

ENERGY

DOE/CS/54209-10  
(DE83003283)

NASA-CR-169801  
19830008587

TESTING OF THE EAGLE-PICHER NICKEL-IRON, THE  
GLOBE ISOA LEAD-ACID, AND THE WESTINGHOUSE  
NICKEL-IRON BATTERY SUBSYSTEMS IN AN  
ELECTRIC-VEHICLE ENVIRONMENT

By  
Robin Hewitt  
Jim Bryant

LIBRARY COPY

FEB 22 1983

LANGLEY RESEARCH CENTER  
LIBRARY, NASA  
HAMPTON, VIRGINIA

July 15, 1982

Work Performed Under Contract No. AI01-78CS54209

Jet Propulsion Laboratory  
California Institute of Technology  
Pasadena, California



U. S. DEPARTMENT OF ENERGY

## DISCLAIMER

"This report was prepared as an account of work sponsored by an agency of the United States Government. Neither the United States Government nor any agency thereof, nor any of their employees, makes any warranty, express or implied, or assumes any legal liability or responsibility for the accuracy, completeness, or usefulness of any information, apparatus, product, or process disclosed, or represents that its use would not infringe privately owned rights. Reference herein to any specific commercial product, process, or service by trade name, trademark, manufacturer, or otherwise, does not necessarily constitute or imply its endorsement, recommendation, or favoring by the United States Government or any agency thereof. The views and opinions of authors expressed herein do not necessarily state or reflect those of the United States Government or any agency thereof."

This report has been reproduced directly from the best available copy.

Available from the National Technical Information Service, U. S. Department of Commerce, Springfield, Virginia 22161.

Price: Printed Copy A14  
Microfiche A01

Codes are used for pricing all publications. The code is determined by the number of pages in the publication. Information pertaining to the pricing codes can be found in the current issues of the following publications, which are generally available in most libraries: *Energy Research Abstracts, (ERA)*; *Government Reports Announcements and Index (GRA and I)*; *Scientific and Technical Abstract Reports (STAR)*; and publication, NTIS-PR-360 available from (NTIS) at the above address.

# Testing of the Eagle-Picher Nickel-Iron, the Globe ISOA Lead-Acid, and the Westinghouse Nickel-Iron Battery Subsystems in an Electric-Vehicle Environment

Robin Hewitt  
Jim Bryant

July 15, 1982

Prepared for  
U.S. Department of Energy  
Through an Agreement with  
National Aeronautics and Space Administration  
by  
Jet Propulsion Laboratory  
California Institute of Technology  
Pasadena, California

(JPL PUBLICATION 82-91)

*NP3-16858<sup>74</sup>*





## ABSTRACT

Three full-size developmental batteries were tested with electric vehicles: the Eagle-Picher nickel-iron battery, the Globe ISOA lead-acid battery, and the Westinghouse nickel-iron battery. Constant-speed and driving-schedule tests were done on a chassis dynamometer. Several aspects of battery performance were evaluated, including capacity, recharge efficiency, voltage response, and self-discharge. Each of these three batteries exhibited some strengths and some weaknesses, but the Westinghouse battery was found to have significant limitations in several important areas.

## ACKNOWLEDGMENTS

Many people made important contributions to the work covered in this report. Test operation and instrumentation were done by Jim Allison, Bob Burleson, Mike Hasbach, Lou Johnson, and Don Palmieri. Data reduction was done by Barb Bonzo, Debbie Brown, and Dick Cowley. I wish to thank Ron Banes, Bob Burleson, Clint Christiansen (ANL), Gene Cynkin, Steve DeGrey, Dan Griffin, Don Kurtz, Dick Levin, Jim Miller (ANL), Don Palmieri, Ted Price, Jack Rowlette, and Mike Yao (ANL), for their helpfulness in reviewing this report and in providing comments and information. Special thanks goes to Marilyn Shaw for typing the manuscript.

This work was sponsored by the U.S. Department of Energy through an interagency agreement, DE-AI01-78CS 54209, with the National Aeronautics and Space Administration (Task RD 152, Amendment 170).

## GLOSSARY

### ABBREVIATIONS AND ACRONYMS

EPI	Eagle-Picher Industries, Incorporated
JPL	Jet Propulsion Laboratory
ISOA	Improved State of the Art
ANL	Argonne National Laboratory
EHV	Electric and Hybrid Vehicle
DOE	Department of Energy
OEPM	Office for Electrochemical Project Management
NBTL	National Battery Test Laboratory
EMS	Electrolyte Management System
ETV	Electric Test Vehicle
SCT	South Coast Technology
IDAC	Integrated Data Acquisition and Control



## CONTENTS

I.	INTRODUCTION . . . . .	1-1
A.	SCOPE . . . . .	1-1
B.	BACKGROUND INFORMATION . . . . .	1-1
1.	General . . . . .	1-1
2.	The EPI Ni-Fe Battery . . . . .	1-2
3.	The Globe ISOA Pb-A Battery . . . . .	1-2
4.	The Westinghouse Ni-Fe Battery . . . . .	1-2
II.	EXECUTIVE SUMMARY . . . . .	2-1
A.	BATTERY DESCRIPTIONS . . . . .	2-1
1.	The EPI Ni-Fe Battery . . . . .	2-1
2.	The Globe ISOA Pb-A Battery . . . . .	2-1
3.	The Westinghouse Ni-Fe Battery . . . . .	2-2
B.	TEST METHODOLOGY . . . . .	2-5
1.	General . . . . .	2-5
2.	Testing the EPI Battery . . . . .	2-6
3.	Testing the Globe Battery . . . . .	2-6
4.	Testing the Westinghouse Battery . . . . .	2-7
C.	DISCUSSION OF TEST RESULTS . . . . .	2-8
1.	Capacity . . . . .	2-8
2.	Self-Discharge . . . . .	2-8
3.	Internal Resistance . . . . .	2-12
4.	Recharge Characteristics . . . . .	2-12
5.	Gassing . . . . .	2-14

D.	CONCLUSIONS . . . . .	2-14
E.	RECOMMENDATIONS . . . . .	2-15
III.	BATTERY DESCRIPTIONS . . . . .	3-1
A.	THE EPI Ni-Fe BATTERY . . . . .	3-1
B.	THE GLOBE ISOA Pb-A BATTERY . . . . .	3-1
C.	THE WESTINGHOUSE Ni-Fe BATTERY . . . . .	3-11
IV.	TEST METHODOLOGY . . . . .	4-1
A.	INTRODUCTION . . . . .	4-1
B.	ELECTRIC-VEHICLE TEST PROCEDURE . . . . .	4-1
	1. Pretest Preparation . . . . .	4-1
	2. Conducting the Test . . . . .	4-2
	3. Test-Termination Criteria . . . . .	4-8
	4. Post-Test Processing of Data . . . . .	4-8
C.	GASSING-RATE MEASUREMENT . . . . .	4-9
D.	TEST-BED ELECTRIC VEHICLES . . . . .	4-9
	1. ETV-1-1 and ETV-1-2 . . . . .	4-9
	2. SCT-2 . . . . .	4-12
E.	TESTING OF THE EPI BATTERY . . . . .	4-12
	1. General . . . . .	4-12
	2. Range Tests . . . . .	4-14
	3. Self-Discharge Tests. . . . .	4-14
	4. Test History. . . . .	4-15
F.	TESTING OF THE GLOBE BATTERY . . . . .	4-17
	1. General . . . . .	4-17
	2. Range Tests . . . . .	4-18

3.	Discharge-Rate Memory Tests . . . . .	4-19
4.	Elevated Temperature Tests . . . . .	4-19
5.	Test History . . . . .	4-20
G.	TESTING OF THE WESTINGHOUSE BATTERY . . . . .	4-22
1.	General . . . . .	4-22
2.	Range Tests . . . . .	4-22
3.	Discharge-Rate Memory Tests . . . . .	4-23
4.	Self-Discharge Tests . . . . .	4-23
5.	Test History . . . . .	4-23
V.	TEST RESULTS . . . . .	5-1
A.	EPI NI-FE BATTERY . . . . .	5-1
1.	Range . . . . .	5-1
2.	Self-Discharge . . . . .	5-4
3.	Self-Heating . . . . .	5-6
4.	Internal Resistance . . . . .	5-7
5.	Recharge Characteristics. . . . .	5-7
6.	Gassing . . . . .	5-7
B.	GLOBE ISOA PB-A BATTERY . . . . .	5-7
1.	Range . . . . .	5-7
2.	Discharge-Rate Memory . . . . .	5-7
3.	Internal Resistance . . . . .	5-15
4.	Effects of Excessive Overcharge . . . . .	5-15
5.	Self-Heating . . . . .	5-15
6.	Temperature Effects . . . . .	5-21

7.	Recharge Characteristics . . . . .	5-21
8.	Gassing . . . . .	5-21
C.	WESTINGHOUSE NI-FE BATTERY . . . . .	5-26
1.	Range . . . . .	5-26
2.	Discharge-Rate Memory . . . . .	5-26
3.	Self-Discharge . . . . .	5-28
4.	Self-Heating . . . . .	5-30
5.	Internal Resistance . . . . .	5-30
6.	Recharge Characteristics . . . . .	5-32
7.	Gassing . . . . .	5-32
VI.	DISCUSSION OF RESULTS . . . . .	6-1
A.	CAPACITY CHARACTERIZATION . . . . .	6-1
1.	Constant-Speed Driving . . . . .	6-1
a.	Westinghouse and EPI Ni-Fe Batteries . . . . .	6-1
b.	Earlier Version of the Westinghouse Battery . . . . .	6-3
c.	Globe ISOA Pb-A Battery . . . . .	6-3
d.	Sensitivity to Discharge Rate . . . . .	6-3
2.	Variable-Speed Driving . . . . .	6-6
3.	Discharge-Rate Memory . . . . .	6-7
4.	Effect of Self-Discharge on Capacity . . . . .	6-7
5.	Effect of Temperature on Capacity . . . . .	6-9
6.	Comparison: Pb-A and Ni-Fe Batteries . . . . .	6-11
B.	RESPONSE UNDER LOAD . . . . .	6-14
1.	Internal Resistance . . . . .	6-14



2.	Effect of Temperature on Internal Resistance . . . . .	6-16
C.	SELF-HEATING . . . . .	6-17
D.	RECHARGE CONSIDERATIONS . . . . .	6-18
1.	Procedure for the EPI Battery . . . . .	6-18
2.	Procedure for the Globe Battery . . . . .	6-18
3.	Procedure for the Westinghouse Battery . . . . .	6-19
4.	Efficiency . . . . .	6-19
5.	Power Requirements . . . . .	6-21
E.	SAFETY AND MAINTENANCE CONSIDERATIONS . . . . .	6-21
1.	Gassing . . . . .	6-21
2.	Watering . . . . .	6-21
3.	Leaks . . . . .	6-22
4.	Reliability . . . . .	6-22
VII.	CONCLUSIONS . . . . .	7-1
A.	EPI BATTERY PERFORMANCE . . . . .	7-1
B.	GLOBE BATTERY PERFORMANCE . . . . .	7-1
C.	WESTINGHOUSE BATTERY PERFORMANCE . . . . .	7-2
VIII.	RECOMMENDATIONS . . . . .	8-1
	REFERENCES . . . . .	9-1
APPENDICES		
A.	BATTERY SYSTEM SPECIFICATIONS . . . . .	A-1
B.	SUPPORTING CALCULATIONS AND DATA ANALYSIS TECHNIQUES . . .	B-1
C.	DATA ACQUISITION CAPABILITIES . . . . .	C-1

D.	RECORDED PARAMETERS . . . . .	D-1
E.	DATA FROM TESTS OF THE 80-CELL EPI BATTERY . . . . .	E-1
F.	DATA FROM TESTS OF THE 90-CELL EPI BATTERY . . . . .	F-1
G.	DATA FROM TESTS OF THE GLOBE ISOA-1 BATTERY . . . . .	G-1
H.	DATA FROM TESTS OF THE GLOBE ISOA-2 BATTERY . . . . .	H-1
I.	DATA FROM TESTS OF THE W-220-1 BATTERY . . . . .	I-1
J.	DATA FROM TESTS OF THE W-220-2 BATTERY . . . . .	J-1
K.	DATA FROM TESTS OF THE W-220-3 BATTERY . . . . .	K-1

## Figures

2-1.	Globe ISOA Pb-A Battery, Electrolyte Stirring Action . . . . .	2-3
2-2.	Westinghouse Ni-Fe Battery, Electrolyte Management System (EMS) . . . . .	2-4
2-3.	EPI and Westinghouse Batteries, Specific Energy versus Power . . . . .	2-9
2-4.	Globe ISOA Battery, Specific Energy versus Power . . . . .	2-10
2-5.	EPI and Westinghouse Batteries, Effect of an Open-Circuit Stand Between End of Charge and Start of Discharge . . . . .	2-11
2-6.	EPI, Globe, and Westinghouse Batteries: Voltage- Normalized Effective Internal Resistance versus Depth-of-Discharge . . . . .	2-13
3-1.	The EPI Ni-Fe Battery, JPL Installation in a Plywood Box . . . . .	3-2
3-2.	EPI Ni-Fe Battery, a String of Five Cells . . . . .	3-3
3-3.	An EPI Ni-Fe Cell . . . . .	3-4
3-4.	The Globe ISOA Pb-A Battery . . . . .	3-5
3-5.	Globe ISOA Pb-A Battery, Vent/Watering System . . . . .	3-7

3-6.	Globe ISOA Pb-A Battery, Electrolyte Stirring Action . . . . .	3-8
3-7.	Globe ISOA Pb-A Battery, Block Diagram of the Electrolyte Stirring System . . . . .	3-9
3-8.	Globe ISOA Pb-A Battery Electrolyte Stirring System, Sequence of Operations . . . . .	3-10
3-9.	The Westinghouse Ni-Fe Battery . . . . .	3-12
3-10.	Westinghouse Ni-Fe Battery, Electrolyte Management System (EMS) . . . . .	3-13
3-11.	Westinghouse Ni-Fe Battery, Plumbing for the EMS . . . . .	3-14
4-1.	Dynamometer Set-up for a Vehicle Test . . . . .	4-3
4-2.	JPL Standardized J227a C and D Driving Schedules . . . . .	4-4
4-3.	EPA Urban Driving Cycle Profile . . . . .	4-7
4-4.	Set-Up Used for Gassing-Rate Measurements . . . . .	4-10
4-5.	An ETV-1 Vehicle . . . . .	4-11
4-6.	SCT-2 . . . . .	4-13
5-1.	80-Cell EPI Ni-Fe Battery: Specific Energy versus Power . . .	5-3
5-2.	EPI Ni-Fe Battery: Effect of an Open-Circuit Stand Between End of Charge and Start of Discharge . . . . .	5-5
5-3.	80-Cell EPI Ni-Fe Battery: Effective Internal Resistance versus Depth-of-Discharge . . . . .	5-8
5-4.	90-Cell EPI Ni-Fe Battery: Effective Internal Resistance versus Depth-of-Discharge . . . . .	5-9
5-5.	90-Cell EPI Ni-Fe Battery: Voltage During Recharge . . . . .	5-10
5-6.	90-Cell EPI Ni-Fe Battery: Recharge Power . . . . .	5-11
5-7.	90-Cell EPI Ni-Fe Battery: Temperature Rise During Recharge . . . . .	5-12
5-8.	Globe ISOA Pb-A Battery: Specific Energy versus Power . . . .	5-14
5-9.	Globe ISOA Pb-A Battery: Effective Internal Resistance versus Depth-of-Discharge . . . . .	5-16

5-10.	Globe ISOA Pb-A Battery: Thermal Runaway Response During Charge with No Temperature Compensation . . . . .	5-17
5-11.	Globe ISOA Pb-A Battery: Increased Internal Resistance as a Result of Damage Caused by a Thermal Runaway Charge . . . .	5-18
5-12.	Globe ISOA Pb-A Battery: Self-Heating During Simulation of Normal Vehicle Use . . . . .	5-20
5-13.	Globe ISOA Pb-A Battery: Voltage During Recharge . . . . .	5-22
5-14.	Globe ISOA Pb-A Battery: Recharge Current . . . . .	5-23
5-15.	Globe ISOA Pb-A Battery: Recharge Power . . . . .	5-24
5-16.	Globe ISOA Pb-A Battery: Temperature During Recharge . . . . .	5-25
5-17.	Westinghouse Ni-Fe Battery: Specific Energy versus Power . . . .	5-27
5-18.	Westinghouse Ni-Fe Battery: Effect of an Open-Circuit Stand Between End of Charge and Start of Discharge . . . . .	5-29
5-19.	Westinghouse Ni-Fe Battery: Effective Internal Resistance versus Depth-of-Discharge . . . . .	5-31
5-20.	Westinghouse Ni-Fe Battery: Voltage During Recharge . . . . .	5-33
5-21.	Westinghouse Ni-Fe Battery: Recharge Current . . . . .	5-34
5-22.	Westinghouse Ni-Fe Battery: Recharge Power . . . . .	5-35
5-23.	Westinghouse Ni-Fe Battery: Temperature During Recharge (low initial temperature) . . . . .	5-36
5-24.	Westinghouse Ni-Fe Battery: Temperature During Recharge (high initial temperature) . . . . .	5-37
5-25.	Westinghouse Ni-Fe Battery: Gassing Rate During a Standard Taper Charge with 40-A Finish Current . . . . .	5-38
5-26.	Westinghouse Ni-Fe Battery: Gassing Rate During an Experimental Taper Charge with 10-A Finish Current . . . . .	5-39
6-1.	EPI and Westinghouse Batteries: Specific Energy versus Power. . . . .	6-2
6-2.	Capacity of the Westinghouse Battery Compared with an Earlier Version of the Battery . . . . .	6-4

6-3.	Globe ISOA Battery, ETV-1 Baseline Battery, and SCT-2 Baseline Battery: Specific Energy versus Power . . . . .	6-5
6-4.	EPI and Westinghouse Batteries: Effect of an Open-Circuit Stand Between End of Charge and Start of Discharge . . . . .	6-8
6-5.	Effect of Temperature on the Capacity of Ni-Fe Batteries, Typical . . . . .	6-10
6-6.	Capacity of the EPI, Globe, and Westinghouse Batteries Immediately After Charge Termination . . . . .	6-12
6-7.	Capacity of the EPI, Globe, and Westinghouse Batteries After an Overnight, Open-Circuit Stand . . . . .	6-13
6-8.	EPI, Globe, and Westinghouse Batteries: Voltage- Normalized Effective Internal Resistance versus Depth-of-Discharge . . . . .	6-15
B-1.	Points in the Driving Cycle that were used for Reading Data for Internal Resistance Calculations . . . . .	B-24
C-1.	Automotive Research Facility, Central Instrumentation Area . .	C-4
C-2.	IDAC, Block Diagram . . . . .	C-5
C-3.	A Power-Measurement Box with Six Wideband-Wattmeter Cards . . .	C-9
C-4.	Wideband Wattmeter, Block Diagram . . . . .	C-10
C-5.	Back Panel of Power-Measurement Box Showing Signal Outputs . .	C-12

## Tables

2-1.	Typical Energy, Coulombic, and Voltage Efficiencies . . . . .	2-14
4-1.	JPL-Standardized Version of J227a Schedule C . . . . .	4-5
4-2.	JPL-Standardized Version of J227a Schedule D . . . . .	4-6
4-3.	Globe ISOA Battery: Test Sequence to Observe Discharge-Rate Memory Effects . . . . .	4-19
4-4.	Westinghouse Battery: Test Sequence to Observe Discharge-Rate Memory Effects . . . . .	4-23
4-5.	Westinghouse Battery: Self Discharge Tests . . . . .	4-24

5-1.	80-Cell EPI Ni-Fe Battery: Averaged Results of All Range Tests with SCT-2 . . . . .	5-1
5-2.	80-Cell EPI Ni-Fe Battery: Averaged Results of All Cell Range Tests with ETV-1-2 . . . . .	5-2
5-3.	90-Cell EPI Ni-Fe Battery: Averaged Results of All Range Tests with SCT-2 . . . . .	5-2
5-4.	80-Cell EPI Ni-Fe Battery: Effect of an Open-Circuit Stand Between End of Charge and Start of Discharge . . . . .	5-4
5-5.	EPI Ni-Fe Battery: Average Temperature Rise Due to Self-Heating During Vehicle Testing . . . . .	5-6
5-6.	Globe ISOA Pb-A Battery: Averaged Results of All Range Tests with ETV-1-1 and ETV-1-2 . . . . .	5-13
5-7.	Globe ISOA Pb-A Battery: Results of Memory Test Series . . . . .	5-13
5-8.	Globe ISOA Pb-A Battery: Average Temperature Rise Due to Self-Heating During Vehicle Testing . . . . .	5-19
5-9.	Westinghouse Ni-Fe Battery: Averaged Results of All Range Tests with SCT-2 . . . . .	5-26
5-10.	Westinghouse Ni-Fe Battery: Results of Memory Tests . . . . .	5-28
5-11.	Westinghouse Ni-Fe Battery: Effect of an Open-Circuit Stand Between End of Charge and Start of Discharge . . . . .	5-28
5-12.	Westinghouse Ni-Fe Battery: Average Temperature Rise Due to Self-Heating During Vehicle Testing . . . . .	5-30
6-1.	Mean Gradient of Specific Energy as a Function of Discharge Power Between 5 kW and 15 kW . . . . .	6-3
6-2.	Typical Energy, Coulombic, and Voltage Efficiencies . . . . .	6-20
B-1.	Data Sources for Table 5-1 . . . . .	B-3
B-2.	Data Sources for Table 5-2 . . . . .	B-4
B-3.	Data Sources for Table 5-3 . . . . .	B-4
B-4.	Data Sources for Table 5-6 . . . . .	B-5
B-5.	Data Sources for Table 5-9 . . . . .	B-5
B-6.	Tabulation of Data Shown in Figure 5-1 . . . . .	B-6

B-7.	Tabulation of Data Shown in Figure 5-8 . . . . .	B-7
B-8.	Tabulation of Data Shown in Figure 5-17 . . . . .	B-8
B-9.	Data for the 1979 Version of the Westinghouse Battery . . . . .	B-9
B-10	Data for the SCT-2 Baseline Battery . . . . .	B-9
B-11.	Data for the ETV-1 Baseline Battery . . . . .	B-10
B-12	EPI Battery: Temperature Rise During 56 km/h (35 mi/h) Tests . . . . .	B-11
B-13.	EPI Battery: Temperature Rise During 72 km/h (45 mi/h) Tests . . . . .	B-11
B-14.	EPI Battery: Temperature Rise During 88 km/h (55 mi/h) Tests . . . . .	B-12
B-15.	EPI Battery: Temperature Rise During Schedule C Tests . . . . .	B-12
B-16.	EPI Battery: Temperature Rise During Schedule D Tests . . . . .	B-12
B-17.	EPI Battery: Temperature Rise to 50% Depth-of- Discharge During 56 km/h (35 mi/h) Tests . . . . .	B-13
B-18.	EPI Battery: Temperature Rise to 50% Depth-of-Discharge During 72 km/h (45 mi/h) Tests . . . . .	B-13
B-19.	EPI Battery: Temperature Rise to 50% Depth-of- Discharge During 88 km/h (55 mi/h) Tests . . . . .	B-13
B-20.	EPI Battery: Temperature Rise to 50% Depth-of-Discharge During Schedule C Tests . . . . .	B-13
B-21.	EPI Battery: Temperature Rise to 50% Depth-of-Discharge During Schedule D Tests . . . . .	B-14
B-22.	EPI Battery: Temperature Rise During Recharge After a Partial Discharge . . . . .	B-14
B-23.	EPI Battery: Temperature Rise During Recharge After a Full Discharge . . . . .	B-14
B-24.	Globe ISOA Battery: Temperature Rise During 56 km/h (35 mi/h) Tests . . . . .	B-16
B-25.	Globe ISOA Battery: Temperature Rise During 72 km/h (45 mi/h) Tests . . . . .	B-16

B-26.	Globe ISOA Battery: Temperature Rise During 88 km/h (55 mi/h) Tests . . . . .	B-16
B-27.	Globe ISOA Battery: Temperature Rise During Schedule C Tests . . . . .	B-17
B-28.	Globe ISOA Battery: Temperature Rise During Schedule C Tests . . . . .	B-17
B-29.	Globe ISOA Battery: Temperature Rise to 50% Depth-of- Discharge During 56 km/h (35 mi/h) Tests . . . . .	B-17
B-30.	Globe ISOA Battery: Temperature Rise to 50% Depth-of- Discharge During 72 km/h (45 mi/h) Tests . . . . .	B-18
B-31.	Globe ISOA Battery: Temperature Rise to 50% Depth-of- Discharge During 88 km/h (55 mi/h) Tests . . . . .	B-18
B-32.	Globe ISOA Battery: Temperature Rise to 50% Depth-of- Discharge During Schedule C Tests . . . . .	B-18
B-33.	Globe ISOA Battery: Temperature Rise to 50% Depth-of- Discharge During Schedule D Tests . . . . .	B-19
B-34.	Globe ISOA Battery: Temperature Rise During Recharge after a Partial Discharge . . . . .	B-19
B-35.	Globe ISOA Battery: Temperature Rise During Recharge After a Full Discharge . . . . .	B-19
B-36.	Westinghouse Battery: Temperature Rise During 56 km/h (35 mi/h) Tests . . . . .	B-20
B-37.	Westinghouse Battery: Temperature Rise During 72 km/h (45 mi/h) Tests . . . . .	B-20
B-38.	Westinghouse Battery: Temperature Rise During 88 km/h (55 mi/h) Tests . . . . .	B-21
B-39.	Westinghouse Battery: Temperature Rise During Schedule C Tests . . . . .	B-21
B-40.	Westinghouse Battery: Temperature Rise to 50% Depth-of- Discharge During 56 km/h (35 mi/h) Tests . . . . .	B-21
B-41.	Westinghouse Battery: Temperature Rise to 50% Depth-of- Discharge During 72 km/h (45 mi/h) Tests . . . . .	B-22
B-42.	Westinghouse Battery: Temperature Rise to 50% Depth-of- Discharge During 88 km/h (55 mi/h) Tests . . . . .	B-22



B-43.	Westinghouse Battery: Temperature Rise to 50% Depth-of-Discharge During Schedule C Tests . . . . .	B-22
B-44.	80-Cell EPI Battery Cycle 112 (Schedule C): Internal Resistance Data . . . . .	B-26
B-45.	90-Cell EPI Battery Cycle 137 (Schedule C): Internal Resistance Data . . . . .	B-28
B-46.	90-Cell EPI Battery Cycle 140 (Schedule D): Internal Resistance Data . . . . .	B-32
B-47.	Globe ISOA-1 Battery Cycle 59 (Schedule D): Internal Resistance Data . . . . .	B-34
B-48.	Globe ISOA-1 Battery Cycle 65 (Schedule D): Internal Resistance Data . . . . .	B-36
B-49.	Globe ISOA-2 Battery Cycle 65 (Schedule D): Internal Resistance Data . . . . .	B-38
B-50.	Westinghouse Battery Cycle 9 (Schedule D): Internal Resistance Data . . . . .	B-40
B-51.	Westinghouse Battery Cycle 20 (Schedule C): Internal Resistance Data . . . . .	B-43
B-52.	Globe ISOA-2 Battery Cycle 76: Gassing-Rate Measurements During Recharge . . . . .	B-48
B-53.	W-220-3 Battery Cycle 56: Gassing-Rate Measurements During Recharge . . . . .	B-48
B-54.	W-220-3 Battery Cycles 68 and 70: Gassing-Rate Measurements During Recharge . . . . .	B-49
B-55.	Data Used for Computing the Mean Gradient of Specific Energy as a Function of Discharge Power . . . . .	B-51



## SECTION I

### INTRODUCTION

#### A. SCOPE

This report covers testing, done by the Jet Propulsion Laboratory (JPL), of three battery subsystems designed for use in electric vehicles:

- (1) The VNF300, a nickel-iron (Ni-Fe) battery being developed by Eagle-Picher Industries, Incorporated (EPI).
- (2) The ISOA (Improved State-of-the-Art) battery, a lead-acid (Pb-A) battery being developed by the Globe Battery Division of Johnson Controls, Incorporated (Globe).
- (3) A Ni-Fe battery being developed by Westinghouse Electric Corporation.

These batteries were tested during the period beginning October 1980 and ending May 1982.

Battery performance in a vehicle environment was evaluated by testing the batteries in conjunction with electric vehicles on a chassis dynamometer. The procedures used for testing each battery subsystem are described, and the test results are presented. A discussion of the significance of these results is included, and, whenever possible, direct comparisons between the three battery subsystems are made. In addition, the Westinghouse battery is compared with an earlier version of the battery that was tested by JPL in 1979. Specific recommendations for further development and testing of the three battery subsystems are given at the end of the report.

#### B. BACKGROUND INFORMATION

##### 1. General

In September 1976, Congress passed Public Law 94-413 (The Electric and Hybrid Vehicle Research, Development, and Demonstration Act). The purpose of this Act was to reduce national dependence on imported petroleum by speeding the rate at which advanced electric and hybrid vehicle technology becomes available. In support of this law, the United States Department of Energy (DOE) was chartered to conduct a research and development program.

At JPL, the Electric and Hybrid Vehicle (EHV) project was started in April 1977 to support the DOE efforts in vehicle-systems research and development. Under contract to DOE, this project has done testing of state-of-the-art electric and hybrid vehicles and research into advanced concepts for vehicles that use non-petroleum-based propulsion systems.

At Argonne National Laboratory (ANL), the Office for Electrochemical Project Management (ANL/OEPM) was formed to support the DOE efforts in energy-

storage-systems research and development. ANL/OEPM has managed contracts with several battery manufacturers to develop improved battery technology for electric and hybrid vehicles. As new battery technology is developed under these contracts, it is tested at the ANL National Battery Test Laboratory (NBTL).

The EPI Ni-Fe, the Globe ISOA Pb-A, and the Westinghouse Ni-Fe batteries were all developed under ANL/OEPM contracts. Before being tested at JPL, each of these battery technologies had demonstrated good performance characteristics, at the cell and/or module level, in tests at NBTL.

Testing of battery systems at JPL is not meant to replace, but rather to supplement, the testing done at NBTL. The testing at NBTL is done mostly at the cell or module level, and the emphasis is on acquiring data under controlled, laboratory conditions for the purpose of evaluating, on a common basis, battery technology from various contractors (Reference 1). In contrast, the testing at JPL is done with full-scale battery subsystems, and the emphasis is on system-level characterization of battery performance in a vehicle environment. By testing electric vehicles on a dynamometer, any vehicle/battery interface problems are brought to light, and the overall viability of the battery as a vehicle subsystem can be evaluated.

The vehicle/battery combinations used for these tests do not necessarily demonstrate the best electric vehicle performance that is possible with the developmental batteries. The test combinations were constrained by the existing design of batteries and the limited availability of test vehicles. In some cases, vehicles were tested with batteries having a system voltage that was lower than the vehicle's design voltage. Therefore, vehicle range data are not necessarily representative of the range that could be obtained with an optimized vehicle system. Of more significance are the data that describe battery performance in a vehicle environment. These data are presented in terms of specific energy, internal resistance, self-discharge rate, and recharge efficiency--not in terms of vehicle range.

## 2. The EPI Ni-Fe Battery

The EPI Ni-Fe battery has been part of the ANL/OEPM program since 1977. Tests of the EPI battery were conducted at JPL from October 1980 to January 1981. This battery was tested in two configurations: 80 cells and 90 cells.

## 3. The Globe ISOA Pb-A Battery

Globe has been in the ANL/OEPM program since 1977. The ISOA battery represents their 1981 level of Pb-A battery technology. Tests of the ISOA battery were conducted at JPL from February 1981 to May 1982. Two ISOA batteries were used for these tests.

## 4. The Westinghouse Ni-Fe Battery

During the time period from May 1979 to April 1980, four developmental batteries from the ANL/OPEM program were tested in conjunction with state-of-the-art electric vehicles (see Reference 2). One of the batteries

tested was the Westinghouse Ni-Fe. This battery had a circulating electrolyte system to provide cooling and to manage the gasses generated during charging. Based on these tests, the following recommendation was made to DOE:

"The Westinghouse nickel-iron battery shows potential for extending vehicle range and performance. Considerable effort is needed, however, to improve the electrolyte circulation system before this battery can be considered suitable for installation within a vehicle. It is recommended that additional work be done on the electrolyte circulation system, with emphasis being placed on the safe handling of the relatively large quantity of hydrogen generated during charge."<sup>1</sup>

Based on the results of the May 1979 to April 1980 testing, DOE funded JPL to manage a contract, under which Westinghouse was to develop their Ni-Fe battery sufficiently for integration into an electric vehicle. This contract was initiated in 1980. Meanwhile, the Westinghouse Ni-Fe battery continued in the ANL/OEPM program and continued to be tested at NBTL. Two updated versions of the Westinghouse battery were tested at JPL from February 1981 to March 1982.

---

<sup>1</sup>Reference 2.



## SECTION II

### EXECUTIVE SUMMARY

This report covers testing, done by the Jet Propulsion Laboratory, of three battery subsystems designed for use in electric vehicles:

- (1) A nickel-iron (Ni-Fe) battery being developed by Eagle-Picher Industries, Incorporated (EPI).
- (2) The ISOA (Improved State-of-the-Art) battery, a lead-acid (Pb-A) battery being developed by the Globe Battery Division of Johnson Controls, Incorporated (Globe).
- (3) A Ni-Fe battery being developed by Westinghouse Electric Corporation.

These batteries were tested during the period beginning October 1980 and ending May 1982.

#### A. BATTERY DESCRIPTIONS

##### 1. The EPI Ni-Fe Battery

EPI is developing their Ni-Fe battery under a cooperative agreement with the Swedish National Development Company. The testing covered in this report was done with a developmental prototype version of the battery. This developmental battery consisted of a collection of cells packaged as 10-cell strings with air gaps between each cell for cooling. There was no provision for handling gasses, and no single-point watering system; each cell was vented directly to the atmosphere, and each cell was watered separately.

Sintered plates are used for both electrodes. The design of the negative electrode is based on iron-electrode technology from the Swedish National Development Company. It consists of a sintered, iron-powder plate on an expanded, iron substrate. The positive electrode is an unusually thick (2.0 mm), sintered, nickel plaque which has been electrochemically impregnated with active material.

The EPI battery was tested in two configurations: as an 80-cell battery and as a 90-cell battery. The mass of the 80-cell battery was 595 kg, and the mass of the 90-cell battery was 670 kg.

##### 2. The Globe ISOA Pb-A Battery

The Globe battery is a complete battery subsystem. It is comprised of eight 12-V modules (connected in series electrically), a vent/watering system, and an electrolyte stirring system. The vent/watering system vents gasses during charge and discharge, and also provides a single-point access for watering. The electrolyte stirring system lifts dense electrolyte from the bottom to the top of the cell to prevent electrolyte stratification during

charge and discharge. The reasons for inclusion of the stirring system are as follows:

- Promote uniform utilization of active materials.
- Minimize the amount of overcharge required.
- Thermal maintenance.

The electrolyte stirring system is used during both charge and discharge. The stirring action occurs as shown in Figure 2-1: air pulses periodically travel to individual cells, depressing a column of high-density electrolyte in one leg of a U-shaped tube in each cell. Most of the electrolyte in the U-shaped tube is thereby lifted up the second leg and emitted above the electrodes; then, because of its high density, it flows down between the plates. A small hole near the bottom of the U-shaped tube allows high-density electrolyte from the bottom of the cell to refill the tube in preparation for the next air pulse. In this manner, the stirring system prevents stratification without bubbling air through the electrolyte.

Pasted plates are used for both the negative and the positive electrodes. The end electrodes in each module are thinner than the interior electrodes, and a patented grid design is used for all electrodes. The negative plates are bagged in envelope-type separators. The mass of the Globe battery was 602 kg.

### 3. The Westinghouse Ni-Fe Battery

The Westinghouse battery is also a complete subsystem. It is comprised of ninety cells (connected in series electrically) and an electrolyte management system (EMS). The EMS has the following functions:

- Control battery temperature.
- Separate gas from electrolyte and safely vent the gas.
- Contain excess electrolyte during charge and supply electrolyte to cells during discharge.
- Prevent over-pressure in the system.
- Isolate electrolyte from outside air.
- Provide a single access for water and electrolyte replenishment.

The EMS is plumbed to the cells through a manifold/header system.

The operation of the EMS is shown in Figure 2-2. Electrolyte and gas are circulated from the cells to a stainless-steel reservoir. Within the reservoir, heat exchanger coils are immersed in the electrolyte, and tap water is used to maintain electrolyte temperature during charge. The reservoir is only partially filled with liquid, so it also serves as a separation chamber for gas and electrolyte. The gas is removed from the reservoir and



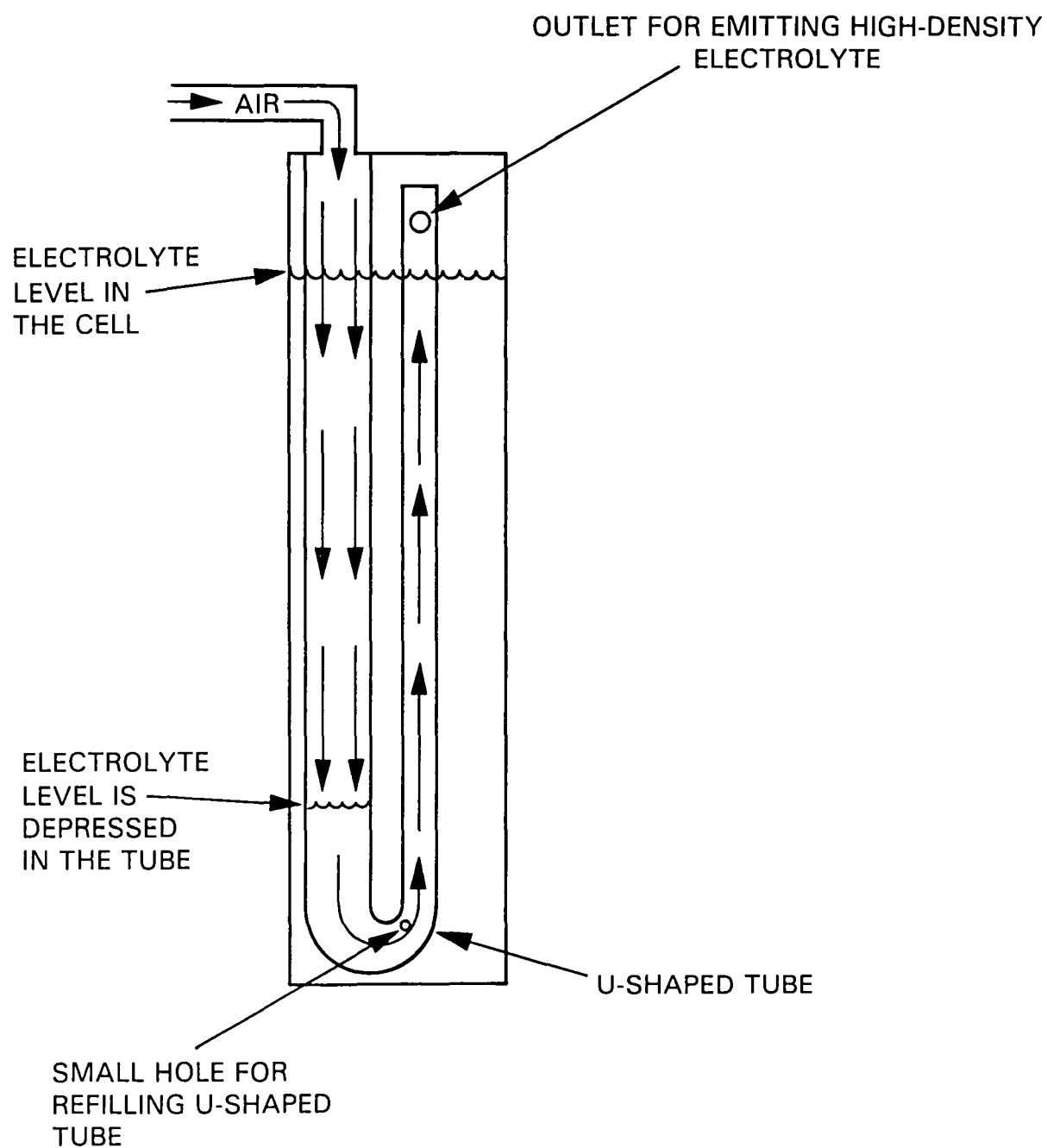


Figure 2-1. Globe ISOA Pb-A Battery, Electrolyte Stirring Action

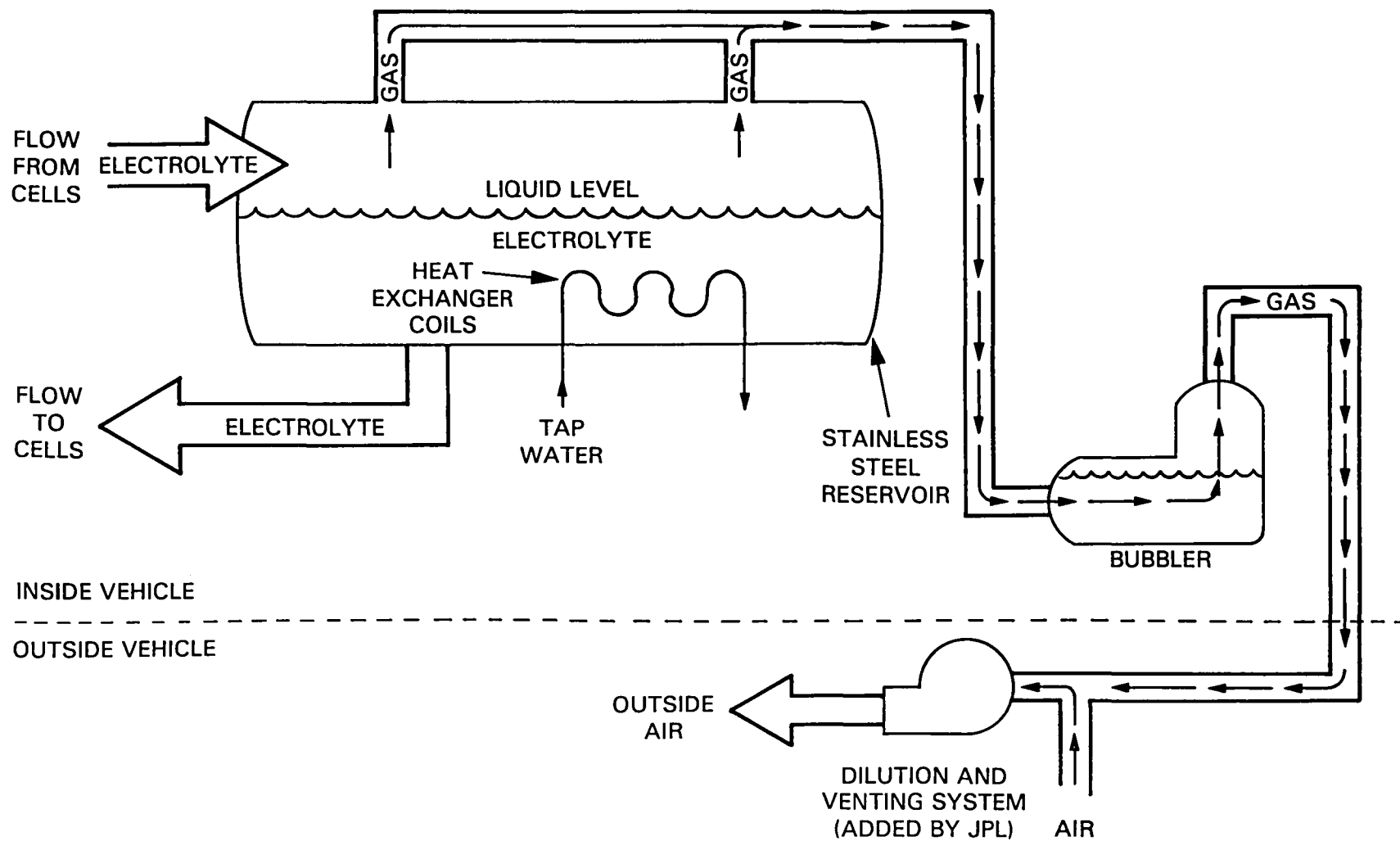


Figure 2-2. Westinghouse Ni-Fe Battery, Electrolyte Management System (EMS)

exhausted through a tank of water--the bubbler. The bubbler serves as a flame arrestor and also isolates the electrolyte from the outside air to prevent carbonation. In addition to the EMS supplied by Westinghouse, hardware for diluting and venting the gas was added by JPL.

A substrate of sintered, steel fiber is used for both positive and negative electrodes. Active material for the iron electrode is loaded in the form of a thick, water-based paste which is pressed into the plaque and dried. The steel-fiber substrate for the positive, nickel electrode is nickel plated. Active material is loaded into the pores of the nickel-plated, steel-fiber substrate by electrochemical precipitation. The mass of the Westinghouse battery was 607 kg.

## B. TEST METHODOLOGY

### 1. General

Battery subsystem performance was evaluated primarily by driving electric vehicles on a chassis dynamometer. In some instances, the batteries were installed in the vehicle, but, in other instances, the batteries were connected to the vehicle by an umbilical cord. Two types of vehicle tests were done: constant-speed tests and driving-schedule tests.

Before a vehicle-range test, the battery is charged fully. If the battery type is Ni-Fe, the discharge normally begins within 10 min after completion of recharge. If the battery type is Pb-A, the battery is normally left standing after completion of recharge until battery temperature is at  $23 \pm 3^\circ\text{C}$ . The time interval between the end of charge and the start of discharge for a Pb-A battery is usually about 10 to 20 h. These pretest criteria were established to provide repeatable data. It was felt that self-discharge would be the parameter having the most effect on the performance of Ni-Fe batteries, so the time interval during which self-discharge could occur was limited to 10 min to minimize variation in test results. Similarly, it was felt that temperature would be the parameter having the most effect on the performance of Pb-A batteries, so the allowable variation in pretest battery temperature was restricted. However, some vehicle tests were done specifically to evaluate the effects of self-discharge and temperature; for the purposes of this evaluation, the pretest criteria of time between charge and discharge and of battery temperature were varied.

The termination criteria used for range tests are as follows:

- (1) Low voltage. If battery voltage drops below a minimum level, the test is terminated. There are two minimum-voltage criteria specified for each battery: one during cruise or idle and one during acceleration.
- (2) Speed. During constant-speed tests, if vehicle speed cannot be maintained within 95% of the specified value, the test is terminated.

- (3) Acceleration. During driving-schedule tests, if the acceleration portion of the profile cannot be completed within 2 s of the time specified by the procedure, the test is terminated.

## 2. Testing of the EPI Battery

Fifteen vehicle range tests of the 80-cell EPI battery were attempted. Ten of these tests were successful. Five vehicle-range tests of SCT-2 with the 90-cell EPI battery were attempted. All of these range tests were successful. The voltage-termination criteria used for all range tests was 1.0 V/cell during cruise or idle, 0.5 V/cell during acceleration.

A limited amount of testing was done with the 80-cell battery to determine the effect of self-discharge on the capacity of the EPI battery. The purpose of these tests was not to provide data for a detailed analysis, but rather to assess the importance of this effect. The procedure for these tests was similar to the procedure used for the range tests. As for the range tests, a full recharge was done first, but the battery was left standing for a longer time between the end of charge and the start of discharge.

The same charge procedure was used before all vehicle tests of the EPI battery: after a full discharge, the battery was recharged until 300 Ah had been returned; after a partial discharge, the battery was recharged until 120% of the previous discharge (on a coulombic basis) had been returned. Charging was always done at a constant, 60-A rate. This charge procedure was specified by the manufacturer.

Maintenance was performed every second charge/discharge cycle. The maintenance procedure consisted of watering the individual cells until the sight glass on each cell indicated that it was full, cleaning salt deposits off the tops of the cells, and checking the vents on each cell.

## 3. Testing of the Globe Battery

Two Globe ISOA batteries were used for the vehicle tests. The first battery (designated ISOA-1) underwent twenty charge/discharge cycles in the vehicle-test program and then began to show a loss of capacity. The vehicle testing was, therefore, continued with a second battery (designated ISOA-2). The ISOA-1 battery was returned to Globe for analysis, and the capacity loss was found to be the result of inadequate electrolyte stirring. Shortly after the start of testing with the ISOA-2 battery, this battery was inadvertently subjected to an excessive overcharge. Damage to the battery as a result of the overcharge affected performance during driving-schedule tests, but did not affect performance during constant-speed driving.

Eight vehicle-range tests with the ISOA-1 battery were attempted. All of these range tests were successful. Twenty-one vehicle-range tests of the ISOA-2 battery were attempted. Nine of these tests were successful. The voltage-termination criteria used for range tests with the ISOA-1 battery was 1.65 V/cell during cruise or idle, 1.3 V/cell during acceleration. The voltage-termination criterion during cruise was raised to 1.75 V/cell for tests with the ISOA-2 battery because it was felt that the lower termination voltage might be damaging to the battery.

A limited amount of testing was done with the ISOA-2 battery to observe the effects of temperature on battery performance. Two consecutive 72 km/h (45 mi/h) range tests were done to observe the effect of temperature on capacity. In addition, a Schedule D test was done at an elevated temperature to observe the effect of temperature on effective internal resistance.

A taper-charge procedure was used with the Globe battery: the battery was charged at 48 A until voltage reached a maximum level; voltage was then maintained for 9 h. The maximum voltage level is temperature compensated: it is reduced at high temperatures and increased at low temperatures. At 27°C, the maximum voltage level is 2.67 V/cell, and the temperature compensation used with this battery is -0.007 V/°C/cell.

Watering of the Globe ISOA battery is required after every 3,000 Ah of charge. Several attempts to use the battery's watering system resulted in the battery being overfilled. Every time this happened, electrolyte would be forced out of the battery through the watering and electrolyte stirring systems during the subsequent recharge. However, when the watering system was used immediately after recharge (while the electrolyte level was raised by gas bubbles on the plates), it worked correctly, and the battery was not overfilled.

#### 4. Testing of the Westinghouse Battery

Fifteen vehicle-range tests of the Westinghouse battery were attempted. Thirteen of these tests were successful. The voltage-termination criteria used for range tests was 1.0 V/cell during cruise or idle, 0.5 V/cell during acceleration.

A limited amount of testing was done to determine the effect of self-discharge on the capacity of the Westinghouse battery. The purpose of these tests was not to provide data for a detailed analysis, but rather to assess the importance of this effect. The procedure for these tests was similar to the procedure used for the range tests. As for the range tests, a full recharge was done first, but the battery was left standing for a longer time between the end of charge and the start of discharge.

Several problems were encountered during testing of the Westinghouse battery, including the following:

- ° Electrolyte leaks.
- ° Cracks in cell cases.
- ° Cell failures.

The charge procedure used during range tests with the Westinghouse battery is as follows: the battery is charged at 70 A until it reaches 157 V; the voltage is then maintained, and current is allowed to taper; the charge is terminated at 300 Ah.

Maintenance was performed as needed. Lights on the charger indicate whether the electrolyte level in the reservoir or the water level in the

bubbler are low. Water was added to the reservoir every second charge/discharge cycle. Water was added to the bubbler approximately every twenty cycles.

## C. DISCUSSION OF TEST RESULTS

### 1. Capacity

Figure 2-3, a plot of specific energy versus power, shows the capacity obtained from each of the two Ni-Fe batteries during constant-speed-range tests. As shown in this figure, the specific energy of the EPI battery is substantially higher than the specific energy of the Westinghouse battery.

Figure 2-4 shows the capacity obtained from the Globe battery during constant-speed-range tests at 23°C. In addition, the estimated capacity of the Globe battery at 33°C (the average end-of-charge temperature of the Globe battery) is shown in this figure.

The sensitivity of capacity to discharge rate is an important aspect of electric-vehicle batteries. In electric-vehicle applications, it is advantageous for battery capacity to have little sensitivity to discharge rate because the power demands during normal use will vary. If battery capacity is relatively insensitive to these variations, vehicle range will be more consistent and predictable--especially under strenuous driving conditions. The capacity of the Ni-Fe batteries is less sensitive to discharge rate than is the capacity of the Globe ISOA battery. The EPI Ni-Fe battery performs especially well in this respect.

### 2. Self-Discharge

In general, the capacity of a fully-charged Pb-A battery will remain relatively stable over a period of several days, but the capacity of a Ni-Fe battery will decrease substantially, due to self-discharge, as the battery stands without an applied load. Because of this self-discharge, the capacity data obtained from vehicle-range tests of the two Ni-Fe batteries is only representative of the capacity available immediately following charge termination. If the vehicle-range tests with the Ni-Fe batteries had been preceded by a one or two day open-circuit stand, as were the range tests with the Globe Pb-A battery, less capacity would have been obtained. Figure 2-5, a plot of capacity loss versus open-circuit stand time, compares the effect of self-discharge on the capacity of each of the two Ni-Fe batteries.

As shown in Figure 2-5, the EPI and the Westinghouse batteries have differing self-discharge characteristics: for the first 24 h, both batteries lose capacity at about the same rate, but after 24 h, the rate of self-discharge is substantially less for the EPI battery than for the Westinghouse battery. Thus, over a period of several days, self-discharge would be less of a problem with the EPI battery than with the Westinghouse battery.

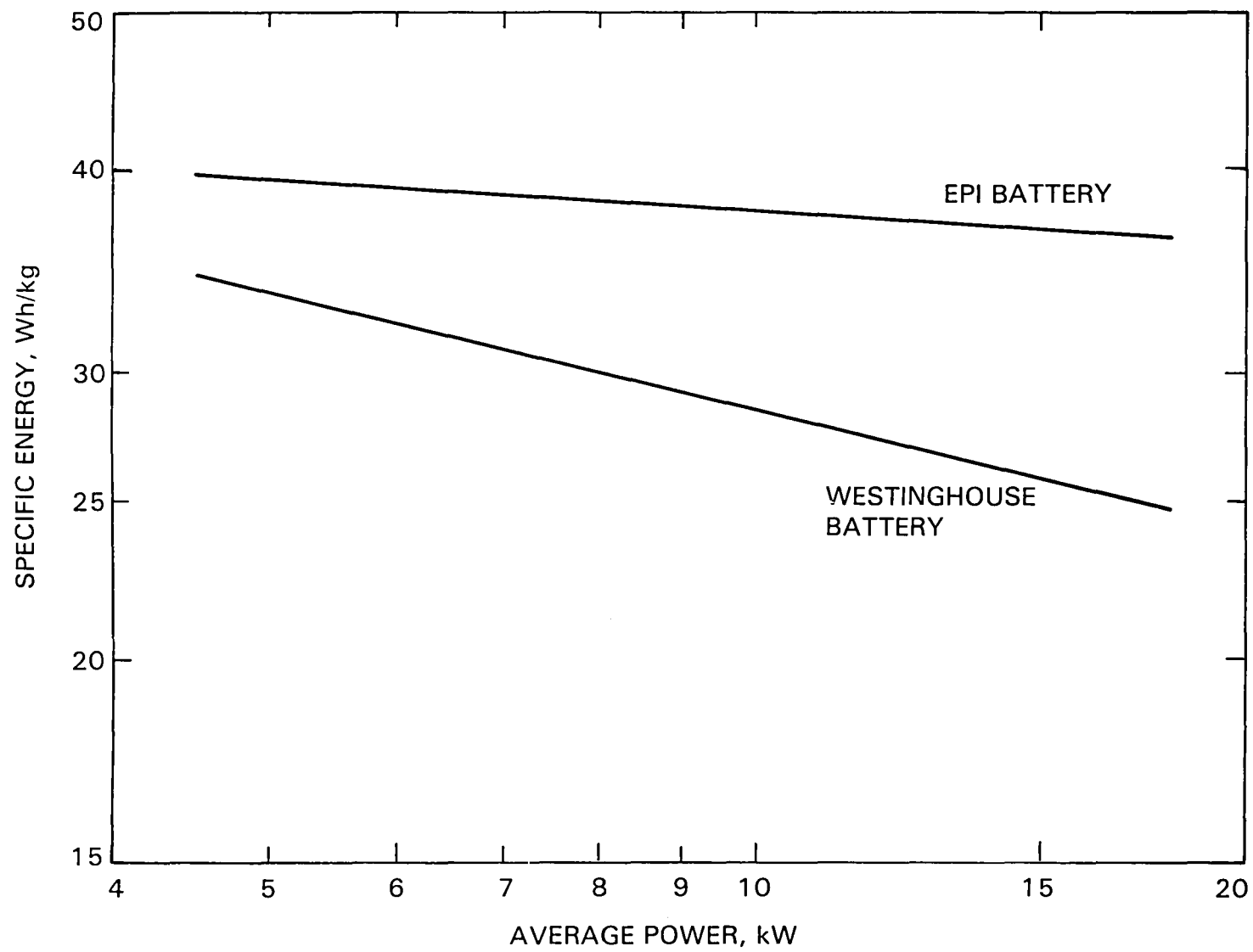


Figure 2-3. EPI and Westinghouse Batteries, Specific Energy versus Power

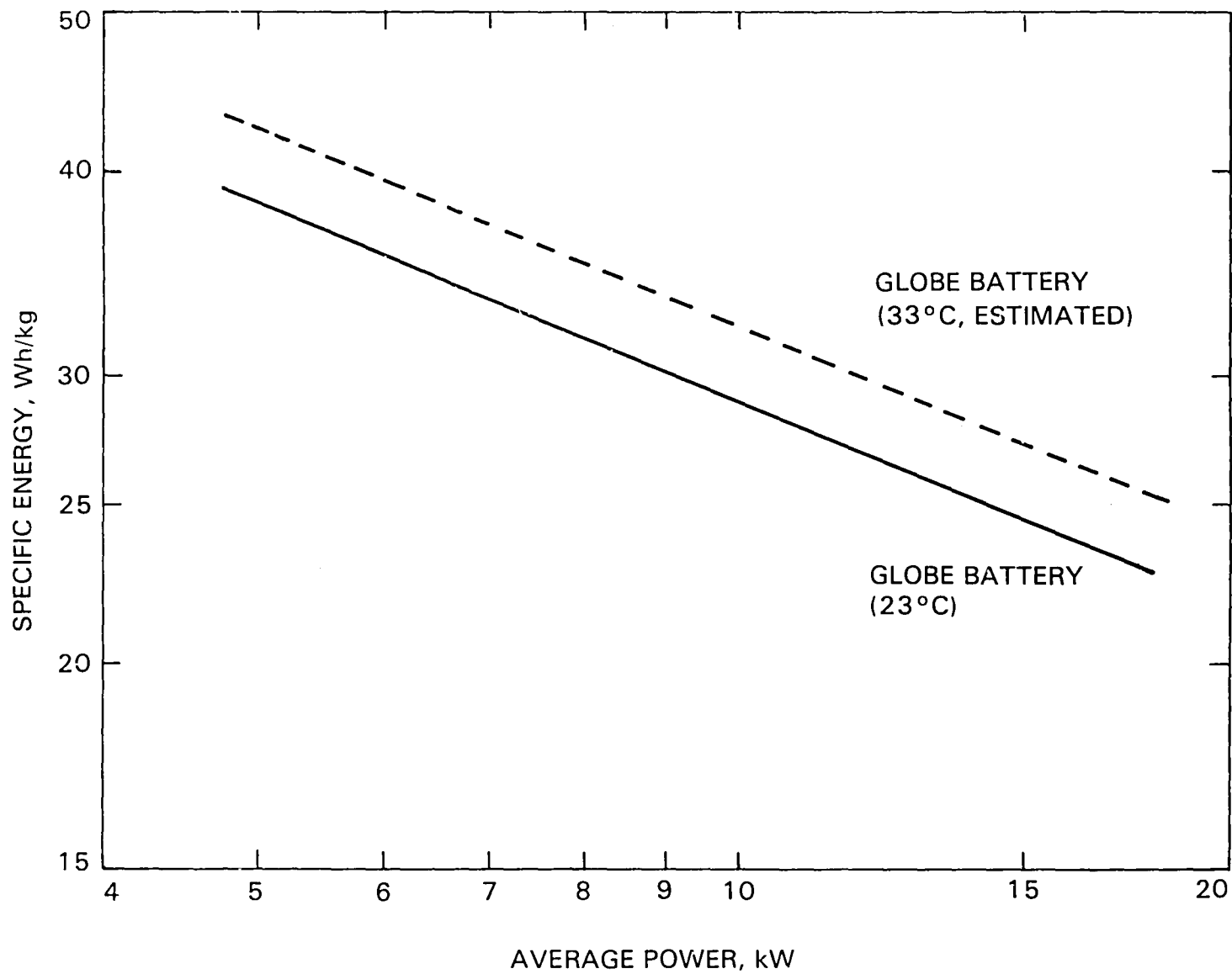


Figure 2-4. Globe ISOA Battery, Specific Energy versus Power



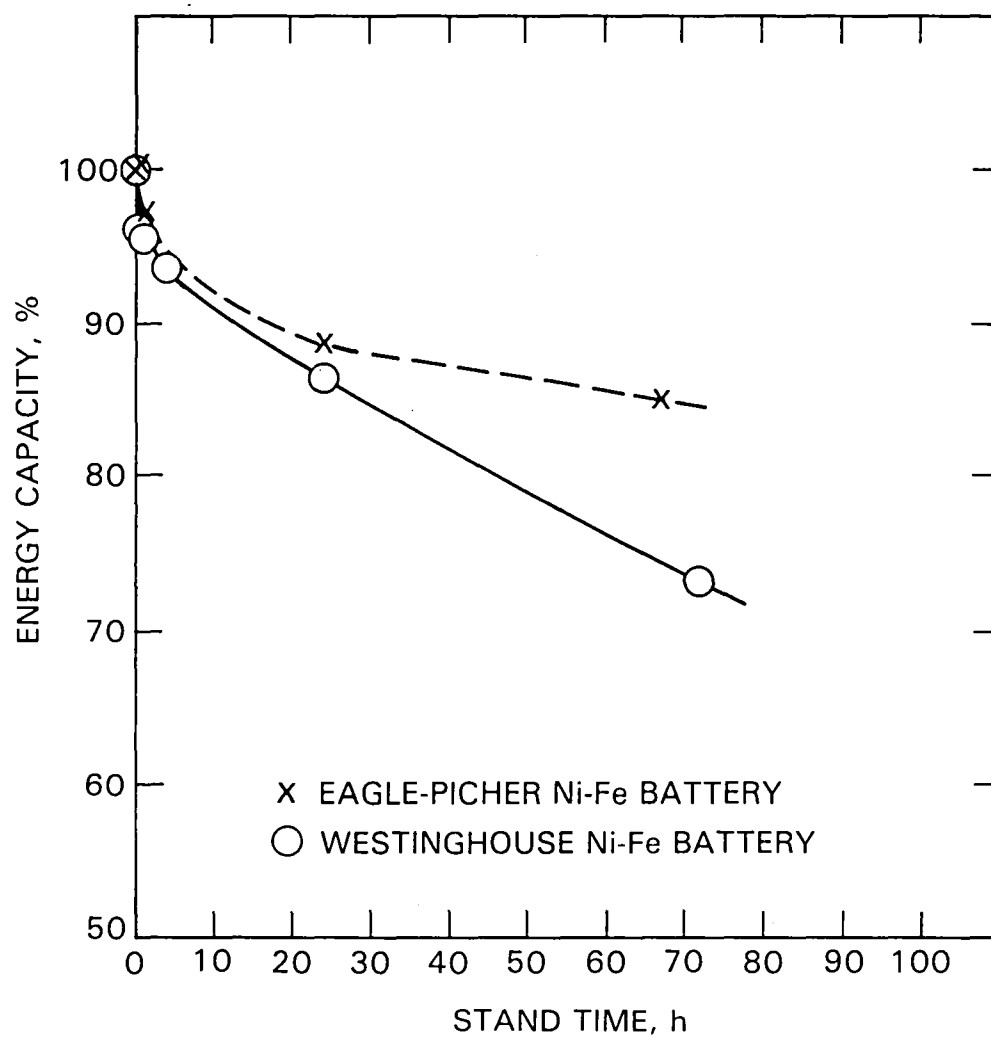


Figure 2-5. EPI and Westinghouse Batteries, Effect of an Open-Circuit Stand Between End of Charge and Start of Discharge

### 3. Internal Resistance

In a vehicle application, the vehicle/battery interface must be given consideration. The voltage response of the battery under a load is an important part of this interface: if a momentary load presented to the battery produces a large voltage drop, a high battery current will be required to satisfy the power demand.

High momentary loads occur during acceleration. For the following reasons, it is disadvantageous for the momentary loads presented to the battery, during normal vehicle operation, to produce a large voltage drop:

- ° The resulting high battery current can cause damage to components through resistive heating.
- ° The motor operates less efficiently under conditions of low voltage and high current.
- ° Battery capacity is depleted more quickly and less efficiently at higher current densities.

For a given power requirement, the greater the battery's effective internal resistance, the larger the voltage drop. The effective internal resistance of a battery varies with depth-of-discharge.

In Figure 2-6, the effective internal resistance of each of the three developmental batteries has been voltage-normalized and plotted versus depth-of-discharge. As shown in this figure, the Globe battery has less internal resistance than either of the two Ni-Fe batteries. Thus the Globe battery could be expected to exhibit the least voltage drop during acceleration.

### 4. Recharge Characteristics

The recharge efficiencies typically obtained from the three developmental batteries during vehicle testing are shown in Table 2-1. During vehicle testing, discharges were seldom terminated before 100% depth-of-discharge, whereas, during normal use, the batteries would seldom be discharged below about 80% depth-of-discharge. In addition, the charge procedures generally were tailored to provide maximum capacity rather than maximum recharge efficiency. Because vehicle-range testing is not representative of normal use patterns, the recharge efficiency data shown in Table 2-1 may not be representative of the efficiencies that would be obtained in a vehicle application.

Although the efficiency data in Table 2-1 was not obtained under conditions of normal use, these data provide information on the relative charge efficiencies of these battery technologies. As shown in Table 2-1, the Globe ISOA battery demonstrated the highest energy efficiency (71%). The energy efficiency of the Westinghouse battery (39%) is much lower than that of the other batteries.

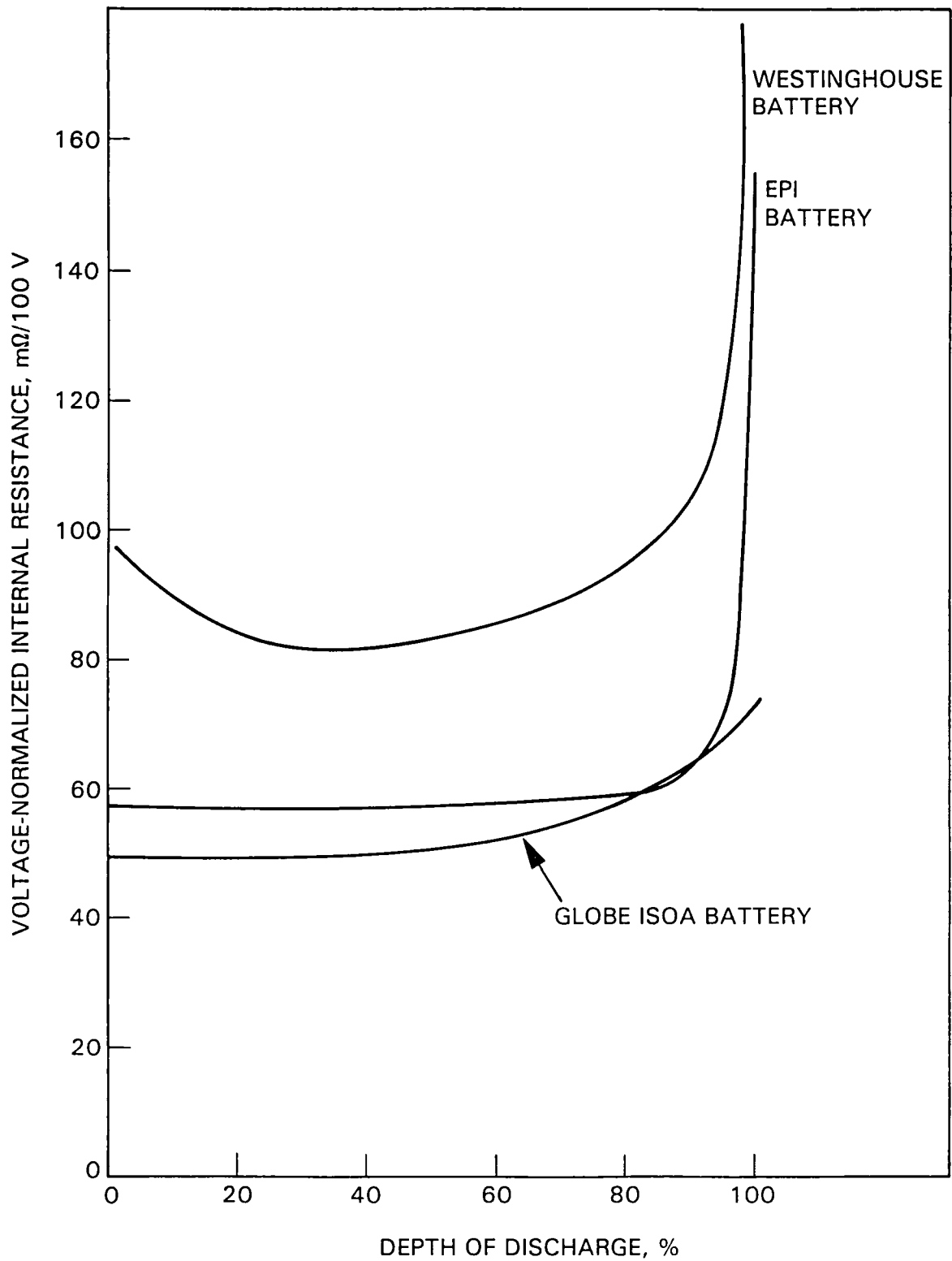


Figure 2-6. EPI, Globe, and Westinghouse Batteries: Voltage-Normalized Effective Internal Resistance versus Depth-of-Discharge

Table 2-1. Typical Energy, Coulombic, and Voltage Efficiencies

Battery	Recharge Energy Efficiency, %	Coulombic Recharge Efficiency, %	Recharge Voltage Efficiency, %
EPI	60	77	79
Globe	71	86	83
Westinghouse	39	56	70

The power requirements for charging these batteries are substantial: 9 kW for the 90-cell EPI battery, 5 kW for the Globe battery, and 10 kW for the Westinghouse battery. These requirements include only the dc power into the battery from the charger. The power required from a wall outlet would be higher because of charger inefficiencies. The high power required to charge these batteries may present difficulties for residential users.

#### 5. Gassing

These batteries release large amounts of hydrogen gas each charge/discharge cycle. The 90-cell EPI battery releases about 2300  $\ell$ . The Globe battery releases about 900  $\ell$ . The Westinghouse battery releases about 2600  $\ell$ . Hydrogen has a broad flammability range in air. Safety provisions should be carefully considered, especially for the Ni-Fe batteries.

#### D. CONCLUSIONS

The EPI Ni-Fe battery was found to have the highest specific energy. The capacity of this battery is relatively insensitive to discharge rate, so specific energy at high discharge rates is especially good. The Globe ISOA Pb-A battery also demonstrated good specific energy characteristics. The Globe battery was found to have a higher specific energy than Pb-A batteries previously tested at JPL. The specific energy of the Westinghouse Ni-Fe battery was found to be lower than that of the other two developmental batteries.

The EPI and the Westinghouse batteries lose capacity during open-circuit stand as a result of self-discharge. Although significant, the magnitude of the self-discharge effect is not large enough to preclude use of the Ni-Fe batteries for electric-vehicle propulsion.

Both the EPI and the Globe battery exhibited a moderate voltage drop during acceleration. In a well-designed vehicle system, voltage drop is not likely to be a problem with these batteries. However, the Westinghouse battery exhibited much more voltage drop during acceleration.

The Globe battery demonstrated the highest recharge efficiency during the vehicle tests. The recharge efficiency of the EPI battery was moderate, but the efficiency of the Westinghouse battery was quite poor.

During charge, the amount of hydrogen gas released by the Ni-Fe batteries is about twice as much as that released by the Globe battery. Therefore, safety during recharge is of greater concern with the two Ni-Fe batteries than with the Globe battery.

#### E. RECOMMENDATIONS

The following recommendations are based on the results of the vehicle tests and on the experience gained in handling the battery systems during testing:

- (1) The performance of the EPI Ni-Fe battery system is promising, especially in terms of energy capacity, and continued development is encouraged.
- (2) The Globe ISOA battery technology offers the potential for good battery performance with a minimum of maintenance and safety requirements. Development of this technology should be continued.
- (3) If development work with the Westinghouse Ni-Fe battery is to be continued, the reasons for the low capacity, high internal resistance, and poor recharge efficiency of this battery should be determined. Any further development work on this battery technology should be concentrated on alleviating these problems.
- (4) More research should be done to determine the optimum recharge procedure for the EPI Ni-Fe battery.
- (5) The cooling requirements of the EPI battery during operation in high ambient temperature conditions should be investigated.
- (6) Further development work should be done to improve the Globe watering system.
- (7) Further testing should be done to quantify the effects of temperature on these batteries and to fully characterize self-discharge of the Ni-Fe batteries.
- (8) All three developmental batteries generate hydrogen gas, and adequate safety precautions should be a primary consideration in their use.



## SECTION III

### BATTERY DESCRIPTIONS

#### A. THE EPI NI-FE BATTERY

EPI is developing their Ni-Fe battery under a cooperative agreement with the Swedish National Development Company. The testing covered in this report was done with a developmental prototype version of the battery. This developmental battery consisted of a collection of cells packaged as 10-cell strings. There was no provision for handling gasses, and no single-point watering system; each cell was vented directly to the atmosphere, and each cell was watered separately. At JPL, nine 10-cell battery strings were installed in a plywood box (shown in Figure 3-1). This box had two 100-ft<sup>3</sup>/min, squirrel-cage fans mounted on opposite sides for cooling and hydrogen dilution. A 4-in. diameter hose was installed to collect the gas mixture and vent it outside. During charge and discharge, the box was kept covered. For tests of the 90-cell battery, all nine strings were connected in series; for tests of the 80-cell battery, one 10-cell string was bypassed.

Sintered plates are used for both electrodes. The design of the negative electrode is based on iron-electrode technology from the Swedish National Development Company. It consists of a sintered, iron-powder plate on an expanded, iron substrate. The positive electrode is an unusually thick (2.0 mm), sintered, nickel plaque which has been electrochemically impregnated with active material (Reference 3).

The cells are packaged individually, and have the following dimensions: 5.5-cm wide, 17.5-cm long, and 28.0-cm high. The cells are joined into strings as shown in Figure 3-2. There are air gaps between each cell for cooling (Reference 3). A single cell is shown in Figure 3-3. The vent plug and the watering point are visible on the top of the cell, and the intercell connector is visible on the side of the cell. Each 10-cell string is contained within a separate frame. The mass of a 10-cell string and frame is 74 kg.

#### B. THE GLOBE ISOA PB-A BATTERY

The Globe battery (shown in Figure 3-4) is a complete battery subsystem. It is comprised of eight 12-V modules (connected in series electrically), a vent/watering system, and an electrolyte stirring system. The vent/watering system vents gasses during charge and discharge, and also provides a single-point access for watering. The electrolyte stirring system lifts dense electrolyte from the bottom to the top of the cell to prevent electrolyte stratification during charge and discharge. The reasons for inclusion of the stirring system (Reference 4) are as follows:

- (1) Promote uniform utilization of active materials.

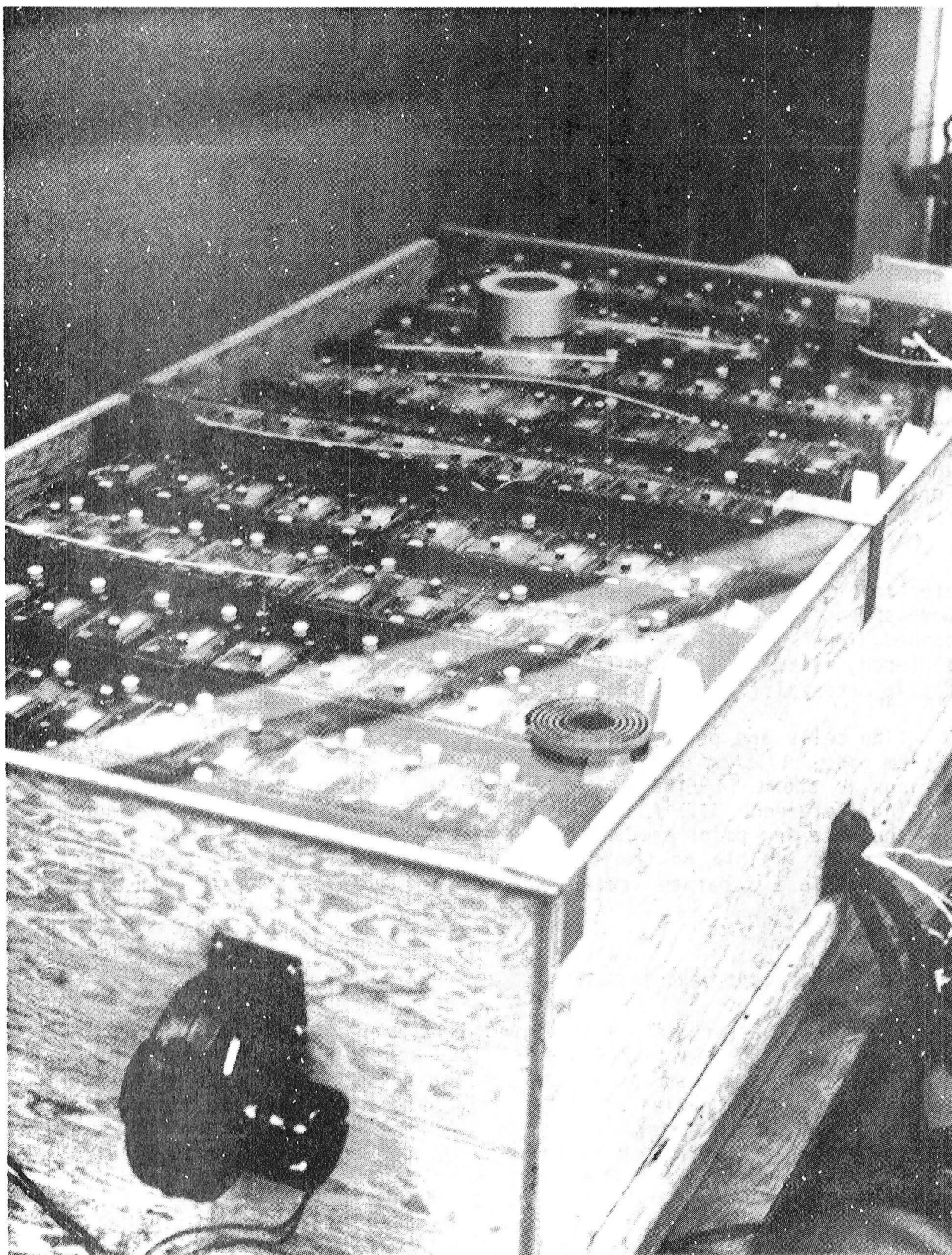


Figure 3-1. The EPI Ni-Fe Battery, JPL Installation in a Plywood Box



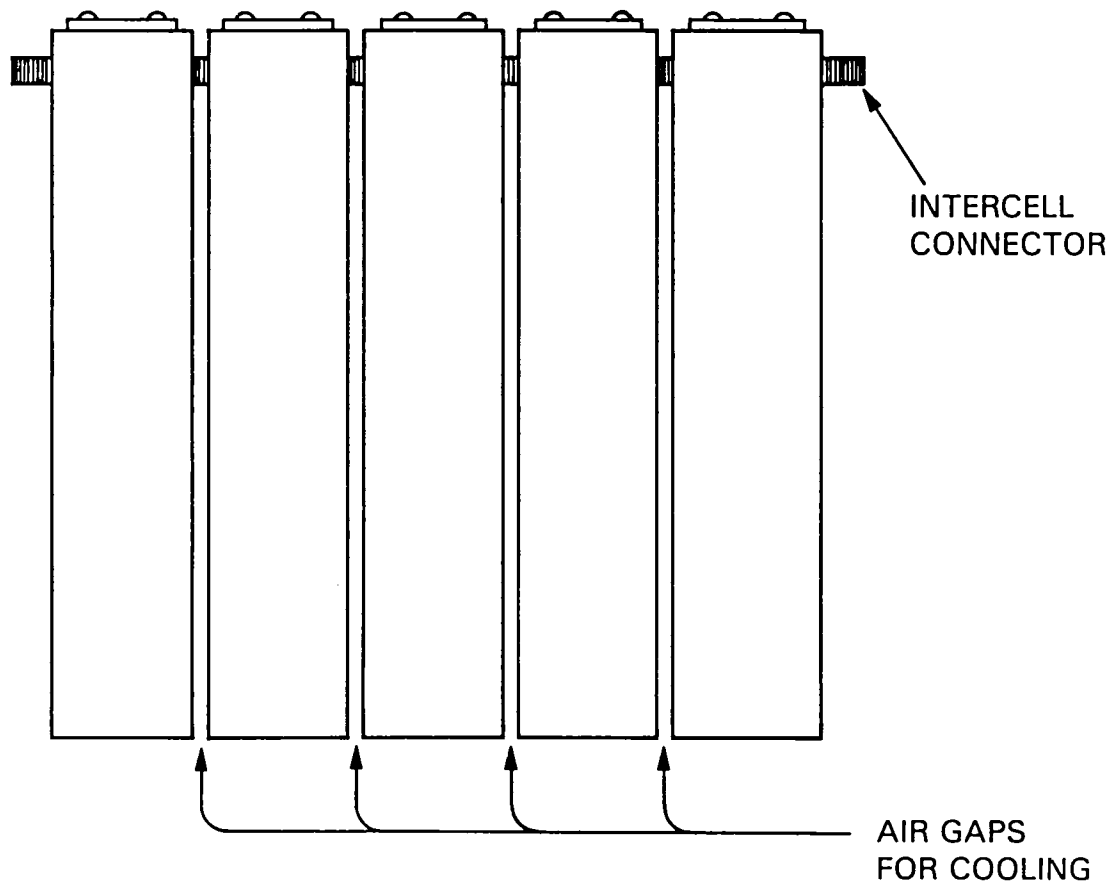


Figure 3-2. EPI Ni-Fe Battery, a String of Five Cells

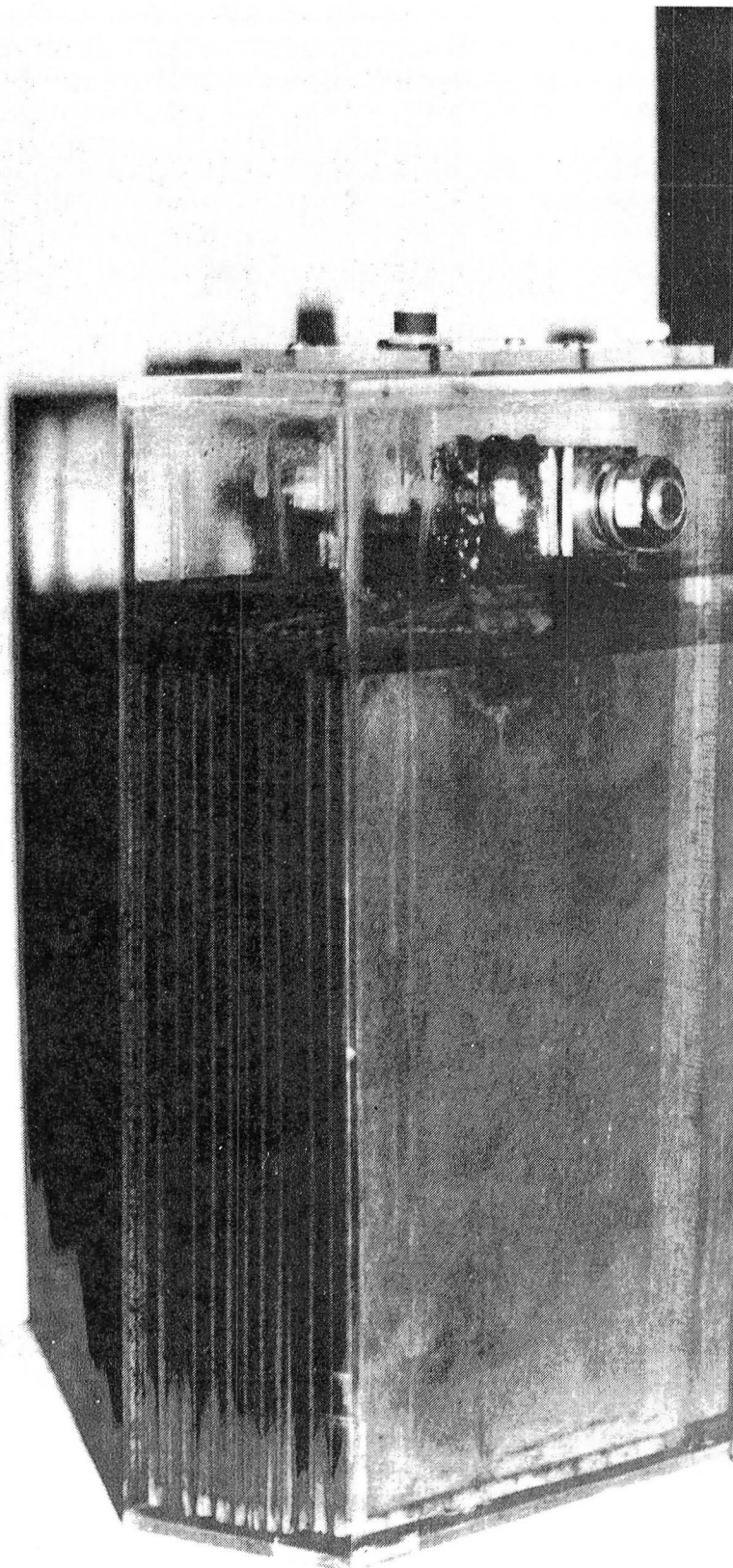


Figure 3-3. An EPI Ni-Fe Cell



Figure 3-4. The Globe ISOA Pb-A Battery

- (2) Minimize the amount of overcharge required.
- (3) Thermal maintenance.

Both the vent/watering and the electrolyte stirring systems are controlled by a single electronics package. The system operating mode is selected with a switch that can be set to one of three positions: CIRCULATE, WATER, or OFF.

A diagram of the vent/watering system is shown in Figure 3-5. A common manifold is used both for venting gasses during operation and for watering. Two valves determine the configuration of the system. Normally, the valves are positioned so the manifold vents the battery gasses through flame arrestors to the outside air. When the batteries are being watered, these two valves are positioned so that the inlet side of the manifold is open to the water reservoir and the outlet side is open to the vacuum pump. The manifold is directional, so water from the reservoir fills each cell consecutively and then the vacuum pump circulates excess water back to the reservoir. The vacuum pump runs only during watering.

The electrolyte stirring system operates whenever the main, three-position switch is set to the CIRCULATE position. It is used during both charge and discharge. The stirring action occurs as shown in Figure 3-6: air pulses periodically travel to individual cells, depressing a column of high-density electrolyte in one leg of a U-shaped tube in each cell. Most of the electrolyte in the U-shaped tube is thereby lifted up the second leg and emitted above the electrodes; then, because of its high density, it flows down between the plates. A small hole near the bottom of the U-shaped tube allows high-density electrolyte from the bottom of the cell to refill the tube in preparation for the next air pulse. In this manner, the stirring system prevents stratification without bubbling air through the electrolyte (Reference 4).

A diagram of the electrolyte stirring system is shown in Figure 3-7. When one of the valves opens, air pulses travel to all the cells in four of the eight modules. The sequence of operations for this system is shown in Figure 3-8. The air pump turns on every 20 s, and runs until the accumulator pressure reaches an upper limit. The pump is then turned off and one of the valves is opened, initiating an air pulse. The air pulse lasts until the accumulator pressure drops to a lower limit. The valve then closes, terminating the pulse. The valves are operated electronically, and they are activated alternately so that (as shown in Figure 3-7) one air pulse will pass through Valve 1 to one half of the cells, and the next air pulse will pass through Valve 2 to the other half of the cells. The air pump is powered by the battery and, when it is on, it draws 9.8 W.

Pasted plates are used for both the negative and the positive electrodes. The end electrodes in each module are thinner than the interior electrodes, and a patented grid design is used for all electrodes. The negative plates are bagged in envelope-type separators. Module cases are made of polypropylene and have the following dimensions: 33-cm wide, 38-cm long, and 30-cm

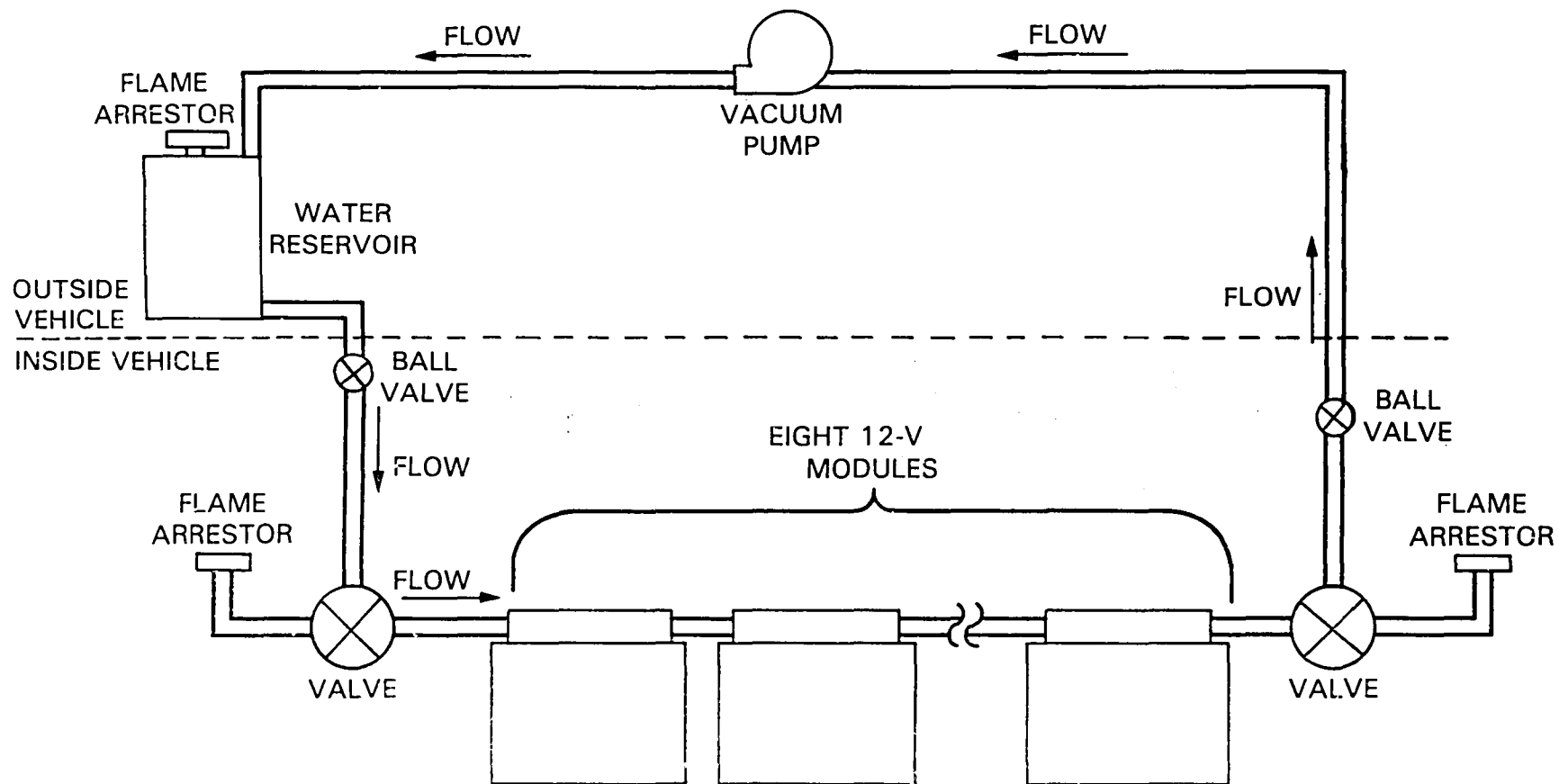


Figure 3-5. Globe ISOA Pb-A Battery, Vent/Watering System

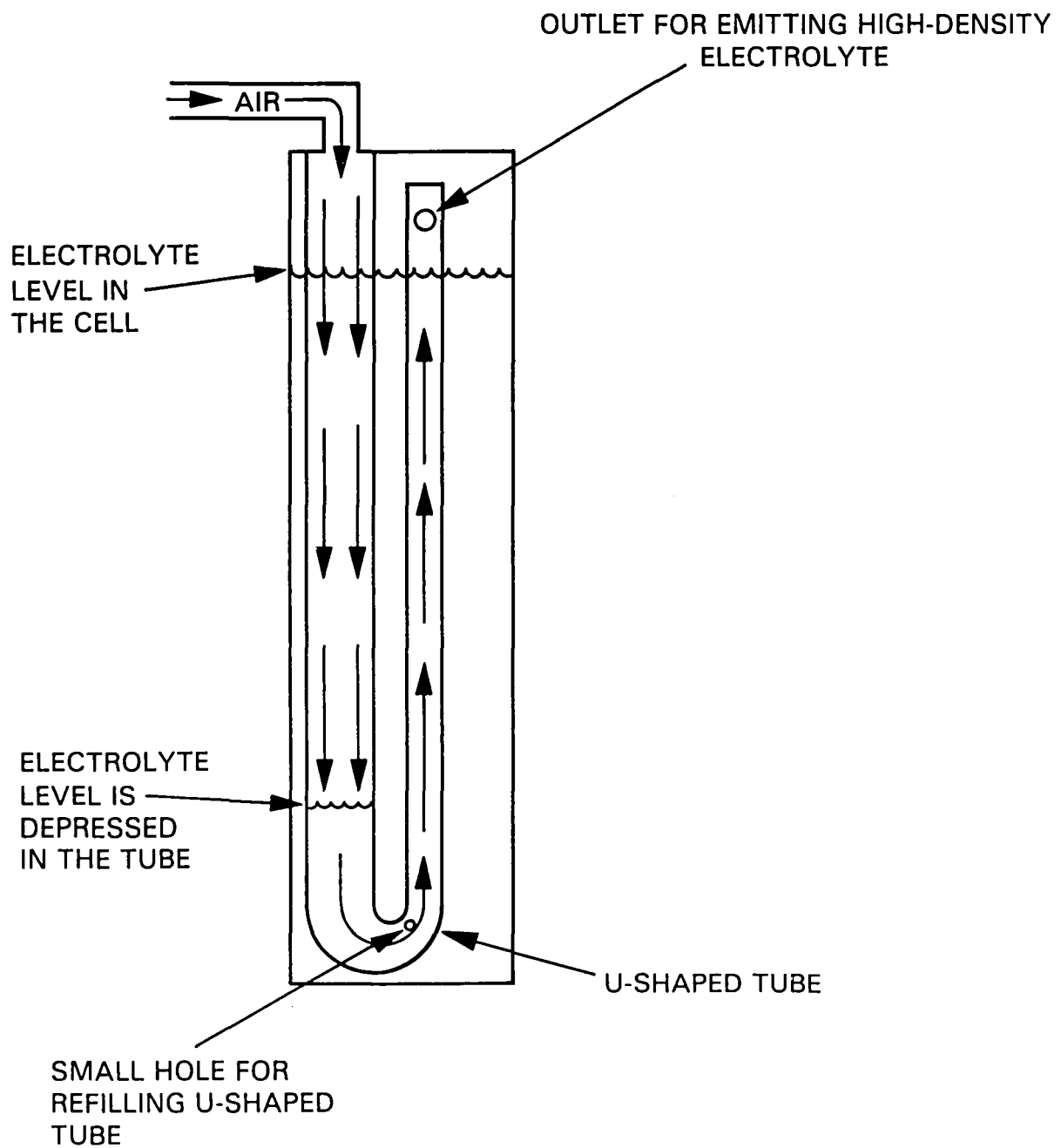


Figure 3-6. Globe ISOA Pb-A Battery, Electrolyte Stirring Action

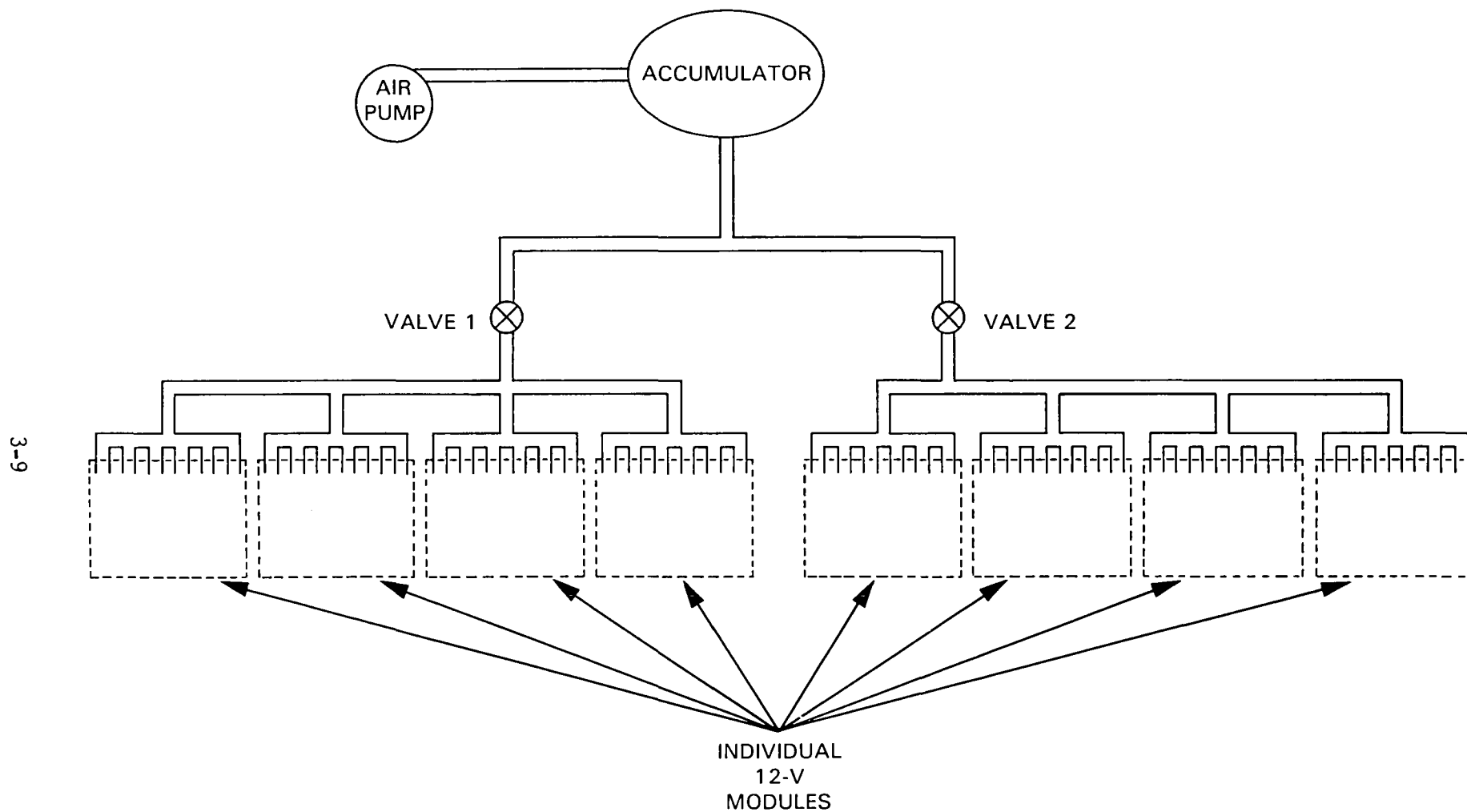


Figure 3-7. Globe ISOA Pb-A Battery, Block Diagram of the Electrolyte Stirring System

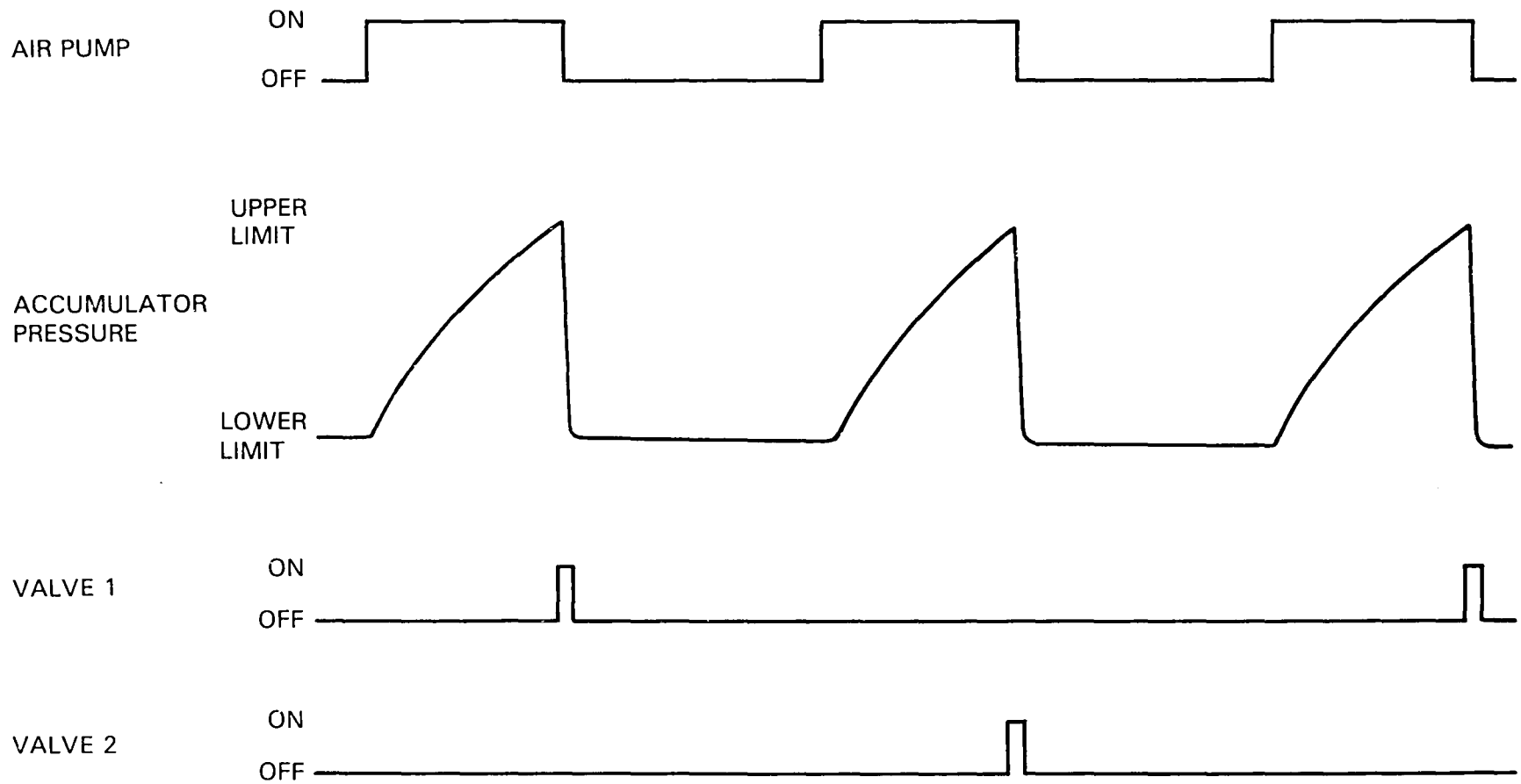


Figure 3-8. Globe ISOA Pb-A Battery Electrolyte Stirring System, Sequence of Operations



high. The mass of a single module is about 74 kg; the mass of the air pump is 4.6 kg; the total mass of the other accessories, excluding intermodule cables, is 1.5 kg.

### C. THE WESTINGHOUSE NI-FE BATTERY

The Westinghouse battery (shown in Figure 3-9) is also a complete subsystem. It is comprised of ninety cells (connected in series electrically) and an electrolyte management system (EMS). The EMS has the following functions:

- (1) Control battery temperature.
- (2) Separate gas from electrolyte and safely vent the gas.
- (3) Contain excess electrolyte during charge and supply electrolyte to cells during discharge.
- (4) Prevent over-pressure in the system.
- (5) Isolate electrolyte from outside air.
- (6) Provide a single access for water and electrolyte replenishment.

The EMS is plumbed to the cells through a manifold/header system.

The operation of the EMS is shown in Figure 3-10. Electrolyte and gas are circulated from the cells to a stainless-steel reservoir. Within the reservoir, heat exchanger coils are immersed in the electrolyte, and tap water is used to maintain electrolyte temperature during charge. The reservoir is only partially filled with liquid, so it also serves as a separation chamber for gas and electrolyte. The gas is removed from the reservoir and exhausted through a tank of water--the bubbler. The bubbler serves as a flame arrestor and also isolates the electrolyte from the outside air to prevent carbonation. In addition to the EMS supplied by Westinghouse, hardware for diluting and venting the gas was added by JPL: exhaust gas from the bubbler is captured by a vent tube and diluted with air by a blower before being exhausted outside (Reference 5).

Plumbing for the EMS is shown in Figure 3-11. The electrolyte pump is in the feed line from the reservoir to the cells. The pump can be run either continuously or at regular intervals, and the on/off timing can be varied. The pump draws 242 W when it is running. System pressure is monitored by a pressure guage in the feed line. Flow through the cells is controlled by a bypass line which allows electrolyte to be shunted back to the reservoir; a valve controls flow through the bypass line. Each cell has a separate fluid inlet and outlet for electrolyte circulation, and flow paths through each of the cells are in parallel.

A substrate of sintered, steel fiber is used for both positive and negative electrodes. Active material for the iron electrode is loaded in the

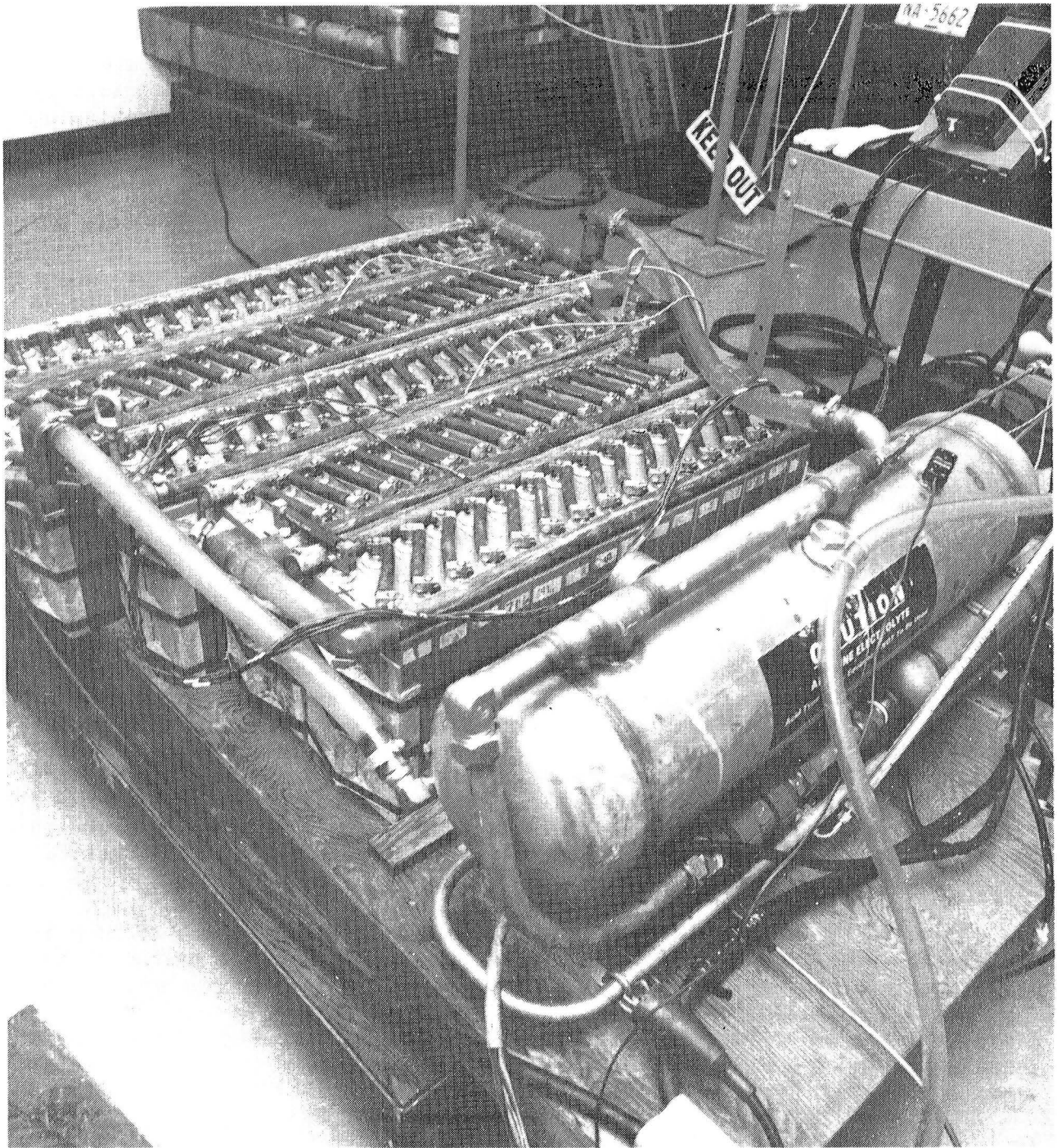


Figure 3-9. The Westinghouse Ni-Fe Battery

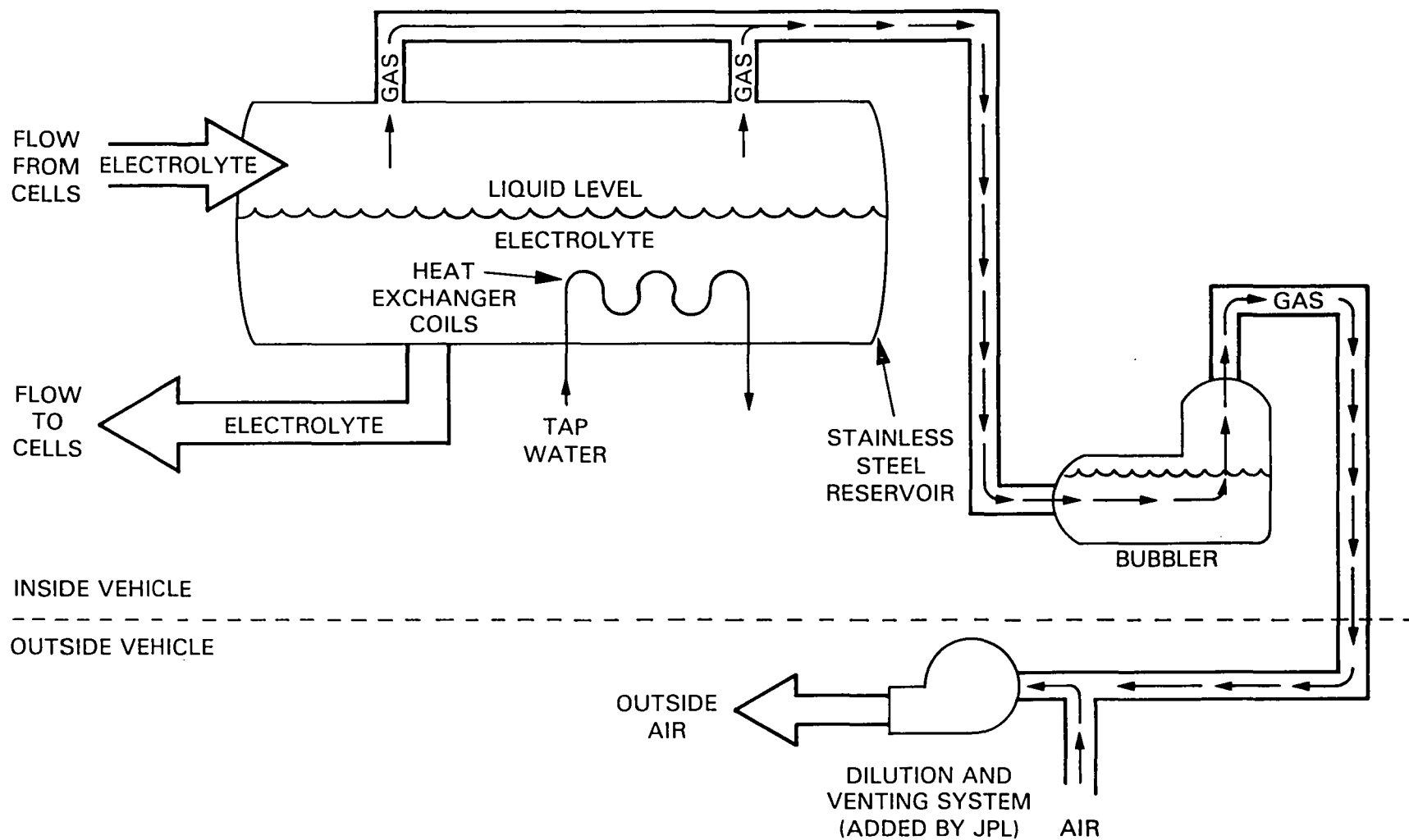


Figure 3-10. Westinghouse Ni-Fe Battery, Electrolyte Management System (EMS)

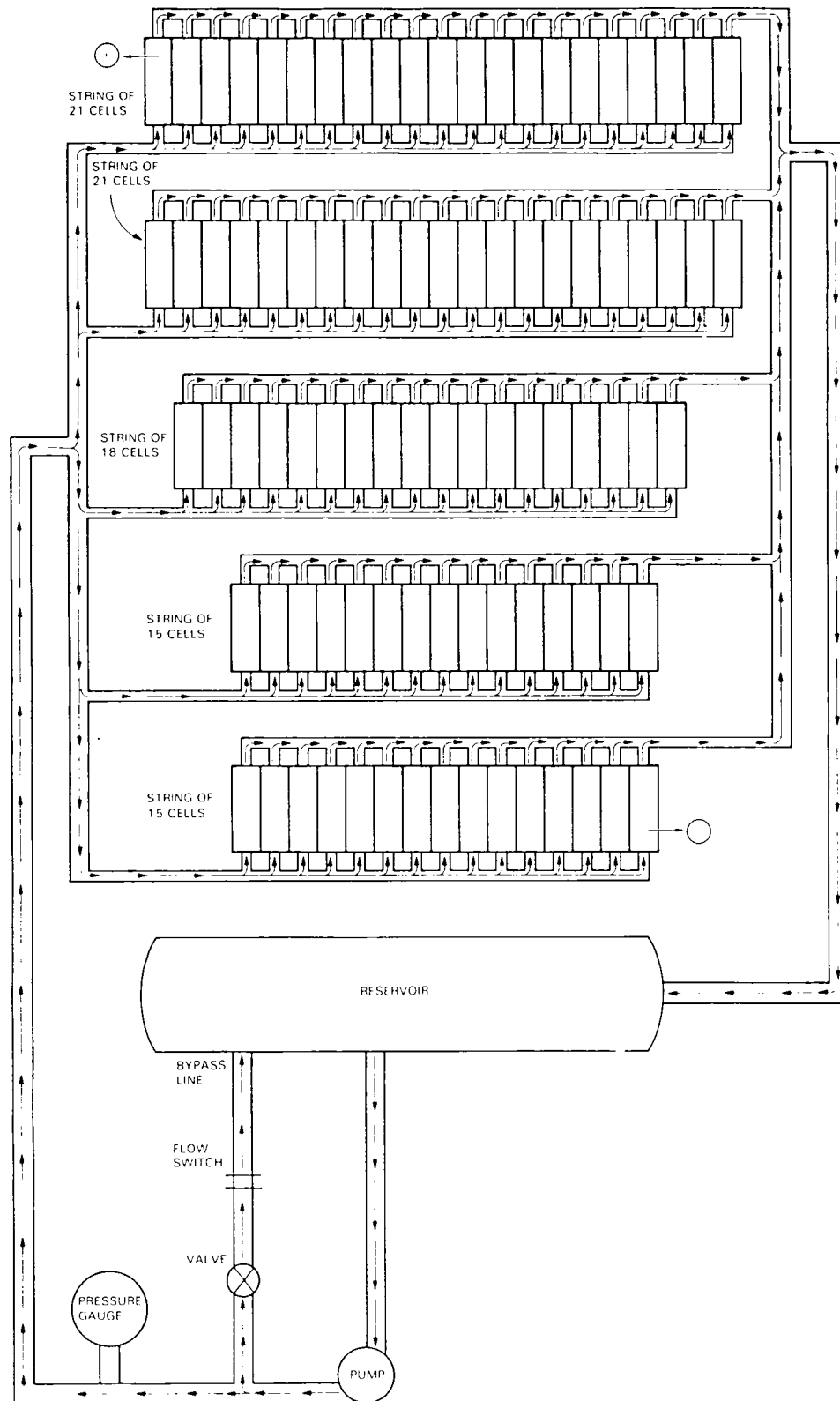


Figure 3-11. Westinghouse Ni-Fe Battery, Plumbing for the EMS

form of a thick, water-based paste which is pressed into the plaque and dried. The steel-fiber substrate for the positive, nickel electrode is nickel plated. Active material is loaded into the pores of the nickel-plated, steel-fiber substrate by electrochemical precipitation. The cell cases are made of injection molded polyphenylene oxide. Cell dimensions are 4.4-cm wide, 18-cm long, and 27-cm high. Each row of cells is bracketed by two end plates and bound with steel bands. The mass of a single cell is 5.42 kg; the mass of the intercell cables is 11 kg; the total mass of the two tanks is 44 kg; the mass of the electrolyte is 57 kg; the total mass of the hoses and manifolds is 7 kg.



## SECTION IV

### TEST METHODOLOGY

#### A. INTRODUCTION

Battery subsystem performance was evaluated primarily by driving electric vehicles on a chassis dynamometer. In some instances, the batteries were installed in the vehicle; in other instances, the batteries were connected to the vehicle by an umbilical cord. The specific test configurations for each battery are described later in this section. The test vehicles, general test procedures, and specific details of test procedures for each battery are also described in this section. The test results are presented in Section V. The vehicle tests were conducted in JPL's Automotive Research Facility. The data acquisition capabilities of this facility are described in Appendix C. During the tests, both analog and digital data were acquired and recorded on magnetic tape. The parameters that were normally recorded during each test are listed in Appendix D.

A Clayton twin-roll dynamometer, with 218-mm (8.6-in.) diameter rollers and direct-drive inertia weights in increments of 57 kg (125 lb), was used for the vehicle tests. Aerodynamic loads are simulated with a hydraulic power-absorption unit. The load due to the power-absorption unit is nominally proportional to the cube of roller speed. The magnitude of the proportionality constant can be varied, and it is set by adjusting the power-absorption unit to a specified load while operating the dynamometer at a specified, constant speed. Rolling losses are simulated by adjusting the tire pressure and the proportion of vehicle weight which is on the rollers. The dynamometer-calibration procedure is described in Reference 6.

In addition to the vehicle tests, a few constant-current-discharge tests were also done. These tests were done to condition the batteries and for various special purposes as explained by the test history for each battery. A resistive load was used for these tests.

#### B. ELECTRIC-VEHICLE TEST PROCEDURE

##### 1. Pretest Preparation

Before a vehicle-range test, the battery is charged fully. If the battery type is Ni-Fe, the discharge normally begins within 10 min after completion of recharge. If the battery type is Pb-A, the battery is normally left standing after completion of recharge until battery temperature is at  $23 \pm 3^\circ\text{C}$ . The time interval between the end of charge and the start of discharge for a Pb-A battery is usually about 10 to 20 h. These pretest criteria were established to provide repeatable data. It was felt that self-discharge would be the parameter having the most effect on the performance of Ni-Fe batteries, so the time interval during which self-discharge could occur was limited to 10 min to minimize variation in test results. Similarly, it was felt that temperature would be the parameter having the most effect on the

performance of Pb-A batteries, so the allowable variation in pretest battery temperature was restricted. However, some vehicle tests were done specifically to evaluate the effects of self-discharge and temperature; for the purposes of this evaluation, the pretest criteria of time between charge and discharge and of battery temperature were varied.

The test-vehicle temperature and the ambient temperature of the dynamometer room must be  $23 \pm 3^{\circ}\text{C}$  at the start of the test. Before each test, a dynamometer warm-up is done by spinning the rollers at 80 km/h (50 mi/h) for 5 min and then at 56 km/h (35 mi/h) for 5 min.

The test vehicle is then winched onto the dynamometer and configured for testing. For each vehicle, there is a predetermined vehicle/dynamometer configuration which consists of an aerodynamic load setting at 80 km/h (50 mi/h), an inertia weight setting, the tire pressure, and the proportion of vehicle weight which is on the rollers. The proportion of vehicle weight on the rollers is controlled by a pneumatic lift under the test vehicle. A fan, positioned in front of the car, is used to simulate the forced-convection cooling from airflow while driving. Figure 4-1 shows the test set-up. In this figure, the test vehicle is on the dynamometer rollers; the pneumatic lift and the fan are positioned as for a test.

Before beginning the test, the following data are recorded:

- (1) Battery recharge energy.
- (2) Amount of coulombic recharge.
- (3) Battery temperature.
- (4) Dynamometer aerodynamic load setting.
- (5) Tire pressure.
- (6) Pneumatic lift pressure.
- (7) Vehicle's odometer reading.

## 2. Conducting the Test

Three types of vehicle tests were done: constant-speed tests, J227a driving-schedule tests, and EPA Urban Driving Cycle tests. Constant-speed tests are started by accelerating the vehicle as quickly as possible to cruise speed. During the test, speed is maintained within 5% of the nominal cruise speed. The test is terminated by bringing the vehicle quickly to a stop. The J227a driving-schedules, shown in Figure 4-2, are JPL-standardized versions of the SAE J227a profiles. Schedule C and Schedule D tests were done. Tables 4-1 and 4-2 give a time-versus-velocity breakdown of these profiles. The EPA Urban Driving Cycle profile is shown in Figure 4-3.

While following the driving schedule, the driver is aided by a dual-pen strip-chart recorder. The time-versus-velocity profile, which is to be followed, is drawn in blue ink and, as the test progresses, actual vehicle velo-





Figure 4-1. Dynamometer Set-Up for a Vehicle Test

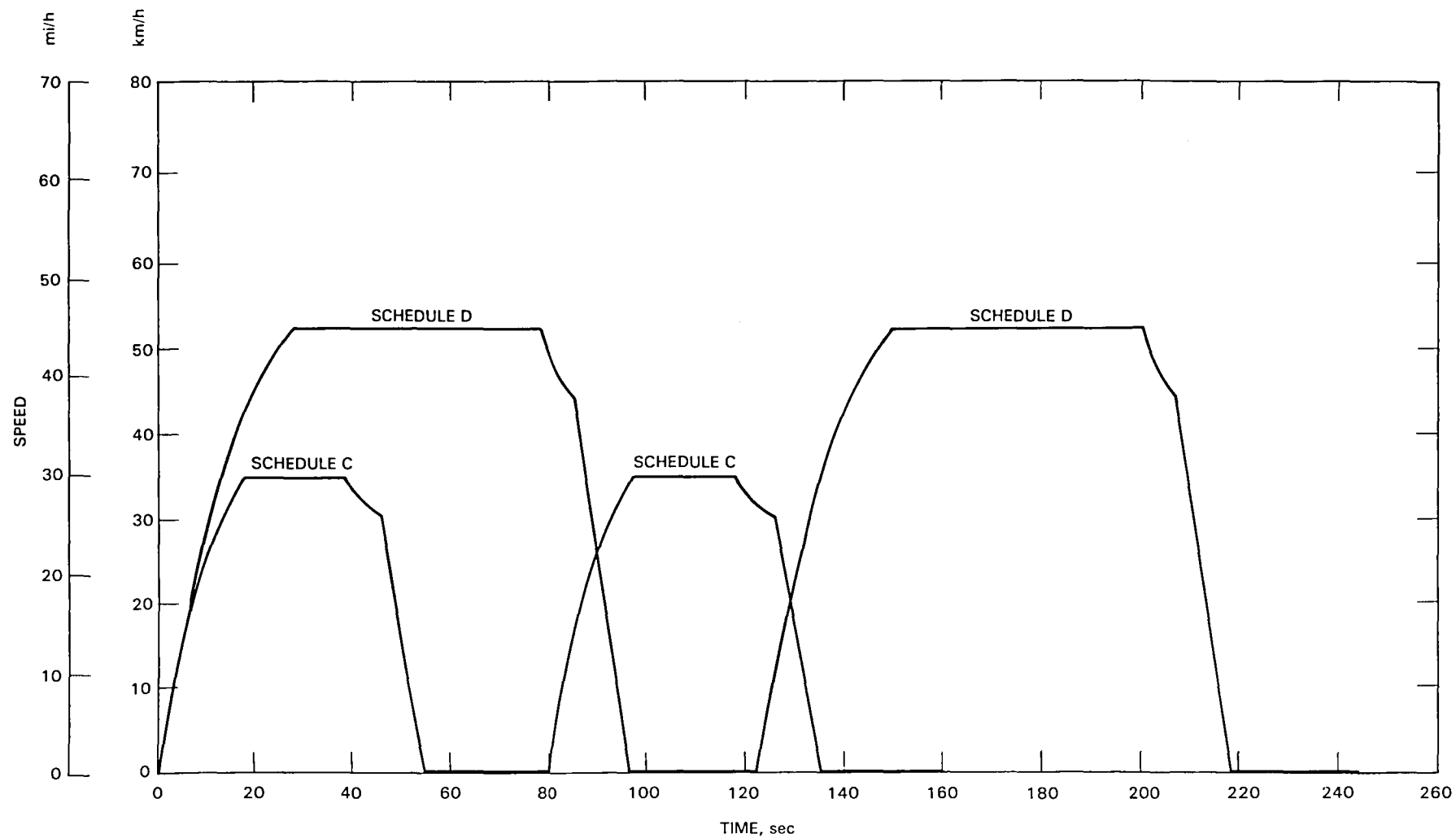


Figure 4-2. JPL Standardized J227a C and D Driving Schedules

Table 4-1. JPL-Standardized Version of J227a Schedule C

Time, s	Speed, mi/h	Time, s	Speed, mi/h	Time, s	Speed, mi/h
0	0	21	30.00	54	2.89
1	2.65	↑	↑	55 <sup>a</sup>	0
2	5.31	↓	↓	56	0
3	7.97			57	0
4	10.60	37	30.00	58	0
5	13.05	38 <sup>a</sup>	30.00	59	0
6	15.28	39	29.19	60	0
7	17.33	40	28.52	↑	↑
8	19.18	41	27.89	↓	↓
9	20.89	42	27.40		
10	22.43	43	26.95	78	0
11	23.83	44	26.59	79	0
12	25.08	45	26.27	80 <sup>a</sup>	Repeat cycle starting at 0 s
13	26.21	46 <sup>a</sup>	26.00		
14	27.20	47	23.11		
15	28.07	48	20.22		
16	28.82	49	17.33		
17	29.45	50	14.44		
18 <sup>a</sup>	30.00	51	11.56		
19	30.00	52	8.67		
20	30.00	53	5.78		

<sup>a</sup>Denotes transition points from one mode to another (i.e., acceleration to cruise).

Table 4-2. JPL Standardized Version of J227a Schedule D

Time, s	Speed, mi/h	Time, s	Speed, mi/h	Time, s	Speed, mi/h
0	0	25	43.31	91	19.00
1	2.56	26	43.93	92	15.83
2	5.12	27	44.49	93	12.67
3	7.68	28 <sup>a</sup>	45.00	94	9.50
4	10.24	29	45.00	95	6.33
5	12.80	30	45.00	96	3.17
6	15.36	↑	↑	97 <sup>a</sup>	0
7	17.79	↓	↓	98	0
8	20.08	↓	↓	99	0
9	22.24	75	45.00	100	0
10	24.28	76	45.00	↑	↑
11	26.20	77	45.00	↓	↓
12	28.01	78 <sup>a</sup>	45.00	↓	↓
13	29.72	79	43.53	120	0
14	31.34	80	42.33	121	0
15	32.85	81	41.33	122 <sup>a</sup>	Repeat cycle starting at 0 s
16	34.27	82	40.40		
17	35.60	83	39.53		
18	36.85	84	38.73		
19	38.01	85 <sup>a</sup>	38.00		
20	39.09	86	34.83		
21	40.08	87	31.67		
22	41.00	88	28.50		
23	41.85	89	25.33		
24	42.61	90	22.17		

<sup>a</sup>Denotes transition points from one mode to another (i.e., acceleration to cruise).

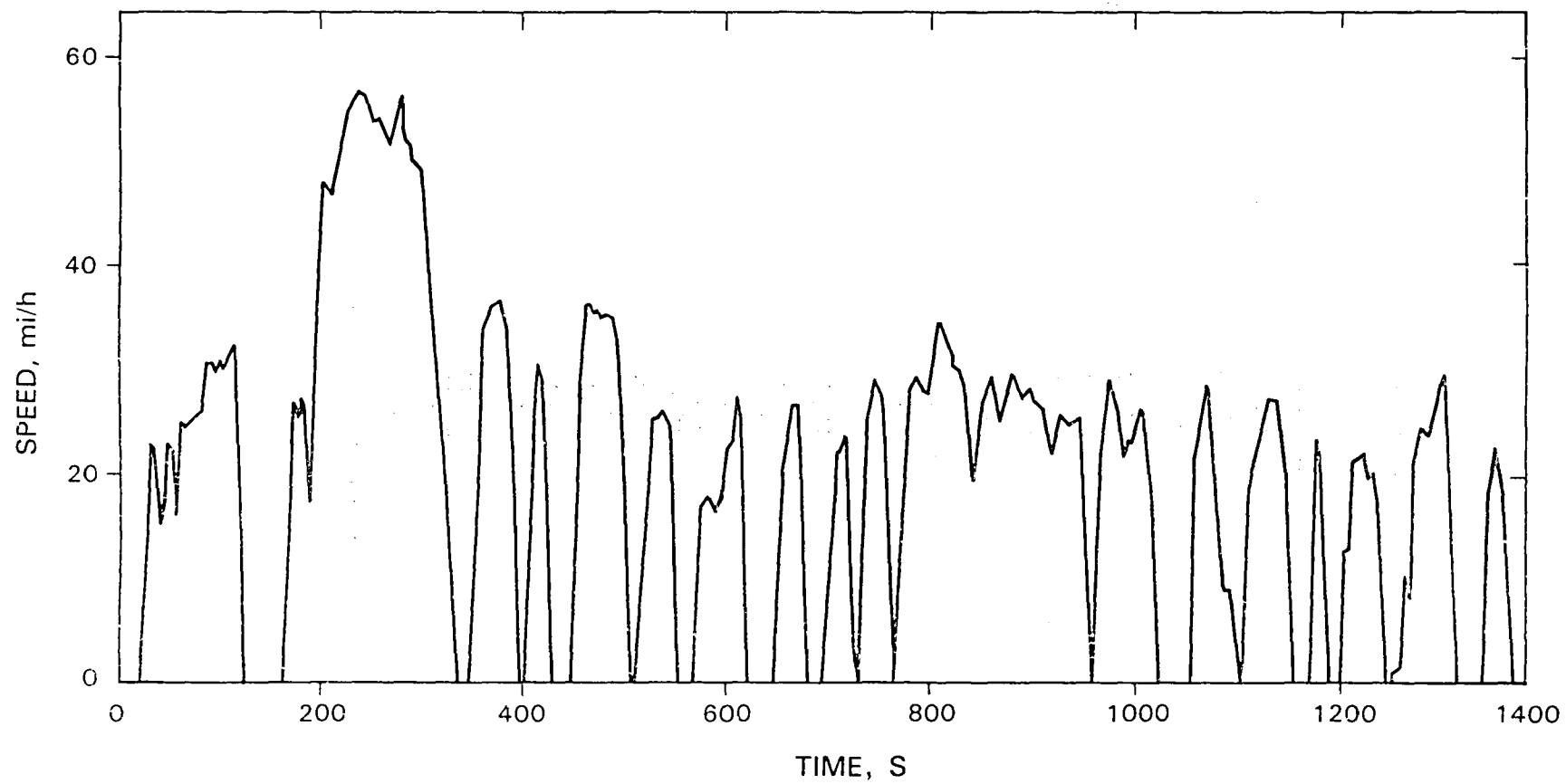


Figure 4-3. EPA Urban Driving Cycle Profile

city is plotted in red ink over the desired profile. Thus, a visual representation of driving accuracy is continuously available as feedback to the driver. The purpose of the strip-chart recorder is to enhance the repeatability of driving-schedule tests.

The instrumentation hardware used for data acquisition and power measurement during electric-vehicle testing is described in Appendix C. During a test, about 40 data channels are scanned, at a rate of about 500 channels/s, and written to magnetic tape for later processing. Test data are also printed by an alphanumeric printer for a "quick-look" capability during the test.

### 3. Test Termination Criteria

Normal termination of a vehicle-range test occurs when the battery is fully discharged. The termination criteria used for range tests are as follows:

- (1) Low voltage. If battery voltage drops below a minimum level, the test is terminated. There are two minimum-voltage criteria specified for each battery: one during cruise or idle and one during acceleration. Minimum voltages for each battery are given in Appendix A.
- (2) Speed. During constant-speed tests, if vehicle speed cannot be maintained within 95% of the specified value, the test is terminated.
- (3) Acceleration. During J227a driving-schedule tests, if the acceleration portion of the profile cannot be completed within 2 s of the time specified by the procedure, the test is terminated.

In actual testing, valid constant-speed range tests are almost invariably terminated by the low-voltage criterion, and valid driving-schedule range tests are usually terminated by the acceleration criterion.

In addition to these criteria, vehicle tests are terminated if any component (motor, battery, controller, etc.) overheats. Also, tests are sometimes terminated by vehicle or equipment failures. A test that is terminated by component overheating, or by vehicle or equipment failure is considered an invalid range test.

### 4. Post-Test Processing of Data

Test data are recorded on magnetic tape during the test and processed later with a main-frame computer. Test data from the magnetic-tape record are routinely plotted and tabulated on printouts. The magnetic-tape data can also be manipulated in a number of ways: calculations involving data from one or more channels can be done; the data can be integrated or differentiated with respect to time; and expanded plots of a portion of the test can be made. Additional operations are also possible.

## C. GASSING-RATE MEASUREMENTS

The gassing rate of the Globe and the Westinghouse batteries was measured during charge using the set-up shown in Figure 4-4. A large container (the outer tube) was filled with water. A pipe was inserted into the bottom of this outer tube and extended upwards to open above the surface of the water. The battery gasses were channelled into this pipe. A second container (the inner tube) was inverted and placed inside the outer tube to trap the gas from the pipe. As gas is evolved by the battery, the inner tube rises, sliding along two guide rails. Pressure inside the inner tube is controlled with a counterweight and monitored with a U-tube manometer. A scale on the side of the inner tube is used for taking volumetric measurements. Volume and fill time are measured at intervals during charge, and gassing rate is calculated from these measurements.

## D. TEST-BED ELECTRIC VEHICLES

### 1. ETV-1-1 and ETV-1-2

Two of the vehicles used for testing these batteries were DOE's Electric-Test-Vehicle-One (ETV-1) vehicles. These two cars are essentially identical, although there are some performance differences between them. They were designed and built by the General Electric Company and the Chrysler Corporation under contract to DOE. Construction was completed in 1979. The vehicles are two-door fastbacks, and the vehicle dimensions are 4.30-m (169.4-in.) long, 1.67-m (65.7-in.) wide, 1.31-m (51.6-in.) high, with a 2.49-m (98.0-in.) wheelbase (Reference 7). A picture of an ETV-1 vehicle is shown in Figure 4-5.

The ETV-1 vehicles have a curb weight of 1520 kg (3350 lb) and a gross-vehicle weight of 1792 kg (3950 lb). They are front-wheel-drive vehicles, with 1978 Dodge Omni front suspensions. A single-speed transaxle developed by the Chrysler Corporation is used.

The motor, made by General Electric, is a separately-excited, shunt-wound, dc motor. The continuous-power-output rating is 15 kW (Reference 7).

At low speeds, field strength is at a maximum, and motor speed is controlled by varying armature power with a chopper circuit. At higher speeds, full battery voltage is maintained across the armature, and motor speed is controlled by varying the field strength with another chopper circuit. A quick-disconnect system prevents battery current from going above 400 A (Reference 7). During deceleration, regenerative braking occurs at all motor speeds.

The accessories are powered by an auxiliary 12-V battery. A gasoline-fueled heater, with a 1-gal fuel tank, is provided to heat the passenger compartment and to defrost the windshield.

The two ETV-1 vehicles have been designated ETV-1-1 and ETV-1-2. Most of the ETV-1 testing was done with ETV-1-2. However, during tests of the

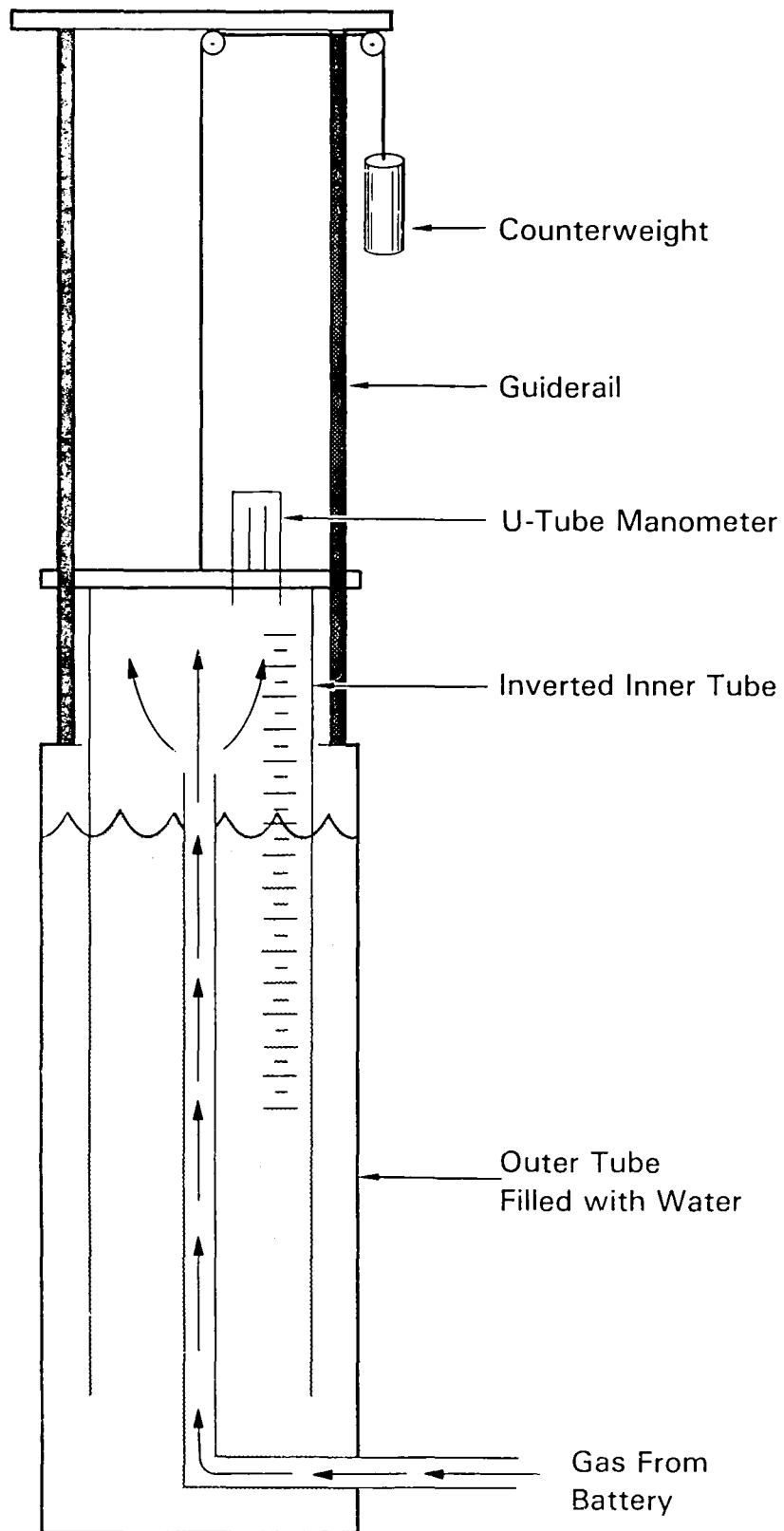


Figure 4-4. Set-Up Used for Gassing-Rate Measurements





Figure 4-5. An ETV-1 Vehicle

Globe ISOA battery, ETV-1-2 developed operational problems requiring extensive repair. Therefore, testing of the ISOA battery was completed with ETV-1-1. The only discernable performance difference between the two vehicles occurs during deceleration: ETV-1-2 returns more regenerative energy to the battery during deceleration than does ETV-1-1.

## 2. SCT-2

Another electric vehicle used for the battery testing was an R-1 Electric by South Coast Technology (SCT), designated SCT-2. SCT-2 is a 1979 Volkswagen Rabbit that has been modified by SCT to operate as an electric vehicle. Its dimensions are 3.94-m (155.3-in.) long, 1.61-m (63.4-in.) wide, 1.41-m (55.5-in.) high, with a 2.40-m (94.5-in) wheelbase. It is a two-door, hatch-back model. A picture of SCT-2 is shown in Figure 4-6.

As a result of the conversion, the curb weight was increased from 880 kg (1940 lb) to 1424 kg (3140 lb), and the gross-vehicle weight was increased from 1309 kg (2887 lb) to 1633 kg (3600 lb). Several modifications were made to handle the increased vehicle weight: the rear suspension was redesigned, and the front and rear shock absorbers were replaced by heavy-duty Koni shock absorbers. SCT-2 is a front-wheel-drive vehicle, and the Rabbit's four-speed, manual transaxle and clutch assembly have been retained.

The motor, made by Siemens Motor Company of Germany, is a separately-excited, shunt-wound, dc traction motor. The continuous-power-output rating is 17 kW, and the peak-power-output rating is 33 kW. Base (idle) speed is 1800 rev/min, and the recommended maximum speed is 6700 rev/min. Motor temperature is monitored by two internal thermistors. A two-speed blower cools the motor while the vehicle is being driven. The blower remains on low speed unless motor temperature rises to 75°C; then it switches to high speed.

Vehicle speed is controlled by varying the motor's field strength with a 20-Hz chopper. Under normal conditions, armature current varies in response to changes in the field strength, but the armature current is limited to a maximum of 300 A. In addition to the logic for speed control under normal conditions, logic has been added to limit armature current to a maximum of 150 A if the motor temperature reaches 115°C. During deceleration, regenerative braking occurs as long as motor speed is above 1800 rev/min.

The accessories are powered by an auxiliary 12-V battery. A gasoline-fueled heater, with a 1-gal fuel tank, is provided to heat the passenger compartment and to defrost the windshield.

## E. TESTING OF THE EPI BATTERY

### 1. General

At the time of these tests, development of the EPI battery was not sufficiently advanced to allow installation in a vehicle. The battery was, therefore, kept in a plywood box. Fans, for cooling the battery and for



Figure 4-6. SCT-2

purging gasses, were installed in the box. A 20-ft umbilical cord was used to carry battery power to the vehicle being tested. The umbilical cord consisted of two cables of 4/0 annealed copper wire (resistance =  $4.9 \times 10^{-5} \Omega/\text{ft}$ ) and two 350-A connectors (resistance =  $50 \mu\Omega/\text{contact}$ ). The EPI battery was tested in both an 80-cell and a 90-cell configuration with SCT-2, and it was tested in an 80-cell configuration with ETV-1-2.

The same charge procedure was used before all vehicle tests of the EPI battery: after a full discharge, the battery was recharged until 300 Ah had been returned; after a partial discharge, the battery was recharged until 120% of the previous discharge (on a coulombic basis) had been returned. Charging was always done at a constant, 60-A rate. This charge procedure was specified by the manufacturer.

Maintenance was performed every second charge/discharge cycle. The maintenance procedure consisted of watering the individual cells until the sight glass on each cell indicated that it was full, cleaning salt deposits off the tops of the cells, and checking the vents on each cell.

## 2. Range Tests

Fifteen vehicle range tests of the 80-cell EPI battery were attempted. Ten of these tests (Battery Cycles 106, 110, 118, 120, 121, 122, 123, 124, 125, and 126) were successful. Three of the attempted range tests (Battery Cycles 107, 108, and 109) were invalidated by operational problems with ETV-1-2. Two of the attempted range tests with SCT-2 were invalidated by motor overheating. These two range tests were an 88 km/h (55 mi/h) test and a Schedule D test. Because SCT-2 limits armature current when the motor overheats (see description of SCT-2 in this section), speed could not be maintained during the 88 km/h (55 mi/h) test, and the acceleration profile could not be met during the Schedule D test. The successful range tests with SCT-2 consisted of constant-speed tests at 56 km/h (35 mi/h), 72 km/h (45 mi/h), and 80 km/h (50 mi/h), and of Schedule C driving tests. The successful range tests with ETV-1-2 consisted of constant-speed tests at 56 km/h (35 mi/h), 72 km/h (45 mi/h), and 88 km/h (55 mi/h) and of Schedule C and Schedule D driving tests.

Five vehicle-range tests (Battery Cycles 135, 136, 137, 138, and 140) of SCT-2 with the the 90-cell EPI battery were attempted; all of these range tests were successful. These range tests consisted of constant-speed tests at 56 km/h (35 mi/h), 72 km/h (45 mi/h), and 88 km/h (55 mi/h), and of Schedule C and Schedule D driving tests.

The voltage-termination criteria used for all range tests were 1.0 V/cell during cruise or idle, 0.5 V/cell during acceleration.

## 3. Self-Discharge Tests

A limited amount of testing (Battery Cycles 116, 117, 119, and 128) was done with the 80-cell battery to determine the effects of self-discharge and temperature on the capacity of the EPI battery. The purpose of these tests was not to provide data for a detailed analysis, but rather to assess the importance of these effects.

The procedure for these tests was similar to the procedure used for the range tests. As for the range tests, a full recharge was done first, but the battery was left standing for a longer time between the end of charge and the start of discharge. Two tests (Battery Cycles 116 and 119) were done with a 24-h stand period between charge and discharge. During the stand period for Battery Cycle 119, a 120-V float charge was maintained across the battery to prevent self-discharge, but during the stand period for the other test, no such self-discharge compensation was used. Similarly, two tests (Battery Cycles 117 and 128) were done with a 67-h stand period between charge and discharge. Again, this was done both ways: once with the 120-V float charge and once with no self-discharge compensation.

In addition to these tests, the 80-cell battery was inadvertently left to stand for 0.5 h between the end of charge and the start of discharge during Battery Cycle 115.

#### 4. Test History

The EPI battery was received at JPL on October 17, 1980. Prior to testing at JPL, it had been tested by EPI and had been through about one hundred charge/discharge cycles.<sup>1</sup> The charge/discharge cycles accumulated on this battery during testing at JPL have been numbered starting at Battery Cycle 101. During testing by EPI, this battery was installed in an electric vehicle and driven on city streets in July and August. No cooling was provided during driving, and, as the ambient temperature was 30 to 40°C during these two months of testing, battery temperature frequently rose above 65°C. Testing by EPI has indicated that a subsequent loss of capacity can occur when battery temperature is allowed to rise this high during discharge.<sup>2</sup>

The following charge/discharge cycles were done after the battery arrived at JPL:

---

Battery Cycles (90-cell battery)	Description
-------------------------------------	-------------

---

101-103	First use after arriving at JPL. Conditioning cycles. Discharge at 75 A.
---------	--

---

---

<sup>1</sup>The exact number of cycles is not known.

<sup>2</sup>EPI has found that addition of LiOH to the electrolyte will restore capacity, but this was not done with the battery tested at JPL (information obtained by telephone from Ray Cooper of EPI on 8/16/82).



On October 24, 1980, the battery was configured to a pack of 80 cells to be used for vehicle testing. The following charge/discharge cycles were done with the 80-cell battery:

---

Battery Cycles (80-cell battery)	Description
104 and 105	Verification tests. Discharge at 75 A.
106	First vehicle test. 72 km/h (45 mi/h) range test with ETV-1-2.
107-109	Invalid range/diagnostic tests with ETV-1-2. Operational problems with ETV-1-2 during these tests.
110-115	Various range tests with SCT-2.
116 and 117	Self-discharge tests with SCT-2.
118	72 km/h (45 mi/h) range test with SCT-2.
119	Self-discharge test with SCT-2.
120	80 km/h (50 mi/h) range test with SCT-2.
121-126	Various range tests with ETV-1-2.
127	Invalid range test. Operational problems with ETV-1-2 during this test.
128	Self-discharge test with SCT-2.
129	Schedule C range test with ETV-1-2.
130	Schedule C range test with SCT-2.

---

On December 15, 1980, two weak cells were replaced and a leaking cell was repaired. The battery was then reconfigured to a pack of 90 cells. The following charge/discharge cycles were done with the 90-cell battery:

---

Battery Cycles (90-cell battery)	Description
131-133	Conditioning cycles. Charge to 300 Ah. Discharge at 75 A.

---

---

Battery Cycles  
(90-cell battery, cont'd)

Description

---

134	Conditioning cycle. Charge to 450 Ah. Discharge at 58 A.
135-138	Various range tests with SCT-2.
139	Special 72 km/h (45 mi/h) test with SCT-2 to 50% depth-of-discharge.
140	Obtained magnetic-tape record of data during charge following partial discharge. Schedule D range test with SCT-2.
141	Charge to 300 Ah. Obtained magnetic-tape record of data during charge. Discharge at 75 A.

---

Additional information regarding each charge/discharge cycle is given in Appendices E and F.

#### F. TESTING OF THE GLOBE BATTERY

##### 1. General

Two Globe ISOA batteries were used for the vehicle tests. The first battery (designated ISOA-1) underwent twenty charge/discharge cycles in the vehicle-test program and then began to show a loss of capacity. The vehicle testing was therefore continued with a second battery (designated ISOA-2). The ISOA-1 battery was returned to Globe for analysis, and the capacity loss was found to be the result of inadequate electrolyte stirring.

During the vehicle testing, the ISOA battery was installed in an SCT R-1 Electric. Vehicle tests were conducted with ETV-1-1 and ETV-1-2. A 20-ft umbilical cord was used to carry battery power from the SCT vehicle to the test vehicle. The umbilical cord consisted of two cables of 4/0 annealed copper wire (resistance =  $4.9 \times 10^{-5} \Omega/\text{ft}$ ) and two 350-A connectors (resistance =  $50 \mu\Omega/\text{contact}$ ).

One of the test criteria for vehicle-range tests with Pb-A batteries is that battery temperature must be  $23 \pm 3^\circ\text{C}$  at the start of discharge. During testing of the ISOA-1 battery, this was accomplished by using a 300-ft<sup>3</sup>/min fan to cool the battery during charge. The fan was not used with the ISOA-2

battery. Instead, this battery was allowed to stand until battery temperature was  $23 \pm 3^\circ\text{C}$ .

A taper-charge procedure was used with the Globe battery: the battery was charged at 48 A until voltage reached a maximum level; voltage was then maintained for 9 h. The maximum voltage level is temperature compensated: it is reduced at high temperatures and increased at low temperatures. At  $27^\circ\text{C}$ , the maximum voltage level is 2.67 V/cell, and the temperature compensation used with this battery is  $-0.007 \text{ V}/^\circ\text{C}/\text{cell}$ .

Shortly after the start of testing with the ISOA-2 battery, this battery was inadvertently charged without temperature compensation. As a result, the battery went into thermal runaway during charge,<sup>3</sup> and received an excessive overcharge. Damage to the battery as a result of this incident affected performance during driving-schedule tests, but did not affect performance during constant-speed driving.

Watering of the Globe ISOA battery is required after every 3,000 Ah of charge. Several attempts to use the battery's watering system resulted in the battery being overfilled. Every time this happened, electrolyte was forced out of the battery through the watering and electrolyte stirring systems during the subsequent recharge. However, when the watering system was used immediately after recharge (while the electrolyte level was raised by gas bubbles on the plates), it worked correctly, and the battery was not overfilled.

## 2. Range Tests

Eight vehicle-range tests (Battery Cycles 58, 59, 60, 61, 62, 63, 64, and 65) of ETV-1-2 with the ISOA-1 battery were attempted; all of these range tests were successful. These range tests consisted of constant-speed tests at 56 km/h (35 mi/h), 72 km/h (45 mi/h), and 88 km/h (55 mi/h) and of Schedule C and Schedule D driving tests.

Twenty-one vehicle-range tests of the ISOA-2 battery were attempted. ETV-1-2 was used for the first seven tests, and ETV-1-1 was used for the rest. Nine of these tests (Battery Cycles 36, 42, 43, 52, 59, 60, 61, 63, and 64) were valid range tests. All of the driving-schedule tests with the ISOA-2 battery are considered to be invalid range tests because damage from the excessive overcharge affected battery performance during these tests. The valid range tests with the ISOA-2 battery consisted of constant-speed tests at 56 km/h (35 mi/h), 72 km/h (45 mi/h), and 88 km/h (55 mi/h).

The voltage-termination criteria used for range tests with the ISOA-1 battery were 1.65 V/cell during cruise or idle, 1.3 V/cell during acceleration. The voltage-termination criterion during cruise was raised to 1.75 V/cell

---

<sup>3</sup>A thermal runaway response can occur when a Pb-A battery is charged at a voltage which is too high. If the voltage is too high, temperature rise will reduce the internal resistance, and charge current will begin to increase. The increased charge current causes temperature to continue rising which further increases the charge current.



for tests with the ISOA-2 battery because it was felt that the lower termination voltage might be damaging to the battery.

### 3. Discharge-Rate Memory Tests

A series of five range tests was done with the ISOA-2 battery to determine to what extent battery capacity is affected by the rate of the previous discharge.<sup>4</sup> The purpose of these tests was to determine whether discharge-rate memory has a significant effect on the capacity of the Globe ISOA battery. These range tests were done with ETV-1-1 in the sequence shown in Table 4-3. Battery Cycle 62 (the third test in this series) was an invalid range test because the test was inadvertently terminated at 1.77 V/cell rather than at 1.75 V/cell.

Table 4-3. Globe ISOA Battery: Test Sequence to Observe Discharge-Rate Memory Effects

Test Sequence Number	ISOA-2 Battery Cycle	Test Type
1	60	56 km/h (35 mi/h)
2	61	56 km/h (35 mi/h)
3	62	88 km/h (55 mi/h)
4	63	88 km/h (55 mi/h)
5	64	56 km/h (35 mi/h)

### 4. Elevated Temperature Tests

A limited amount of testing was done with the ISOA-2 battery to observe the effects of temperature on battery performance. Two consecutive 72 km/h (45 mi/h) range tests (Battery Cycles 74 and 75) were done. The range test of Battery Cycle 74 was started with battery temperature at 28.7°C, and the range test of Battery Cycle 75 was started with battery temperature at 22.7°C. These two tests were done to observe the effect of temperature on capacity. In addition, a Schedule D test (Battery Cycle 66) was done at an elevated temperature to observe the effect of temperature on effective internal resistance.

---

<sup>4</sup>See Section VI for a discussion of discharge-rate memory.

## 5. Test History

The first Globe ISOA battery (ISOA-1) arrived at JPL in February 1981. Prior to testing at JPL, it had been tested by Globe and by the NBTL, and had been through 49 charge/discharge cycles. The charge/discharge cycles accumulated on this battery during testing at JPL have been numbered starting at Battery Cycle 50. After two conditioning cycles were completed, the ISOA-1 battery was installed in an SCT R-1 Electric.

The following charge/discharge cycles were done with the ISOA-1 battery:

---

Battery Cycles (ISOA-1)	Description
50-57	Conditioning and verification. Discharge at 83 A.
58-66	Various range tests with ETV-1-2.
67	Diagnostic test with ETV-1-2.
68 and 69	Conditioning cycles. Discharge at 83 A.

---

A capacity loss was observed after cycle 66, and the ISOA-1 battery was returned to Globe for analysis following Battery Cycle 69.

The second Globe battery (ISOA-2) arrived at JPL in August 1981. Prior to testing at JPL, it had been tested by Globe and by the NBTL, and had been through 32 charge/discharge cycles. The charge/discharge cycles accumulated on this battery during testing at JPL have been numbered starting at Battery Cycle 33.

After the discharge of Battery Cycle 36, the ISOA-2 battery was inadvertently charged with no temperature compensation. As a result, the battery received an excessive overcharge. During this charge, the following occurred:

- (1) The battery went into thermal runaway.
- (2) Electrolyte temperature rose to a maximum of 68°C.
- (3) A total charge of 402 Ah was delivered.
- (4) Approximately 1 gal of electrolyte was lost.
- (5) Electrolyte level fell below the plates in 8 cells.

After the excessive overcharge, electrolyte levels and specific gravities were adjusted in all of the cells. Five conditioning cycles were done, and vehicle testing was then resumed. The following charge/discharge cycles were done with the ISOA-2 battery:

Battery Cycle (ISOA-2)	Description
33-35	Conditioning and verification. Discharge at 83 A.
36	72 km/h (45 mi/h) range test with ETV-1-2. Thermal runaway during recharge resulted in excessive overcharge.
37-41	Conditioning cycles.
42 and 43	Various range tests with ETV-1-2.
44	Invalid Schedule D range test with ETV-1-2.
45 and 46	Conditioning cycles.
47-49	Invalid Schedule D range test with ETV-1-2.
51	Diagnostic test with ETV-1-1.
52	72 km/h (45 mi/h) range test with ETV-1-1.
53-58	Conditioning cycles.
59-61	Various range tests with ETV-1-1.
62	Invalid 88 km/h (55 mi/h) range test with ETV-1-1.
63-66	Various range tests with ETV-1-1.
67	Invalid 72 km/h (45 mi/h) range test with ETV-1-1.
68	Conditioning cycle.
69	Invalid 72 km/h (45 mi/h) range test with ETV-1-1.
70-73	Self-heating tests.
74 and 75	Various range tests with ETV-1-1.
76	Conditioning cycle. Measured gassing rate during charge.

Additional information regarding each charge/discharge cycle is given in Appendices G and H.

## G. TESTING OF THE WESTINGHOUSE BATTERY

### 1. General

In 1979, JPL contracted Westinghouse to build two Ni-Fe battery systems which could be installed in SCT R-1 Electrics such as SCT-2. The emphasis of this contract was on developing the system-level aspects of the battery. During tests of these two battery systems (designated W-220-1 and W-220-2) at JPL, reliability problems, especially cell failures during charging, precluded meaningful results being obtained from testing.

To improve the battery's reliability, charge-algorithm tests were done, and a JPL-standardized charge procedure was developed for use with the Westinghouse battery. A new battery was assembled from the best 90 cells of the W-220-1 and W-220-2 batteries. This new battery was designated W-220-3. Reliability improved, and the JPL-standardized charge procedure was used for all subsequent vehicle tests of the Westinghouse battery. During vehicle testing, the battery was installed in SCT-2.

The JPL-standardized charge procedure for use with the Westinghouse battery is as follows: The battery is charged at 70 A until it reaches 157 V; the voltage is then maintained, and current is allowed to taper; the charge is terminated at 300 Ah.

Maintenance was performed as needed. Lights on the charger indicate whether the electrolyte level in the reservoir or the water level in the bubbler are low. Water was added to the reservoir every second charge/discharge cycle. Water was added to the bubbler approximately every twenty cycles.

### 2. Range Tests

Fifteen vehicle-range tests of the W-220-3 battery were attempted. Thirteen of these tests were successful (Battery Cycles 10, 11, 12, 13, 14, 15, 19, 20, 21, 22, 23, 24, and 25). All vehicle-range tests of the W-220-3 battery were done with SCT-2. One of the attempted range tests (Battery Cycle 9) was invalidated by motor overheating. This range test was a Schedule D test. Because SCT-2 limits armature current when the motor overheats, the acceleration profile could not be met during this test. The successful range tests consisted of constant-speed tests at 56 km/h (35 mi/h), 72 km/h (45 mi/h), and 88 km/h (55 mi/h), and of Schedule C driving tests.

A few range tests of the W-220-1 and W-220-2 batteries were also done. However, the reliability problems experienced during testing and the small number of tests completed precludes a meaningful evaluation of those tests. Therefore, only the results of range tests with the W-220-3 battery are discussed in this report.

The voltage-termination criteria used for range tests were 1.0 V/cell during cruise or idle, 0.5 V/cell during acceleration.

### 3. Discharge-Rate Memory Tests

A series of four range tests was done with the W-220-3 battery to determine to what extent battery capacity is affected by the rate of the previous discharge.<sup>5</sup> The purpose of these tests was to determine whether discharge-rate memory has a significant effect on the capacity of the Westinghouse battery. These range tests were done with SCT-2 in the sequence shown in Table 4-4.

Table 4-4. Westinghouse Battery: Test Sequence to Observe Discharge-Rate Memory Effects

Test Sequence Number	W-220-3 Battery Cycle Number	Test Type
1	22	88 km/h (55 mi/h)
2	23	88 km/h (55 mi/h)
3	24	56 km/h (35 mi/h)
4	25	56 km/h (35 mi/h)

### 4. Self-Discharge Tests

A limited amount of testing (Battery Cycles 7, 26, 27, 28, and 29) was done to determine the effect of self-discharge on the capacity of the Westinghouse battery. The purpose of these tests was not to provide data for a detailed analysis, but rather to assess the importance of this effect.

The procedure for these tests was similar to the procedure used for the range tests. As for the range tests, a full recharge was done first, but the battery was left standing for a longer time between the end of charge and the start of discharge. The open-circuit stand time between the end of charge and the start of discharge for each of the self-discharge tests is shown in Table 4-5.

### 5. Test History

The first of the two Westinghouse batteries built under contract to JPL (designated W-220-1) arrived for testing in July 1980. The W-220-1 battery was installed in SCT-2 in August 1980. Following Battery Cycle 8, the battery was removed from SCT-2, and the interconnects were modified in an attempt to reduce ohmic resistance. Before Battery Cycle 17, the battery was dismantled and moved to another location. During reassembly, 42 of the

---

<sup>5</sup>See Section VI for a discussion of discharge-rate memory.

Table 4-5. Westinghouse Battery: Self-Discharge Tests

W-220-3 Battery Cycle Number	Open-Circuit Stand Time, h	Test Type
7	0.5	72 km/h (45 mi/h)
28	1.0	72 km/h (45 mi/h)
29	4.0	72 km/h (45 mi/h)
26	24	72 km/h (45 mi/h)
27	72	72 km/h (45 mi/h)

90 cells were inadvertently installed backwards and, thereby, electrically reversed. During the subsequent recharge, these 42 cells were driven negative for 4 h before the error was discovered and corrected. Subsequent tests showed no decrease in capacity, and it was concluded that these cells were not damaged by the reversal. This battery was always charged at a constant, 70-A rate. The following charge/discharge cycles were done with the W-220-1 battery:

---

Battery Cycles  
(W-220-1)

Description

---

1-4	Conditioning and verification. Discharge at 70 A.
5 and 6	Invalid range tests with SCT-2.
7	88 km/h (55 mi/h) range test with ETV-1-2. Done with 84 cells to reduce voltage.
8-11	Constant-current-discharge tests to measure battery internal resistance.
12-19	Constant-current-discharge tests.
20-22	Conditioning cycles.
23 and 24	Tests conducted by Westinghouse personnel. Testing to select best cells for use in W-220-3 battery.

---

Page 4-25 through 5-12 intentionally left blank.





Table 5-6. Globe ISOA Pb-A Battery: Averaged Results of All Range Tests with ETV-1-1 and ETV-1-2.

Test Type	Range, km (mi)	Specific Energy, Wh/kg	Recharge Energy Efficiency, %	Coulombic Recharge Efficiency, %
56 km/h (35 mi/h)	217.8 (135.3)	36.1	72.0	85.4
72 km/h (45 mi/h)	170.1 (105.7)	32.0	70.6	85.5
88 km/h (55 mi/h)	123.0 (76.4)	27.4	70.2	86.1
Schedule C	104.2 (64.8)	33.4	--	--
Schedule D	90.7 (56.4)	28.9	--	--

Table 5-7. Globe ISOA Pb-A Battery: Results of Memory Test Series

Test Sequence Number	Type of Discharge	Battery Discharge Energy, kWh
1	56 km/h (35 mi/h)	22.2
2	56 km/h (35 mi/h)	22.4
3	88 km/h (55 mi/h)	N.A. <sup>a</sup>
4	88 km/h (55 mi/h)	16.5
5	56 km/h (35 mi/h)	21.9

<sup>a</sup>This discharge was inadvertently terminated before 100% depth-of-discharge was reached.

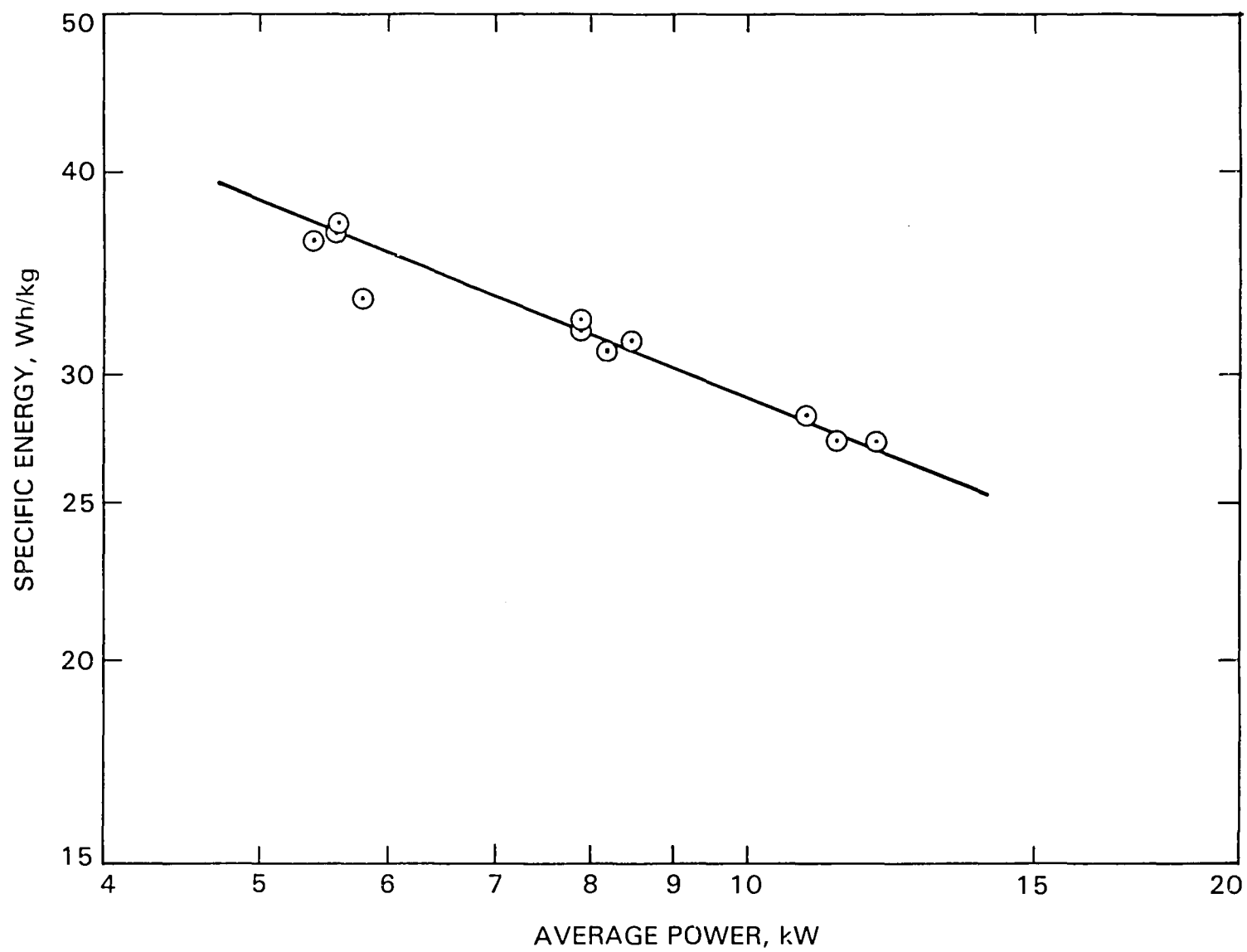


Figure 5-8. Globe ISOA Pb-A Battery: Specific Energy versus Power

It appears that there may be a small memory effect: battery capacity at 56 km/h (35 mi/h) increased slightly when this low-power test was repeated and decreased slightly following the high-power, 88 km/h (55 mi/h) tests. The usefulness of these results is somewhat limited because the battery was not completely discharged on the third test of the sequence. Also, immediately after these tests, battery capacity began to decline (probably as a result of the excessive overcharge given at the start of the vehicle testing). The small magnitude of the variation in capacity indicates, however, that any discharge-rate memory effect which may be present is of only minor importance.

### 3. Internal Resistance

The effective internal resistance of the Globe battery was calculated using voltage-drop data that were recorded during the acceleration portions of driving-schedule tests.<sup>4</sup> Figure 5-9 shows the effective internal resistance of this battery versus depth-of-discharge. The results of individual resistance calculations are shown as data points.

### 4. Effects of Excessive Overcharge

After the first vehicle test with the second Globe ISOA battery, the battery was inadvertently charged without temperature compensation--resulting in an excessive overcharge due to thermal runaway.<sup>5</sup> Recharge current and battery temperature during this charge are shown in Figure 5-10. The total charge was 402 Ah, and battery temperature rose to 68°C.

In discussions with JPL, Globe indicated that several deleterious effects were likely to occur as a result of the overcharge, including corrosion of the positive grid. They further indicated that a short cycle life and loss of capacity at high discharge rates, due to reduced grid conductivity, would probably occur as a result of damage sustained during the excessive overcharge. It appears that both these predictions were accurate: Schedule D tests were conducted after the overcharge, and internal resistance during these tests was found to be significantly higher than the internal resistance of the first battery. This higher internal resistance resulted in significantly less capacity for Schedule D range tests. The effect of the overcharge on internal resistance is shown in Figure 5-11. In addition, battery capacity began to decline after Cycle 66--indicating a short cycle life as a result of the overcharge.

### 5. Self-Heating

A test series, consisting of Urban Driving Cycles done on consecutive days, was conducted to observe the cumulative temperature rise due to

---

<sup>4</sup>A detailed description of the internal resistance calculations is given in Appendix B.

<sup>5</sup>A thermal runaway response can occur when a Pb-A battery is charged at a voltage which is too high. If the charge current does not taper, battery temperature increases rapidly. As temperature increases, the charge current must also increase to maintain the voltage level.

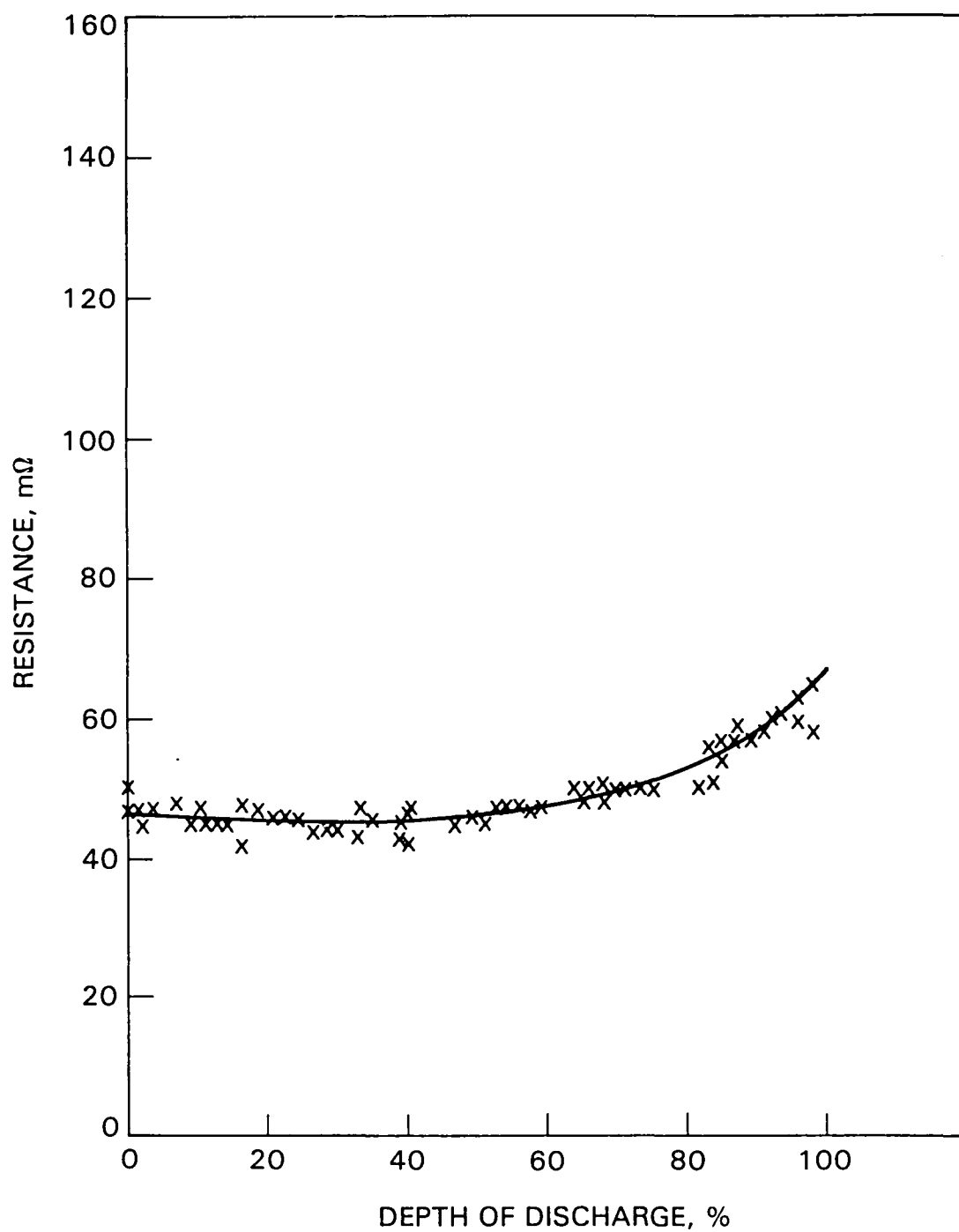


Figure 5-9. Globe ISOA Pb-A Battery: Effective Internal Resistance versus Depth-of-Discharge

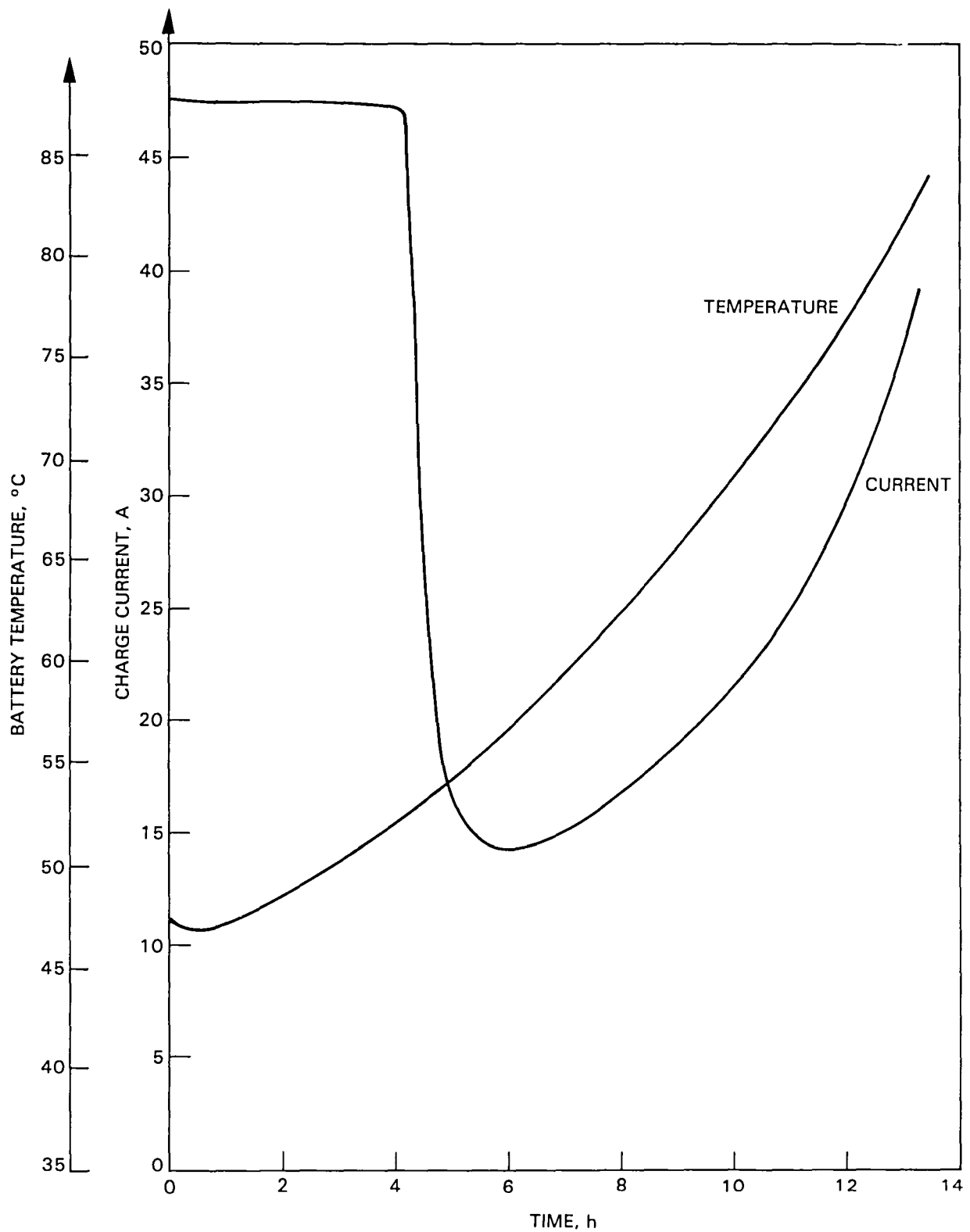


Figure 5-10. Globe ISOA Pb-A Battery: Thermal Runaway Response During Charge with No Temperature Compensation

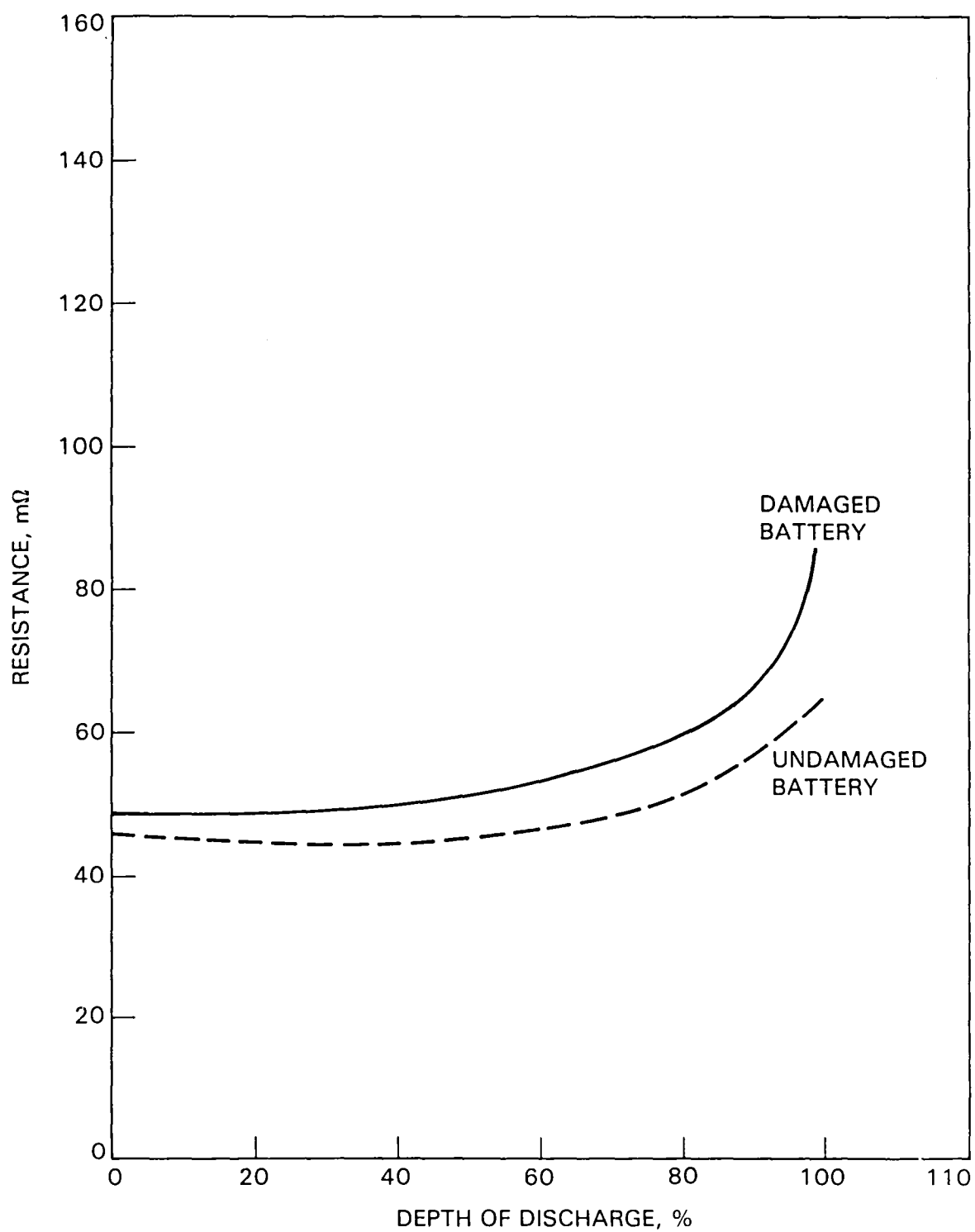


Figure 5-11. Globe ISOA Pb-A Battery: Increased Internal Resistance as a Result of Damage Caused by a Thermal Runaway Charge

self-heating during normal vehicle use.<sup>6</sup> Average battery temperature during this test series is shown in Figure 5-12. At the end of the test series, the spread in module temperatures was 5.7°C.

Table 5-8 shows the average temperature rise of the Globe battery during vehicle-range tests with ETV-1-1 and ETV-1-2. Average temperature rise at 50% and at 100% depth-of-discharge is shown in this table. The average temperature rise during recharge is also shown.

Table 5-8. Globe ISOA Pb-A Battery: Average Temperature Rise Due to Self-Heating During Vehicle Testing

Activity	Average Temperature Rise, <sup>a</sup> °C
56 km/h to battery depletion	3.7
72 km/h to battery depletion	5.4
88 km/h to battery depletion	6.2
56 km/h to 50% depth-of-discharge	2.4
72 km/h to 50% depth-of-discharge	3.2
88 km/h to 50% depth-of-discharge	3.7
Schedule C to battery depletion	6.8
Schedule D to battery depletion	9.2
Schedule C to 50% depth-of-discharge	2.9
Schedule D to 50% depth-of-discharge	3.8
Recharge after a full discharge	6.6
Recharge after a partial discharge	3.2
<sup>a</sup> Ambient temperature was maintained at 23 $\pm$ 3 °C.	

<sup>6</sup>See Section IV for a description of this test series.

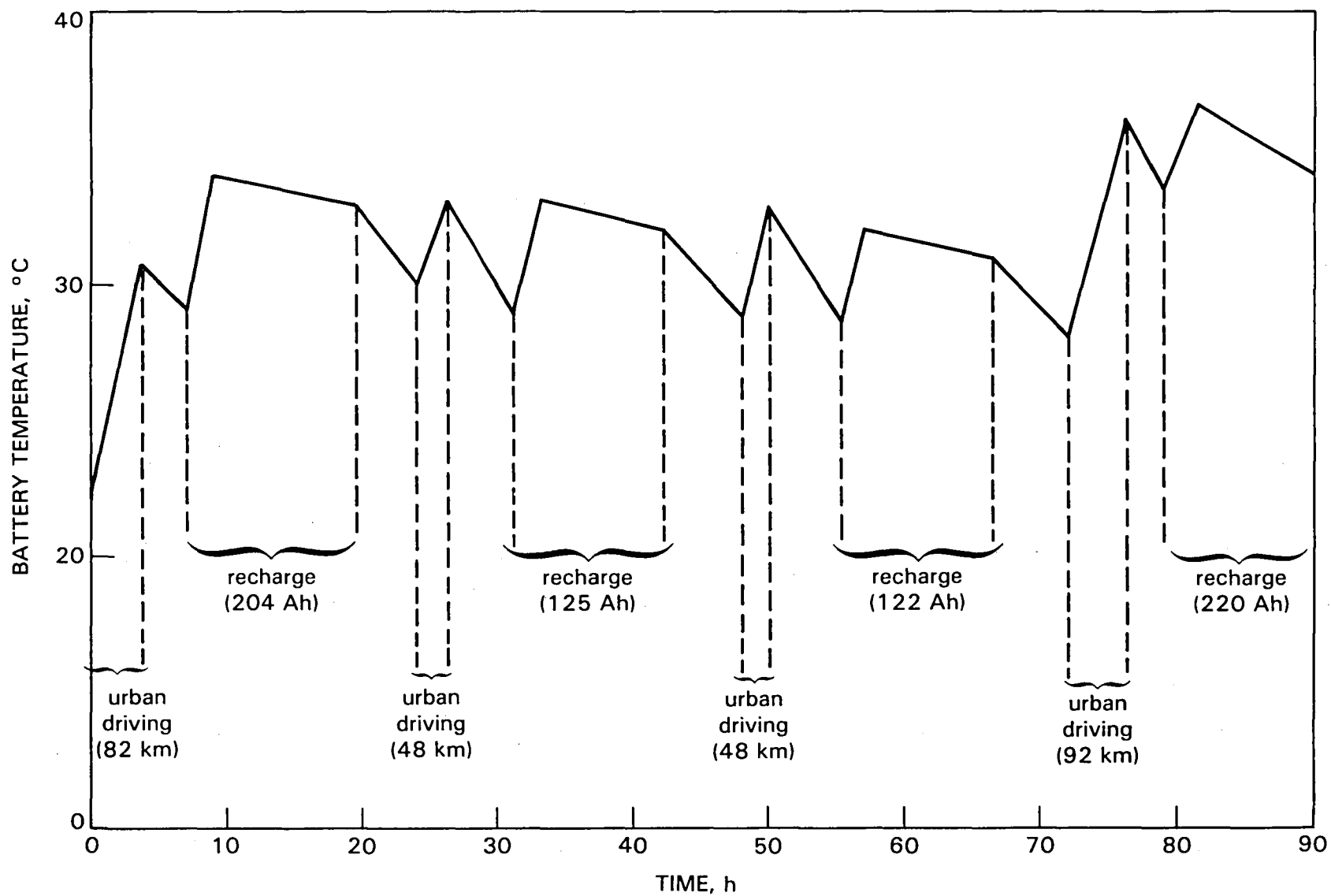


Figure 5-12. Globe ISOA Pb-A Battery: Self-Heating During Simulation of Normal Vehicle Use (Ambient temperature was maintained at  $23 \pm 3^{\circ}\text{C}.$ )



## 6. Temperature Effects

A limited amount of testing was done to observe the effect of temperature on the capacity and on the effective internal resistance of the Globe battery. These tests were conducted on the second battery after it had been damaged by the excessive overcharge. Therefore, the absolute magnitude of the results may not be representative of the performance of an undamaged battery. However, the relative results provide a basis for making some preliminary observations on the effect of temperature.

Energy capacity during a 72 km/h (45 mi/h) range test was found to increase with temperature by 1.1% per °C. Internal resistance was found to decrease with temperature by 0.8% per °C at 0% depth-of-discharge and by 0.7% per °C at 50% depth-of-discharge. Thus, temperature appears to be an important parameter affecting the performance of the Globe battery.

## 7. Recharge Characteristics

A two-part charge was used with the Globe battery. During the first part, a constant, 48-A charge current is maintained until battery voltage reaches a temperature-compensated, voltage-clamp level; voltage is then maintained at this level for the remainder of the charge. Battery voltage, current, power, and temperature during recharge are shown in Figures 5-13 through 5-16. As shown in Figure 5-13, battery voltage increases fairly steadily during about the first two hours of charge; voltage then increases very rapidly until the voltage-clamp level is reached. As shown in Figure 5-14, charge current tapers to about 3.5 A by the end of charge. As shown in Figure 5-16, battery temperature rises until the charge current falls below about 7 A. Temperature levels off at this point and remains fairly constant through the remainder of the charge. As shown in Table 5-6, the recharge efficiency of the Globe battery was about 71% on an energy basis and about 86% on a coulombic basis.

## 8. Gassing

Because of difficulties with the watering system (see the Globe battery test history, Section IV), the water consumption of the Globe battery could not be determined. Thus, the quantity of water dissociated into hydrogen and oxygen gasses each charge/discharge cycle could not be calculated. Based on the amount of coulombic overcharge,<sup>7</sup> however, the maximum amount of hydrogen gas that can be released each charge/discharge cycle is 900 ℓ (at standard conditions).

The gassing rate of the Globe battery during charge was measured, and these data are shown in Appendix B. Calculations based on these gassing-rate measurements (see Appendix B) indicate that only about 100 ℓ of hydrogen gas are released each charge/discharge cycle. As it seems unlikely that only 1/9 of the coulombic overcharge is used for electrolysis, the gassing rate data are probably too low. Possibly the measurements were taken during a non-representative charge. There may also have been some leaks in the system which allowed gas to escape into the atmosphere.

---

<sup>7</sup>Calculations are shown in Appendix B.

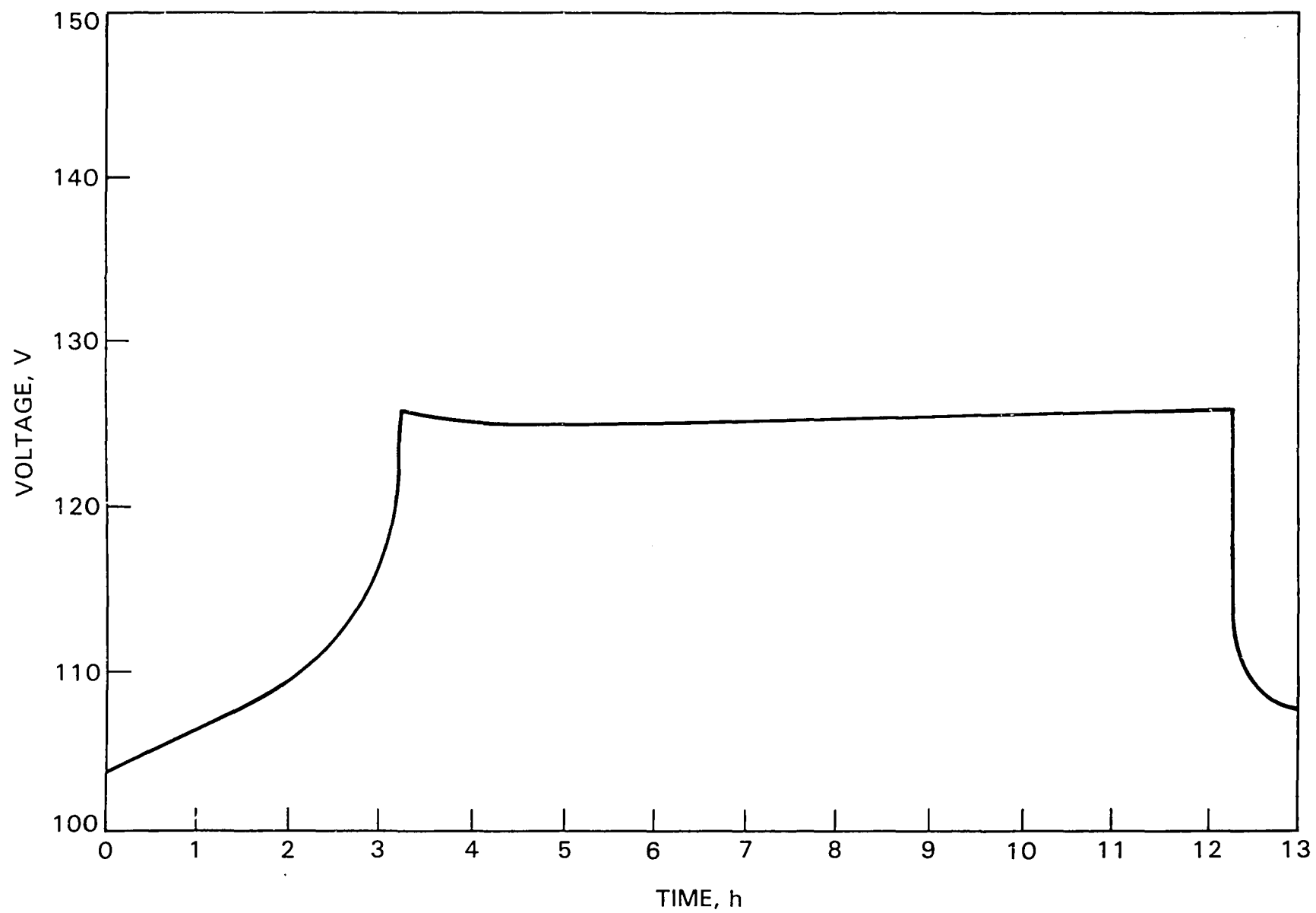


Figure 5-13. Globe ISOA Pb-A Battery: Voltage During Recharge

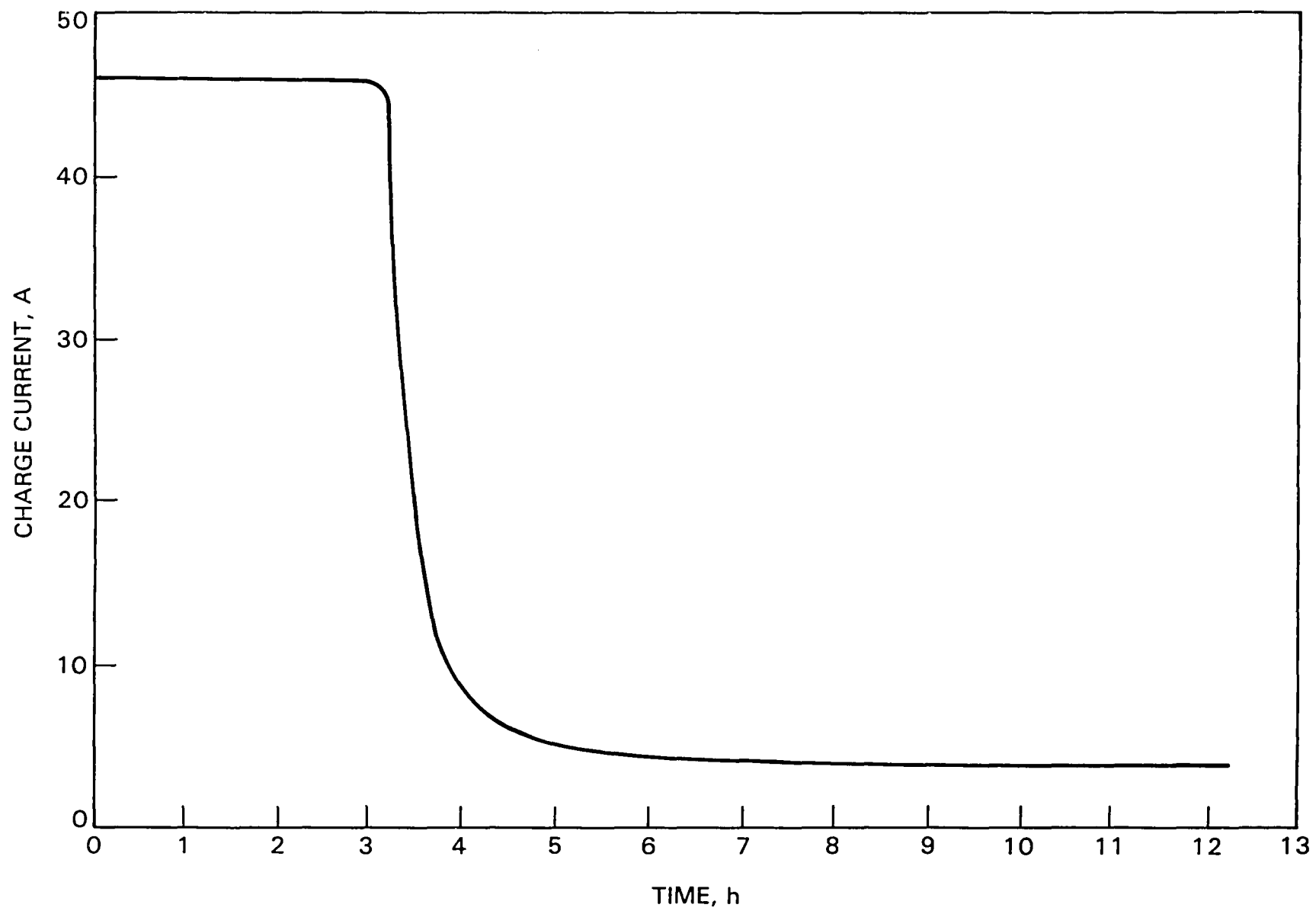


Figure 5-14. Globe ISOA Pb-A Battery: Recharge Current

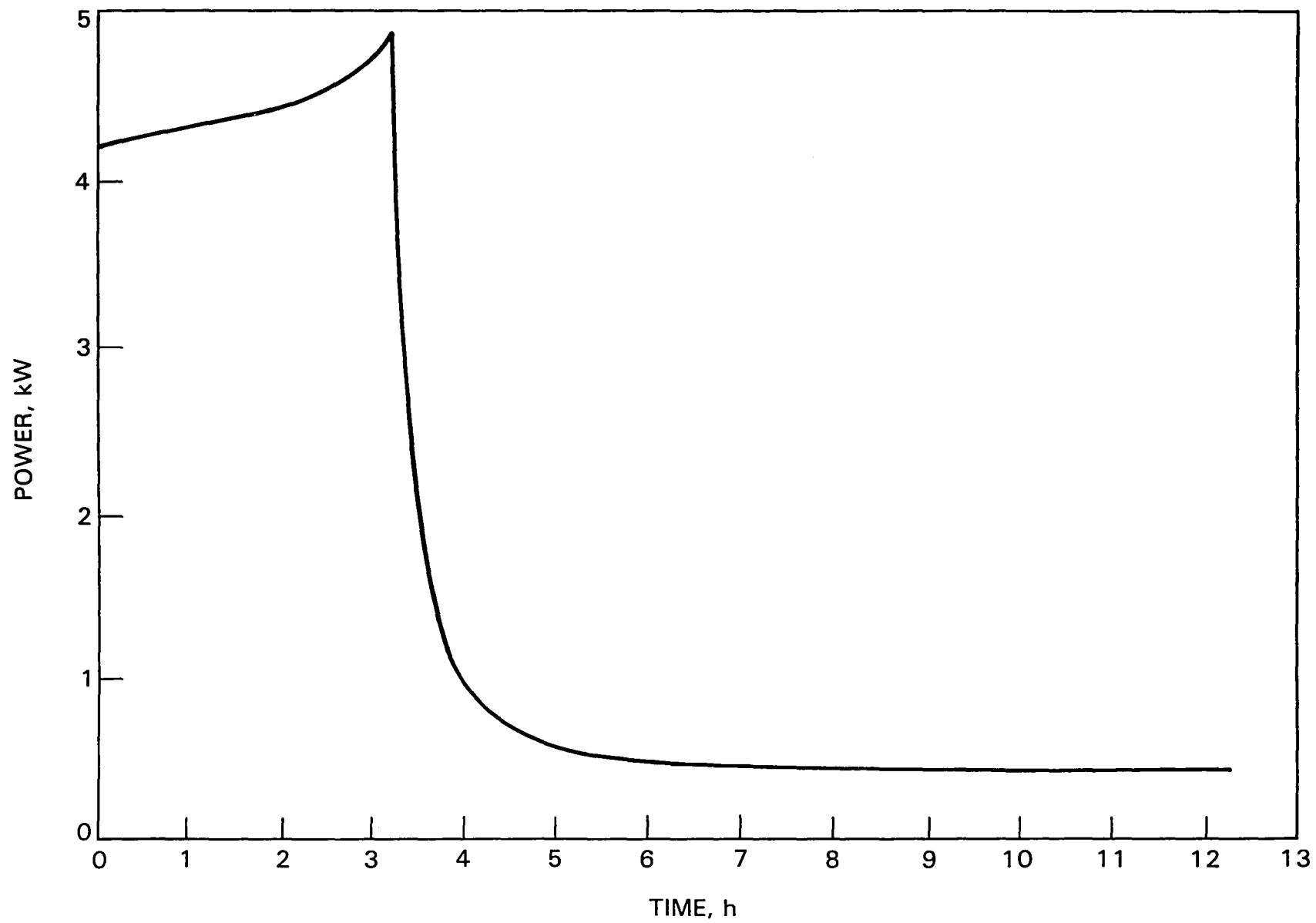


Figure 5-15. Globe ISOA Pb-A Battery: Recharge Power

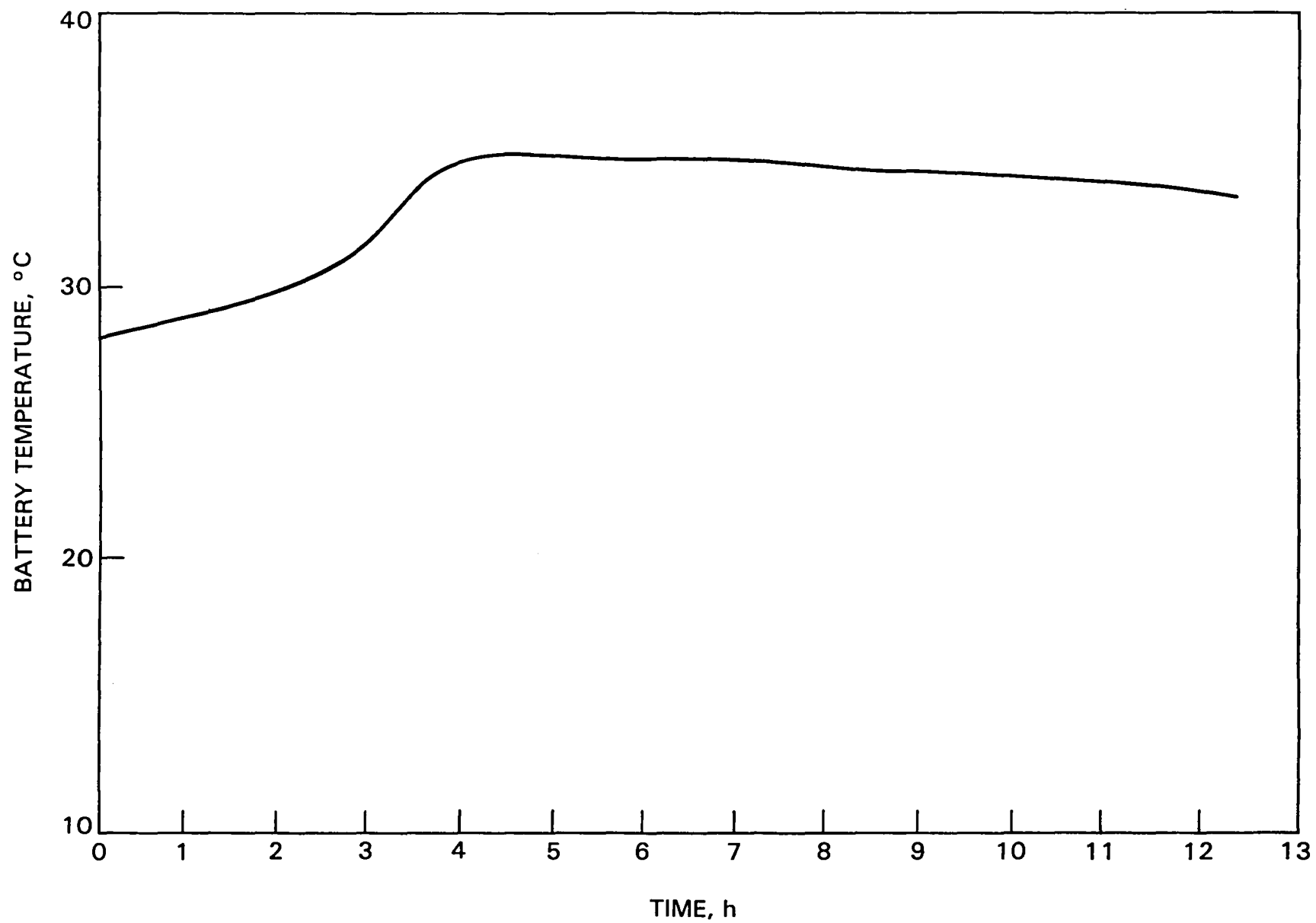


Figure 5-16. Globe ISOA Pb-A Battery: Temperature During Recharge

## C. WESTINGHOUSE NI-FE BATTERY

### 1. Range

Ten range tests of the SCT-2 powered by the Westinghouse Ni-Fe battery were completed. The results of these tests are summarized in Table 5-9. A Schedule D test was attempted, but battery voltage-drop resulted in high currents during acceleration, causing the motor to overheat. A plot of specific energy versus power, based on constant-speed-range tests, is shown in Figure 5-17.

Table 5-9. Westinghouse Ni-Fe Battery: Averaged Results of All Range Tests with SCT-2

Test Type	Range, km (mi)	Specific Energy, Wh/kg	Recharge Energy Efficiency, %	Coulombic Recharge Efficiency, %
56 km/h (35 mi/h)	160.1 (99.5)	31.3	42.8	59.1
72 km/h (45 mi/h)	135.5 (84.2)	29.1	39.5	56.3
88 km/h (55 mi/h)	91.2 (56.7)	25.7	34.9	51.6
Schedule C	76.9 (47.8)	28.9	--	--

### 2. Discharge-Rate Memory

A test sequence consisting of four constant-speed-range tests was done to determine the importance of discharge-rate memory as a parameter affecting the capacity of the Westinghouse battery.<sup>8</sup> The results of this test sequence are shown in Table 5-10.

There does appear to be a small memory effect: the data in Table 5-10 show a 1% variation in range between repeated tests. The magnitude of this variation indicates, however, that discharge-rate memory has only a minor impact on energy capacity.

---

<sup>8</sup>See Section IV for a description of the memory tests.

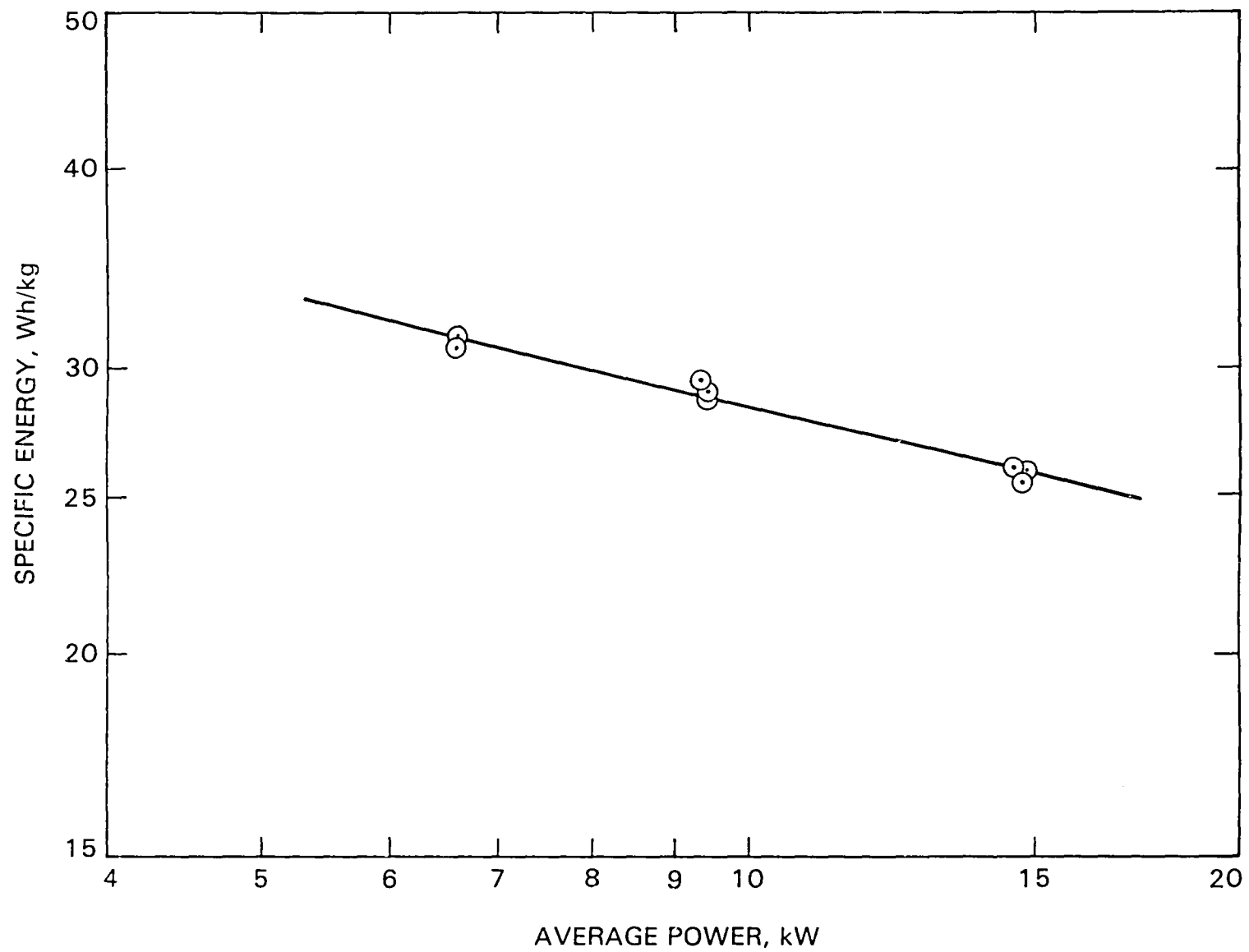


Figure 5-17. Westinghouse Ni-Fe Battery: Specific Energy versus Power

Table 5-10. Westinghouse Ni-Fe Battery: Results of Memory Tests

Test Sequence Number	Type of Discharge	Battery Discharge Energy, kWh
1	88 km/h (55 mi/h)	15.8
2	88 km/h (55 mi/h)	15.6
3	56 km/h (35 mi/h)	18.9
4	56 km/h (35 mi/h)	19.1

### 3. Self-Discharge

A limited amount of testing was done to observe the effect of self-discharge on battery capacity. (See Section IV for a description of the test procedures.) The results of the self-discharge tests are shown in Table 5-11 and in Figure 5-18. Figure 5-18 indicates that the rate of self-discharge decreases after a few hours, but that--even after several days--self-discharge continues to reduce capacity at a substantial rate.

Table 5-11. Westinghouse Ni-Fe Battery: Effect of an Open-Circuit Stand Between End of Charge and Start of Discharge<sup>a</sup>

Duration of Open-Circuit Stand, h	Discharge Energy, kWh	Energy Capacity Loss, %
0.5	17.0	4.0
1	16.9	4.5
4	16.5	6.8
24	15.3	13.6
72	12.9	27.1

<sup>a</sup>All data are from 72 km/h (45 mi/h) dynamometer tests of SCT-2.



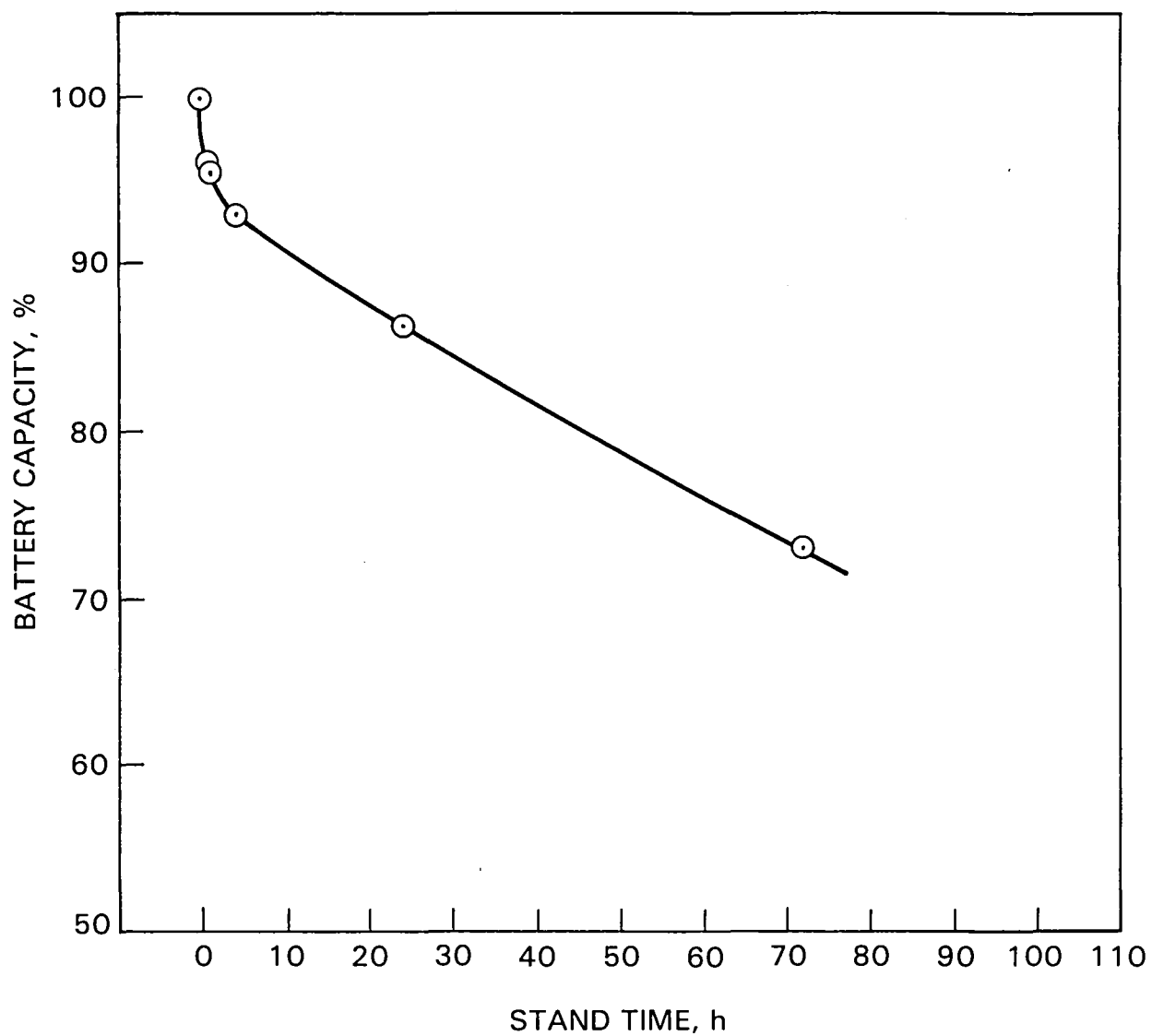


Figure 5-18. Westinghouse Ni-Fe Battery: Effect of an Open-Circuit Stand Between End of Charge and Start of Discharge

#### 4. Self-Heating

Table 5-12 shows the average temperature rise of the Westinghouse battery during vehicle-range tests. Average temperature rise at 50% depth-of-discharge is also shown in this table.

Table 5-12. Westinghouse Ni-Fe Battery: Average Temperature Rise Due to Self-Heating During Vehicle Testing

Activity	Average Temperature Rise, <sup>a</sup> °C
56 km/h to battery depletion	21.8
72 km/h to battery depletion	23.4
88 km/h to battery depletion	24.1
56 km/h to 50% depth-of-discharge	10.2
72 km/h to 50% depth-of-discharge	10.8
88 km/h to 50% depth-of-discharge	10.0
Schedule C to battery depletion	27.0
Schedule C to 50% depth-of-discharge	11.6
<sup>a</sup> Ambient temperature was maintained at 23 $\pm$ 3°C.	

#### 5. Internal Resistance

The effective internal resistance of the Westinghouse battery was calculated using voltage-drop data that were recorded during the acceleration portions of driving-schedule tests.<sup>9</sup> Figure 5-19 shows the effective internal resistance of this battery versus depth-of-discharge. The results of individual resistance calculations are shown as data points.

<sup>9</sup>A detailed description of the internal resistance calculations is given in Appendix B.

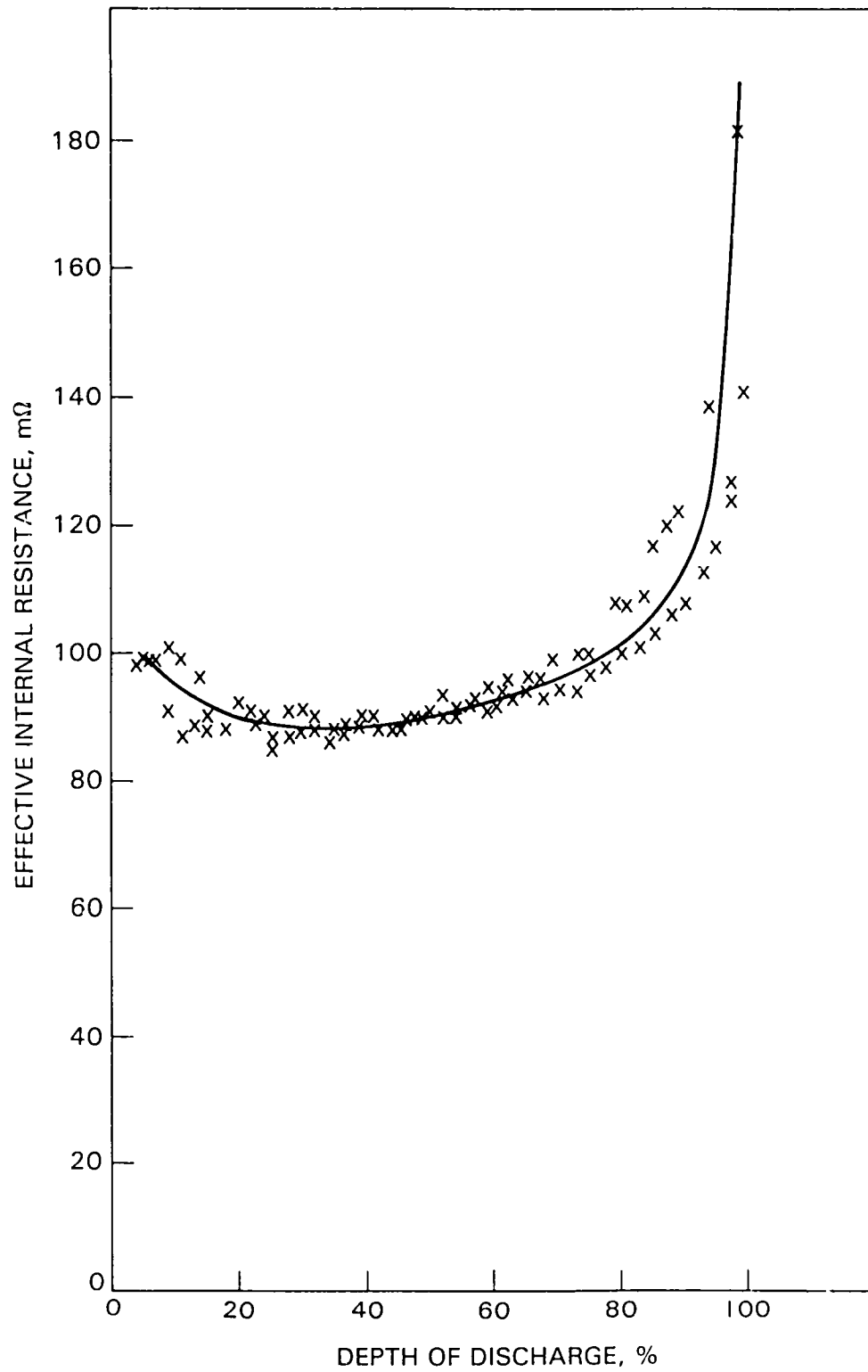


Figure 5-19. Westinghouse Ni-Fe Battery: Effective Internal Resistance versus Depth-of-Discharge

## 6. Recharge Characteristics

During the vehicle tests, the battery was charged at 70 A until it reached 156 V. This voltage was then maintained until 300 Ah had been delivered to the battery. With this procedure, current tapers to about 40 A by the end of charge. Battery voltage, current, and power during the taper charge are shown in Figures 5-20, 5-21, and 5-22. As shown in Table 5-9, the recharge efficiency of the Westinghouse battery during vehicle testing was about 40% on an energy basis and about 56% on a coulombic basis.

Battery temperature during recharge is shown for two different initial conditions in Figures 5-23 and 5-24. In Figure 5-23, battery temperature was low at the start of recharge, and it rose slowly throughout the charge. Figure 5-24 shows a recharge that was started while battery temperature was high. When the charge was started, the Electrolyte Management System cooled the battery, and the temperature dropped during the first part of recharge.

## 7. Gassing

The gassing rate of the Westinghouse battery during the standard taper charge is shown in Figure 5-25. As shown in this figure, gassing begins after about 0.5 h of charge. The rate increases throughout the charge, and begins to level off somewhat near the end of charge. Figure 5-26 shows the gassing rate during charge when the voltage-clamp level is lowered so that current tapers to about 10 A by the end of charge. In this case, the gassing rate peaks as current begins to taper, and then the rate remains fairly constant through the end of charge.

The proportion of hydrogen to oxygen in the gas generated at various times during the charge may vary, and these proportions are not known. However, the total amount of hydrogen and of oxygen generated during each charge/discharge cycle was determined by integration of the gassing-rate data shown in Figure 5-25. Based on these data,<sup>10</sup> about 3000  $\ell$  of hydrogen gas are released each charge/discharge cycle.

---

<sup>10</sup>Calculations of electrolysis by-products are shown in Appendix B.

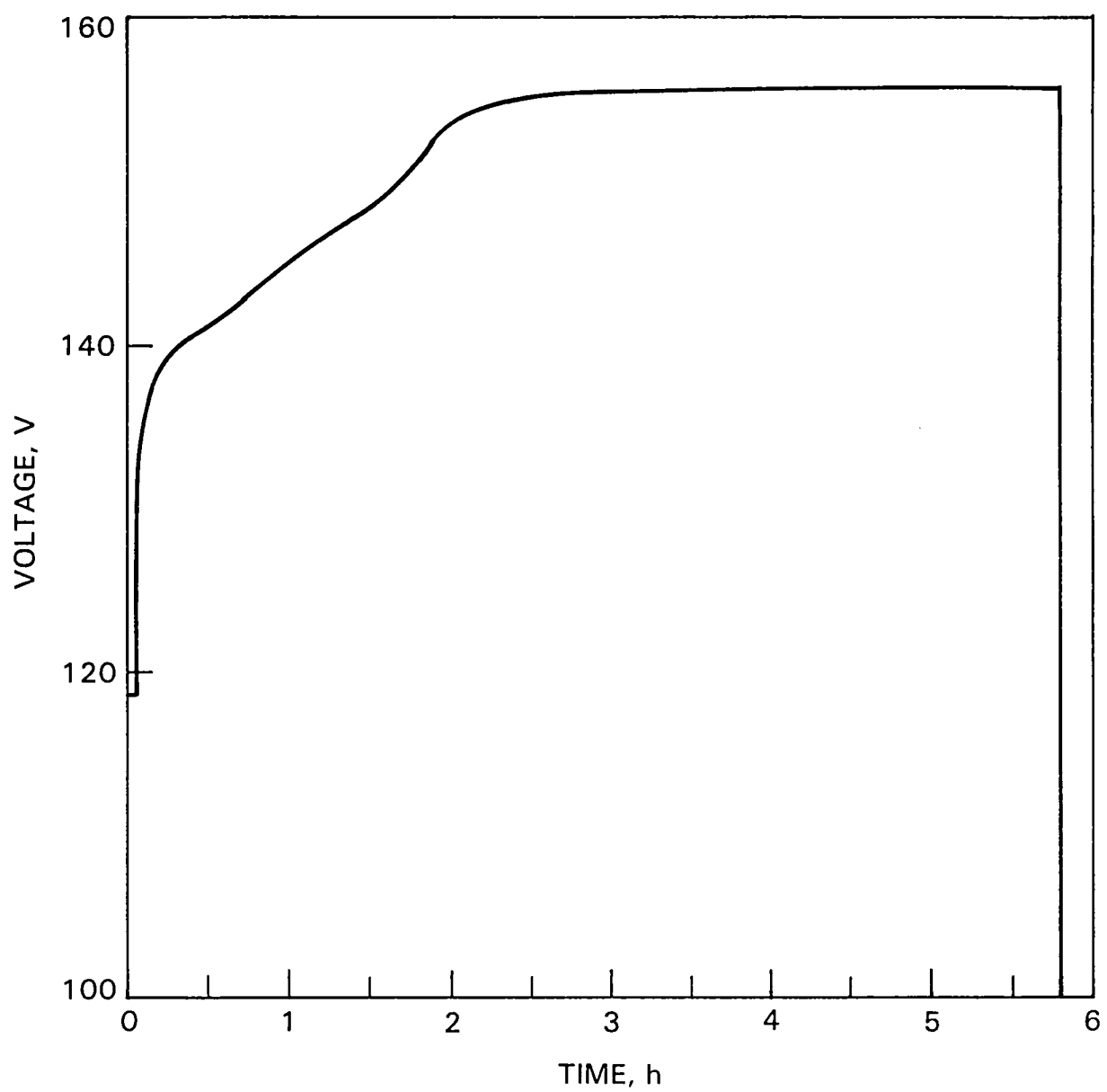


Figure 5-20. Westinghouse Ni-Fe Battery: Voltage During Recharge

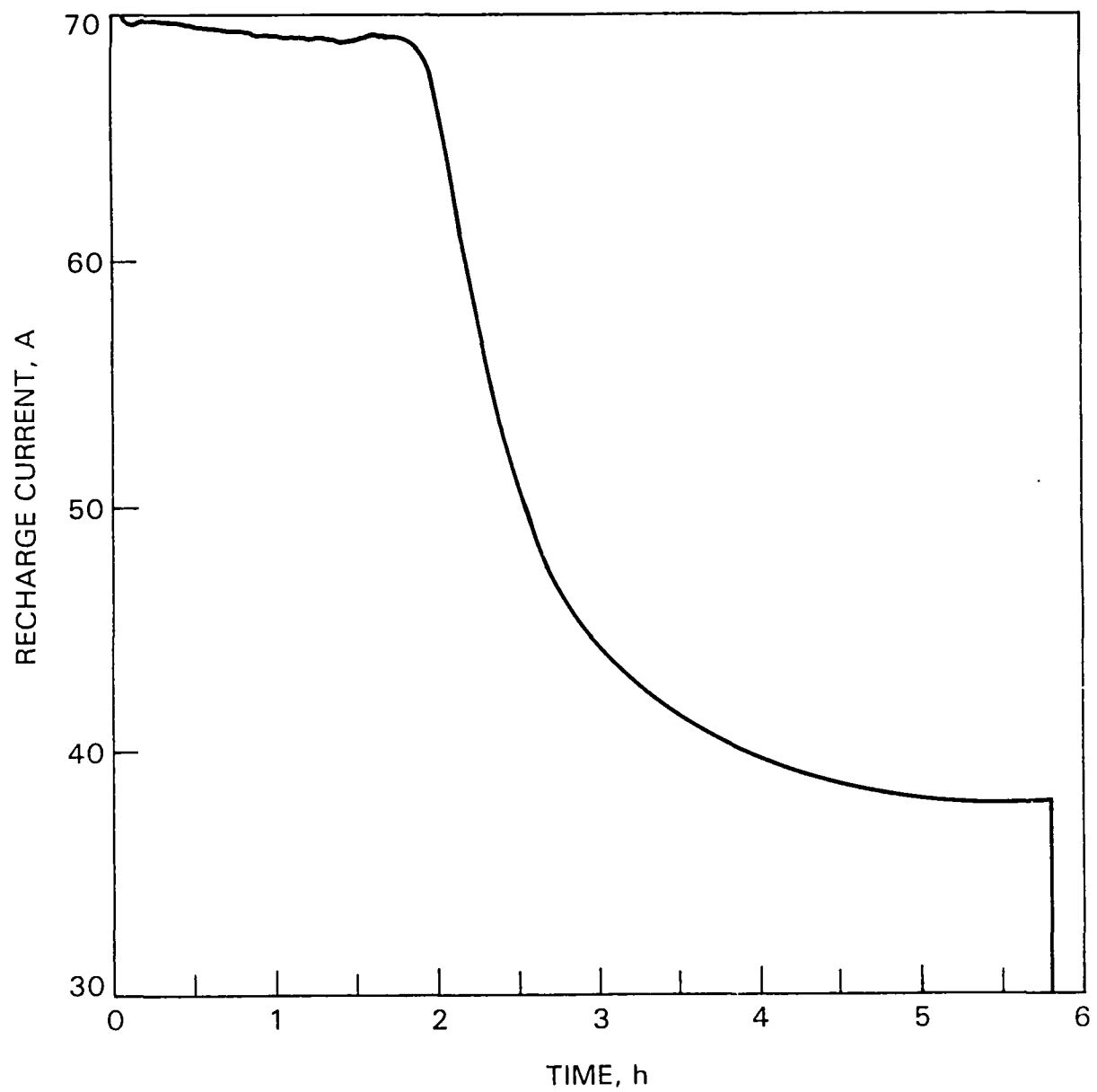


Figure 5-21. Westinghouse Ni-Fe Battery: Recharge Current

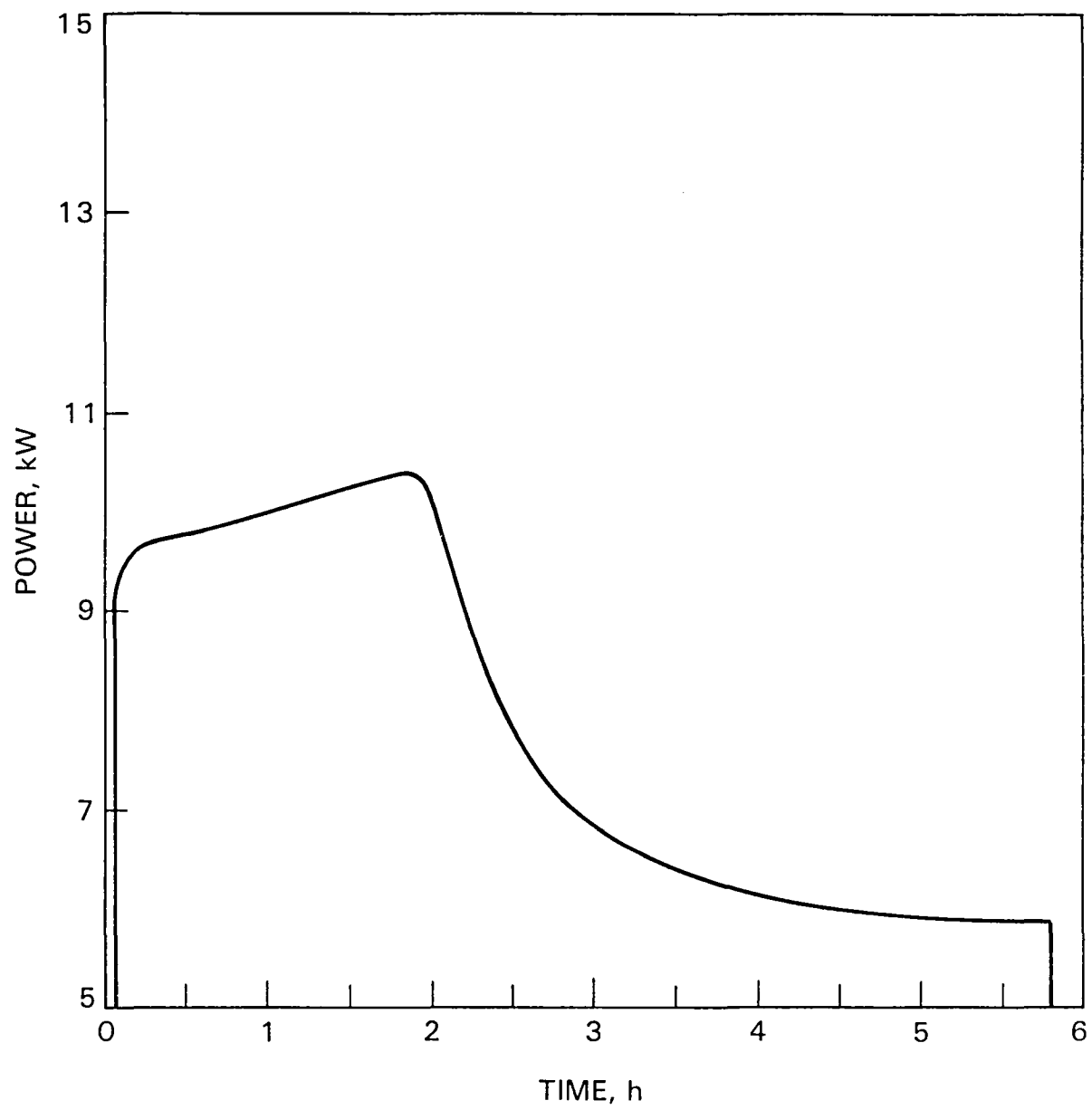


Figure 5-22. Westinghouse Ni-Fe Battery: Recharge Power

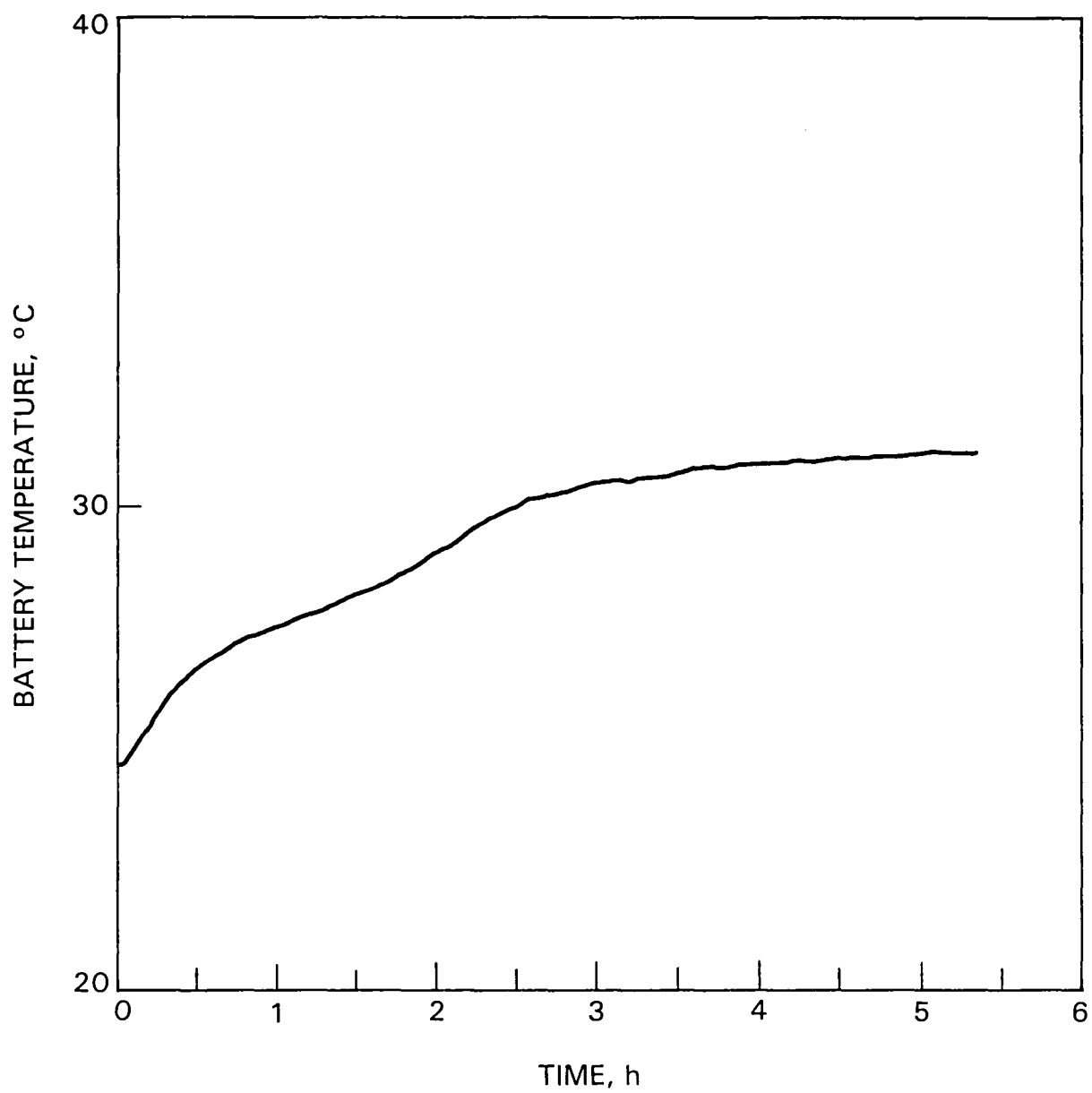


Figure 5-23. Westinghouse Ni-Fe Battery: Temperature During Recharge (low initial temperature)



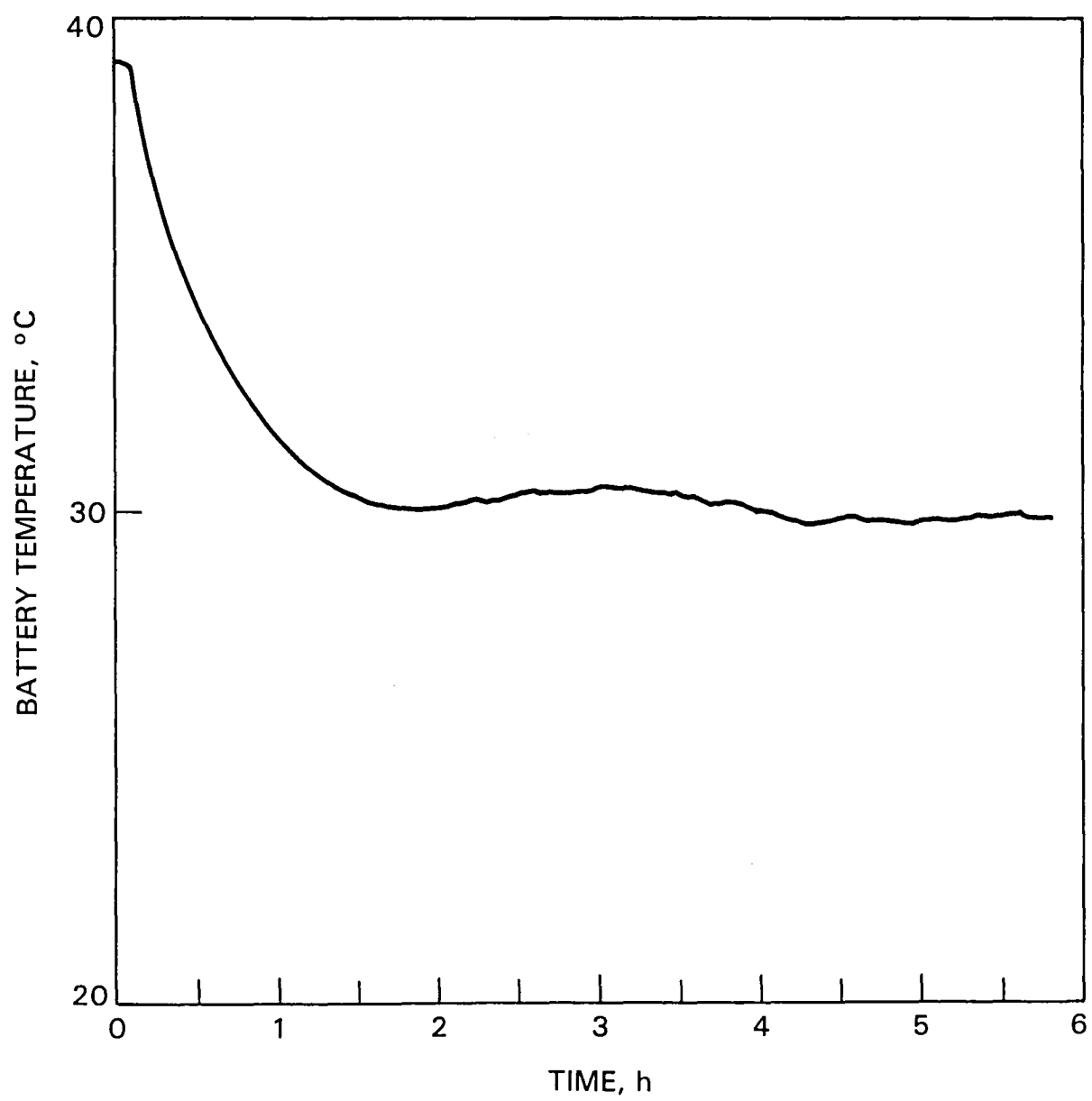


Figure 5-24. Westinghouse Ni-Fe Battery: Temperature During Recharge (high initial temperature)

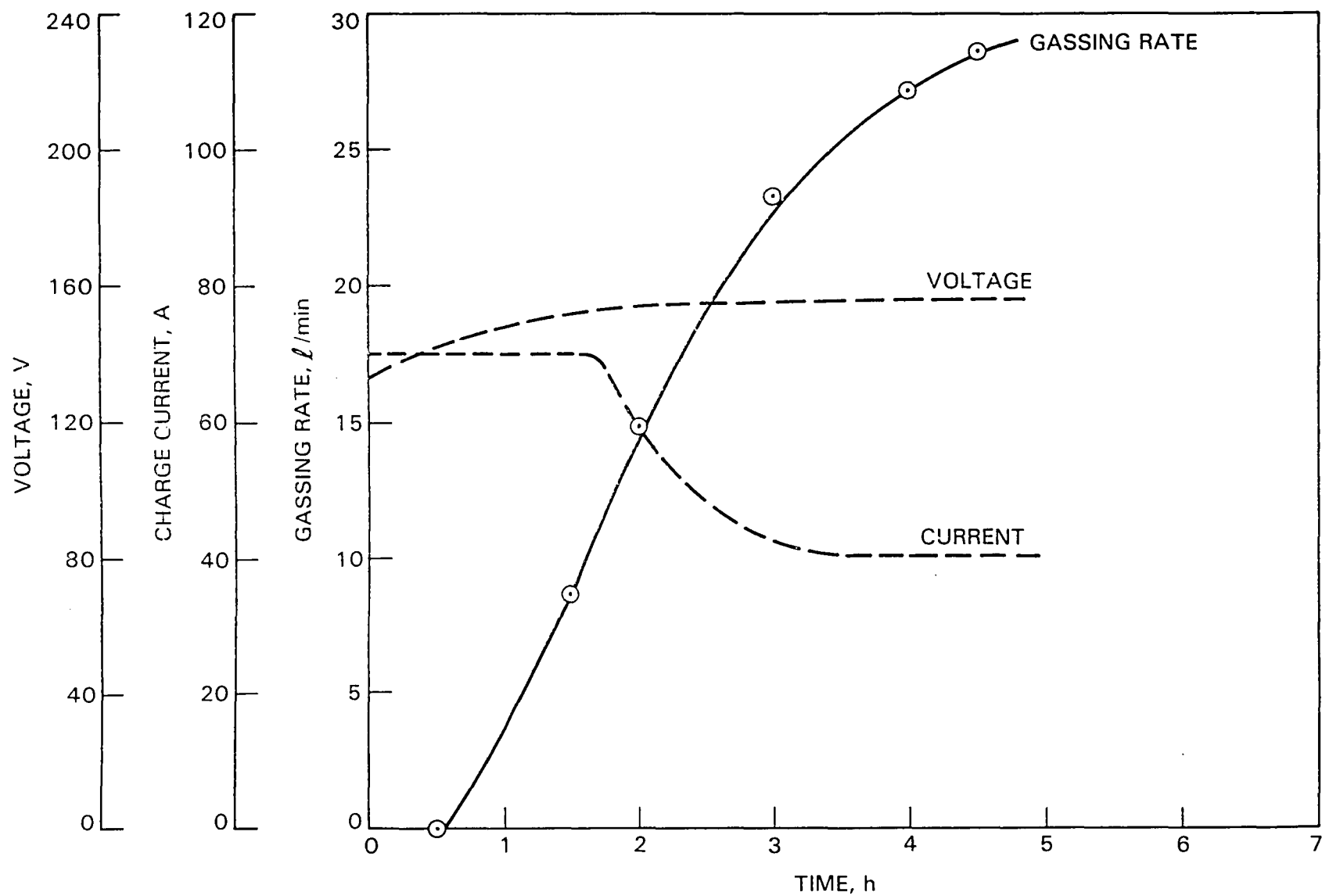


Figure 5-25. Westinghouse Ni-Fe Battery: Gassing Rate During a Standard Taper Charge with 40-A Finish Current

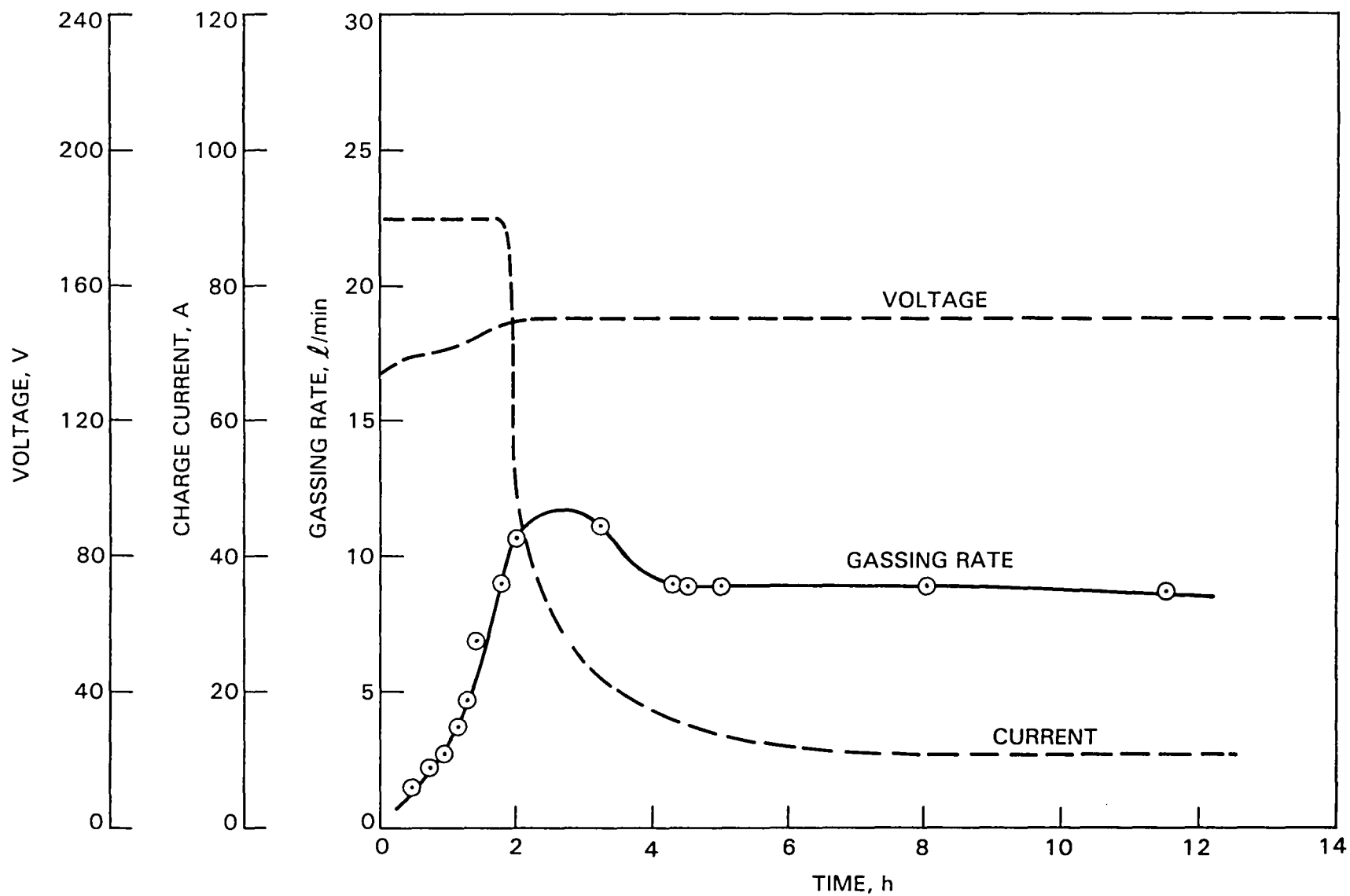


Figure 5-26. Westinghouse Ni-Fe Battery: Gassing Rate During an Experimental Taper Charge with 10-A Finish Current



## SECTION VI

### DISCUSSION OF RESULTS

In this section, data from the vehicle tests are analyzed in detail. All aspects of battery performance that were covered by the vehicle testing are evaluated. Comparisons are made between battery systems, and areas where further development or additional testing is likely to be worthwhile are identified.

#### A. CAPACITY CHARACTERIZATION

##### 1. Constant-Speed Driving

a. The Westinghouse and EPI Ni-Fe Batteries. Figure 6-1, a plot of specific energy versus power, shows the capacity obtained from each of the two Ni-Fe batteries during constant-speed-range tests at JPL. These two batteries were tested at different levels of developmental maturity, and therefore capacity comparisons based on the vehicle testing done to date should be viewed as tentative.

As shown in Figure 6-1, the specific energy of the EPI battery is substantially higher than the specific energy of the Westinghouse battery: 16% higher at 5 kW and 41% higher at 15 kW. It may appear that the Westinghouse battery is penalized, in terms of specific energy, because the battery mass includes the EMS hardware whereas, during the vehicle testing at JPL, the EPI battery did not have any similar hardware. However, since then, EPI has developed hardware for watering, venting of gasses, and cooling, and, with the approach taken by EPI, the mass of this hardware is negligible compared to the battery mass.<sup>1</sup>

During vehicle tests, the Westinghouse battery was always charged to 300 Ah. Constant-current test data indicate that about 6% more capacity could have been obtained from this battery by increasing the amount of charge to 350 Ah. This was not done, however, because reliability problems were experienced when the battery was repeatedly charged with more than 300 Ah. An estimate of the capacity increase that could be obtained with increased overcharge is shown as a dashed line in Figure 6-1. As shown in this figure, even with a 350-Ah charge, the specific energy of the Westinghouse battery would still be substantially less than that of the EPI battery.

It was mentioned, in Section IV, that the EPI battery may have suffered some loss of capacity as a result of operation at elevated temperatures before being tested at JPL. Thus, it is possible that the results of the vehicle testing at JPL understate the capacity of the EPI battery. Unfortunately,

---

<sup>1</sup>EPI Ni-Fe batteries are presently being field tested in electric vehicles, and, in these batteries, the additional hardware consists of hoses for watering and a 300-ft<sup>3</sup>/min fan for cooling. The total mass of this hardware is estimated to be less than 5 kg.

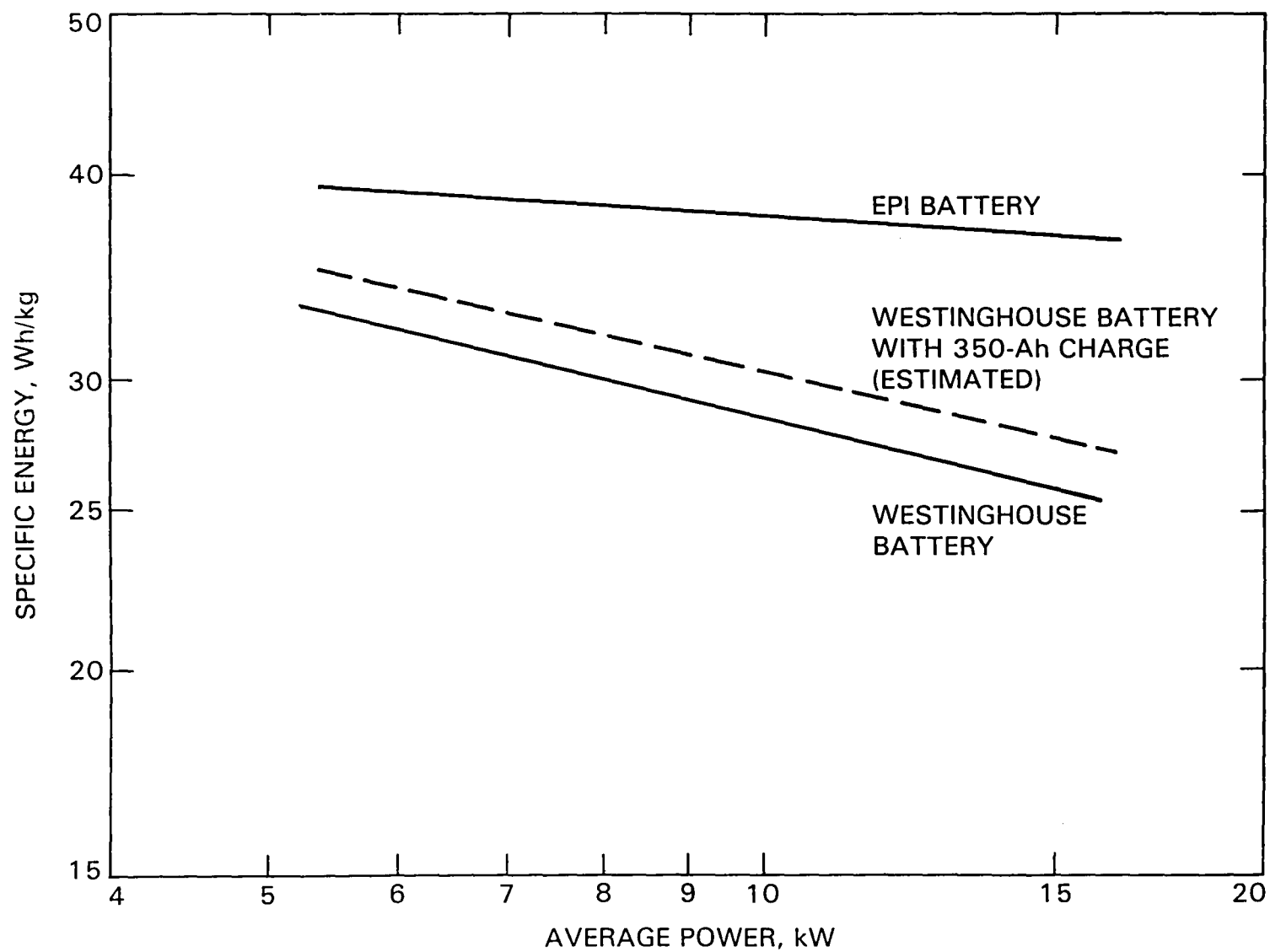


Figure 6-1. EPI and Westinghouse Batteries: Specific Energy versus Power

insufficient data are available to estimate the magnitude of the capacity loss of the EPI battery (if any) due to the elevated-temperature operation.

b. Earlier Version of the Westinghouse Battery. In Figure 6-2, the capacity of the Westinghouse battery is compared with the capacity of the earlier version of that battery that was tested at JPL in 1979. As this figure shows, the earlier version had more capacity at high discharge rates than the present version. Insufficient data were obtained to determine the capacity of the earlier version at low discharge rates: only two low-power, constant-speed-range tests were completed, and the results from these two tests differ by 18%.

c. Globe ISOA Pb-A Battery. Figure 6-3 shows the capacity of the Globe ISOA battery, the ETV-1 baseline battery, and the SCT-2 baseline battery<sup>2</sup> during constant-speed-range tests. As shown in this figure, the specific energy of the Globe ISOA battery is 10 to 20% higher than the specific energy of the two baseline Pb-A batteries.

d. Sensitivity to Discharge Rate. In Table 6-1, the sensitivity of battery capacity to constant-power discharge rate has been expressed as the mean gradient of the curves shown in Figures 6-1 and 6-3 (specific energy as a function of discharge power) between 5 kW and 15 kW ( $G_{5-15}$ )<sup>3</sup> for each of the three developmental batteries and for the two commercially-available

Table 6-1. Mean Gradient of Specific Energy as a Function of Discharge Power Between 5 kW and 15 kW

Battery	$G_{5-15}$ , Wh/kW-kg
EPI Ni-Fe	-0.30
Globe ISOA Pb-A	-1.1
Westinghouse Ni-Fe	-0.82
ETV-1-2 baseline	-1.4
SCT-2 baseline	-1.2

<sup>2</sup>The baseline configuration of a test vehicle is the configuration when delivered by the manufacturer. The baseline battery for ETV-1-2 is a prototype version of the Globe EV1000, and the baseline battery for SCT-2 is the Exide XPV-23.

<sup>3</sup>5 kW represents roughly the lower limit and 15 kW represents roughly the upper limit for power requirements during constant-speed operation.

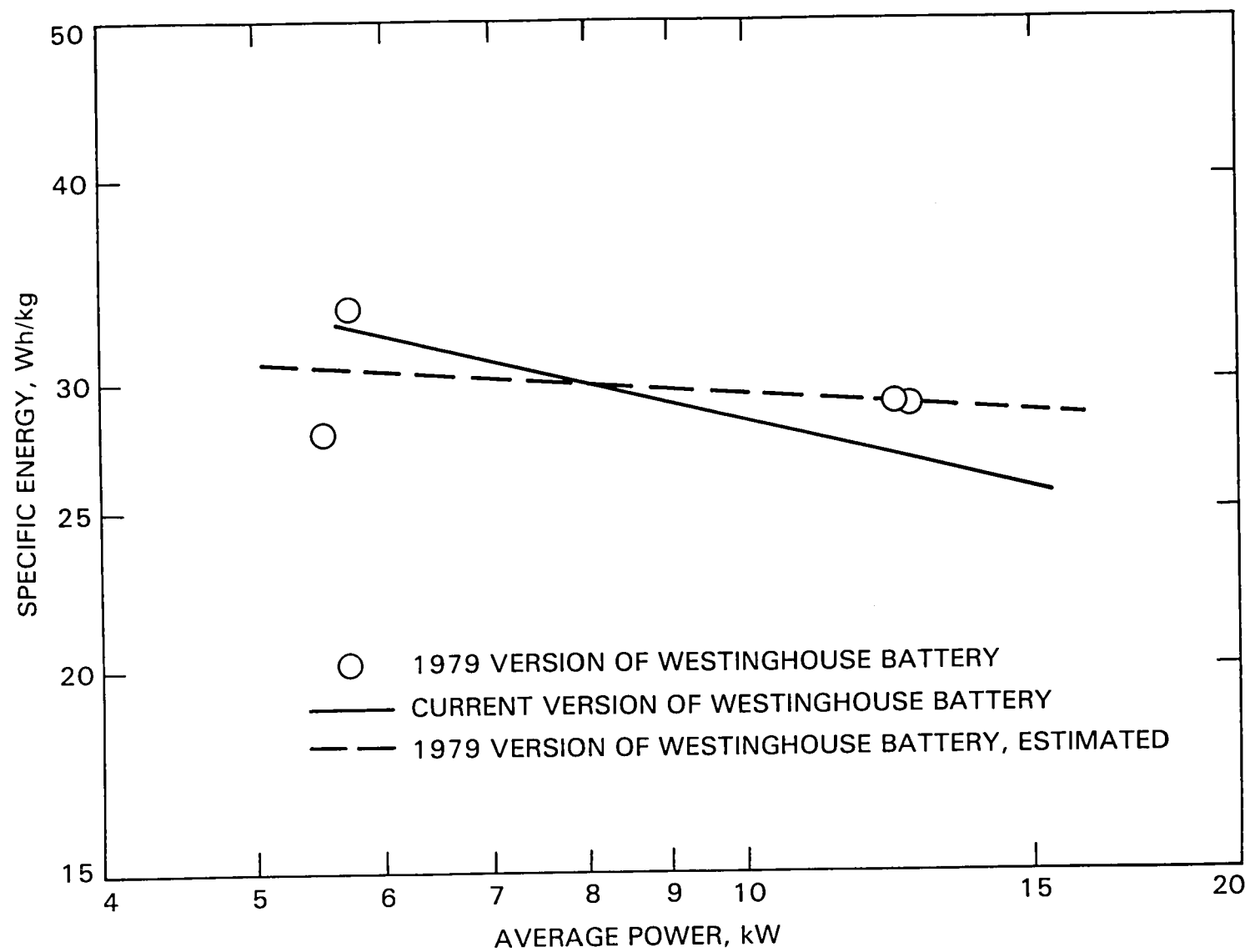


Figure 6-2. Capacity of the Westinghouse Battery Compared with an Earlier Version of the Battery



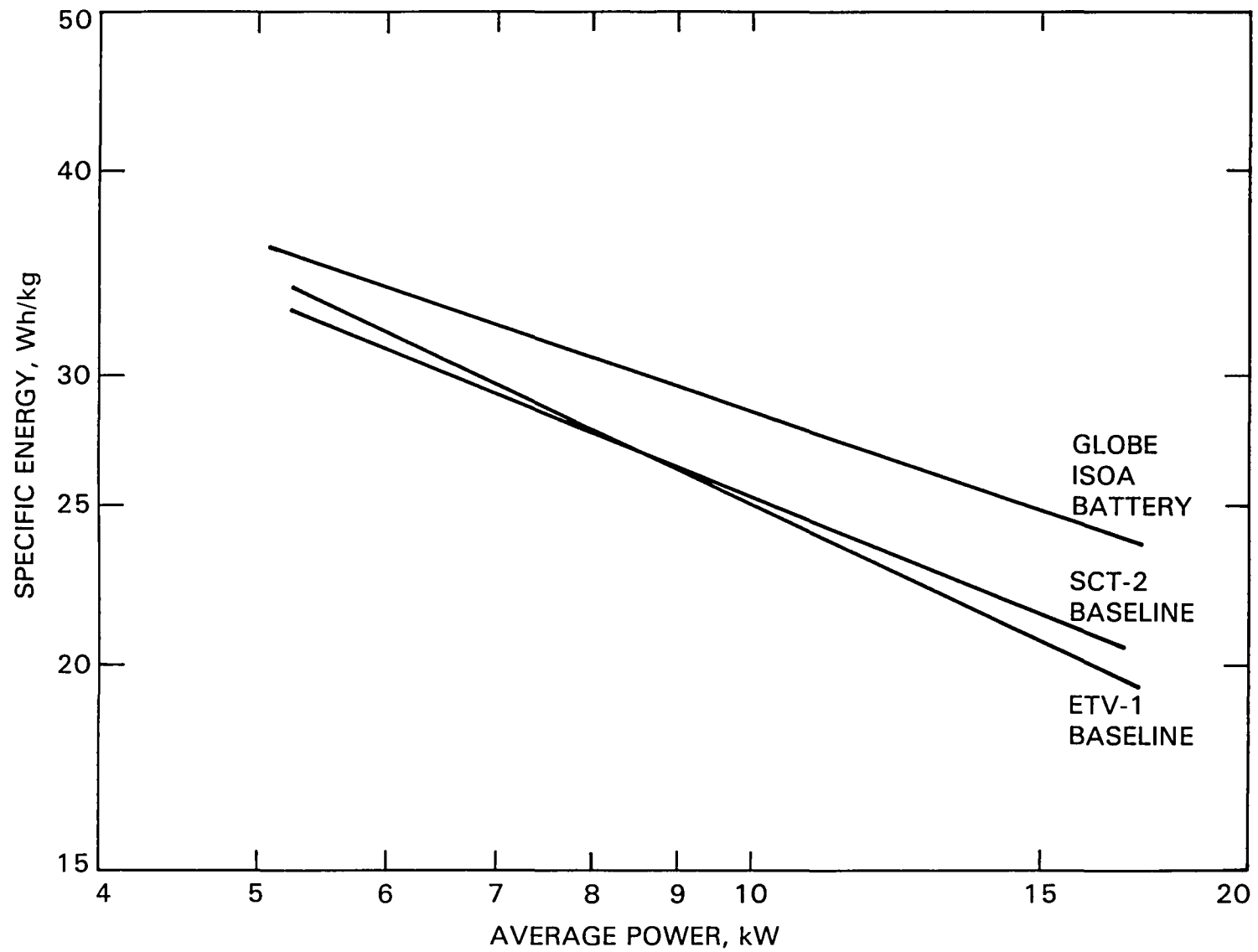


Figure 6-3. Globe ISOA Battery, ETV-1 Baseline Battery, and SCT-2 Baseline Battery: Specific Energy versus Power

baseline batteries.<sup>4</sup> A shallow gradient (i.e. close to zero) indicates that the capacity of the battery has little sensitivity to discharge rate.

The sensitivity of capacity to discharge rate is an important aspect of electric-vehicle batteries. In electric-vehicle applications, it is advantageous for battery capacity to have little sensitivity to discharge rate because the power demands during normal use will vary. If battery capacity is relatively insensitive to these variations, vehicle range will be more consistent and predictable--especially under strenuous driving conditions.

As indicated in Table 6-1, the gradient is shallower for the two Ni-Fe batteries than for the Pb-A batteries--indicating that, within the power range considered, the capacity of the Ni-Fe batteries is less sensitive to discharge rate than is the capacity of the Pb-A batteries. The EPI Ni-Fe battery performs especially well in this respect. The Globe ISOA battery has a shallower gradient than the two Pb-A baseline batteries, demonstrating that a performance improvement in this area was obtained with the ISOA technology.

## 2. Variable-Speed Driving

A limited amount of capacity characterization under variable-speed driving conditions was done. The variable-speed tests consisted mostly of SAE Schedule C and Schedule D range tests. Although the SAE schedules are composed of the basic elements of variable-speed driving (i.e., acceleration, cruise, coast, brake, and idle), the velocity-time profiles are not (nor are they intended to be) representative of typical driving patterns during normal vehicle use. For this reason, the results of the Schedule C and Schedule D range tests should not be considered predictions either of the vehicle range or of the battery capacity which would be obtained during normal vehicle use. However, these tests do provide a repeatable basis for comparing the capacity of the batteries tested under the dynamic power requirements of variable-speed driving.

Both the 90-cell EPI Ni-Fe battery and the Westinghouse Ni-Fe battery were tested with SCT-2; Schedule C range tests were done with both batteries. The specific energy of the Westinghouse battery was 28.9 Wh/kg, and the specific energy of the EPI battery was 38.1 Wh/kg--a difference of over 20%--during Schedule C range tests with SCT-2. Thus it appears that the capacity of the EPI battery under the conditions of variable-speed driving is substantially greater than the capacity of the Westinghouse battery.

Both the Globe ISOA battery and the ETV-1 baseline battery were tested with ETV-1-2. For Schedule D driving, the specific energy of the ISOA battery was about 6% higher than the specific energy of the ETV-1 baseline battery. Thus, although an increase in specific energy was obtained with the ISOA battery, the magnitude of this increase is only moderate.

---

<sup>4</sup>Calculations are shown in Appendix B.

### 3. Discharge-Rate Memory

Some batteries show a discharge-rate memory effect during repetitive charge/discharge cycling (Reference 8). That is, the capacity available under a given set of discharge conditions is influenced by the previous discharge. If a discharge is done at a high power (resulting in reduced capacity), battery capacity will be impaired during the subsequent discharge. If a discharge is done at a low power (resulting in increased capacity), battery capacity will be enhanced during the subsequent discharge. This memory effect is undesirable because it adds to the uncertainty already present in the predictions of battery capacity which are used to estimate depth-of-discharge during use.

The Westinghouse battery and the Globe battery were tested for discharge-rate memory. A memory effect was observed in both batteries, but, in both cases, it was so small that it can undoubtedly be neglected. Although the EPI battery was not tested for discharge-rate memory, the capacity of this battery was found to be unusually consistent: in Reference 9, it is shown that, throughout the entire series of vehicle tests, the maximum deviation in the net coulombic capacity of the EPI battery was 1.5%. Therefore, it appears that memory effects are not significant in this battery. Thus, all three of these batteries appear to be essentially free of discharge-rate memory.

There is another memory effect which can occur when a battery is subjected to repeated partial discharge. In this case, a capacity loss occurs when a full discharge is preceded by a number of partial discharges. Several full charge/discharge cycles are then required to restore battery capacity. This memory effect was not quantified during the vehicle tests.

### 4. Effect of Self-Discharge on Capacity

In general, the capacity of a fully-charged Pb-A battery will remain relatively stable over a period of several days, but the capacity of a Ni-Fe battery will decrease substantially, due to self-discharge, as the battery stands without an applied load (Reference 10). Because of this self-discharge, the capacity data obtained from vehicle-range tests of the two Ni-Fe batteries is only representative of the capacity available immediately following charge termination. If the vehicle-range tests with the Ni-Fe batteries had been preceded by a one or two day open-circuit stand, as were the range tests with the Globe Pb-A battery, less capacity would have been obtained. Figure 6-4, a plot of capacity loss versus open-circuit stand time, compares the effect of self-discharge on the capacity of each of the two Ni-Fe batteries.

As shown in Figure 6-4, the EPI and the Westinghouse batteries have differing self-discharge characteristics: for the first 24 h, both batteries lose capacity at about the same rate, but after 24 h, the rate of self-discharge is substantially less for the EPI battery than for the Westinghouse battery. Thus, over a period of several days, self-discharge would be less of a problem with the EPI battery than with the Westinghouse battery.

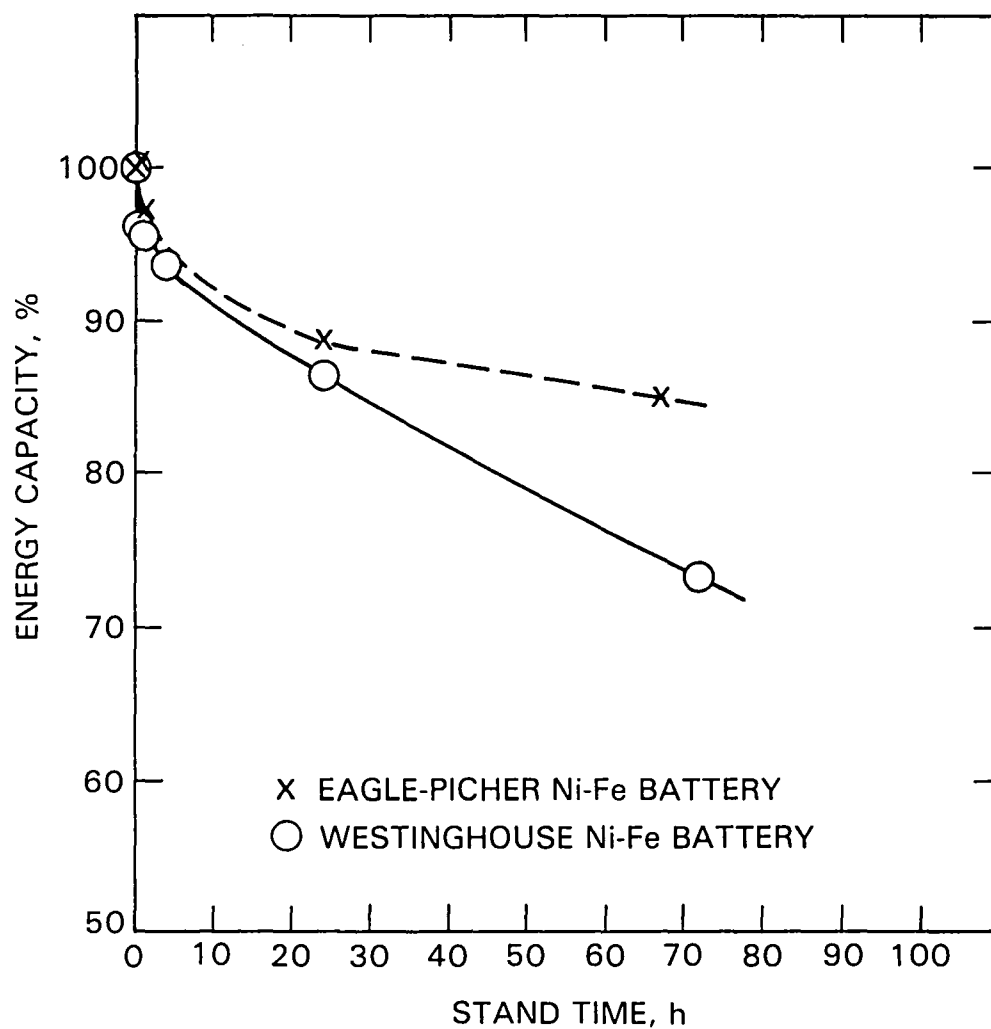


Figure 6-4. EPI and Westinghouse Batteries: Effect of an Open-Circuit Stand Between End of Charge and Start of Discharge

The purpose of the self-discharge tests was not to provide data for a detailed analysis, but rather to assess the importance of this parameter. The self-discharge characteristics presented in Figure 6-4 should be considered preliminary, because this figure is based on a limited amount of testing (three tests of the EPI battery and five tests of the Westinghouse battery). All the self-discharge tests were done at an ambient temperature of  $23 \pm 3^\circ\text{C}$ . Since chemical reaction rates are generally temperature dependent, the self-discharge characteristics of these batteries are probably functions of temperature.

The occurrence of self-discharge in the Ni-Fe batteries must be considered when evaluating battery performance during normal vehicle use. There are several possible ways of handling this problem of self-discharge:

- (1) One approach would be to plan on using the vehicle within a few minutes after terminating the charge. This might not always be practical, but whenever it could be done, it would ensure maximum capacity and energy efficiency from these batteries.
- (2) A second approach would be to adjust battery capacity predictions to include the self-discharge losses based on the time interval between end of charge and start of discharge.
- (3) A third approach would be to prevent self-discharge by applying a trickle charge to the battery when there must be a wait period between charge and discharge. The trade-off with this approach would be reduced recharge efficiency because additional energy must be used for the trickle charge. Further testing would be required to determine the effectiveness of trickle charging and the energy trade-offs involved.

## 5. Effect of Temperature on Capacity

At the end of charge, the temperature of all three batteries was typically about  $30$  to  $35^\circ\text{C}$ . During vehicle-range tests, both the EPI and the Westinghouse batteries were discharged shortly after charge termination, but the Globe battery was allowed to cool to  $23 \pm 3^\circ\text{C}$  before discharge (see Section IV). The capacity of Ni-Fe and of Pb-A batteries is temperature dependent. In the case of Pb-A batteries in general, capacity has been found empirically to vary linearly with temperature (Reference 11). In Ni-Fe batteries, the influence of temperature on capacity is generally as shown in Figure 6-5: above some critical temperature, approximately full capacity is available, but below the critical temperature, capacity rapidly decreases. The critical temperature for a Ni-Fe battery varies with discharge rate (Reference 8).

The effect of temperature on the capacity of the developmental batteries (over the full temperature range likely to be experienced during normal vehicle use) must be determined before a meaningful evaluation of battery capacity

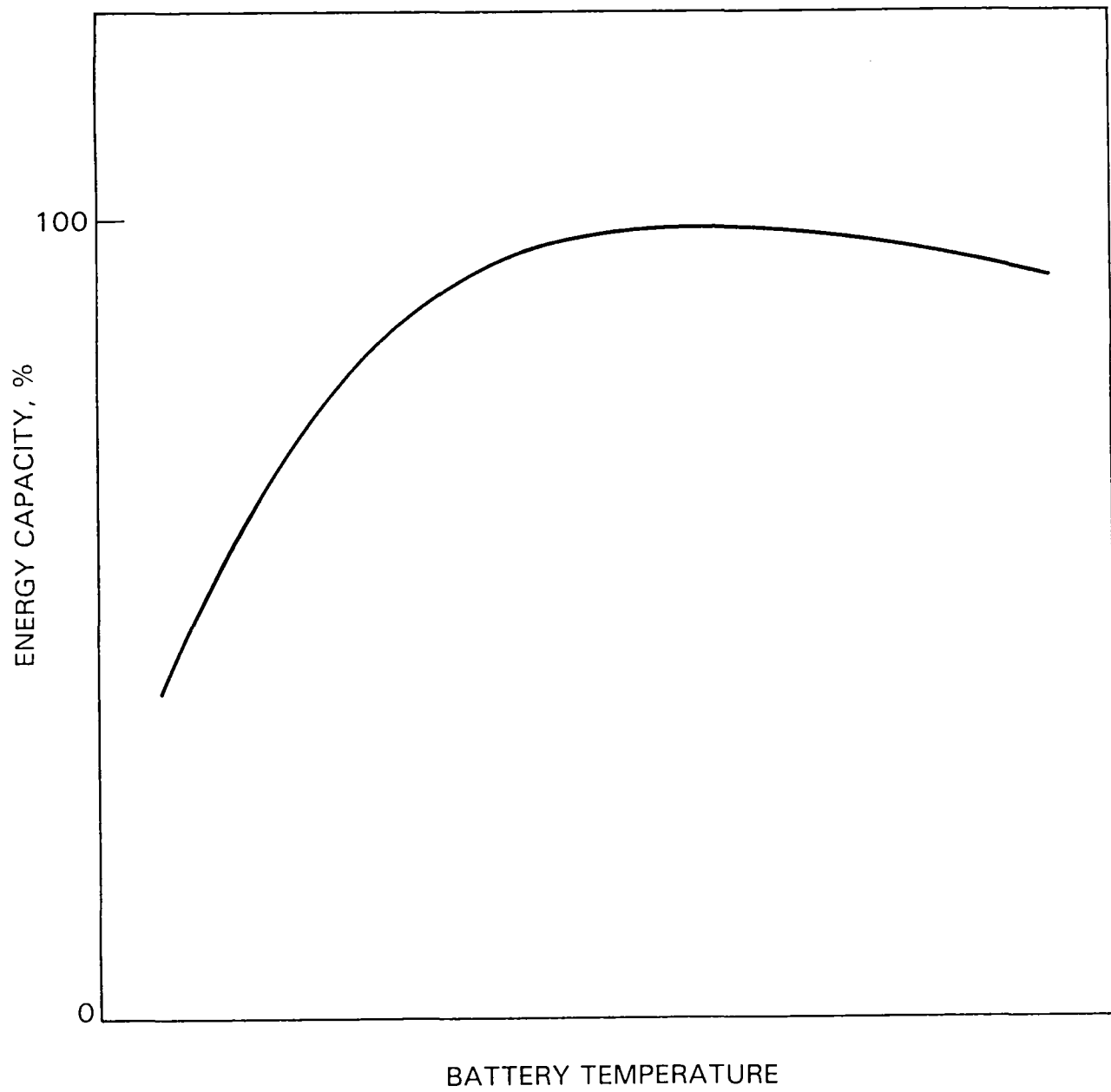


Figure 6-5. Effect of Temperature on the Capacity of Ni-Fe Batteries, Typical

can be made.<sup>5</sup> This was not done during the vehicle testing. However, a limited amount of testing was done which provides some preliminary data. More extensive testing of the effect of temperature on capacity is being done at the NBTL.

In tests done by EPI (Reference 3), the capacity of the EPI Ni-Fe cells was found to be approximately constant when operated at ambient temperatures down to about 0°C. Even at ambient temperatures of -20°C, the EPI cells were found to have over 80% of full capacity. In tests done by Westinghouse (Reference 12), the Westinghouse Ni-Fe cells were found to have about 70% of full capacity at 0°C.

A capacity increase of 1.1% per °C was observed in the Globe battery during vehicle testing. A temperature sensitivity of this magnitude seems reasonable because a similar temperature sensitivity has been observed in other Pb-A batteries (References 8 and 11).

#### 6. Comparison: Pb-A and Ni-Fe Batteries

A comparison of the capacity of the Globe battery to the capacities of the two Ni-Fe batteries based solely on the results of the vehicle-range tests shown in Figures 6-1 and 6-3 would not be valid. Such a comparison should also include, at the least, the effects of self-discharge and temperature. A comparison which includes an estimate<sup>6</sup> of these effects is shown in Figures 6-6 and 6-7.

In Figure 6-6, the estimated capacity of the Globe battery at 33°C (the average end-of-charge temperature of the Globe battery) is shown along with the data from range tests of the two Ni-Fe batteries. This figure represents capacity available, immediately after charge termination, for each of the three developmental batteries. As shown in this figure, the specific energy of the EPI battery is substantially higher than the other two batteries, and the specific energy of the Globe battery is higher than the Westinghouse battery. Under warmer or cooler ambient conditions, the end-of-charge temperatures of the batteries would be different. The effect of temperature on capacity is different for each of the two types of batteries, and a complete comparison should include capacity data over a large temperature range. However, at this time, such a comparison would have a great deal of uncertainty because of the preliminary nature of the data available.

In Figure 6-7, the estimated capacity of the two Ni-Fe batteries after an overnight open-circuit stand is shown along with the data from range tests of the Globe battery. The relationship between the capacities of the three batteries in this figure is similar to the relationship shown in Figure 6-6.

---

<sup>5</sup>Even if a thermal management system is used to control battery temperature, capacity will still be affected by the ambient temperature because power will be required to regulate battery temperature.

<sup>6</sup>Calculations are explained in Appendix B.

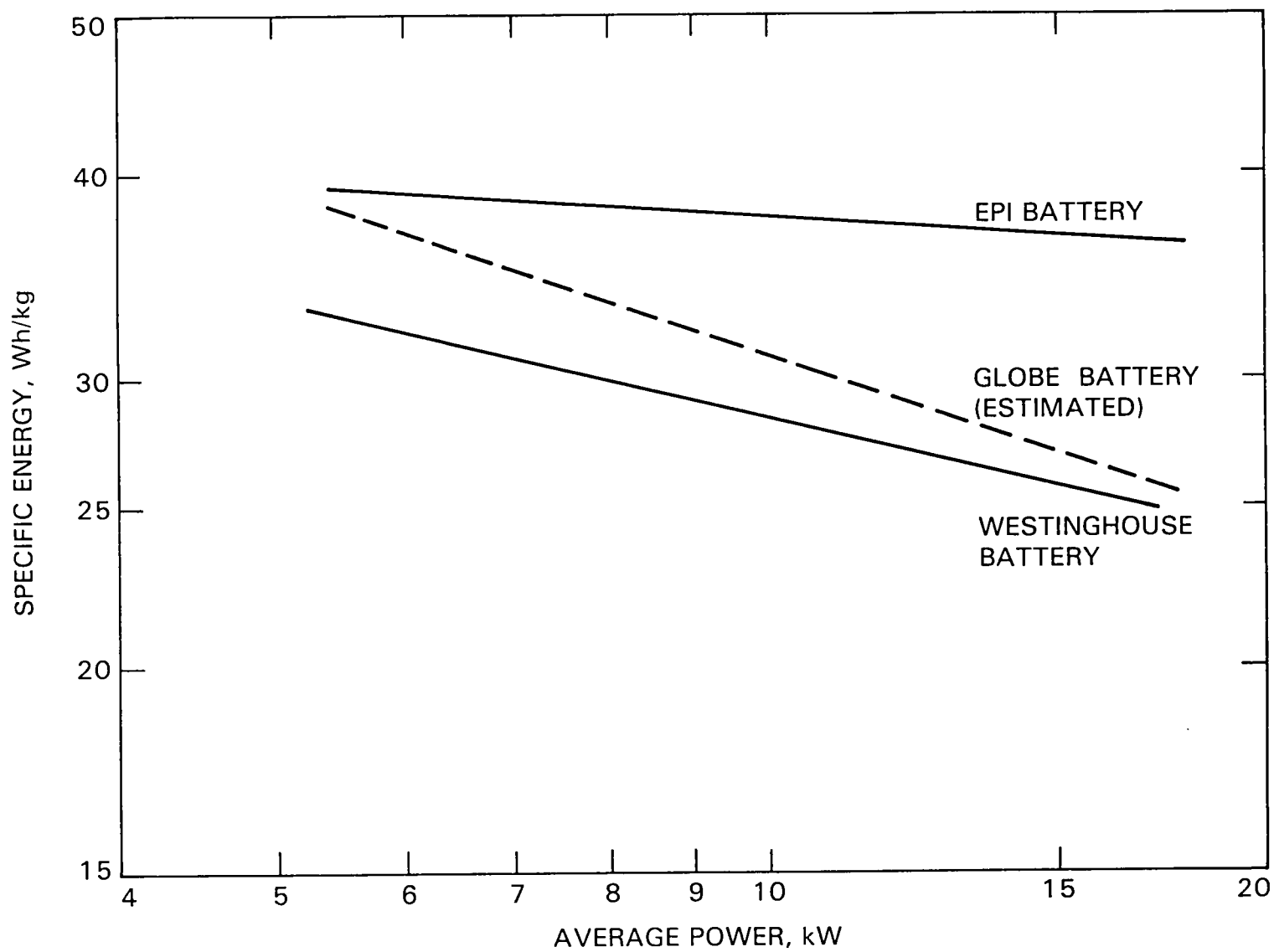


Figure 6-6. Capacity of the EPI, Globe, and Westinghouse Batteries Immediately After Charge Termination



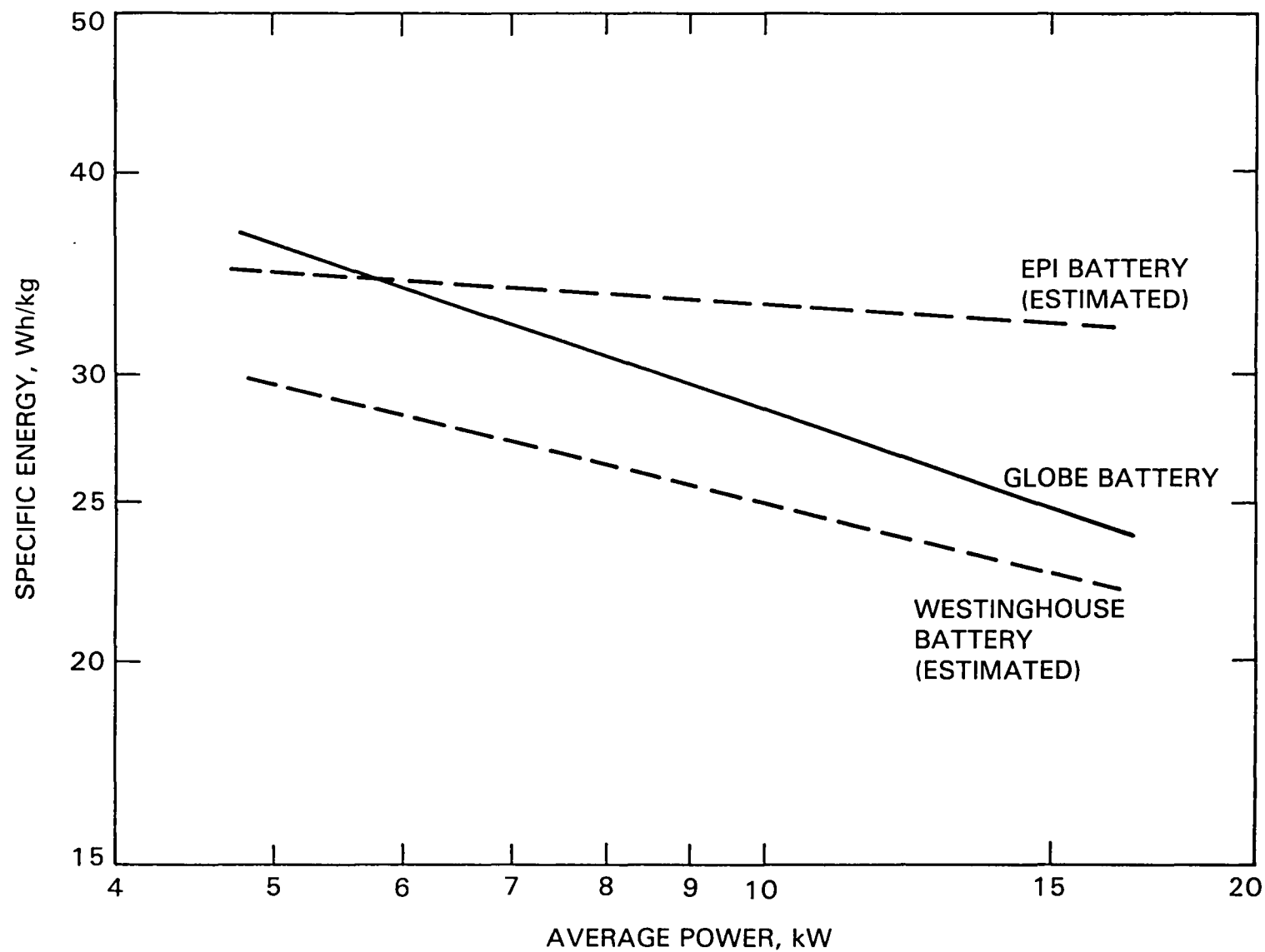


Figure 6-7. Capacity of the EPI, Globe, and Westinghouse Batteries After an Overnight, Open-Circuit Stand

## B. RESPONSE UNDER LOAD

### 1. Internal Resistance

In a vehicle application, the vehicle/battery interface must be given consideration. The voltage response of the battery under a load is an important part of this interface: if a momentary load presented to the battery produces a large voltage drop, a high battery current will be required to satisfy the power demand.

High momentary loads occur during acceleration. For the following reasons, it is disadvantageous for the momentary loads presented to the battery, during normal vehicle operation, to produce a large voltage drop:

- (1) The resulting high battery current can cause damage to components through resistive heating.
- (2) The motor operates less efficiently under conditions of low voltage and high current.
- (3) Battery capacity is depleted more quickly and less efficiently at higher current densities.

For a given power requirement, the greater the battery's effective internal resistance, the larger the voltage drop. The effective internal resistance of a battery varies with depth-of-discharge.

In Figure 6-8, the effective internal resistance of each of the three development batteries has been voltage-normalized<sup>7</sup> and plotted versus depth-of-discharge. As shown in this figure, the Globe battery has less internal resistance than either of the two Ni-Fe batteries. Thus the Globe battery could be expected to exhibit the least voltage drop during acceleration. The internal resistance of the EPI battery is only slightly higher than that of the Globe battery. The internal resistance of the Westinghouse battery, however, is significantly higher than that of the other two batteries. Depending on the vehicle/battery combination, the high internal resistance of the Westinghouse battery could cause difficulties due to voltage drop during acceleration. Indeed, attempts to do a Schedule D range test using SCT-2 with the Westinghouse battery had to be abandoned because voltage drop during acceleration resulted in motor overheating after 32 driving cycles. Yet, SCT-2 completed 66 driving cycles during a Schedule D range test with the 90-cell EPI battery, and no motor overheating was observed.

The way in which effective internal resistance varies with depth-of-discharge is also important. Figure 6-8 shows that in both the EPI battery and the Globe battery, internal resistance remains nearly constant until about 75 to 80% depth-of-discharge. During normal use, the battery would seldom be discharged more than about 80%, so internal resistance would not fluctuate much. In the Westinghouse battery, however, internal resistance

---

<sup>7</sup>Calculations are shown in Appendix B.

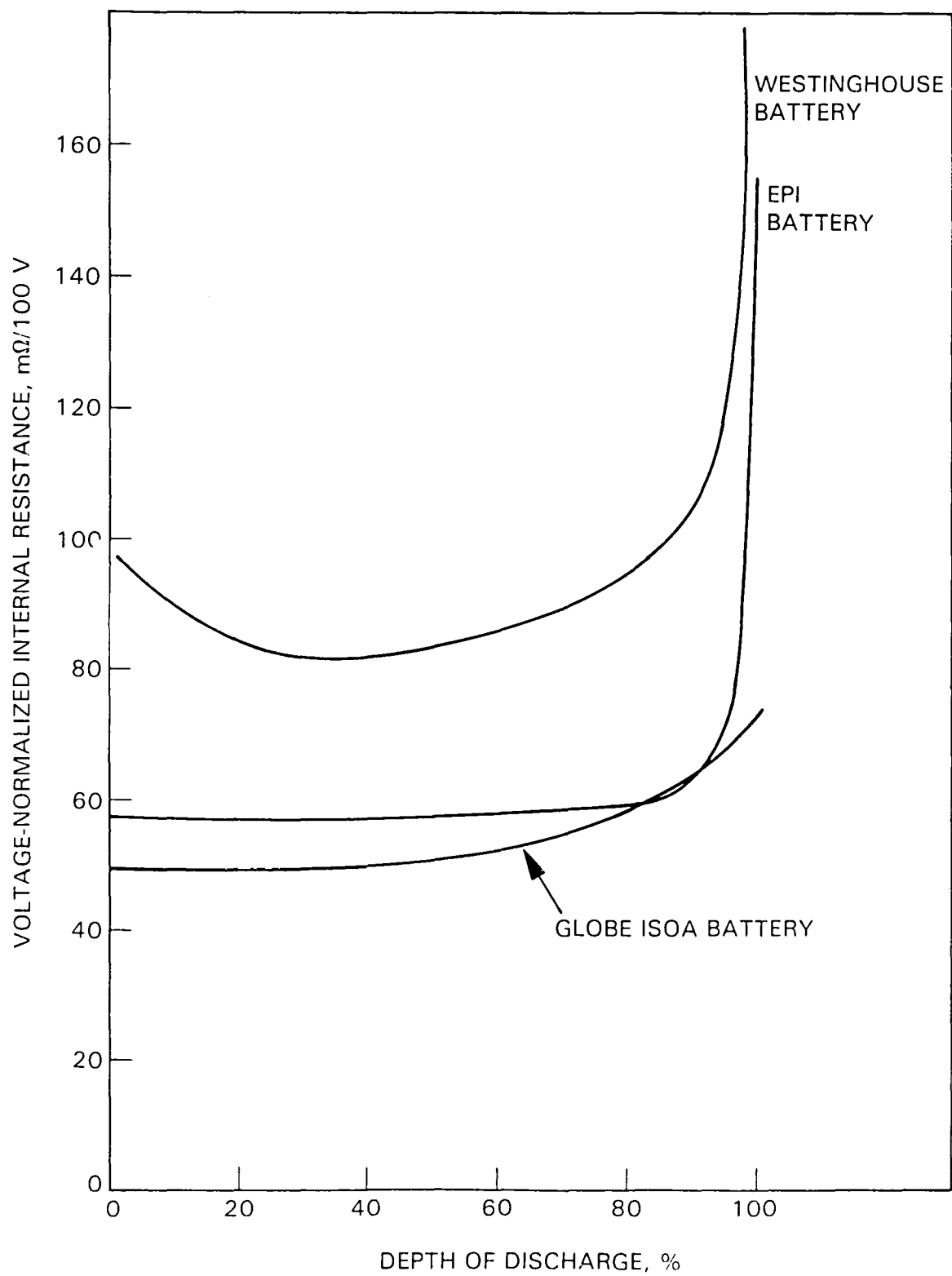


Figure 6-8. EPI, Globe, and Westinghouse Batteries: Voltage-Normalized Effective Internal Resistance versus Depth-of-Discharge

decreases between 0% depth-of-discharge and about 25% depth-of-discharge; after about 40% depth-of-discharge, internal resistance begins to increase rather rapidly through the end of discharge. Thus, the voltage response of the Westinghouse battery during acceleration would be less consistent throughout discharge than that of the other two batteries.

The reasons for the differences in the shape of each of the three curves shown in Figure 6-8 are not clearly understood, but some possible explanations can be postulated:

- (1) The very rapid increase in the internal resistance of the two Ni-Fe batteries, after about 95% depth-of-discharge, is undoubtedly due to final depletion of the active material. The Pb-A battery does not show this rapid increase because the voltage cut-off criterion is such that it is not discharged as deeply as the Ni-Fe batteries during Schedule C and Schedule D range tests.
- (2) The decreasing internal resistance of the Westinghouse battery from 0% depth-of-discharge to about 25% depth-of-discharge may be the result of self-heating. The EPI and the Globe batteries do not show this decrease in internal resistance during the first part of discharge, but neither does the temperature of these two batteries rise as much as that of the Westinghouse battery.
- (3) Differences in electrode construction may explain the rather rapid increase of internal resistance, after about 40% depth-of-discharge, in the Westinghouse battery as opposed to the very gradual increase in the EPI battery: a sintered, iron-powder plate is used in the EPI battery (Reference 3), whereas the active material for the iron electrode in the Westinghouse battery is pressed into a steel-fiber substrate (Reference 12). Thus, in the Westinghouse iron electrode, the interlacing of active material and conductive substrate is likely to be coarser than in the EPI iron electrode. Assuming the structure of the Westinghouse iron electrode to be coarser than that of the EPI iron electrode, the more rapid increase of internal resistance in the Westinghouse battery may be due to depletion of active material in the immediate vicinity of the conductive substrate. Internal resistance rises because the remaining active material is not in as close contact with the conductive substrate.

## 2. Effect of Temperature on Internal Resistance

The resistivity of sulfuric acid (the electrolyte in Pb-A batteries) and of potassium hydroxide (the electrolyte in Ni-Fe batteries) decreases as temperature increases. The electrolyte is responsible for a large portion of the battery's internal resistance (Reference 8), so internal resistance should also decrease as temperature increases. This was found to be true for the Globe battery: internal resistance decreased by 0.7-0.8% per °C during discharge. The effect of temperature on the internal resistance of the two Ni-Fe batteries was not tested. Increasing internal resistance at lower temperatures should be included in the vehicle/battery interface

considerations. If acceleration capability is only marginal with a warm battery, it is likely to be inadequate when the battery is cold.

### C. SELF-HEATING

High ambient temperatures can adversely affect battery performance. The degree to which high ambient temperatures present a problem depends on the self-heating of the battery system and on the effectiveness of the thermal management techniques used. If battery temperature is allowed to rise too high, the battery system may be permanently damaged. In addition, the charge acceptance of Ni-Fe batteries is impaired at elevated temperatures, even when battery temperature is not high enough to cause damage (Reference 11).

Of the three developmental batteries, the Globe battery exhibited the least amount of self-heating. During discharge, battery temperature seldom rose by as much as 10°C. During charge, temperature rises at first, but then remains constant, or even decreases as current tapers below about 7 A. A test series, consisting of four consecutive days of urban driving, was conducted to simulate normal vehicle use. During this test series, battery temperature fluctuated between 33°C and 28°C, and there was no overall increase in temperature, due to cumulative heating, when driving range was limited to about 30 mi. On the fourth day, a full discharge was done and battery temperature reached 36°C (13°C above ambient) by the end of this discharge. These temperatures are well below safe limits, and it does not appear that self-heating will be a problem for the Globe battery.

The EPI battery was charged and discharged daily during vehicle testing. The cells in the EPI battery are spaced apart to allow forced-air cooling, and air circulation was maintained with blowers. Nevertheless, some cumulative heating effects were seen in the EPI battery: temperature typically rose by about 4°C during a week of testing. During a full discharge, temperature typically rose by about 15°C. Unless a more effective means of cooling is used during charge, decreased charge acceptance at elevated temperatures is likely to impair capacity when the EPI battery is used at high ambient temperatures.

The Westinghouse battery was also charged and discharged daily during vehicle testing. However, cumulative temperature rise was prevented by the water cooling that was used during charge. Figure 5-24 shows a charge that was started at a high initial temperature. During the first part of charge, the EMS reduced battery temperature by 9°C. The water cooling in the EMS seems to be an effective means of controlling battery temperature during charge. During discharge, however, there is no cooling, and battery temperature rose by as much as 27°C during a full discharge. This self-heating during discharge is likely to present a problem at high ambient temperatures.

## D. RECHARGE CONSIDERATIONS

### 1. Procedure for the EPI Battery

The EPI battery was recharged at 60 A for 5 h (300 Ah) after every complete discharge; after a partial discharge, it was charged at 60 A until 120% of the previous discharge (on a coulombic basis) had been returned.

The voltage response of the battery during recharge is shown in Figure 5-5. As seen in this figure, the voltage of the 90-cell battery rises during the first 3.5 h of charge to a peak of about 152 V. The voltage remains fixed at this peak value for the remaining 1.5 h of charge. This last 1.5 h seems to be the least efficient portion of the charge. There are two indications that, during this time, the battery is not able to accept as much of the charge current as during the first 3.5 h:

- (1) During the last part of charge, there is a visible increase in the rate of gassing. This increased gassing is evidence of a drop in charge efficiency during this period: more of the current passing through the battery is being used for electrolysis so less is available for charging.
- (2) Figure 5-7 shows the temperature rise that occurs during the last part of charge, which indicates that some of the power going into the battery is being lost as heat rather than being stored as useful energy. Although battery temperature rises continually during charge, there is a sharp increase in the rate of this temperature rise during the last part of charge.

Battery response during this last portion of the charge is especially important, because during normal use, the battery would seldom be fully discharged.

More experimentation with the charge procedure for this battery would likely prove to be valuable. The increased electrolysis observed during the last 1.5 h of charge indicates that the current during this time is probably higher than is actually needed to charge the battery (Reference 13). It is possible that the battery could be fully charged with a lower current during the last portion of charge, and that this would improve the recharge efficiency--especially following a partial discharge. Lowering the current would at least reduce the recharge power requirement and decrease the gassing rate.

### 2. Procedure for the Globe Battery

A taper-charge procedure was used with the Globe battery. The battery was charged at 48 A until voltage reached 2.67 V/cell;<sup>8</sup> voltage was then maintained for a fixed time period. The length of this time period determined the amount of overcharge that the battery received. For an equalization charge, the time period was 9 h, and for a regular charge, it was 3 h.

---

<sup>8</sup>Referenced to 27°C (temperature compensation = -0.007 V/°C/cell).

A regular charge can be used after a discharge that is terminated at or before 80% depth-of-discharge, but an equalization charge is required after any discharge greater than 80% depth-of-discharge. In addition, an equalization charge is required after every seventh discharge, regardless of depth-of-discharge.

One purpose of the electrolyte stirring system is to increase recharge efficiency, which would reduce the amount of overcharge required. Globe has estimated (Reference 14) that an overcharge of 5% for the regular charges and 10% for the equalization charges (on a coulombic basis) would be sufficient to maintain full battery capacity. With the charge procedure used, the amount of overcharge actually given depends on how low the charge current tapers during the fixed-voltage portion of charge. With the first battery, charge current tapered to about 2.5 A by the end of the equalization charges, and the amount of overcharge was typically about 14%. With the second battery, however, charge current tapered to about 3.5 A by the end of the equalization charges, and the amount of overcharge was typically about 19%. The batteries were seldom discharged to less than 100% depth-of-discharge during vehicle testing, and the regular charge procedure was never used.

### 3. Procedure for the Westinghouse Battery

The manufacturer's recommended recharge procedure is a nominal 350-Ah charge consisting of a 70-A charge current for 5 h. A number of reliability problems were experienced while using this charge regime, and a taper charge was developed to improve reliability. With the taper charge procedure, the battery is charged at 70 A until it reaches 156 V. This voltage is then maintained until 300 Ah has been delivered to the battery.

It is recognized that some capacity is probably sacrificed by reducing the charge from 350 Ah to 300 Ah. However, it was felt that ensuring reliability was of more importance than maximizing capacity. Based on a limited number of constant-current-discharge tests, it appears that a capacity loss of about 6% is suffered when the amount of charge is reduced from 350 Ah to 300 Ah.

### 4. Efficiency

The recharge efficiencies typically obtained from the three developmental batteries during vehicle testing are shown in Table 6-2.<sup>9</sup> Efficiencies of the two baseline batteries and of the earlier version of the Westinghouse battery are also shown in this table.

During vehicle testing, discharges were seldom terminated before 100% depth-of-discharge, whereas, during normal use, the batteries would seldom be discharged below about 80% depth-of-discharge. In addition, the charge procedures generally were tailored to provide maximum capacity rather than maximum recharge efficiency. Because vehicle-range testing is not representative of normal use patterns, the recharge efficiency data shown in Table 6-2

---

<sup>9</sup>The equations used for calculating recharge efficiencies are shown in Appendix B.

Table 6-2. Typical Energy, Coulombic, and Voltage Efficiencies

Battery	Recharge Energy Efficiency, %	Coulombic Recharge Efficiency, %	Recharge Voltage Efficiency, %
EPI	60	77	79
Globe	71	86	83
Westinghouse	39	56	70
ETV-1 Baseline (prototype of Globe EV1000)	64	78	82
SCT-2 Baseline (Exide XPV-23)	62	77	80
Early Westinghouse	47	67	70

may not be representative of the efficiencies that would be obtained in a vehicle application.

Although the efficiency data in Table 6-2 was not obtained under conditions of normal use, these data provide information on the relative charge efficiencies of these battery technologies. As shown in Table 6-2, the Globe ISOA battery demonstrated the highest energy efficiency (71%). The energy efficiency of the EPI battery (60%) is slightly less than that of the two commercially-available, baseline Pb-A batteries (62% and 64%). The energy efficiency of the Westinghouse battery (39%) is much lower than that of the other batteries.

The energy efficiency of the Globe ISOA battery is substantially higher than that of the two baseline Pb-A batteries. As shown in Table 6-2, this improvement in energy efficiency is due to improved coulombic efficiency; voltage efficiency is only slightly higher than that of the other two batteries. The high coulombic efficiency of the ISOA battery indicates that the electrolyte stirring system is effective in preventing electrolyte stratification thus allowing more uniform utilization of active material.

The energy efficiency of the EPI battery is significantly less than that of the Globe ISOA battery. Most of this difference appears to be due to the lower coulombic efficiency of the EPI battery. Both the coulombic and the voltage efficiencies of the EPI battery are about the same as that of the two baseline Pb-A batteries. Thus, the efficiency of the EPI battery is comparable to that of a commercially-available, Pb-A propulsion battery.



The energy efficiency of the Westinghouse battery is much lower than that of either of the other two developmental batteries. This low energy efficiency appears to be due to both coulombic and voltage losses. The low voltage efficiency is probably a result of the high internal resistance of the Westinghouse battery, noted previously. It is surprising that the coulombic loss in the Westinghouse battery is about twice that in the EPI battery, even though the amount of gas released is about the same for both batteries. Apparently, a side reaction occurs in the Westinghouse battery which lowers the coulombic efficiency. The earlier version of the Westinghouse battery, that was tested in 1979, had a somewhat higher energy efficiency due to a higher coulombic efficiency.

## 5. Power Requirements

The recharge power profiles for each battery are shown in Section V (see Figures 5-6, 5-15, and 5-22). As shown by these profiles, the power requirements for charging these batteries are substantial: 9 kW for the 90-cell EPI battery, 5 kW for the Globe battery, and 10 kW for the Westinghouse battery. These requirements include only the dc power into the battery from the charger. The power required from a wall outlet would be higher because of charger inefficiencies.

The power requirement for the Globe battery was less than for the Ni-Fe batteries, but the Globe battery also had a lower system voltage than the Ni-Fe batteries. The high power requirements for charging these batteries may present difficulties for residential users.

## E. SAFETY AND MAINTENANCE CONSIDERATIONS

### 1. Gassing

The two Ni-Fe batteries release large amounts of hydrogen and oxygen gas each charge/discharge cycle. The Globe ISOA battery also releases these gasses, but the amount released is about a half the amount from the Ni-Fe batteries. Hydrogen has a broad flammability range in air, and this range is extended by the presence of oxygen. Safety provisions should be carefully considered, especially for the Ni-Fe batteries.

### 2. Watering

At the time of the vehicle tests, EPI had not yet developed a watering system for their Ni-Fe battery, and it was necessary to water each cell separately. Of the two developmental batteries with watering systems, the Westinghouse system is the easiest to use: water is simply poured into the EMS reservoir through a fill spout. Several difficulties were encountered while attempting to use the Globe watering system.<sup>10</sup>

The Ni-Fe batteries needed watering every second charge/discharge cycle, but the Globe battery only needed watering about every tenth charge/discharge

---

<sup>10</sup>See the test history for the Globe battery in Section IV.

cycle. The more frequent watering required by the Ni-Fe batteries would cause them to be less convenient in a vehicle application.

### 3. Leaks

Both Ni-Fe and Pb-A batteries have electrolyte which, in the case of a leak in the battery system, would pose a safety hazard. It is therefore important that the possibilities for electrolyte leaks be minimized.

The possibility of a leak through the case is probably greatest with the Ni-Fe batteries. Because of the higher gassing rates during charge, the EPI and the Westinghouse cells are likely to be subjected to higher internal pressures than the Globe modules.

The Westinghouse battery is especially likely to develop leaks because the electrolyte is circulated outside the cells through an extensive plumbing network (shown in Figure 3-11). Numerous opportunities for electrolyte leaks exist within this system. Indeed, this battery developed several leaks during the test program.

### 4. Reliability

Although the EMS of the Westinghouse battery facilitates thermal management, venting of gasses, and watering, and the electrolyte stirring system of the Globe battery prevents electrolyte stratification, these auxiliary systems present added complexity which may adversely affect system reliability. The Globe battery system is the most complex: the auxiliary components of this system consist of an air pump, valves, a control system for the pump and valve timing, manifolds, and a vacuum pump. However, if a problem were to develop in one of these components, it would not disable the battery. The Westinghouse battery is more vulnerable: if a problem were to develop in the EMS (such as pump failure), the battery could not be used until after being repaired.

## SECTION VII

### CONCLUSIONS

#### A. EPI BATTERY PERFORMANCE

The most outstanding features of this battery are its high specific energy and its ability to maintain a high energy capacity as discharge rate is increased. The capacity of this battery is very consistent and predictable under a variety of discharge regimes, and capacity under strenuous driving conditions is especially good. There are, however, several disadvantages of the EPI battery:

- (1) Self-discharge occurs when the battery stands without an applied load.
- (2) The power requirement for recharge is considerable.
- (3) Electrolysis during charge produces enough hydrogen gas to be a safety concern.
- (4) Frequent watering is required.

By lowering the current during the last part of charge, it may be possible to reduce the recharge power requirement somewhat, decrease the gassing rate considerably, and slow down water consumption without sacrificing capacity.

Because of its good capacity at high discharge rates, the EPI battery shows promise for electric vehicle applications. Although self-discharge has a significant effect on capacity, the magnitude of this phenomenon should not preclude use of the battery. Voltage drop during acceleration is moderate and should present no problems in a well-designed vehicle system. Recharge efficiency is only fair, but it is high enough for the battery to be viable.

#### B. GLOBE BATTERY PERFORMANCE

The specific energy of the Globe battery is significantly higher than that of the commercially-available Pb-A propulsion batteries tested at JPL. It is also less sensitive to discharge rate. Nevertheless, the specific energy of this battery is not as high as that of the EPI Ni-Fe battery. Voltage drop during acceleration is less than with either of the two Ni-Fe batteries, and should present no problems in a well-designed vehicle system. The use of an electrolyte stirring system has improved specific energy and recharge efficiency, but at the expense of increased system complexity.

As a Pb-A system, the Globe battery has several advantages over the Ni-Fe batteries:

- ° The self-discharge rate of a fully-charged battery is less.
- ° Less hydrogen gas is released during charge.
- ° Watering is required less frequently.
- ° The recharge power requirement is lower.

#### C. WESTINGHOUSE BATTERY PERFORMANCE

Performance limitations in several critical areas were observed in this battery:

- (1) Specific energy is low.
- (2) Voltage drop during acceleration is high.
- (3) Recharge energy efficiency is poor.

In addition, as with the EPI battery, frequent watering is required, large quantities of hydrogen gas are released during charge, and considerable power is required for recharge.

The EMS provides an effective means of cooling the battery during charge and makes watering a simple process. But, the need for electrolyte circulation through an extensive plumbing network, during both charge and discharge, makes the battery vulnerable: both to leaks and to inadequate electrolyte flow.

Recharge efficiency and specific energy were significantly better in the earlier version of the Westinghouse battery, indicating that it may be possible to improve performance in these areas. Unless performance improvements are made, the Westinghouse battery would not be a viable battery for electric-vehicle propulsion.

## SECTION VIII

### RECOMMENDATIONS

The following recommendations are based on the results of the vehicle tests and on the experience gained in handling the battery systems during testing:

- (1) The performance of the EPI Ni-Fe battery system is promising, especially in terms of energy capacity, and continued development is encouraged.
- (2) The Globe ISOA battery technology offers the potential for good battery performance with a minimum of maintenance and safety requirements. Development of this technology should be continued.
- (3) If development work with the Westinghouse Ni-Fe battery is to be continued, the reasons for the low capacity, high internal resistance, and poor recharge efficiency of this battery should be determined. Any further development work on this battery technology should be concentrated on alleviating these problems.
- (4) More research should be done to determine the optimum recharge procedure for the EPI Ni-Fe battery.
- (5) The cooling requirements of the EPI battery during operation in high ambient temperature conditions should be investigated.
- (6) Further development work should be done to improve the Globe watering system.
- (7) Further testing should be done to quantify the effects of temperature on these batteries and to fully characterize self-discharge of the Ni-Fe batteries.
- (8) All three developmental batteries generate hydrogen gas, and adequate safety precautions should be a primary consideration in their use.



## SECTION IX

### REFERENCES

1. Development of Aqueous Batteries for Electric Vehicles, Summary Report, Oct. 1979 - Sept. 1980, Argonne National Laboratory, Argonne, Illinois, Prepared for the U.S. Department of Energy under Contract No. W-31-109-Eng-38.
2. Bryant, J., et al., Upgraded Demonstration Vehicle Task Report, JPL Publication 81-98, Jet Propulsion Laboratory, Pasadena, Calif., Oct. 15, 1981.
3. Design and Cost Study for Nickel-Iron Oxide Electric Vehicle Batteries, Prepared for Argonne National Laboratory, by Eagle-Picher Industries, Inc., Final Report, Contract No. 31-109-38-3709, June 1, 1979.
4. Inkman, Mark S., Method and Apparatus for Storage Battery Electrolyte Circulation, U.S. Patent 4,221,847, (assigned to Globe-Union, Inc.) U.S. Department of Commerce, Washington, Sept. 9, 1980.
5. Hardy, K., Interim Report: Westinghouse Ni-Fe Battery, unpublished JPL report, prepared for the U.S. Department of Energy, Dec. 10, 1980.
6. Price, T.W., Shain, T.W., and Bryant, J.A., Vehicle Test Report: South Coast Technology Electric Conversion of a Volkswagen Rabbit, JPL Publication 81-28, Jet Propulsion Laboratory, Pasadena, Calif., February 15, 1981.
7. Near-Term Electric Vehicle Phase II-Final Report, Contract No. DE-AC03-76CS51294, submitted to the Department of Energy by Corporate Research and Development, General Electric Company, Schenectady, N.Y.
8. Vinal, G.W., Storage Batteries, fourth edition, John Wiley & Sons, Inc., New York, N.Y. 1955.
9. Hewitt, R., Test Results: Electric Test Vehicle-1 with the Eagle-Picher Nickel-Iron Battery, JPL Internal Report 5030-510, Jet Propulsion Laboratory, Pasadena, Calif., Sept. 1, 1981.
10. Morehouse, C.K., Glicksman, R., and Lozier, G.S., "Batteries," Proceedings of the IRE, Vol. 46, No. 8, August 1958; from Selected Papers On New Techniques for Energy Conversion, S.N. Levine, ed., Dover Publications, Inc., New York, N.Y., 1961.
11. Comprehensive Treatise of Electrochemistry, Volume 3: Electrochemical Energy Conversion and Storage. Edited by J. O'M. Bockris, et al., Plenum Press, New York, 1981.
12. Research, Development, and Demonstration of Nickel-Iron Batteries for Electric Vehicle Propulsion, prepared for Argonne National Laboratory by Westinghouse Electric Corporation, Annual Report, Contract No. 31-109-38-4141, March 1981.

13. Mantell, C.L., Batteries and Energy Systems, McGraw-Hill Book Company, 1970.
14. Burke, A.F., The Hybrid Test Vehicle (HTV)-From Concept Through Fabrication and Marketing, SAE Paper 820266, 1982.
15. Mantell, C.L., Industrial Electrochemistry, McGraw-Hill Book Company, 1931.
16. Handbook of Chemistry and Physics, 52nd edition. Edited by R.C. Weast, The Chemical Rubber Publishing Company, Cleveland, Ohio, 1971-1972.



APPENDIX A

BATTERY SYSTEM SPECIFICATIONS



## THE EAGLE-PICHER NICKEL-IRON BATTERY SYSTEM

### Description

Manufacturer's Designation ----- VNF 300

Rated Capacity ----- 270 Ah @ 90 A

Nominal Voltage ----- 1.2 V/cell

Weight (Cells + Frame)

80-Cell Battery ----- 595 kg

90-Cell Battery ----- 670 kg

### Charge Procedure

After a Full Discharge ----- 60 A for 5 h (300 Ah)

After a Partial Discharge ----- 60 A until 120% of previous  
discharge (on an Ah basis) has  
been returned.

### Test Termination Criteria

During Cruise ----- 1.0 V/cell

During Acceleration ----- 0.5 V/cell

## THE GLOBE ISOA LEAD-ACID BATTERY SYSTEM

### Description

Manufacturer's Designation ----- EV-3000  
Rated Capacity ----- 249 Ah @ 83 A  
Nominal Voltage ----- 1.9 V/cell  
Weight<sup>1</sup> ----- 602 kg

### Charge Procedure

Following Discharges of ----- 48 A until voltage reaches  
More Than 80%, or for 2.67 V/cell.<sup>2</sup> Hold temperature-  
Equalization compensated voltage constant until  
110% of previous discharge (on an  
Ah basis) has been returned.

Regular Charge ----- Same as for equalization,  
but return only 103% of previous  
discharge.

### Test Termination Criteria

During Cruise ----- 1.75 V/cell  
During Acceleration ----- 1.3 V/cell

---

<sup>1</sup>Weight includes 5 kg for the pump and the manifolds.

<sup>2</sup>Referenced to 27°C (Temperature Compensation = -0.007 V/°C/cell.)

## THE WESTINGHOUSE NICKEL-IRON BATTERY SYSTEM

### Description

Manufacturer's Designation ----- none  
Rated Capacity ----- 220 Ah @ 73 A  
Nominal Voltage ----- 1.2 V/cell  
Weight<sup>3</sup> ----- 607 kg

### Charge Procedure

After a Full Discharge ----- 70 A until voltage reaches  
157 V. Hold voltage constant;  
continue charge until 300 Ah has  
been returned.  
After a Partial Discharge ----- Has not been determined.

### Test Termination Criteria

During Cruise ----- 1.0 V/cell  
During Acceleration ----- 0.5 V/cell

---

<sup>3</sup>Weight includes cables, hoses, manifolds, circulation pump, electrolyte storage tank, and 40 liters of electrolyte in tank.



APPENDIX B

SUPPORTING CALCULATIONS

AND

DATA ANALYSIS TECHNIQUES





## A. EQUATIONS

Equations that were used for calculating common battery parameters are listed below.

$$\text{Specific energy} = \frac{\text{Discharge energy from battery}}{\text{Battery mass}} \quad (1)$$

$$\text{Recharge energy efficiency} = \frac{\text{Discharge energy from battery}}{\text{Recharge energy}} \quad (2)$$

$$\text{Coulombic recharge efficiency} = \frac{\text{Coulombic battery discharge}}{\text{Coulombic recharge}} \quad (3)$$

$$\text{Recharge voltage efficiency} = \frac{\text{Recharge energy efficiency}}{\text{Coulombic recharge efficiency}} \quad (4)$$

$$\text{Average power} = \frac{\text{Discharge energy from battery}}{\text{Discharge time}} \quad (5)$$

## B. AVERAGED RESULTS OF RANGE TESTS

Tables 5-1, 5-2, 5-3, 5-6, and 5-9 summarize the results of all valid range tests with the developmental batteries. Equations (1), (2), and (3) were used to calculate the parameters in these tables.

Tables 5-1 and 5-2 show the results of range tests with the 80-cell EPI battery. The battery cycles shown in Table B-1 were used as data sources for Table 5-1.

Table B-1. Data Sources for Table 5-1

Test Type	Battery Cycles
56 km/h (35 mi/h)	114
72 km/h (45 mi/h)	110, 118
80 km/h (50 mi/h)	120
Schedule C	112, 130

The battery cycles shown in Table B-2 were used as data sources for Table 5-2.

Table B-2. Data Sources for Table 5-2

Test Type	Battery Cycles
56 km/h (35 mi/h)	121
72 km/h (45 mi/h)	106, 125
88 km/h (55 mi/h)	122
Schedule C	124, 129
Schedule D	123, 126

The raw data from these range tests are shown in Appendix E. For calculations involving the 80-cell EPI battery, a battery mass of 595 kg was used.

Table B-3 shows the results of range tests with the 90-cell EPI battery. The battery cycles shown in Table B-3 were used as data sources for Table 5-3.

Table B-3. Data Sources for Table 5-3

Test Type	Battery Cycles
56 km/h (35 mi/h)	138
72 km/h (45 mi/h)	135
88 km/h (55 mi/h)	136
Schedule C	137
Schedule D	140

The raw data from these range tests are shown in Appendix F. For calculations involving the 90-cell EPI battery, a battery mass of 670 kg was used.

Table 5-6 shows the results of range tests with the Globe ISOA battery. The battery cycles shown in Table B-4 were used as data sources for Table 5-6.

Table B-4. Data Sources for Table 5-6

Test Type	ISOA-1 Battery Cycles	ISOA-2 Battery Cycles
56 km/h (35 mi/h)	60	60, 61, 64
72 km/h (45 mi/h)	58	42, 52, 59
88 km/h (55 mi/h)	61, 62, 64	43, 63
Schedule C	63	--
Schedule D	59, 65	--

The raw data from range tests with the ISOA-1 battery are shown in Appendix G, and the raw data from range tests with the ISOA-2 battery are shown in Appendix H. For calculations involving the Globe ISOA battery, a battery mass of 602 kg was used.

Table 5-9 shows the results of range tests with the Westinghouse battery. Only data from tests with the W-220-3 battery were used in this table. The battery cycles shown in Table B-5 were used as data sources for Table 5-9.

The raw data from range tests with the W-220-3 battery are shown in Appendix K. For calculations involving the Westinghouse battery, a battery mass of 607 kg was used.

Table B-5. Data Sources for Table 5-9

Test Type	W-220-3 Battery Cycles
56 km/h (35 mi/h)	11, 13, 24, 25
72 km/h (45 mi/h)	10, 12, 21
88 km/h (55 mi/h)	15, 19, 22, 23
Schedule C	14, 20

### C. SPECIFIC ENERGY VERSUS AVERAGE POWER

Figures 5-1, 5-8, 5-17, 6-1, 6-2, 6-3, 6-6, and 6-7 show battery specific energy as a function of the average power requirements during constant-speed driving. Equations (1) and (5) were used to calculate the data points shown in these figures.

Figure 5-1 shows the results of all valid constant-speed range tests with the 80-cell EPI battery. A battery mass of 595 kg was used for the 80-cell battery. The data used to generate this figure are listed in Table B-6.

Table B-6. Tabulation of Data Shown in Figure 5-1

Battery Cycle	Battery Discharge Energy, kWh	Specific Energy, Wh/kg	Average Power, kW
106	22.128	37.2	8.066
110	22.757	38.2	9.378
114	22.967	38.6	6.350
118	22.767	38.3	9.186
120	22.233	37.4	11.51
121	22.500	37.8	5.618
122	21.831	36.7	11.38
125	22.467	37.8	8.019

Figure 5-8 shows the results of all valid constant-speed range tests with the Globe ISOA Pb-A battery. A battery mass of 602 kg was used for this battery. Data from tests with both the ISOA-1 and the ISOA-2 batteries are used, but the data from tests of the ISOA-1 battery were corrected to account for the fact that a termination voltage of 1.65 V/cell rather than 1.75 V/cell was used with the ISOA-1 battery. This correction was made for each test by examining the magnetic-tape data, and determining the amount of battery energy removed from the time voltage reached 1.75 V/cell until the start of vehicle deceleration. The battery energy removed during this time interval was subtracted from the total battery discharge energy. The data used to generate Figure 5-8 are listed in Table B-7.

Table B-7. Tabulation of Data Shown in Figure 5-8

ISOA-1 Battery Cycle	Battery Discharge Energy, kWh	Specific Energy, Wh/kg	Average Power, kW
58	19.05	31.64	8.539
60	20.12	33.42	5.793
61	16.6	27.34	11.95
ISOA-2 Battery Cycle	Battery Discharge Energy, kWh	Specific Energy, Wh/kg	Average Power, kW
42	19.68	32.70	7.932
43	17.08	28.37	10.90
52	19.26	31.99	7.915
59	18.65	30.99	8.188
60	22.24	36.94	5.588
61	22.44	37.28	5.568
63	16.47	27.36	11.31
64	21.90	36.38	5.434

Figure 5-17 shows the results of all valid constant-speed range tests with the Westinghouse battery. A battery mass of 607 kg was used for this battery. The data used to generate Figure 5-17 are shown in Table B-8.

Table B-8. Tabulation of Data Shown in Figure 5-17

W-220-3 Battery Cycle	Battery Discharge Energy, kWh	Specific Energy, Wh/kg	Average Power, kW
10	18.006	29.66	9.258
11	19.157	31.56	6.636
14	17.551	28.91	5.870
15	15.680	25.83	14.77
22	15.821	26.06	14.47
23	15.594	25.69	14.64
24	18.872	31.09	6.626
25	19.053	31.39	6.654

In Figure 6-1, the curves of Figure 5-1 and 5-17 have been redrawn as the solid curves for the EPI and the Westinghouse batteries. The dashed curve in Figure 6-1 was obtained from the solid curve for the Westinghouse battery by multiplying the specific energy of the Westinghouse battery by 1.06. This 6% increase in specific energy is an estimate of the increase in capacity that could have been obtained by using a 350-Ah charge rather than a 300-Ah charge with the Westinghouse battery.

This estimate is based on data from constant-current-discharge tests of the W-220-3 battery. A 300-Ah charge was used for Battery Cycles 4 and 5, and energy capacity was 18.8 kWh; a 340-Ah charge was used for the next cycle, and energy capacity increased by 7% to 20.1 kWh. Similarly, 350-Ah charges were used for Battery Cycles 35 and 36, and energy capacity was 19.7 kWh; 300-Ah charges were used for the next two cycles, and energy capacity decreased by 5% to 18.7 kWh. It is therefore estimated that about 6% more energy capacity could be obtained by increasing the amount of recharge from 300 Ah to 350 Ah.

In Figure 6-2, the curve of Figure 5-17 has been redrawn as the solid curve for the current version of the Westinghouse battery. The four data points from tests of the 1979 version of the Westinghouse battery are based on data found in Reference 2. These data are listed in Table B-9. The dashed curve showing the estimated specific energy of the 1979 battery has been placed halfway between the two low-power data points.

Table B-9. Data for the 1979 Version of the Westinghouse Battery

Battery Discharge Energy, kWh	Specific Energy, Wh/kg	Average Power, kW
17.08	28.95	12.65
19.79	33.55	5.69
17.30	29.33	12.32
16.51	27.99	5.47

In Figure 6-3, the curve of Figure 5-8 has been redrawn as the curve for the Globe ISOA battery. The curve for the SCT-2 baseline battery is based on the data listed in Table B-10.

Table B-10. Data for the SCT-2 Baseline Battery

SCT-2 Test	Battery Discharge Energy, kWh	Specific Energy, Wh/kg	Average Power, kW
44	14.54	28.29	9.49
51	14.52	28.81	9.53
57	16.10	31.32	6.26
59	11.68	22.72	14.48
61	13.18	25.65	9.84
62	10.59	20.61	15.24
63	13.61	26.48	9.14
64	10.95	21.31	14.38
65	14.55	28.31	6.08
66	14.34	27.90	6.00

The mass of the SCT-2 baseline battery is 514 kg. The curve for the ETV-1 baseline battery is based on the data listed in Table B-11. The mass of the ETV-1 baseline battery is 490 kg.

Table B-11. Data for the ETV-1 Baseline Battery

ETV-1-2 Test	Battery Discharge Energy, kWh	Specific Energy, Wh/kg	Average Power, kW
5	12.02	24.53	11.21
7	13.86	28.29	8.05
12	13.69	27.94	7.87
-----			
15	13.61	27.77	7.97
16	13.39	27.32	8.24
21	15.79	32.23	5.86
-----			
22	16.20	33.07	5.79
23	13.31	27.16	8.11
24	16.10	32.85	5.73

In Figure 6-6, the curves of Figures 5-1 and 5-17 have been redrawn as the solid curves for the EPI and the Westinghouse batteries. The dashed curve for the Globe ISOA battery was obtained by multiplying the specific energy of the Globe battery by 1.11. This 11% increase in specific energy is an estimate of the amount capacity would be increased if the discharges had been done at 33°C rather than at 23°C. This estimate is based on a capacity increase of 1.1% per °C.

In Figure 6-7, the curve of Figure 5-8 has been redrawn as the solid curve for the Globe battery. The dashed curves for the EPI and for the Westinghouse batteries were obtained by multiplying the specific energy of these batteries by 0.88. This 12% decrease in specific energy is an estimate, based on the data shown in Figure 6-4, of the amount that capacity would be decreased by self-discharge after an overnight stand.



#### D. SELF-HEATING

Tables 5-5, 5-8, and 5-12 show the average temperature rise, due to self-heating, for each battery during charge and discharge. The test data used to generate Table 5-5 are listed in Tables B-12 through B-23. The test data used to generate Table 5-8 are listed in Tables B-24 through B-35. The data used to generate Table 5-12 are listed in Tables B-36 through B-43. No data are shown for self-heating of the Westinghouse battery during charge because, as shown in Figures 5-23 and 5-24, temperature is controlled by the Electrolyte Management System (EMS).

Table B-12. EPI Battery: Temperature Rise  
During 56 km/h (35 mi/h) Tests

Battery	Battery Cycle	Temperature at Start of Discharge, °C	Temperature at End of Discharge, °C	Temperature Rise During Discharge, °C
80-cell	114	30.7	44.4	13.7
80-cell	121	31.3	43.9	12.6
90-cell	138	32.7	41.8	9.1

Table B-13. EPI Battery: Temperature Rise  
During 72 km/h (45 mi/h) Tests

Battery	Battery Cycle	Temperature at Start of Discharge, °C	Temperature at End of Discharge, °C	Temperature Rise During Discharge, °C
80-cell	106	32.4	47.2	14.8
80-cell	110	34.0	49.8	15.8
80-cell	118	33.5	48.7	15.2
80-cell	125	34.0	48.5	14.5
90-cell	135	30.7	44.6	13.9

Table B-14. EPI Battery: Temperature Rise  
During 88 km/h (55 mi/h) Tests

Battery	Battery Cycle	Temperature at Start of Discharge, °C	Temperature at End of Discharge, °C	Temperature Rise During Discharge, °C
80-cell	122	33.9	50.4	16.5
90-cell	136	32.7	47.8	15.1

Table B-15. EPI Battery: Temperature Rise  
During Schedule C Tests

Battery	Battery Cycle	Temperature at Start of Discharge, °C	Temperature at End of Discharge, °C	Temperature Rise During Discharge, °C
80-cell	124	31.5	47.2	15.7
80-cell	129	33.9	50.7	16.8
80-cell	130	33.3	50.0	16.7
90-cell	137	31.9	45.1	13.2

Table B-16. EPI Battery: Temperature Rise  
During Schedule D Tests

Battery	Battery Cycle	Temperature at Start of Discharge, °C	Temperature at End of Discharge, °C	Temperature Rise During Discharge, °C
80-cell	123	33.7	54.8	21.1
80-cell	126	33.7	55.0	21.3
90-cell	140	28.2	46.8	18.6

Table B-17. EPI Battery: Temperature Rise to 50% Depth-of-Discharge During 56 km/h (35 mi/h) Tests

Battery	Battery Cycle	Temperature at Start of Discharge, °C	Temperature at 50% DoD, °C	Temperature Rise to 50% DoD, °C
90-cell	138	32.7	36.2	3.5

Table B-18. EPI Battery: Temperature Rise to 50% Depth-of-Discharge During 72 km/h (45 mi/h) Tests

Battery	Battery Cycle	Temperature at Start of Discharge, °C	Temperature at 50% DoD, °C	Temperature Rise to 50% DoD, °C
80-cell	110	34.0	40.4	6.4
80-cell	118	33.5	39.8	6.3
90-cell	135	30.7	36.4	5.7

Table B-19. EPI Battery: Temperature Rise to 50% Depth-of-Discharge During 88 km/h (55 mi/h) Tests

Battery	Battery Cycle	Temperature at Start of Discharge, °C	Temperature at 50% DoD, °C	Temperature Rise to 50% DoD, °C
90-cell	136	32.7	38.5	5.8

Table B-20. EPI Battery: Temperature Rise to 50% Depth-of-Discharge During Schedule C Tests

Battery	Battery Cycle	Temperature at Start of Discharge, °C	Temperature at 50% DoD, °C	Temperature Rise to 50% DoD, °C
80-cell	130	33.3	40.6	7.3
90-cell	137	31.9	36.2	4.3

Table B-21. EPI Battery: Temperature Rise to 50% Depth-of-Discharge During Schedule D Tests

Battery	Battery Cycle	Temperature at Start of Discharge, °C	Temperature at 50% DoD, °C	Temperature Rise to 50% DoD, °C
90-cell	140	28.2	36.3	8.0

Table B-22. EPI Battery: Temperature Rise During Recharge After a Partial Discharge

Battery	Battery Cycle	Temperature at Start of Recharge, °C	Temperature at End of Recharge, °C	Temperature Rise During Recharge, °C
80-cell	108	25.7	33.8	8.1
80-cell	109	24.9	30.8	5.9
80-cell	112	28.5	35.7	7.2

Table B-23. EPI Battery: Temperature Rise During Recharge After a Full Discharge

Battery	Battery Cycle	Temperature at Start of Recharge, °C	Temperature at End of Recharge, °C	Temperature Rise During Recharge, °C
80-cell	111	26.8	33.3	6.5
80-cell	113	27.1	34.6	7.5
80-cell	114	20.6	28.8	8.2
80-cell	115	25.7	33.5	7.8
80-cell	116	26.5	33.7	9.4
80-cell	118	24.3	33.3	9.0

Table B-23. EPI Battery: Temperature Rise During Recharge  
After a Full Discharge (cont'd)

Battery	Battery Cycle	Temperature at Start of Recharge, °C	Temperature at End of Recharge, °C	Temperature Rise During Recharge, °C
80-cell	119	24.6	34.1	9.5
80-cell	120	25.7	34.4	8.7
80-cell	121	20.6	31.3	10.7
80-cell	122	23.4	33.9	10.5
80-cell	123	26.9	33.7	6.8
80-cell	124	20.6	31.3	10.7
80-cell	125	25.8	33.7	7.9
80-cell	126	26.2	33.7	7.5
80-cell	127	28.1	34.6	6.5
80-cell	129	24.5	33.8	9.3
80-cell	130	21.9	32.9	11.0
90-cell	131	21.9	32.1	10.2
90-cell	133	26.4	33.8	7.4
90-cell	134	20.8	37.5	16.7
90-cell	135	21.1	31.1	10.0
90-cell	136	25.7	33.9	8.2
90-cell	137	25.3	31.8	6.5
90-cell	139	21.0	31.4	10.4

Table B-24. Globe ISOA Battery: Temperature Rise  
During 56 km/h (35 mi/h) Tests

Battery	Battery Cycle	Temperature at Start of Discharge, °C	Temperature at End of Discharge, °C	Temperature Rise During Discharge, °C
ISOA-1	60	22.7	25.6	2.8
ISOA-2	60	23.6	27.6	4.0
ISOA-2	61	23.3	27.3	4.0
ISOA-2	64	22.9	27.0	4.1

Table B-25. Globe ISOA Battery: Temperature Rise  
During 72 km/h (45 mi/h) Tests

Battery	Battery Cycle	Temperature at Start of Discharge, °C	Temperature at End of Discharge, °C	Temperature Rise During Discharge, °C
ISOA-1	58	22.2	26.2	4.0
ISOA-2	42	21.7	26.7	5.0
ISOA-2	51	21.3	27.5	6.2
ISOA-2	52	24.3	29.9	5.6
ISOA-2	59	21.0	27.0	6.0

Table B-26. Globe ISOA Battery: Temperature Rise  
During 88 km/h (55 mi/h) Tests

Battery	Battery Cycle	Temperature at Start of Discharge, °C	Temperature at End of Discharge, °C	Temperature Rise During Discharge, °C
ISOA-1	61	24.1	29.8	5.7
ISOA-2	43	23.9	30.2	6.3
ISOA-2	63	24.3	30.8	6.5

Table B-27. Globe ISOA Battery: Temperature Rise During Schedule C Tests

Battery	Battery Cycle	Temperature at Start of Discharge, °C	Temperature at End of Discharge, °C	Temperature Rise During Discharge, °C
ISOA-1	63	21.4	28.2	6.8

Table B-28. Globe ISOA Battery: Temperature Rise During Schedule D Tests

Battery	Battery Cycle	Temperature at Start of Discharge, °C	Temperature at End of Discharge, °C	Temperature Rise During Discharge, °C
ISOA-1	59	21.4	30.9	9.5
ISOA-1	65	22.1	30.9	8.8

Table B-29. Globe ISOA Battery: Temperature Rise to 50% Depth-of-Discharge During 56 km/h (35 mi/h) Tests

Battery	Battery Cycle	Temperature at Start of Discharge, °C	Temperature at 50% DoD, °C	Temperature Rise to 50% DoD, °C
ISOA-2	60	23.6	26.0	2.4
ISOA-2	61	23.3	25.7	2.4
ISOA-2	64	22.9	25.4	2.5

Table B-30. Globe ISOA Battery: Temperature Rise to 50% Depth-of-Discharge During 72 km/h (45 mi/h) Tests

Battery	Battery Cycle	Temperature at Start of Discharge, °C	Temperature at 50% DoD, °C	Temperature Rise to 50% DoD, °C
ISOA-2	42	21.7	24.3	2.6
ISOA-2	51	21.3	24.7	3.4
ISOA-2	52	24.3	27.6	3.2
ISOA-2	59	21.0	24.6	3.6

Table B-31. Globe ISOA Battery: Temperature Rise to 50% Depth-of-Discharge During 88 km/h (55 mi/h) Tests

Battery	Battery Cycle	Temperature at Start of Discharge, °C	Temperature at 50% DoD, °C	Temperature Rise to 50% DoD, °C
ISOA-2	43	23.9	27.3	3.4
ISOA-2	63	24.3	28.3	4.0

Table B-32. Globe ISOA Battery: Temperature Rise to 50% Depth-of-Discharge During Schedule C Tests

Battery	Battery Cycle	Temperature at Start of Discharge, °C	Temperature at 50% DoD, °C	Temperature Rise to 50% DoD, °C
ISOA-1	62	21.4	24.3	2.9



Table B-33. Globe ISOA Battery: Temperature Rise to 50% Depth-of-Discharge During Schedule D Tests

Battery	Battery Cycle	Temperature at Start of Discharge, °C	Temperature at 50% DoD, °C	Temperature Rise to 50% DoD, °C
ISOA-1	65	22.1	25.9	3.8

Table B-34. Globe ISOA Battery: Temperature Rise During Recharge After a Partial Discharge

Battery	Battery Cycle	Temperature at Start of Recharge, °C	Temperature at End of Recharge, °C	Temperature Rise During Recharge, °C
ISOA-2	49	29.7	34.7	5.0
ISOA-2	71	29.3	31.9	2.3
ISOA-2	72	28.6	31.0	2.4

Table B-35. Globe ISOA Battery: Temperature Rise During Recharge After a Full Discharge

Battery	Battery Cycle	Temperature at Start of Recharge, °C	Temperature at End of Recharge, °C	Temperature Rise During Recharge, °C
ISOA-2	52	27.7	35.9	8.1
ISOA-2	59	26.0	33.7	7.7
ISOA-2	60	25.7	34.3	8.6
ISOA-2	61	26.5	34.6	8.0
ISOA-2	63	27.9	33.9	6.0
ISOA-2	64	26.8	34.6	7.8

Table B-35. Globe ISOA Battery: Temperature Rise During Recharge After a Full Discharge (cont'd)

Battery	Battery Cycle	Temperature at Start of Recharge, °C	Temperature at End of Recharge, °C	Temperature Rise During Recharge, °C
ISOA-2	65	29.3	32.4	3.1
ISOA-2	69	27.9	33.7	5.8
ISOA-2	70	29.2	32.9	3.7
ISOA-2	75	26.7	34.4	7.7

Table B-36. Westinghouse Battery: Temperature Rise During 56 km/h (35 m/h) Tests

Battery	Battery Cycle	Temperature at Start of Discharge, °C	Temperature at End of Discharge, °C	Temperature Rise During Discharge, °C
W-220-3	11	30.1	51.6	21.5
W-220-3	13	31.9	53.6	21.7
W-220-3	24	31.4	53.4	22.0
W-220-3	25	31.9	54.0	22.1

Table B-37. Westinghouse Battery: Temperature Rise During 72 km/h (45 mi/h) Tests

Battery	Battery Cycle	Temperature at Start of Discharge, °C	Temperature at End of Discharge, °C	Temperature Rise During Discharge, °C
W-220-3	10	30.4	53.0	22.6
W-220-3	21	30.1	54.4	24.3

Table B-38. Westinghouse Battery: Temperature Rise During 88 km/h (55 mi/h) Tests

Battery	Battery Cycle	Temperature at Start of Discharge, °C	Temperature at End of Discharge, °C	Temperature Rise During Discharge, °C
W-220-3	15	31.7	55.6	23.9
W-220-3	19	31.8	56.2	24.4
W-220-3	22	31.9	56.0	24.1
W-220-3	23	31.6	55.6	24.0

Table B-39. Westinghouse Battery: Temperature Rise During Schedule C Tests

Battery	Battery Cycle	Temperature at Start of Discharge, °C	Temperature at End of Discharge, °C	Temperature Rise During Discharge, °C
W-220-3	14	31.7	58.0	26.3
W-220-3	20	30.7	58.3	27.6

Table B-40. Westinghouse Battery: Temperature Rise to 50% Depth-of-Discharge During 56 km/h (35 mi/h) Tests

Battery	Battery Cycle	Temperature at Start of Discharge, °C	Temperature at 50% DoD, °C	Temperature Rise to 50% DoD, °C
W-220-3	11	30.1	40.2	10.1
W-220-3	13	31.9	42.2	10.3
W-220-3	24	31.4	41.7	10.3
W-220-3	25	31.9	42.1	10.2

Table B-41. Westinghouse Battery: Temperature Rise to 50% Depth-of-Discharge During 72 km/h (45 mi/h) Tests

Battery	Battery Cycle	Temperature at Start of Discharge, °C	Temperature at 50% DoD, °C	Temperature Rise to 50% DoD, °C
W-220-3	10	30.4	40.5	10.1
W-220-3	21	30.1	41.5	11.4

Table B-42. Westinghouse Battery: Temperature Rise to 50% Depth-of-Discharge During 88 km/h (55 mi/h) Tests

Battery	Battery Cycle	Temperature at Start of Discharge, °C	Temperature at 50% DoD, °C	Temperature Rise to 50% DoD, °C
W-220-3	15	31.7	41.7	10.0
W-220-3	19	31.8	42.0	10.2
W-220-3	22	31.9	41.7	9.8
W-220-3	23	31.6	41.6	10.0

Table B-43. Westinghouse Battery: Temperature Rise to 50% Depth-of-Discharge During Schedule C Tests

Battery	Battery Cycle	Temperature at Start of Discharge, °C	Temperature at 50% DoD, °C	Temperature Rise to 50% DoD, °C
W-220-3	14	31.7	42.8	11.1
W-220-3	20	30.7	42.8	12.1

#### E. EFFECT OF TEMPERATURE ON CAPACITY

Two 72 km/h (45 mi/h) range tests (Battery Cycles 74 and 75) were conducted with the ISOA-2 battery to determine the effect of temperature on capacity. These range tests were conducted after the ISOA-2 battery began to lose capacity as a result of the excessive overcharge. Although the absolute magnitude of battery capacity during these two tests is impaired, it is assumed that the relative effect of temperature on capacity is the same as for an undamaged battery. The following results were obtained:

For Battery Cycle 74

Battery temperature at start of discharge = 28.7°C.  
Battery discharge energy = 18.99 kWh.

For Battery Cycle 75

Battery temperature at start of discharge = 22.7°C.  
Battery discharge energy = 17.75 kWh.

The average discharge energy for these two tests is

$$\text{Average energy} = \frac{(18.99 + 17.75)\text{kWh}}{2} = 18.37 \text{ kWh}$$

Thus,

$$\text{the temperature effect} = \frac{(18.99 - 17.75)\text{kWh}}{18.37 \text{ kWh} \times (28.7 - 22.7)^{\circ}\text{C}} \times 100\% = 1.1\% \text{ per } ^{\circ}\text{C}$$

#### F. INTERNAL RESISTANCE

Figures 5-3, 5-4, 5-9, 5-11, 5-19, and 6-8 show the effective internal resistance of the developmental batteries as a function of depth-of-discharge. The voltage and current information used to develop these curves was obtained from the magnetic-tape data for Schedule C and Schedule D range tests. Figure B-1 shows the two points in the driving cycle that were used for reading voltage and current data to calculate internal resistance. Readings at Point 1 were taken during idle--shortly before the start of acceleration. Readings at Point 2 were taken near the end of acceleration because battery current is highest at that point in the cycle. Battery current at Point 1 is typically about 5 A, and battery current at Point 2 is typically about 350 A.

Figure 5-3 shows the internal resistance of the 80-cell EPI battery. Data from Battery Cycle 112 were used to generate this figure. These data are shown in Table B-44. Figure 5-4 shows the internal resistance of the 90-cell EPI battery. Data from Battery Cycles 137 and 140 were used to generate this figure. These data are shown in Tables B-45 and B-46. Figure 5-9 shows the internal resistance of the Globe ISOA battery. Data from ISOA-1 Battery Cycles 59 and 65 were used to generate this figure. These data are shown in Tables B-47 and B-48. Figure 5-11 shows the effect of the thermal-runaway charge on the internal resistance of the Globe ISOA battery.

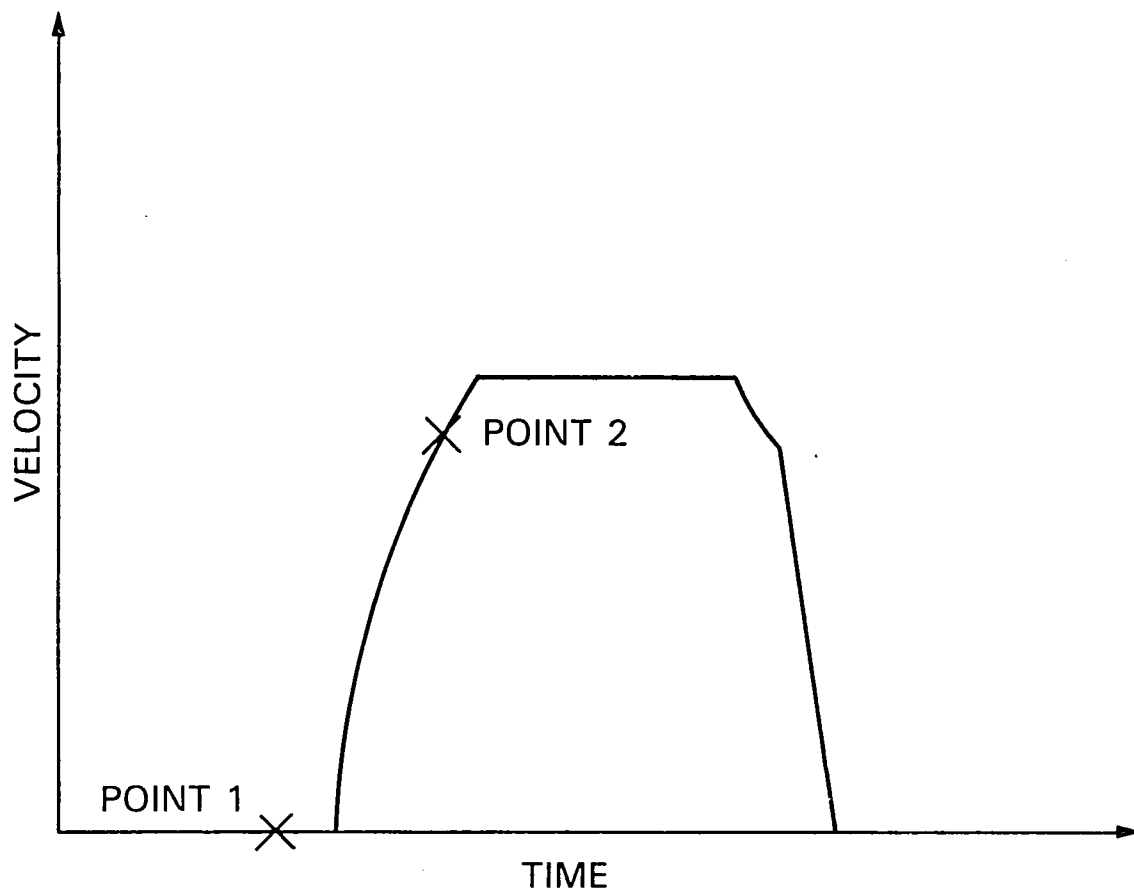


Figure B-1. Points in the Driving Cycle That Were Used for Reading Data for Internal Resistance Calculations

the dashed curve (undamaged battery) is the same as the curve shown in Figure 5-9, and the solid curve (damaged battery) is based on data from ISOA-2 Battery Cycle 65. These data are shown in Table B-49. Figure 5-19 shows the internal resistance of the Westinghouse battery. Data from W-220-3 Battery Cycles 9 and 20 were used to generate this figure. These data are shown in Tables B-50 and B-51.

In Figure 6-8, the internal resistance curves of Figures 5-4, 5-9, and 5-19 have been voltage normalized. The following average system voltages were used for each battery:

Average voltage of the Globe battery =  $(1.9 \text{ V/cell}) \times (48 \text{ cells}) = 91.2 \text{ V}$ .

Average voltage of the 90-cell EPI battery =  $(1.2 \text{ V/cell}) \times (90 \text{ cells}) = 108 \text{ V}$ .

Average voltage of the Westinghouse battery =  $(1.2 \text{ V/cell}) \times (90 \text{ cells}) = 108 \text{ V}$ .

Voltage-normalized resistance curves were calculated for each battery as follows:

$$\text{Voltage-Normalized Resistance} = (100 \text{ V}) \times \frac{\text{Internal Resistance}}{\text{Average System Voltage}}$$

Table B-44. 80-Cell EPI Battery Cycle 112 (Schedule C):  
Internal Resistance Data

Driving Cycle Number	Effective Internal Resistance, m $\Omega$	Depth-of-Discharge, %
1	45.4	0.24
2	44.1	0.81
6	45.4	2.9
9	46.3	4.5
15	47.9	7.8
21	44.8	11.1
27	47.7	14.3
30	47.7	16.0
36	51.1	19.2
39	47.4	20.9
42	48.9	22.5
48	45.5	25.8
51	47.8	27.4
63	47.1	34.0
67	51.2	36.3
68	49.9	36.8
69	48.7	37.3
72	45.8	38.9
75	49.7	40.5
78	48.5	42.2
87	49.5	47.1



Table B-44. 80-Cell EPI Battery Cycle 112 (Schedule C):  
Internal Resistance Data (cont'd)

Driving Cycle Number	Effective Internal Resistance, m $\Omega$	Depth-of-Discharge, %
97	51.3	52.6
102	48.5	55.3
105	44.4	57.1
114	45.5	61.8
117	46.4	63.4
120	47.4	65.1
123	47.0	66.7
126	50.1	68.3
132	49.1	71.6
139	50.7	75.5
140	50.4	76.1
149	50.7	81.4
155	51.8	84.7
158	51.5	86.5
161	51.9	88.0
164	51.9	89.6
168	55.2	91.9
172	57.8	94.1
175	62.6	95.8
178	68.7	97.4
179	75.7	98.0
180	79.0	98.5
181	87.6	99.0

Table B-45. 90-Cell EPI Battery Cycle 137 (Schedule C): Internal Resistance Data

Driving Cycle Number	Effective Internal Resistance, m $\Omega$	Depth-of-Discharge, %
1	56.0	0.2
2	56.0	0.7
3	61.6	1.1
6	57.0	2.7
9	64.0	4.2
12	62.2	5.7
15	63.5	7.2
18	64.3	8.7
21	64.3	10.2
24	65.8	11.7
27	66.8	13.2
30	70.6	14.8
32	64.8	16.2
35	68.1	17.7
38	64.1	19.3
41	66.6	20.8
44	66.0	22.3
47	62.1	23.8

Table B-45. 90-Cell EPI Battery Cycle 137 (Schedule C): Internal Resistance Data (Cont'd)

Driving Cycle Number	Effective Internal Resistance, $m\Omega$	Depth-of-Discharge, %
50	62.1	25.3
53	62.6	26.8
56	62.2	28.3
-----		
59	58.5	30.0
62	67.3	31.3
65	64.3	32.8
-----		
68	64.6	34.3
71	60.0	35.8
74	57.1	37.4
-----		
75	57.5	37.9
76	57.5	38.4
82	59.5	41.3
-----		
88	61.6	44.4
91	60.7	45.9
94	64.6	47.4
-----		
100	58.5	50.4
102	60.5	52.0
105	65.9	53.5
-----		

Table B-45. 90-Cell EPI Battery Cycle 137 (Schedule C): Internal Resistance Data (Cont'd)

Driving Cycle Number	Effective Internal Resistance, m $\Omega$	Depth-of-Discharge, %
111	66.0	56.4
114	66.6	57.9
117	68.6	59.4
120	66.9	60.9
123	67.3	62.5
126	65.8	62.7
129	58.8	65.5
132	66.7	67.0
135	60.1	68.5
138	64.0	70.0
141	68.1	71.5
144	67.5	73.0
150	67.1	76.0
153	67.2	77.6
154	60.7	78.1
155	59.9	78.6
157	59.8	79.5
158	62.1	80.0

Table B-45. 90-Cell EPI Battery Cycle 137 (Schedule C): Internal Resistance Data (Cont'd)

Driving Cycle Number	Effective Internal Resistance, m $\Omega$	Depth-of-Discharge, %
161	65.4	81.5
164	61.1	83.0
166	66.9	84.2
169	64.7	85.1
172	69.2	87.2
175	67.6	88.7
178	67.4	90.2
181	66.9	91.7
184	69.8	93.3
187	78.3	94.7
190	84.8	96.2
193	107.0	97.7
195	116.0	98.8
196	132.0	99.3

Table B-46. 90-Cell EPI Battery Cycle 140 (Schedule D): Internal Resistance Data

Driving Cycle Number	Effective Internal Resistance, m $\Omega$	Depth-of-Discharge, %
1	57.5	0.36
2	61.6	1.91
3	64.5	3.26
4	63.1	4.72
6	62.6	7.70
7	61.7	9.13
8	60.6	10.6
13	64.7	17.8
14	63.1	19.4
15	62.8	20.8
17	62.1	23.7
18	60.1	25.1
19	59.8	26.5
20	60.7	28.0
25	61.6	35.3
26	61.0	36.8
27	62.7	38.2
28	61.2	39.7

Table B-46. 90-Cell EPI Battery Cycle 140 (Schedule D): Internal Resistance Data (Cont'd)

Driving Cycle Number	Effective Internal Resistance, m $\Omega$	Depth-of-Discharge, %
29	59.2	41.1
39	61.4	55.6
40	61.4	57.1
-----		
47	63.5	67.3
48	63.0	68.8
49	60.6	70.2
-----		
50	60.5	71.7
51	62.5	73.2
58	64.7	83.3
-----		
59	64.6	84.8
60	63.5	86.2
-----		
61	62.6	87.6
66	78.1	95.0

Table B-47. Globe ISOA-1 Battery Cycle 59 (Schedule D): Internal Resistance Data

Driving Cycle Number	Effective Internal Resistance, m $\Omega$	Depth-of-Discharge, %
1	49.9	0.1
2	47.2	1.9
3	47.3	3.4
5	47.8	7.0
7	47.3	10.4
11	47.7	17.3
12	47.2	18.9
13	46.3	20.8
14	46.0	22.5
15	45.6	24.1
20	47.2	33.6
21	45.6	35.4
22	45.6	37.1
23	45.9	38.8
24	47.3	40.4
31	47.3	52.6
32	47.6	54.3
33	47.4	55.9



Table B-47. Globe ISOA-1 Battery Cycle 59 (Schedule D): Internal Resistance Data (Cont'd)

Driving Cycle Number	Effective Internal Resistance, mΩ	Depth-of-Discharge, %
34	46.9	57.6
35	47.5	59.3
38	49.7	64.5
39	50.1	66.2
40	50.8	67.9
41	49.8	69.7
42	50.2	71.4
43	49.7	73.1
44	50.4	74.8
49	55.9	83.2
50	57.1	85.1
51	57.2	86.9
52	56.8	89.1
53	58.1	90.7
54	59.8	92.5
55	61.5	94.2
56	62.9	95.9
57	65.4	97.6

Table B-48. Globe ISOA-1 Battery Cycle 65 (Schedule D): Internal Resistance Data

Driving Cycle Number	Effective Internal Resistance, m $\Omega$	Depth-of-Discharge, %
1	46.7	0.5
2	44.5	2.2
6	44.8	9.2
7	45.1	10.9
8	45.2	12.6
9	45.7	14.3
10	41.6	16.0
16	43.6	26.5
17	44.3	28.2
18	44.0	29.9
20	43.4	33.3
23	42.4	38.6
24	42.2	40.3
28	45.5	47.2
29	46.0	48.9
30	45.1	50.7
38	47.7	64.6
39	49.2	66.3

Table B-48. Globe ISOA-1 Battery Cycle 65 (Schedule D): Internal Resistance Data (Cont'd)

Driving Cycle Number	Effective Internal Resistance, $m\Omega$	Depth-of-Discharge, %
40	47.6	68.0
48	49.5	81.9
49	50.6	83.7
50	54.1	85.3
51	59.1	87.2
56	58.9	95.8
57	58.0	98.1

Table B-49. Globe ISOA-2 Battery Cycle 65 (Schedule D): Internal Resistance Data

Driving Cycle Number	Effective Internal Resistance, $m\Omega$	Depth-of-Discharge, %
1	50.4	0.8
2	48.7	2.7
3	48.9	4.7
9	49.8	16.7
11	49.1	20.8
12	48.3	22.8
16	51.1	30.9
17	50.8	32.8
18	51.6	34.8
19	51.8	36.9
20	50.6	38.9
21	50.9	40.9
22	50.2	43.0
23	50.3	45.0
27	52.0	53.0
28	53.1	55.0
29	52.6	56.9
30	53.3	59.0

Table B-49. Globe ISOA-2 Battery Cycle 65 (Schedule D): Internal Resistance Data (Cont'd)

Driving Cycle Number	Effective Internal Resistance, m $\Omega$	Depth-of-Discharge, %
31	53.6	60.9
32	53.6	64.1
33	53.5	66.1
34	57.2	67.9
37	57.7	74.2
38	58.1	76.1
39	58.7	78.1
41	60.4	82.2
42	60.6	84.2
43	62.7	86.2
44	64.7	88.2
45	67.9	90.5
46	70.7	92.8
47	73.2	94.9
48	77.8	96.4
49	85.9	98.5

Table B-50. Westinghouse Battery Cycle 9 (Schedule D): Internal Resistance Data

Driving Cycle Number	Effective Internal Resistance, $m\Omega$	Depth-of-Discharge, %
1	98.7	0
2	99.1	1.8
3	101.0	4.3
4	98.9	6.0
5	96.3	8.5
6	89.9	10.2
8	91.7	14.4
9	91.2	16.6
10	89.6	18.6
11	85.3	20.3
12	91.4	22.8
13	90.6	24.5
14	90.5	27.0
15	86.1	28.9
16	86.9	30.9
17	89.8	33.8
18	89.6	35.4
20	88.3	39.2

Table B-50. Westinghouse Battery Cycle 9 (Schedule D): Internal Resistance Data (Cont'd)

Driving Cycle Number	Effective Internal Resistance, $m\Omega$	Depth-of-Discharge, %
21	90.3	41.4
22	89.9	43.6
23	91.2	45.2
24	93.5	47.3
25	90.8	49.3
26	92.6	52.3
27	94.9	53.7
28	94.0	55.7
29	96.2	57.4
30	96.5	59.9
31	95.6	61.8
32	99.1	64.1
34	99.8	67.8
35	99.8	70.0
37	108.0	73.9
38	108.0	75.9
39	109.0	78.4
40	117.0	80.3

Table B-50. Westinghouse Battery Cycle 9 (Schedule D): Internal Resistance Data (Cont'd)

Driving Cycle Number	Effective Internal Resistance, $m\Omega$	Depth-of-Discharge, %
41	120.0	82.1
42	122.0	84.3
-----		
44	139.0	88.5
46	182.0	92.8



Table B-51. Westinghouse Battery Cycle 20 (Schedule C): Internal Resistance Data

Driving Cycle Number	Effective Internal Resistance, $m\Omega$	Depth-of-Discharge, %
5	97.5	3.6
8	99.0	6.2
10	82.0	8.0
11	90.6	8.5
14	87.0	11.0
17	88.7	13.4
20	88.3	15.4
23	87.5	18.1
29	89.2	22.8
32	86.7	25.3
35	86.8	27.6
38	87.7	29.9
41	87.6	32.2
44	88.4	34.7
47	88.7	36.8
50	89.4	39.4
54	88.4	42.3
57	88.0	44.7

Table B-51. Westinghouse Battery Cycle 20 (Schedule C): Internal Resistance Data (Cont'd)

Driving Cycle Number	Effective Internal Resistance, mΩ	Depth-of-Discharge, %
60	89.9	47.0
63	90.1	49.4
66	89.9	52.0
69	89.7	54.4
72	91.7	56.5
75	90.9	58.9
78	91.9	60.4
81	92.7	62.8
84	93.6	65.3
87	92.9	67.8
90	94.3	70.3
93	94.0	72.7
96	96.8	75.2
99	98.3	77.7
102	99.5	80.1
105	101.0	82.6
108	103.0	85.1
111	106.0	87.5

Table B-51. Westinghouse Battery Cycle 20 (Schedule C): Internal Resistance Data (Cont'd)

Driving Cycle Number	Effective Internal Resistance, $m\Omega$	Depth-of-Discharge, %
114	108.0	90.0
117	113.0	92.5
120	117.0	95.0
123	127.0	97.1
126	141.0	99.4

## G. ELECTROLYSIS BY-PRODUCTS

### 1. EPI Battery

Based on the amount of water consumed by the 80-cell EPI battery during daily use, the amount of hydrogen gas released during a charge/discharge cycle was calculated as follows (References 15, 16):

$$\text{Amount of water added per charge/discharge cycle} = 1.5 \ell$$

or

$$(1.5 \ell \text{ H}_2\text{O}) \times (1000 \text{ g H}_2\text{O}/\ell) = 1500 \text{ g H}_2\text{O}$$

The atomic weight of hydrogen is 1.0 g, and the atomic weight of oxygen is 16.0 g, so the amount of hydrogen gas liberated per charge/discharge cycle was

$$(1500 \text{ g H}_2\text{O}) \times (2 \text{ g H}_2) / (18 \text{ g H}_2\text{O}) = 166.7 \text{ g H}_2$$

To determine the volume of hydrogen gas at standard conditions, the perfect gas law was used:

$$V = \frac{nRT}{P}$$

where

$$n = (166.7 \text{ g H}_2) / (2 \text{ g H}_2/\text{g-mole}) = 83.33 \text{ g/mole}$$

$$R = 0.08205 \frac{\text{atm} \cdot \ell}{\text{g-mole} \cdot \text{K}}$$

$$T = 297 \text{ K}$$

$$P = 1 \text{ atm}$$

so,

$$V = \frac{83.33 \times 0.08205 \times 297}{1} = 2031 \ell$$

The amount of hydrogen gas released by the 90-cell battery each charge/discharge cycle would, therefore, be

$$V = \frac{2031 \ell}{80 \text{ cells}} \times 90 \text{ cells} = 2284 \ell$$

### 2. Globe ISOA Battery

Because of difficulties with the watering system, the water consumption of the Globe battery could not be determined. Therefore, the approach used for calculating the amount of hydrogen gas released by the EPI battery could not be used with this battery. However, the amount which can be released is limited by the amount of coulombic overcharge. The maximum possible amount of hydrogen gas which could be released each charge/discharge

cycle was calculated as follows:

Average coulombic overcharge = 45 Ah.

One faraday = 26.8 Ah/equivalent (Reference 16), and one equivalent<sup>1</sup> of H<sub>2</sub> = 11.2 ℓ/cell at standard conditions (Reference 15). If all of the coulombic overcharge is used to produce hydrogen, the amount of hydrogen gas released would be

$$\frac{45 \text{ Ah}}{26.8 \text{ Ah/equiv}} \times (11.2 \text{ ℓ/cell-equiv}) \times (48 \text{ cells}) = 900 \text{ ℓ}.$$

The amount of hydrogen gas released by the Globe battery was also calculated using gassing-rate measurements taken during charge. These measurements were taken during ISOA-2 Battery Cycle 76. The data are shown in Table B-52. As shown in this table, the measured gassing rate was about 0.2 ℓ/min during most of the charge. The following assumptions were used to estimate the amount of hydrogen gas released each charge/discharge cycle:

- (1) Assume a steady gassing rate of 0.2 ℓ/min throughout charge.
- (2) Recharge time = 13 h.
- (3) Hydrogen and oxygen gasses are released in a stoichiometric ratio of 2:1 during charge.
- (4) No electrolysis occurs during discharge.

Using these assumptions, the volume of hydrogen gas released each charge/discharge cycle is calculated as follows:

$$(0.2 \text{ ℓ/min}) \times (60 \text{ min/h}) \times (13 \text{ h}) \times (2 \text{ parts H}_2) / (2 \text{ parts H}_2 + 1 \text{ part O}_2) = 104 \text{ ℓ}$$

As explained in Section V, these gassing-rate measurements are probably inaccurate because it seems unlikely that only 1/9 of the total coulombic overcharge is used for electrolysis.

### 3. Westinghouse Battery

Figures 5-25 and 5-26 show the gassing rate of the Westinghouse battery during charge. The data shown Figure 5-25 were obtained during a normal charge (W-220-3 Battery Cycle 56). These data are listed in Table B-53. The data shown in Figure 5-26 were obtained during experimental charges (Battery Cycles 68 and 70) in which a lower clamping voltage was used, allowing charge current to taper to about 10 A. These data are listed in Table B-54.

---

<sup>1</sup>The equivalent weight of an element is defined as its atomic weight divided by its valence (Reference 16).

Table B-52. Globe ISOA-2 Battery Cycle 76: Gassing-Rate Measurements During Recharge

Time Since Charge Start, h	Volume of Gas Collected, $\ell$	Elapsed Time, min	Gassing Rate, $\ell/\text{min}$
1.0	0.0	10.0	0.0
4.0	1.2	3.8	0.32
5.0	1.2	5.3	0.23
6.0	1.2	5.0	0.24
7.0	1.2	6.6	0.18
9.0	1.2	5.2	0.23
11.0	1.2	7.0	0.17

Table B-53. W-220-3 Battery Cycle 56: Gassing-Rate Measurements During Recharge

Time Since Charge Start, h	Volume of Gas Collected, $\ell$	Elapsed Time, min	Gassing Rate, $\ell/\text{min}$
0.5	0.0	10.0	0.0
1.0	0.0	10.0	0.0
1.5	18.3	2.1	8.6
2.0	24.5	1.6	14.9
3.0	24.5	1.1	23.3
4.0	24.5	0.90	27.2
4.5	24.5	0.85	28.7

Table B-54. W-220-3 Battery Cycles 68 and 70: Gassing-Rate Measurements During Recharge

Time Since Charge Start, h	Volume of Gas Collected, $\ell$	Elapsed Time, min	Gassing Rate, $\ell/\text{min}$
0.5	6.4	4.2	1.5
0.75	6.4	2.9	2.2
0.92	6.4	2.4	2.7
1.17	12.6	3.4	3.7
1.25	12.6	2.7	4.7
1.42	18.8	2.8	6.8
1.75	18.8	2.1	9.0
2.0	18.8	1.8	10.7
3.25	18.8	1.7	11.0
4.25	18.8	2.1	8.9
4.50	18.8	2.1	8.8
5.0	18.8	2.1	8.8
8.0	18.8	2.2	8.7
11.5	18.8	2.2	8.6

The total volume of hydrogen gas released by the Westinghouse battery during a normal charge/discharge cycle was calculated from the gassing-rate measurements listed in Table B-53. The following assumptions were used to estimate the amount of hydrogen gas released:

- 1) Hydrogen and oxygen gasses are released in a stoichiometric ratio of 2:1 during charge.
- 2) No electrolysis occurs during discharge.

Numerical integration of the data in Table B-53 was used to calculate the total volume of gas released during charge. The integration was done by using trapezoids to approximate the area under the gassing-rate curve. Five trapezoids were used, and their area was summed to give the total area under the curve as follows:

$$A_1 = 1/2 \times (0 + 8.6) \text{ } \ell/\text{min} \times (1.5 - 1.0)\text{h} \times 60 \text{ min/h} = 129 \ell$$

$$A_2 = 1/2 \times (8.6 + 14.9) \text{ } \ell/\text{min} \times (2.0 - 1.5)\text{h} \times 60 \text{ min/h} = 352.5 \ell$$

$$A_3 = 1/2 \times (14.9 + 23.3) \text{ } \ell/\text{min} \times (3.0 - 2.0)\text{h} \times 60 \text{ min/h} = 1146 \ell$$

$$A_4 = 1/2 \times (23.3 + 27.2) \text{ } \ell/\text{min} \times (4.0 - 3.0)\text{h} \times 60 \text{ min/h} = 1515 \ell$$

$$A_5 = 1/2 \times (27.2 + 28.7) \text{ } \ell/\text{min} \times (4.5 - 4.0)\text{h} \times 60 \text{ min/h} = 838.5 \ell$$

$$\text{Total volume of gas released} = A_1 + A_2 + A_3 + A_4 + A_5 = 3981 \ell$$

Using the assumptions stated above, the volume of hydrogen gas released each charge/discharge cycle was estimated to be

$$3981 \ell \times (2 \text{ parts } H_2)/(2 \text{ parts } H_2 + 1 \text{ part } O_2) = 2654 \ell$$

The magnitude of this volume calculation is corroborated by the fact that the water consumption of the Westinghouse battery was approximately the same as that of the EPI battery.

#### H. SENSITIVITY TO DISCHARGE RATE

In Table 6-1, the sensitivity of battery capacity to constant-power discharge rate has been expressed as the mean gradient of specific energy as a function of average discharge power between 5 and 15 kW. This parameter was calculated as follows:

$$G_{5-15} = \frac{E_{15} - E_5}{(15 - 5)\text{kW}} = \frac{E_{15} - E_5}{10 \text{ kW}}$$



where  $E_{15}$  = specific energy at 15 kW discharge rate.

$E_5$  = specific energy at 5 kW discharge rate.

The data used for these calculations are listed in Table B-55.

Table B-55. Data Used for Computing the Mean Gradient of Specific Energy as a Function of Discharge Power

Battery	$E_5$ , Wh/kg	$E_{15}$ , Wh/kg
EPI Ni-Fe	39.9	36.9
Globe ISOA Pb-A	36.1	25.0
Westinghouse Ni-Fe	33.8	25.6
ETV-1-2 baseline	34.9	20.6
SCT-2 baseline	33.8	21.5



## APPENDIX C

### DATA ACQUISITION CAPABILITIES



## A. INTRODUCTION

Dynamometer testing of electric vehicles is done in JPL's Automotive Research Facility. This facility was started in 1973 as a small laboratory for internal-combustion engine research and, since that time, it has been expanded to include capabilities for exhaust emissions analysis, Stirling engine testing, and electric vehicle testing.

The primary means of recording data in the Automotive Research Facility is with IDAC (Integrated Data Acquisition and Control). IDAC is a data logger/computer that was designed and built by JPL. Other instrumentation in the Automotive Research Facility includes an oscillograph for recording high-speed data, strip chart recorders, x-y plotters, and special power measurement instrumentation for electric vehicle testing. The central instrumentation area of this facility is shown in Figure C-1.

## B. IDAC

### 1. Analog Inputs

A block diagram of IDAC is shown in Figure C-2. Analog data signals are multiplexed for a maximum capability of five-hundred data channels. A capability of two-hundred analog channels has been implemented. The sampling sequence of analog channels is determined by software, and the number and order of channels sampled can be changed by software modifications. The sampling rate can be varied from 50 to 5000 samples per second. The characteristics of the multiplexer input channels are as follows:

Input type:	Guarded differential, three wires per channel.
Input resistance:	$> 10^6 \Omega$ .
Input capacitance:	1200 pf.
Common mode rejection:	Each input: 120 dB, dc to 60 Hz, 1000 $\Omega$ , source unbalanced.  Input-to-input: 100 dB, dc to 60 Hz.
Common mode input resistance:	$10^6 \Omega$ .

The first level of switching in the multiplexer unit is done by field-effect transistors having a maximum pump-out current of 1.5 nA. The full-scale sensitivity settings available for analog data are +5, +10, +20, +50, and +100 mV, and the output word size from the analog-to-digital converter is fourteen bits plus sign. The performance of the multiplexer and the analog-to-digital converter is as follows:

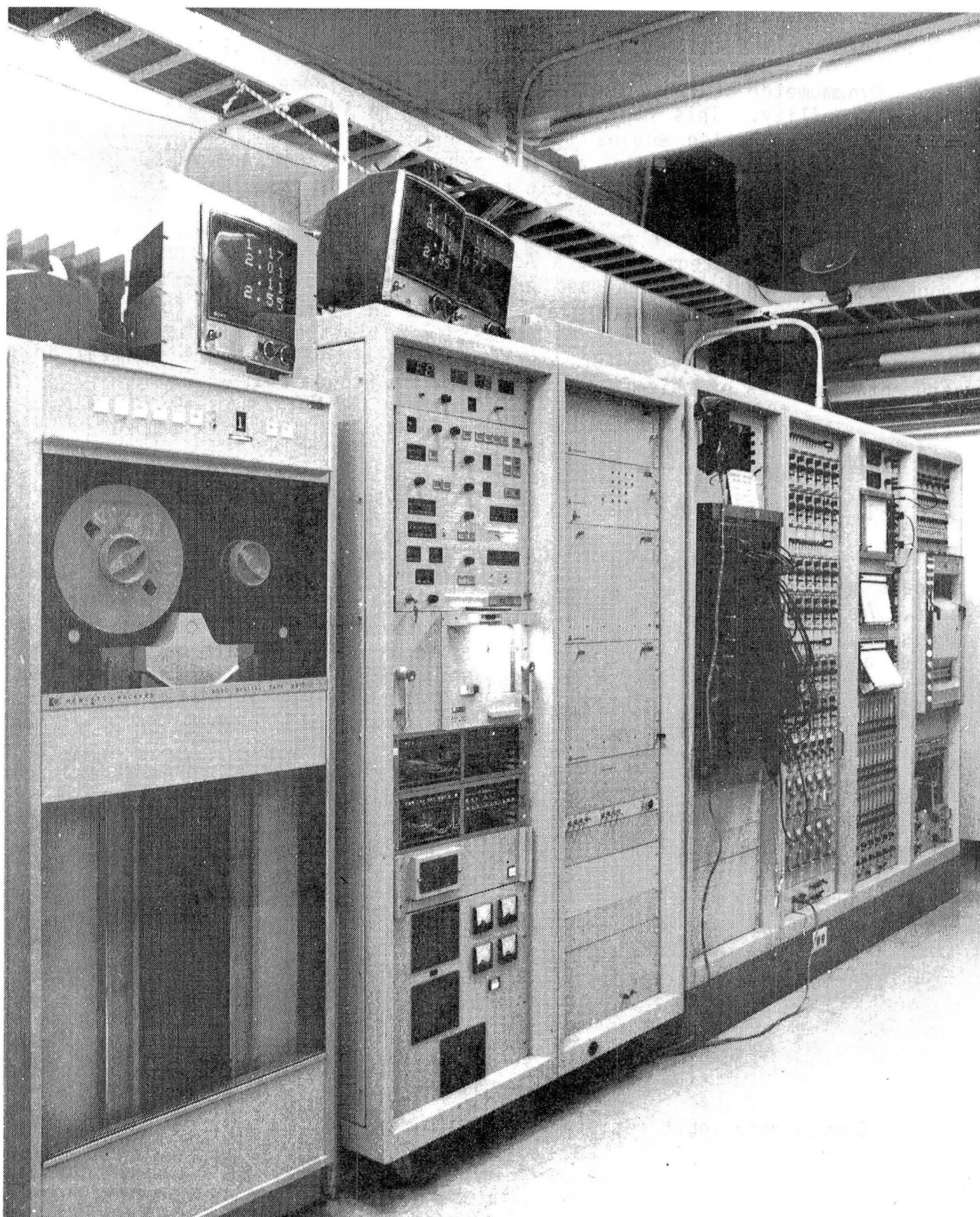


Figure C-1. Automotive Research Facility,  
Central Instrumentation Area

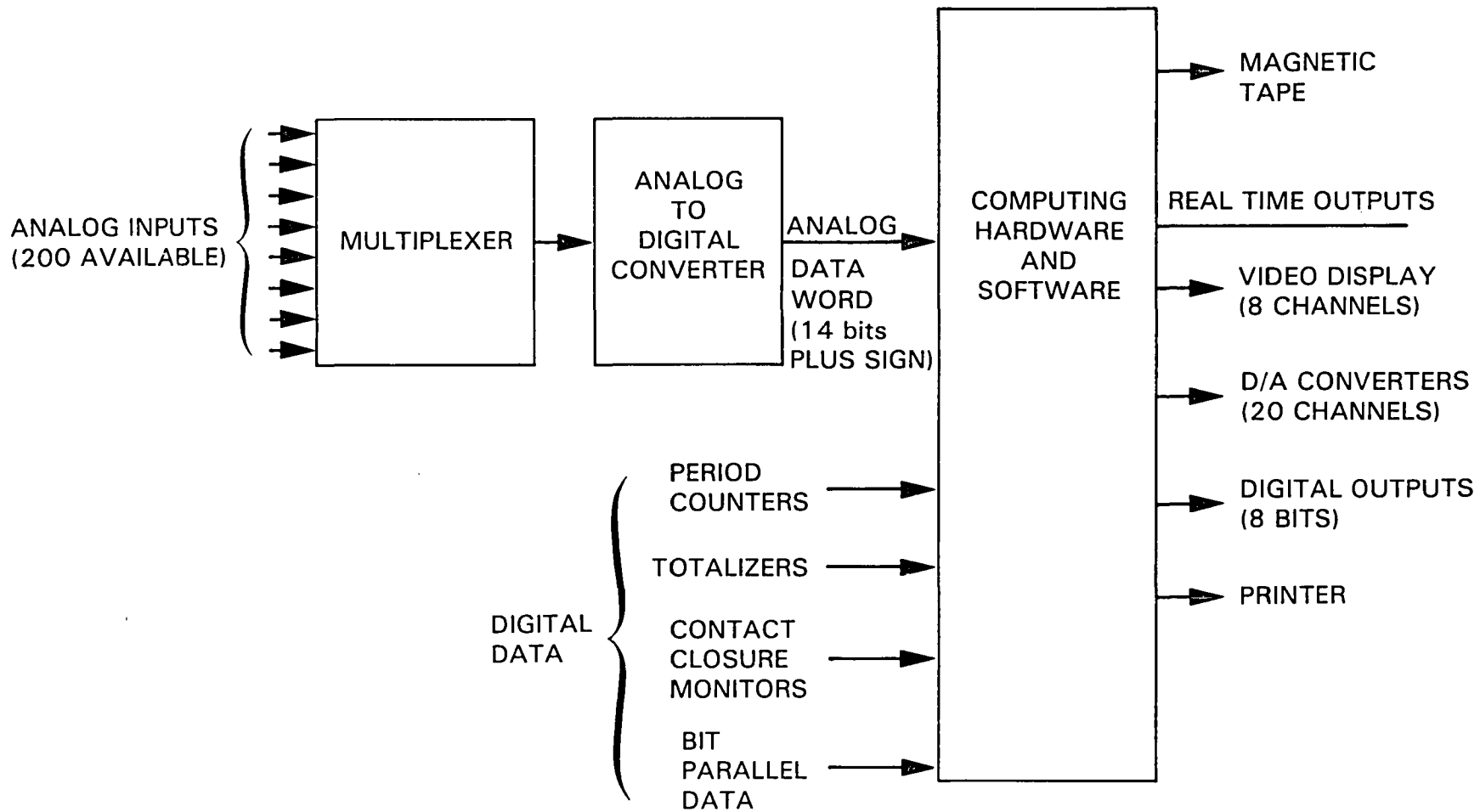


Figure C-2. IDAC, Block Diagram

Gain accuracy (one month):	<u>+0.05%</u> .
Gain stability (8 h):	<u>+0.01%</u> .
Offset drift (8 h):	0.5 $\mu$ V Referred To Input (RTI) plus 0.005% of full scale.
Linearity:	+0.02% of full scale, best straight line.
Noise, peak 3 sigma:	(4 + 6(10 <sup>-4</sup> )x(scan rate)) $\mu$ V RTI or 0.02% of full scale, whichever is greater.
Cross talk:	<u>+2 <math>\mu</math>V RTI</u> or <u>+0.025(10<sup>-4</sup>)x(scan rate))%</u> of previous channel amplitude, which- ever is greater.
Channel-to-channel offset:	<u>+(3 + 15(10<sup>-4</sup>)x(scan rate)) <math>\mu</math>V RTI.</u>
Temperature coefficient (offset):	<u>+1.0 <math>\mu</math>V</u> and <u>+1.0 nA RTI per °C</u> over any 10°C variation between 0°C and 50°C.
Maximum input overload:	<u>+10 V.</u>
Maximum common mode voltage:	Total of input signal and common mode signal must be less than 10 V.

## 2. Digital Inputs

There are four types of digital inputs: period counters, totalizers, contact closure monitors, and bit parallel data. Four period counters are available. These counters record frequency data within a range of 7.5 Hz to 100 kHz with an accuracy of +0.2%. Eight totalizers are available to record the total counts of a frequency source. Eight contact closure monitors are available to record the status of contacts. Four bit parallel data inputs are available. Two of these inputs record 16-bit data, and two record 30-bit data.

## 3. Real-Time Capabilities

IDAC can be used to do calculations in real time, and a floating-point arithmetic capability with five significant decimal figures is available for this purpose. Real-time calculations can be based on data from either analog or digital channels, and data from several channels can be used simultaneously in calculations. In addition, limits can be assigned to analog data, digital data, and to the results of calculations. The status of these limits is checked continuously.



There are four types of real-time data outputs: video display channels, digital-to-analog (D/A) converters, digital output channels, and a printer. There are eight video display channels, and these can be used to show analog, digital, or calculated data in decimal format with engineering units. If the parameter displayed has been assigned a limit, the limit status (LO, GO, or HI) will also be displayed. There are twenty D/A converters that can output a signal proportional to time, digital, analog, or calculated data. The output from these D/A converters are  $\pm 10$ -V signals with a nominal 0.1% resolution. These outputs can be used to run an analog device such as a strip chart recorder or an x-y plotter, or they can be used for feedback in a control circuit. Eight digital outputs are available. These outputs can be used to sound an alarm or to shut off a test if a limit is exceeded, or they can be set and cleared periodically by software for control purposes. A thirty-two column alphanumeric printer is available for printing analog, digital, or calculated data at a rate of 50 channels per second. Printing can be initiated manually, at preset time intervals, or by a change in a limit status. The list of parameters to be printed can be varied, and one of seven prestored lists can be selected manually or by software at each initiation of printing.

## 5. Magnetic Tape Recording

In addition to the real-time data-examination capabilities, IDAC can also produce a magnetic-tape recording of test data. Whenever data scans are written to tape, the analog channels are sampled in a sequence determined by software. As the analog channels are being sampled, digital channels may input data. If digital data are input during a data scan, they are immediately written to tape by a hardware interrupt scheme. Analog and digital data are recorded on tape only when the recording capability is enabled by a data scan. The rate at which analog data is scanned and written to tape can be varied from 50 to 5000 samples per second.

Three recording modes are available for writing magnetic tapes: continuous, intervalometer, and single scan. In continuous mode, the data channels are scanned and written to tape continuously; this mode is used for tests with rapidly varying data. In intervalometer mode, data scans are written to tape at fixed intervals; this mode is used for tests with slowly varying data. In single scan mode, each data scan must be manually initiated; this mode is used for steady-state testing. In intervalometer and single scan modes, eight samples of each analog channel are taken every data scan.

During a test, raw data are written to tape each time a channel is sampled. Time resolution for these data is 1 ms. Before and after the test, headers are written. The headers contain the information needed to convert the raw channel data to engineering units, the test number (input manually), the date, the time of day, and other test information.

The magnetic tape is later processed by software on a Univac 1100/81 computer. If the data were recorded in single scan or intervalometer mode, the eight samples from each data scan are averaged to reduce the influence of noise. Various data reduction programs are available to do calculations with the test data, and to print and plot either raw or calculated data.

## B. ADDITIONAL DATA ACQUISITION HARDWARE

### 1. High-Speed Data Acquisition

A Honeywell 1912 oscillograph is also available for high-speed, analog data recording. It has thirty-six channels, and paper speeds can be varied from 0.1 in./s to 160 in./s. Galvanometers are available for recording data at up to 5 kHz.

### 2. Plotting Hardware

Two Hewlett-Packard 7100B strip chart recorders are available. These are dual-pen recorders, and paper speed can be varied from 1 in./h to 2 in./s. Full-scale sensitivity can be varied from 0.1 mV to 100 V, and response time is less than 0.5 s for a full-scale excursion.

A Moseley 7030A x-y plotter is available, and this plotter is often controlled by the IDAC analog outputs during a test. This plotter has a 7x10 in. grid and a single pen. Full-scale sensitivity can be varied from 1.0 mV to 200 V, and response time is 1 s for a full-scale excursion. Several other, similar, x-y plotters are also available.

### 3. Electric Vehicle Test Equipment

When testing electric vehicles, differential amplifiers are used to isolate signals that might reach battery potential. In addition, some special instrumentation is used in the Automotive Research Facility for testing electric vehicles. High-frequency, coaxial shunts are used for measuring current. Two sizes are used: 50-A shunts and 500-A shunts. The full-scale output of both types is nominally 250 mV.

Wideband wattmeters are used for power measurement. These wattmeters were designed and built by JPL. A power-measurement box with six wattmeter cards is shown in Figure C-3. Each of these wattmeters continuously outputs signals for four parameters: voltage, current, positive power, and negative power. Two power-measurement boxes (twelve wattmeters) are available.

A block diagram of a wattmeter card is shown in Figure C-4. Voltage and current input signals are connected directly to each card to minimize noise. These signals pass through several stages of amplification. Frequency response during amplification is within +3% from 0 to 50 kHz. The 50 kHz voltage and current signals are output, and these outputs can be used for facility checkout or for examining the pulsed-power waveforms typically used for speed control in electric vehicles. Voltage and current signals that have been filtered to 5 Hz are also output. Because the signals from the filtered outputs are proportional to average (rather than instantaneous) input data, these signals are used as the analog inputs to IDAC for voltage and current.

The 50 kHz signals also go to an analog multiplier where a signal proportional to instantaneous power is derived. The signal from the multiplier goes to two voltage-to-frequency (V/F) converters. The output from the V/F converters is pulsed, and the frequency of the output is proportional to the magnitude of the power measurement. Because the outputs are frequen-

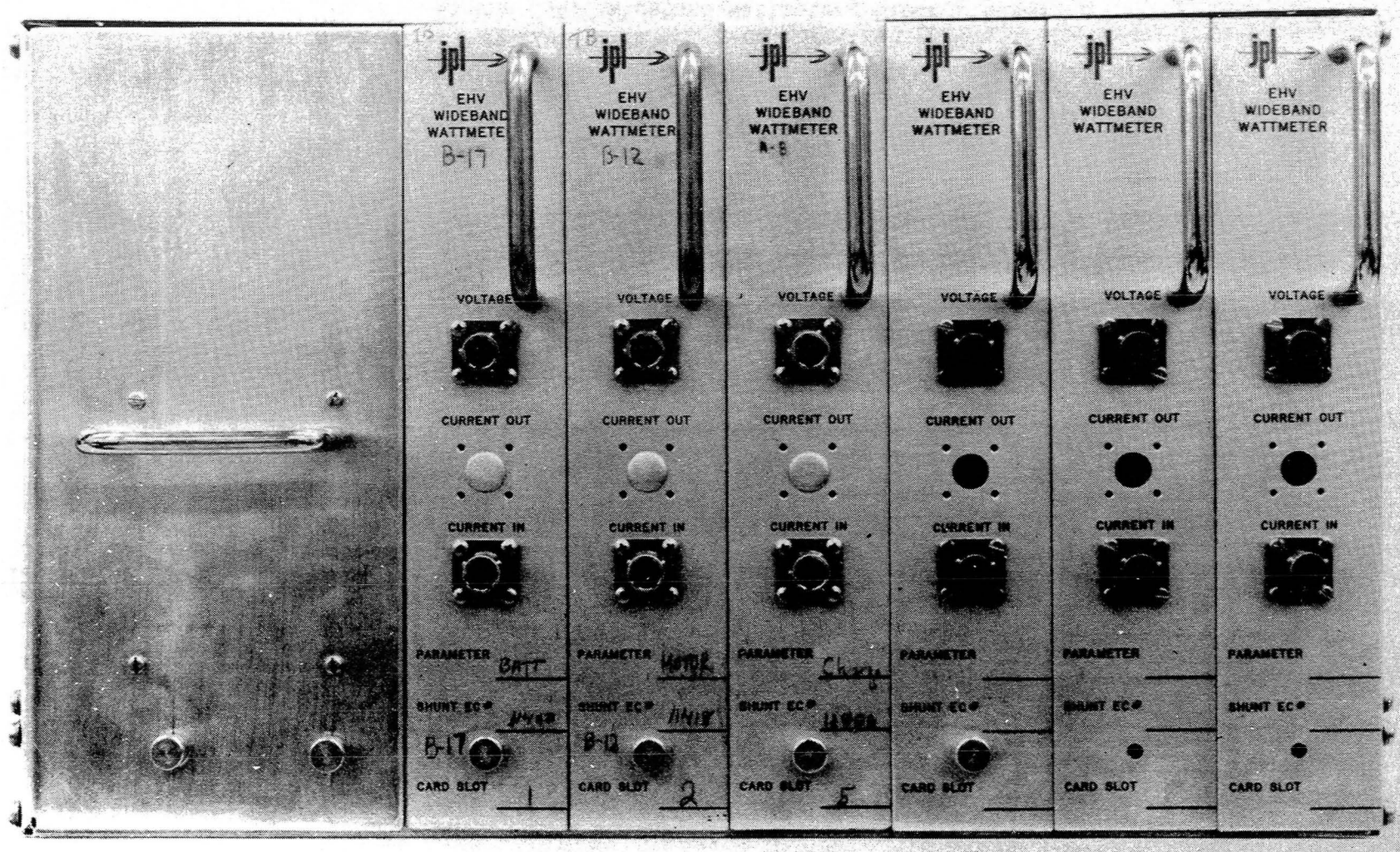


Figure C-3. A Power-Measurement Box with Six Wideband-Wattmeter Cards

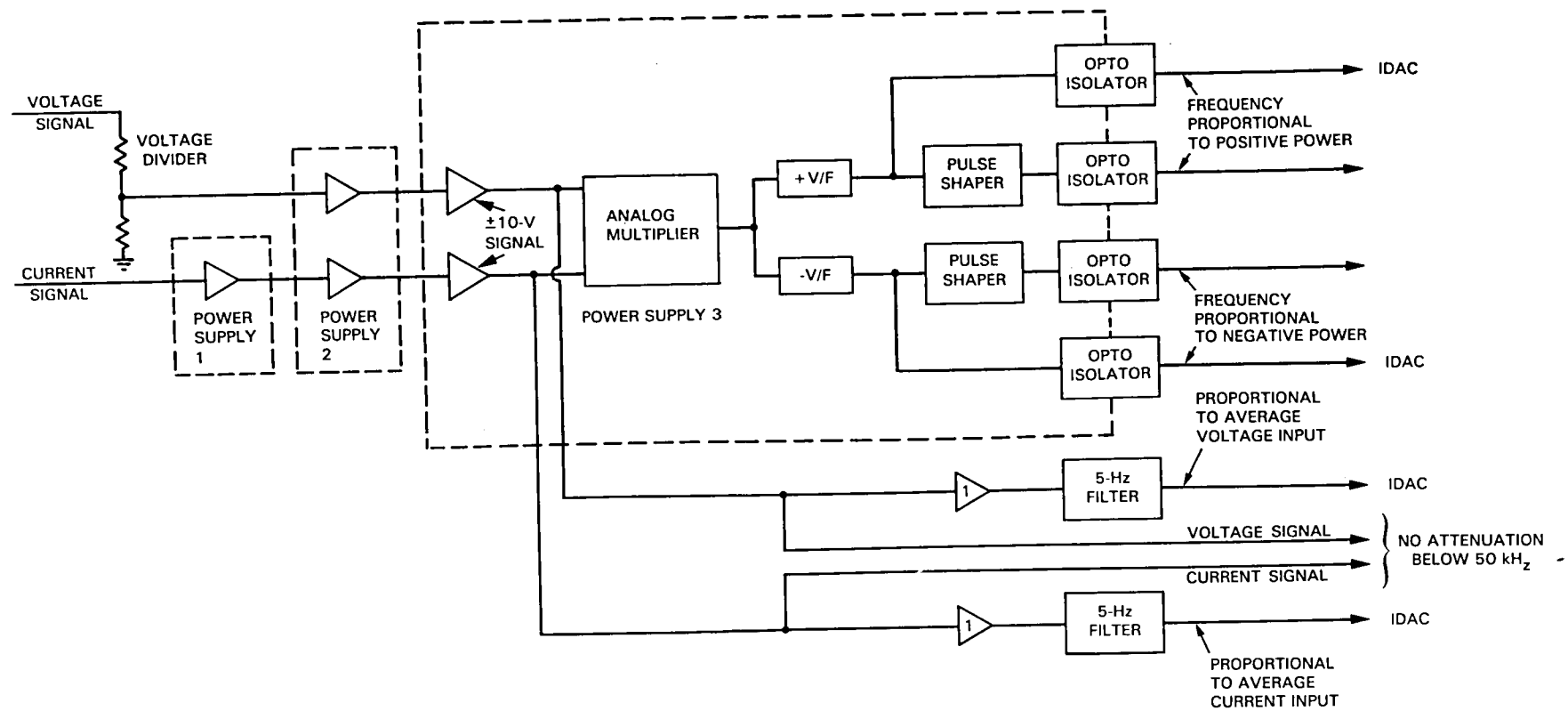


Figure C-4. Wideband Wattmeter, Block Diagram

cies, the power signals can be integrated by totalizers to obtain energy data. There are two outputs for each polarity: one output for each polarity is processed by a pulse shaper so mechanical counters can be used to totalize energy; the other pulsed output is processed by a pulse-rate converter to obtain an analog signal proportional to average power, and this signal is used as an analog input to IDAC. All power-signal outputs are optically isolated. The wattmeter outputs are located in the rear of the power-measurement box--shown in Figure C-5.

Specifications for the wideband wattmeters are as follows:

#### Output Signals

Voltage measurement:	<u>+10</u> V.
Current measurement:	<u>+10</u> V.
Power measurements:	0 to 10 kHz.

#### Full-Scale Sensitivity

Voltage measurement:	<u>+200</u> V.
Current measurement:	<u>+25</u> A to <u>+500</u> A.

#### DC Accuracy

Low-frequency voltage signal:	1.0%.
Low-frequency current signal:	1.0%.
Positive power signal:	0.2%.
Negative power signal:	0.2%.

#### Frequency Response

High-frequency voltage measurement:	<u>+3%</u> from 0 to 50 kHz.
High-frequency current measurement:	<u>+3%</u> from 0 to 50 kHz.
Low-frequency voltage measurement:	5 Hz.
Low-frequency current measurement:	5 Hz.

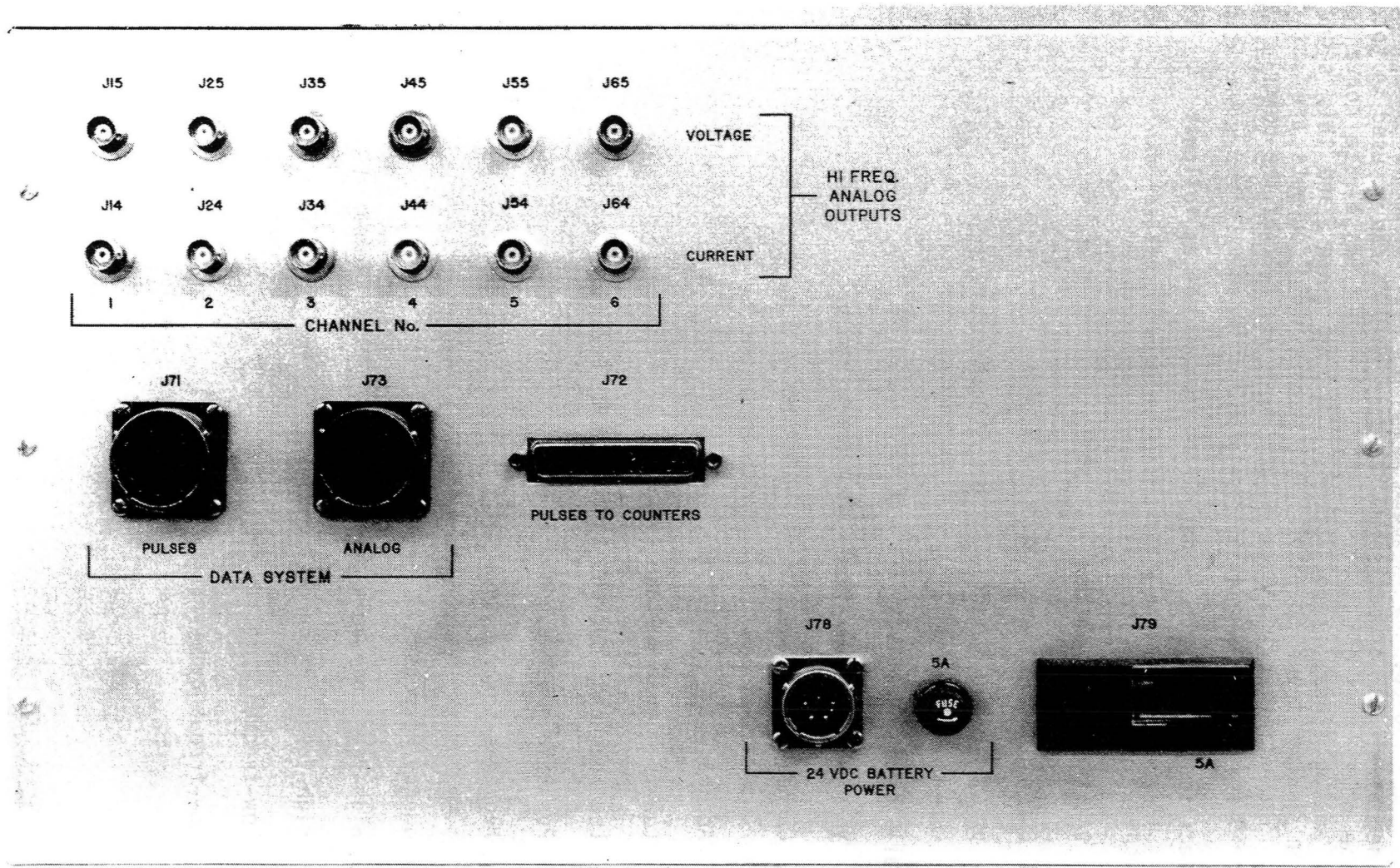


Figure C-5. Back Panel of Power-Measurement Box Showing Signal Outputs

APPENDIX D

RECORDED PARAMETERS





The following data are recorded during electric vehicle tests:

Magnetic Tape Data

Analog Channels

Parameter	Resolution
Battery Voltage	0.1 V
Battery Current	0.1 A
Power Out of Battery	0.01 kW
Power Into Battery	0.01 kW
Battery Temperature <sup>1</sup>	0.1 °F
Armature Voltage	0.1 V
Armature Current	0.1 A
Power Into Armature	0.01 kW
Power Out of Armature	0.01 kW
Field Voltage	0.1 V
Field Current	0.01 A
Field Power	0.001 kW
Motor Speed	1.0 rev/min
Motor Temperature <sup>2</sup>	0.1 °F
Controller Temperature	0.1 °F
Torque on Dynamometer Load Roller	0.01 lb-ft
Load-Roller Speed	0.1 rev/min
Idle-Roller Speed <sup>3</sup>	0.1 rev/min

<sup>1</sup>There are five battery temperature channels.

<sup>2</sup>There are two motor temperature channels.

<sup>3</sup>Idle-roller speed is used to calculate vehicle velocity.

### Analog Channels (Cont'd)

Parameter	Resolution
Inertia-Weight Torque	0.1 lb-ft
Ambient Temperature	0.1 °F
Ambient Pressure	0.01 psia
Relative Humidity	0.01 %

### Digital Channels

Parameter	Type of Digital Input
Energy Out of Battery	Totalizer
Energy Into Battery	Totalizer
Coulombic Charge Removed From Battery	Totalizr
Coulombic Charge Returned to Battery	Totalizer
Energy Into Armature	Totalizer
Energy Out of Armature	Totalizer
Field Energy	Totalizer
Distance	Totalizer

### Hand-Recorded Data

Date

Test Number

Vehicle Tested

Test Type

Battery

Dynamometer Settings

Odometer Reading (recorded both before and after test)

Tire Pressure (recorded both before and after test)

Lift Pressure (recorded both before and after test)

Specific Gravity (recorded both before and after test)

Post-Test Tire Temperature

Test Termination Criterion

Mechanical Counter Data:

Energy Out of Battery

Energy Into Battery

Coulombic Charge Removed From Battery

Coulombic Charge Returned to Battery

Energy Into Armature

Energy Out of Armature

Field Energy

Drivers

Instrumentation Operator



## APPENDIX E

### DATA FROM TESTS OF THE 80-CELL EPI NI-FE BATTERY



DATA FROM TESTS OF THE 80-CELL EPI NI-FE BATTERY

Battery Cycle	104	105	106	107 <sup>a</sup>
Date (Discharge)	10/24/80	10/27/80	10/28/80	10/29/80
Test Vehicle	--	--	ETV-1-2	ETV-1-2
Type of Discharge	75 A	75 A	45 mi/h	D
Distance Traveled, mi	--	--	122.1	57.2
Discharge Time, min	N.A.	N.A.	164.6	117.9
Discharge Energy From Battery, kWh	N.A.	N.A.	22.13	17.46
Regen. Energy To Battery, kWh	--	--	0.04	2.39
Coulombic Battery Discharge, Ah	235.0	231.7	226.0	183.2
Coulombic Regen., Ah	--	--	0.42	20.54
Discharge Termination Criteria	1.0 V/cell	1.0 V/cell	1.0 V/cell	vehicle failure
Recharge Energy, kWh	N.A.	N.A.	N.A.	N.A.
Coulombic Recharge	300.0	316.4	300.0	300.0
Recharge Time, h	5.0	5.3	5.0	5.0
Battery Temp. (Start of Discharge), °F	N.A.	N.A.	87.0	87.3
Battery Temp. (End of Discharge), °F	N.A.	N.A.	109.0	110.5
Battery Temp. (Start of Charge), °F	N.A.	N.A.	N.A.	N.A.
Battery Temp. (End of Charge), °F	N.A.	N.A.	N.A.	N.A.

<sup>a</sup>Invalid range test. Test terminated by vehicle failure.

DATA FROM TESTS OF THE 80-CELL EPI NI-FE BATTERY

Battery Cycle	108 <sup>a</sup>	109 <sup>a</sup>	110	111 <sup>b</sup>
Date (Discharge)	10/30/80	10/31/80	11/4/80	11/5/80
Test Vehicle	ETV-1-2	ETV-1-2	SCT-2	SCT-2
Type of Discharge	55 mi/h	D	45 mi/h	D
Distance Traveled, mi	67.1	61.3	108.5	23.9
Discharge Time, min	75.2	127.1	145.6	49.5
Discharge Energy From Battery, kWh	14.40	18.59	22.76	8.83
Regen. Energy To Battery, kWh	0.04	2.47	0.01	0.22
Coulombic Battery Discharge, Ah	144.6	194.8	230.7	90.3
Coulombic Regen., Ah	0.35	21.24	0.06	1.90
Discharge Termination Criteria	vehicle failure	vehicle failure	1.0 V/cell	motor overheat
Recharge Energy, kWh	N.A.	N.A.	N.A.	N.A.
Coulombic Recharge	N.A.	N.A.	N.A.	300.0
Recharge Time, h	N.A.	N.A.	N.A.	5.0
Battery Temp. (Start of Discharge), °F	92.8	87.8	92.7	92.0
Battery Temp. (End of Discharge), °F	107.0	N.A.	112.0	N.A.
Battery Temp. (Start of Charge), °F	78.2	76.8	71.2	80.2
Battery Temp. (End of Charge), °F	92.8	87.5	92.7	92.0

<sup>a</sup>Invalid range test. Terminated by vehicle failure.

<sup>b</sup>Test terminated early because of motor overheating.



DATA FROM TESTS OF THE 80-CELL EPI NI-FE BATTERY

Battery Cycle	112	113 <sup>a</sup>	114	115 <sup>b</sup>
Date (Discharge)	11/6/80	11/7/80	11/10/80	11/11/80
Test Vehicle	SCT-2	SCT-2	SCT-2	SCT-2
Type of Discharge	C	55 mi/h	35 mi/h	C
Distance Traveled, mi	65.0	81.7	126.0	62.0
Discharge Time, min	245.1	91.2	217.0	233.0
Discharge Energy From Battery, kWh	22.86	21.91	22.97	21.87
Regen. Energy To Battery, kWh	0.63	0.10	0.0	0.57
Coulombic Battery Discharge, Ah	241.4	229.7	232.3	228.2
Coulombic Regen., Ah	5.62	0.09	0.02	5.32
Discharge Termination Criteria	accel. time	1.0 V/cell	1.0 V/cell	accel. time
Recharge Energy, kWh	N.A.	N.A.	N.A.	N.A.
Coulombic Recharge	300.0	300.0	300.0	300.0
Recharge Time, h	5.0	5.0	5.0	5.0
Battery Temp. (Start of Discharge), °F	96.3	94.3	83.8	89.8
Battery Temp. (End of Discharge), °F	N.A.	N.A.	104.2	114.0
Battery Temp. (Start of Charge), °F	83.3	80.7	69.0	78.3
Battery Temp. (End of Charge), °F	96.3	94.3	83.8	92.3

<sup>a</sup>Invalid range test. Motor overheat resulted in current limiting.

<sup>b</sup>Invalid range test. 25-min wait between end of charge and start of discharge.

DATA FROM TESTS OF THE 80-CELL EPI NI-FE BATTERY

Battery Cycle	116 <sup>a</sup>	117 <sup>b</sup>	118	119 <sup>c</sup>
Date (Discharge)	11/13/80	11/17/80	11/18/80	11/20/80
Test Vehicle	SCT-2	SCT-2	SCT-2	SCT-2
Type of Discharge	45 mi/h	45 mi/h	45 mi/h	45 mi/h
Distance Traveled, mi	95.73	92.02	110.71	103.75
Discharge Time, min	128.8	123.8	148.7	139.4
Discharge Energy From Battery, kWh	20.08	19.32	22.77	21.70
Regen. Energy To Battery, kWh	0.02	0.04	0.02	0.01
Coulombic Battery Discharge, Ah	211.0	204.2	232.4	227.0
Coulombic Regen., Ah	0.22	0.04	0.21	0.05
Discharge Termination Criteria	1.0 V/cell	1.0 V/cell	1.0 V/cell	1.0 V/cell
Recharge Energy, kWh	N.A.	N.A.	N.A.	N.A.
Coulombic Recharge	300.0	300.0	300.0	300.0
Recharge Time, h	5.0	5.0	5.0	5.0
Battery Temp. (Start of Discharge), °F	74.0	72.0	93.0	75.7
Battery Temp. (End of Discharge), °F	106.3	105.3	119.0	110.0
Battery Temp. (Start of Charge), °F	79.7	N.A.	75.7	76.3
Battery Temp. (End of Charge), °F	92.7	N.A.	92.0	93.3

<sup>a</sup>24-h open-circuit stand between charge and discharge.

<sup>b</sup>67-h open-circuit stand between charge and discharge.

<sup>c</sup>24-h stand with 120-V float charge between charge and discharge.

DATA FROM TESTS OF THE 80-CELL EPI NI-FE BATTERY

Battery Cycle	120	121	122	123
Date (Discharge)	11/21/80	11/24/80	11/25/80	11/26/80
Test Vehicle	SCT-2	ETV-1-2	ETV-1-2	ETV-1-2
Type of Discharge	50 mi/h	35 mi/h	55 mi/h	D
Distance Traveled, mi	95.67	139.35	103.48	77.09
Discharge Time, min	115.9	240.3	115.1	159.0
Discharge Energy From Battery, kWh	22.23	22.50	21.83	23.25
Regen. Energy To Battery, kWh	0.01	0.03	0.04	3.00
Coulombic Battery Discharge, Ah	227.9	229.7	226.8	249.7
Coulombic Regen., Ah	0.09	0.27	0.34	26.13
Discharge Termination Criteria	1.0 V/cell	1.0 V/cell	1.0 V/cell	accel. time
Recharge Energy, kWh	N.A.	N.A.	N.A.	N.A.
Coulombic Recharge	300.0	300.0	300.0	300.0
Recharge Time, h	5.0	5.0	5.0	5.0
Battery Temp. (Start of Discharge), °F	94.0	88.3	93.0	92.7
Battery Temp. (End of Discharge), °F	123.7	111.0	122.7	130.7
Battery Temp. (Start of Charge), °F	78.2	69.0	74.2	80.5
Battery Temp. (End of Charge), °F	94.0	88.3	93.0	92.7

DATA FROM TESTS OF THE 80-CELL EPI NI-FE BATTERY

Battery Cycle	124	125	126	127 <sup>a</sup>
Date (Discharge)	12/1/80	12/2/80	12/3/80	12/4/80
Test Vehicle	ETV-1-2	ETV-1-2	ETV-1-2	ETV-1-2
Type of Discharge	C	45 mi/h	D	Var.
Distance Traveled, mi	75.55	124.75	78.12	N.A.
Discharge Time, min	286.0	168.1	161.0	N.A.
Discharge Energy From Battery, kWh	23.73	22.47	23.62	N.A.
Regen. Energy To Battery, kWh	2.66	0.04	3.09	N.A.
Coulombic Battery Discharge, Ah	251.2	230.6	250.9	70.6
Coulombic Regen., Ah	23.15	0.41	26.66	N.A.
Discharge Termination Criteria	accel. time	1.0 V/cell	accel. time	vehicle failure
Recharge Energy, kWh	N.A.	N.A.	N.A.	N.A.
Coulombic Recharge	300.0	300.0	300.0	300.0
Recharge Time, h	5.0	5.0	5.0	5.0
Battery Temp. (Start of Discharge), °F	88.7	93.3	92.7	N.A.
Battery Temp. (End of Discharge), °F	117.0	119.3	131.0	N.A.
Battery Temp. (Start of Charge), °F	69.0	78.5	79.2	82.5
Battery Temp. (End of Charge), °F	88.3	92.7	92.7	94.2

<sup>a</sup>Not a range test. Special test at various speeds to examine chopper waveforms. Terminated by vehicle failure.

DATA FROM TESTS OF THE 80-CELL EPI NI-FE BATTERY

Battery Cycle	128 <sup>a</sup>	129	130
Date (Discharge)	12/8/80	12/9/80	12/11/80
Test Vehicle	SCT-2	ETV-1-2	SCT-2
Type of Discharge	45 mi/h	C	C
Distance Traveled, mi	102.24	76.60	64.02
Discharge Time, min	137.8	287.6	241.1
Discharge Energy From Battery, kWh	21.16	23.86	22.30
Regen. Energy To Battery, kWh	0.01	2.81	0.61
Coulombic Battery Discharge, Ah	224.2	253.2	234.4
Coulombic Regen., Ah	0.06	24.53	5.51
Discharge Termination Criteria	1.0 V/cell	accel. time	accel. time
Recharge Energy, kWh	N.A.	N.A.	N.A.
Coulombic Recharge	N.A.	300.0	300.0
Recharge Time, h	N.A.	5.0	5.0
Battery Temp. (Start of Discharge), °F	69.8	93.0	92.0
Battery Temp. (End of Discharge), °F	105.5	123.2	122.0
Battery Temp. (Start of Charge), °F	N.A.	77.8	71.5
Battery Temp. (End of Charge), °F	N.A.	92.8	91.2
<sup>a</sup> 67-h stand with 120-V float charge between charge and discharge.			



## APPENDIX F

### DATA FROM TESTS OF THE 90-CELL EPI NI-FE BATTERY





DATA FROM TESTS OF THE 90-CELL EPI NI-FE BATTERY

Battery Cycle	101 <sup>a</sup>	102	103 <sup>b</sup>
Date (Discharge)	10/21/80	10/22/80	10/23/80
Test Vehicle	--	--	--
Type of Discharge	CC, 75 A	CC, 75 A	CC, 75 A
Distance Traveled, mi	--	--	--
Discharge Time, min	N.A.	N.A.	N.A.
Discharge Energy From Battery, kWh	N.A.	N.A.	N.A.
Regen. Energy To Battery, kWh	--	--	--
Coulmbic Battery Discharge, Ah	258.2	250.1	234.3
Coulombic Regen., Ah	--	--	--
Discharge Termination Criteria	1.0 V/cell	1.0 V/cell	1.0 V/cell
Recharge Energy, kWh	N.A.	N.A.	N.A.
Coulombic Recharge, Ah	400.0	350.0	300.1
Recharge Time, h	N.A.	N.A.	5.0
Battery Temp. (Start of Discharge), °F	N.A.	N.A.	N.A.
Battery Temp. (End of Discharge), °F	N.A.	131.2	N.A.
Battery Temp. (Start of Charge), °F	N.A.	N.A.	78.5
Battery Temp. (End of Charge), °F	N.A.	N.A.	N.A.

<sup>a</sup>First use at JPL. Conditioning cycle.

<sup>b</sup>Battery was configured to 80 cells after this cycle.

DATA FROM TESTS OF THE 90-CELL EPI NI-FE BATTERY

Battery Cycle	131 <sup>a</sup>	132 <sup>b</sup>	133	134 <sup>c</sup>
Date (Discharge)	12/16/80	12/17/80	12/18/80	12/30/80
Test Vehicle	--	--	--	--
Type of Discharge	CC, 75 A	CC, 75 A	CC, 75 A	CC, 58 A
Distance Traveled, mi	--	--	--	--
Discharge Time, min	N.A.	N.A.	N.A.	N.A.
Discharge Energy From Battery, kWh	N.A.	N.A.	N.A.	N.A.
Regen. Energy To Battery, kWh	--	--	--	--
Coulombic Battery Discharge, Ah	237.3	239.3	235.9	223.8
Coulombic Regen., Ah	--	--	--	--
Discharge Termination Criteria	1.0 V/cell	1.0 V/cell	1.0 V/cell	1.0 V/cell
Recharge Energy, kWh	N.A.	N.A.	N.A.	N.A.
Coulombic Recharge, Ah	301.0	300.0	300.0	450.0
Recharge Time, h	5.0	5.0	5.0	N.A.
Battery Temp. (Start of Discharge), °F	89.8	N.A.	92.8	79.5
Battery Temp. (End of Discharge), °F	N.A.	N.A.	N.A.	108.8
Battery Temp. (Start of Charge), °F	71.4	96.0	79.5	69.5
Battery Temp. (End of Charge), °F	89.8	N.A.	92.8	99.5

<sup>a</sup>First cycle after being reconfigured from 80 to 90 cells. Replaced two weak cells and repaired a leaking cell before this cycle.

<sup>b</sup>Replaced two weak cells before this cycle.

<sup>c</sup>Conditioning cycle. Overnight stand between charge and discharge.

DATA FROM TESTS OF THE 90-CELL EPI NI-FE BATTERY

Battery Cycle	135	136	137	138
Date (Discharge)	1/6/81	1/7/81	1/8/81	1/9/81
Test Vehicle	SCT-2	SCT-2	SCT-2	SCT-2
Type of Discharge	45 mi/h	55 mi/h	C	35 mi/h
Distance Traveled, mi	123.7	98.9	70.7	151.8
Discharge Time, min	166.1	109.1	265.0	261.4
Discharge Energy From Battery, kWh	25.55	24.64	25.48	26.21
Regen. Energy To Battery, kWh	0.01	0.01	0.63	0.01
Coulombic Battery Discharge, Ah	231.6	227.0	238.0	236.0
Coulombic Regen., Ah	0.1	0.1	5.1	0.0
Discharge Termination Criteria	1.0 V/cell	1.0 V/cell	accel time	1.0 V/cell
Recharge Energy, kWh	N.A.	N.A.	N.A.	N.A.
Coulombic Recharge, Ah	300.0	300.0	300.0	300.0
Recharge Time, h	5.0	5.0	5.0	5.0
Battery Temp. (Start of Discharge), °F	88.0	93.0	89.2	93.0
Battery Temp. (End of Discharge), °F	110.0	125.0	119.0	107.2
Battery Temp. (Start of Charge), °F	70.0	78.2	77.5	N.A.
Battery Temp. (End of Charge), °F	88.0	93.0	89.2	93.0

DATA FROM TESTS OF THE 90-CELL EPI NI-FE BATTERY

Battery Cycle	139 <sup>a</sup>	140	141
Date (Discharge)	1/12/81	1/13/81	1/15/81
Test Vehicle	SCT-2	SCT-2	--
Type of Discharge	45 mi/h	D	CC, 75 A
Distance Traveled, mi	62.6	66.1	--
Discharge Time, min	85.0	134.8	N.A.
Discharge Energy From Battery, kWh	12.52	23.18	N.A.
Regen. Energy To Battery, kWh	0.0	0.72	--
Coulombic Battery Discharge, Ah	107.0	222.9	235.4
Coulombic Regen., Ah	0.0	5.8	--
Discharge Termination Criteria	107 Ah	accel time	1.0 V/cell
Recharge Energy, kWh	N.A.	N.A.	N.A.
Coulombic Recharge, Ah	300.0	149.7	300.0
Recharge Time, h	5.0	N.A.	5.0
Battery Temp. (Start of Discharge), °F	88.6	82.8	N.A.
Battery Temp. (End of Discharge), °F	96.4	116.0	N.A.
Battery Temp. (Start of Charge), °F	69.8	N.A.	N.A.
Battery Temp. (End of Charge), °F	88.6	82.8	N.A.

<sup>a</sup>Not a range test. Partial discharge.

## APPENDIX G

### DATA FROM TESTS OF THE GLOBE ISOA-1 BATTERY



DATA FROM TESTS OF THE GLOBE ISOA-1 BATTERY

Battery Cycle	50 <sup>a</sup>	51 <sup>b</sup>	52	53
Date (discharge)	2/13/81	3/3/81	3/4/81	3/5/81
Test Vehicle	--	--	--	--
Type of Discharge	CC, 83 A	CC, 83 A	CC, 83 A	CC, 83 A
Distance Traveled, mi	--	--	--	--
Discharge Time, min	N.A.	N.A.	N.A.	N.A.
Discharge Energy from Battery, kWh	N.A.	N.A.	N.A.	N.A.
Regen. Energy To Battery, kWh	--	--	--	--
Coulombic Battery Discharge, Ah	216.0	202.7	216.3	204.3
Coulombic Regen., Ah	--	--	--	--
Discharge Termination Criteria	1.75 V/cell	1.65 V/cell	1.65 V/cell	1.65 V/cell
Recharge Energy, kWh	N.A.	26.30	25.83	24.80
Coulombic Recharge, Ah	N.A.	235.2	234.5	223.5
Recharge Time, h	N.A.	N.A.	N.A.	N.A.
Battery Temp. (Start of Discharge), °F	N.A.	N.A.	N.A.	N.A.
Battery Temp. (End of Discharge), °F	84.0	74.0	82.0	71.0
Battery Temp. (Start of Charge), °F	N.A.	N.A.	N.A.	N.A.
Battery Temp. (End of Charge), °F	N.A.	N.A.	N.A.	N.A.

<sup>a</sup>All previous cycles done at Globe and at ANL.

<sup>b</sup>Top-off charge before this cycle. Acid-stirring pump off until last 15 min of discharge.

DATA FROM TESTS OF THE GLOBE ISOA-1 BATTERY

Battery Cycle	54	55 <sup>a</sup>	56 <sup>b</sup>	57
Date (discharge)	3/23/81	3/24/81	3/25/81	3/26/81
Test Vehicle	--	--	--	--
Type of Discharge	CC, 83 A	CC, 83 A	CC, 83 A	CC, 83 A
Distance Traveled, mi	--	--	--	--
Discharge Time, min	N.A.	N.A.	N.A.	N.A.
Discharge Energy from Battery, kWh	N.A.	N.A.	N.A.	N.A.
Regen. Energy To Battery, kWh	--	--	--	--
Coulombic Battery Discharge, Ah	203.8	220.5	216.7	218.1
Coulombic Regen., Ah	--	--	--	--
Discharge Termination Criteria	1.65 V/cell	1.65 V/cell	1.65 V/cell	1.65 V/cell
Recharge Energy, kWh	27.64	26.24	27.89	N.A.
Coulombic Recharge, Ah	249.1	240.2	251.9	254.9
Recharge Time, h	N.A.	N.A.	N.A.	N.A.
Battery Temp. (Start of Discharge), °F	68.0	N.A.	N.A.	N.A.
Battery Temp. (End of Discharge), °F	77.0	85.0	82.0	84.0
Battery Temp. (Start of Charge), °F	78.0	83.0	81.0	79.7
Battery Temp. (End of Charge), °F	81.0	75.2	79.6	74.7

<sup>a</sup>Charge error: battery undercharged.

<sup>b</sup>Battery terminals cleaned prior to discharge.



DATA FROM TESTS OF THE GLOBE ISOA-1 BATTERY

Battery Cycle	58	59	60	61
Date (discharge)	3/27/81	3/30/81	3/31/81	4/1/81
Test Vehicle	ETV-1-2	ETV-1-2	ETV-1-2	ETV-1-2
Type of Discharge	45 mi/h	D	35 mi/h	55 mi/h
Distance Traveled, mi	101.56	56.33	122.68	77.31
Discharge Time, min	136.4	117.5	211.7	86.1
Discharge Energy from Battery, kWh	19.41	17.60	20.43	17.16
Regen. Energy To Battery, kWh	0.04	2.12	0.03	0.07
Coulombic Battery Discharge, Ah	211.2	202.0	219.8	188.8
Coulombic Regen., Ah	0.35	19.94	0.27	0.70
Discharge Termination Criteria	1.65 V/cell	accel time	1.65 V/cell	1.65 V/cell
Recharge Energy, kWh	26.13	23.10	27.49	23.75
Coulombic Recharge, Ah	235.6	207.2	247.6	213.8
Recharge Time, h	N.A.	N.A.	N.A.	N.A.
Battery Temp. (Start of Discharge), °F	72.0	70.6	72.8	75.4
Battery Temp. (End of Discharge), °F	79.2	87.6	78.0	85.6
Battery Temp. (Start of Charge), °F	81.0	85.6	79.0	78.0
Battery Temp. (End of Charge), °F	75.4	76.0	76.1	76.1

DATA FROM TESTS OF THE GLOBE ISOA-1 BATTERY

Battery Cycle	62 <sup>a</sup>	63	64	65 <sup>b</sup>
Date (discharge)	4/2/81	4/3/81	4/6/81	4/7/81
Test Vehicle	ETV-1-2	ETV-1-2	ETV-1-2	ETV-1-2
Type of Discharge	55 mi/h	C	55 mi/h	D
Distance Traveled, mi	71.50	64.77	71.66	56.44
Discharge Time, min	79.3	246.6	80.0	117.0
Discharge Energy from Battery, kWh	16.09	20.08	15.79	17.15
Regen. Energy To Battery, kWh	0.09	2.01	0.09	2.33
Coulombic Battery Discharge, Ah	177.5	227.6	175.3	196.2
Coulombic Regen., Ah	0.85	18.80	0.85	22.02
Discharge Termination Criteria	1.65 V/cell	1.3 V/cell	1.65 V/cell	accel time
Recharge Energy, kWh	21.93	25.81	22.21	21.93
Coulombic Recharge, Ah	198.3	233.7	199.4	198.0
Recharge Time, h	N.A.	N.A.	N.A.	N.A.
Battery Temp. (Start of Discharge), °F	75.4	70.6	70.0	71.8
Battery Temp. (End of Discharge), °F	83.6	82.8	79.4	87.6
Battery Temp. (Start of Charge), °F	84.5	82.0	79.9	87.8
Battery Temp. (End of Charge), °F	73.6	75.2	77.7	77.1

<sup>a</sup>Watered battery before this cycle.

<sup>b</sup>One weak module. Problem identified later as inadequate circulation.

DATA FROM TESTS OF THE GLOBE ISOA-1 BATTERY

Battery Cycle	66 <sup>a</sup>	67 <sup>b</sup>	68 <sup>c</sup>	69 <sup>d</sup>
Date (discharge)	4/8/81	4/9/81	4/22/81	4/23/81
Test Vehicle	ETV-1-2	ETV-1-2	--	--
Type of Discharge	FTP	45 mi/h	CC, 83 A	CC, 83 A
Distance Traveled, mi	61.39	96.90	--	--
Discharge Time, min	273.2	130.6	N.A.	N.A.
Discharge Energy from Battery, kWh	19.74	18.03	N.A.	N.A.
Regen. Energy To Battery, kWh	2.57	0.06	--	--
Coulombic Battery Discharge, Ah	228.0	196.5	207.0	219.5
Coulombic Regen., Ah	23.55	0.54	--	--
Discharge Termination Criteria	1.3 V/cell	1.65 V/cell	1.65 V/cell	1.65 V/cell
Recharge Energy, kWh	27.88	24.00	N.A.	N.A.
Coulombic Recharge, Ah	247.8	217.3	238.0	270.0
Recharge Time, h	N.A.	N.A.	N.A.	N.A.
Battery Temp. (Start of Discharge), °F	72.4	75.6	N.A.	N.A.
Battery Temp. (End of Discharge), °F	84.8	80.4	N.A.	90.0
Battery Temp. (Start of Charge), °F	82.0	81.5	N.A.	N.A.
Battery Temp. (End of Charge), °F	80.0	77.0	N.A.	N.A.

<sup>a</sup>Charging error: battery overcharged.

<sup>b</sup>Diagnostic test only.

<sup>c</sup>Top-off charge before this cycle.

<sup>d</sup>Charging error: battery overcharged. Returned to Globe for analysis after this cycle.



## APPENDIX H

### DATA FROM TESTS OF THE GLOBE ISOA-2 BATTERY



DATA FROM TESTS OF THE GLOBE ISOA-2 BATTERY

Battery Cycle	33 <sup>a</sup>	34	35	36 <sup>b</sup>
Date (discharge)	8/19/81	9/2/81	9/4/81	9/9/81
Test Vehicle	--	--	--	ETV-1-2
Type of Discharge	CC, 83 A	CC, 83 A	CC, 83 A	45 mi/h
Distance Traveled, mi	--	--	--	109.71
Discharge Time, min	N.A.	N.A.	N.A.	149.7
Discharge Energy from Battery, kWh	N.A.	N.A.	N.A.	19.54
Regen. Energy To Battery, kWh	--	--	--	0.06
Coulombic Battery Discharge, Ah	226.2	193.1	218.4	213.5
Coulombic Regen., Ah	--	--	--	0.56
Discharge Termination Criteria	1.75 V/cell	1.75 V/cell	1.75 V/cell	1.75 V/cell
Recharge Energy, kWh	N.A.	N.A.	N.A.	47.49
Coulombic Recharge, Ah	263.3	263.2	259.8	401.6
Recharge Time, h	N.A.	N.A.	N.A.	N.A.
Battery Temp. (Start of Discharge), °F	N.A.	N.A.	N.A.	75.0
Battery Temp. (End of Discharge), °F	86.0	82.0	85.0	84.8
Battery Temp. (Start of Charge), °F	N.A.	N.A.	N.A.	N.A.
Battery Temp. (End of Charge), °F	N.A.	N.A.	N.A.	N.A.

<sup>a</sup>First cycle at JPL. Gravities adjusted.

<sup>b</sup>Excessive overcharge. Thermal runaway. Added water. Gravities adjusted.

DATA FROM TESTS OF THE GLOBE ISOA-2 BATTERY

Battery Cycle	37	38	39 <sup>a</sup>	40
Date (discharge)	9/17/81	9/21/81	10/16/81	10/19/81
Test Vehicle	--	--	--	--
Type of Discharge	CC, 83 A	CC, 83 A	CC, 83 A	CC, 83 A
Distance Traveled, mi	--	--	--	--
Discharge Time, min	N.A.	N.A.	N.A.	N.A.
Discharge Energy from Battery, kWh	N.A.	N.A.	N.A.	N.A.
Regen. Energy To Battery, kWh	--	--	--	--
Coulombic Battery Discharge, Ah	219.7	212.2	224.4	214.6
Coulombic Regen., Ah	--	--	--	--
Discharge Termination Criteria	1.75 V/cell	1.75 V/cell	1.75 V/cell	1.75 V/cell
Recharge Energy, kWh	N.A.	N.A.	N.A.	N.A.
Coulombic Recharge, Ah	241.2	N.A.	262.3	251.8
Recharge Time, h	N.A.	N.A.	N.A.	N.A.
Battery Temp. (Start of Discharge), °F	N.A.	71.0	81.0	76.0
Battery Temp. (End of Discharge), °F	82.0	79.0	88.0	83.0
Battery Temp. (Start of Charge), °F	N.A.	N.A.	N.A.	83.0
Battery Temp. (End of Charge), °F	N.A.	N.A.	N.A.	N.A.

<sup>a</sup>Top-off charge before this cycle.



DATA FROM TESTS OF THE GLOBE ISOA-2 BATTERY

Battery Cycle	41	42 <sup>a</sup>	43	44 <sup>b</sup>
Date (discharge)	10/20/81	10/28/81	10/30/81	11/2/81
Test Vehicle	--	ETV-1-2	ETV-1-2	ETV-1-2
Type of Discharge	CC, 83 A	45 mi/h	55 mi/h	D
Distance Traveled, mi	--	110.88	83.38	8.87
Discharge Time, min	N.A.	148.9	95.0	19.9
Discharge Energy from Battery, kWh	N.A.	19.68	17.08	2.68
Regen. Energy To Battery, kWh	--	0.05	0.08	0.41
Coulombic Battery Discharge, Ah	235.1	217.2	189.1	29.6
Coulombic Regen., Ah	--	0.49	0.71	3.73
Discharge Termination Criteria	1.75 V/cell	1.75 V/cell	1.75 V/cell	vehicle failure
Recharge Energy, kWh	N.A.	27.67	25.15	N.A.
Coulombic Recharge, Ah	271.1	249.6	225.2	41.4
Recharge Time, h	N.A.	N.A.	N.A.	N.A.
Battery Temp. (Start of Discharge), °F	88.0	71.0	75.0	73.0
Battery Temp. (End of Discharge), °F	94.0	80.0	86.4	76.4
Battery Temp. (Start of Charge), °F	N.A.	78.8	84.2	N.A.
Battery Temp. (End of Charge), °F	N.A.	93.2	91.8	N.A.

<sup>a</sup>Top-off charge before this test.

<sup>b</sup>Invalid range test: terminated by vehicle failure.

DATA FROM TESTS OF THE GLOBE ISOA-2 BATTERY

Battery Cycle	45	46	47 <sup>a</sup>	48 <sup>b</sup>
Date (discharge)	12/11/81	1/6/82	1/8/82	1/13/82
Test Vehicle	--	--	ETV-1-2	ETV-1-2
Type of Discharge	CC, 83 A	CC, 83 A	D	D
Distance Traveled, mi	--	--	52.49	43.44
Discharge Time, min	N.A.	N.A.	114.3	91.0
Discharge Energy from Battery, kWh	N.A.	N.A.	15.88	12.92
Regen. Energy To Battery, kWh	--	--	1.75	1.78
Coulombic Battery Discharge, Ah	180.5	199.7	182.3	149.3
Coulombic Regen., Ah	--	--	16.38	16.45
Discharge Termination Criteria	1.75 V/cell	1.75 V/cell	vehicle failure	accel time
Recharge Energy, kWh	N.A.	N.A.	22.19	18.98
Coulombic Recharge, Ah	242.5	247.8	198.0	166.4
Recharge Time, h	N.A.	N.A.	12.0	11.4
Battery Temp. (Start of Discharge), °F	N.A.	64.0	73.3	66.1
Battery Temp. (End of Discharge), °F	N.A.	74.6	94.7	85.8
Battery Temp. (Start of Charge), °F	N.A.	N.A.	N.A.	N.A.
Battery Temp. (End of Charge), °F	N.A.	N.A.	N.A.	N.A.

<sup>a</sup>Invalid range test: terminated by vehicle failure.

<sup>b</sup>Invalid range test: cold battery.

DATA FROM TESTS OF THE GLOBE ISOA-2 BATTERY

Battery Cycle	49 <sup>a</sup>	50	51 <sup>b</sup>	52
Date (discharge)	1/15/82	2/11/82	2/15/82	2/17/82
Test Vehicle	ETV-1-2	--	ETV-1-1	ETV-1-1
Type of Discharge	D	CC, 83 A	45 mi/h	45 mi/h
Distance Traveled, mi	33.74	--	101.25	108.53
Discharge Time, min	73.8	N.A.	138.2	145.0
Discharge Energy from Battery, kWh	9.95	N.A.	18.11	19.26
Regen. Energy To Battery, kWh	1.34	--	0.04	0.04
Coulombic Battery Discharge, Ah	113.4	174.2	195.2	206.9
Coulombic Regen., Ah	12.22	--	0.41	0.38
Discharge Termination Criteria	vehicle failure	1.75 V/cell	1.75 V/cell	1.75 V/cell
Recharge Energy, kWh	15.69	N.A.	N.A.	28.22
Coulombic Recharge, Ah	136.9	N.A.	229.3	252.0
Recharge Time, h	N.A.	N.A.	12.6	N.A.
Battery Temp. (Start of Discharge), °F	73.8	N.A.	70.4	75.8
Battery Temp. (End of Discharge), °F	87.6	N.A.	81.5	85.9
Battery Temp. (Start of Charge), °F	85.5	N.A.	N.A.	81.8
Battery Temp. (End of Charge), °F	94.4	N.A.	N.A.	96.6

<sup>a</sup>Invalid range test: terminated by vehicle failure.

<sup>b</sup>Not a range test. Diagnostic car test and battery conditioning cycle.

DATA FROM TESTS OF THE GLOBE ISOA-2 BATTERY

Battery Cycle	53 <sup>a</sup>	54	55 <sup>b</sup>	56 <sup>c</sup>
Date (discharge)	2/19/82	2/25/82	3/4/82	3/5/82
Test Vehicle	--	--	--	--
Type of Discharge	CC, 83 A	CC, 83 A	CC, 83 A	CC, 83 A
Distance Traveled, mi	--	--	--	--
Discharge Time, min	N.A.	N.A.	N.A.	N.A.
Discharge Energy from Battery, kWh	N.A.	N.A.	N.A.	N.A.
Regen. Energy To Battery, kWh	--	--	--	--
Coulombic Battery Discharge, Ah	206.5	192.7	200.8	215.6
Coulombic Regen., Ah	--	--	--	--
Discharge Termination Criteria	1.75 V/cell	N.A.	1.75 V/cell	1.75 V/cell
Recharge Energy, kWh	24.02	N.A.	N.A.	N.A.
Coulombic Recharge, Ah	223.0	219.6	244.6	265.6
Recharge Time, h	N.A.	N.A.	N.A.	N.A.
Battery Temp. (Start of Discharge), °F	75.6	N.A.	73.0	84.4
Battery Temp. (End of Discharge), °F	82.6	N.A.	82.2	90.0
Battery Temp. (Start of Charge), °F	N.A.	N.A.	82.2	N.A.
Battery Temp. (End of Charge), °F	N.A.	N.A.	N.A.	N.A.

<sup>a</sup>Watered battery before this cycle. Interrupted charge because electrolyte was coming out of flame arrestors.

<sup>b</sup>Adjusted electrolyte levels and specific gravities in all cells before this cycle.

<sup>c</sup>Interrupted charge because electrolyte was coming out of flame arrestors. Adjusted electrolyte levels and finished charge.

DATA FROM TESTS OF THE GLOBE ISOA-2 BATTERY

Battery Cycle	57	58	59	60
Date (discharge)	3/10/82	3/11/82	3/15/82	3/17/82
Test Vehicle	--	--	ETV-1-1	ETV-1-1
Type of Discharge	CC, 83 A	CC, 83 A	45 mi/h	35 mi/h
Distance Traveled, mi	--	--	101.84	138.85
Discharge Time, min	N.A.	N.A.	136.7	238.8
Discharge Energy from Battery, kWh	N.A.	N.A.	18.65	22.24
Regen. Energy To Battery, kWh	--	--	0.04	0.03
Coulombic Battery Discharge, Ah	215.2	223.5	201.1	236.0
Coulombic Regen., Ah	--	--	0.36	0.25
Discharge Termination Criteria	1.75 V/cell	1.75 V/cell	1.75 V/cell	1.75 V/cell
Recharge Energy, kWh	N.A.	N.A.	27.09	31.18
Coulombic Recharge, Ah	253.1	242.6	241.5	279.5
Recharge Time, h	N.A.	N.A.	13.2	13.9
Battery Temp. (Start of Discharge), °F	75.2	81.8	69.9	74.4
Battery Temp. (End of Discharge), °F	84.2	90.0	80.7	81.7
Battery Temp. (Start of Charge), °F	84.2	90.0	78.9	78.2
Battery Temp. (End of Charge), °F	N.A.	N.A.	92.6	93.7

DATA FROM TESTS OF THE GLOBE ISOA-2 BATTERY

Battery Cycle	61 <sup>a</sup>	62 <sup>b</sup>	63	64
Date (discharge)	3/19/82	3/22/82	3/24/82	3/26/82
Test Vehicle	ETV-1-1	ETV-1-1	ETV-1-1	ETV-1-1
Type of Discharge	35 mi/h	55 mi/h	55 mi/h	35 mi/h
Distance Traveled, mi	139.7	75.33	78.39	140.03
Discharge Time, min	241.8	83.5	87.4	241.8
Discharge Energy from Battery, kWh	22.44	15.87	16.47	21.90
Regen. Energy To Battery, kWh	0.03	0.07	0.08	0.02
Coulombic Battery Discharge, Ah	238.5	173.1	179.3	231.1
Coulombic Regen., Ah	0.27	0.73	0.74	0.25
Discharge Termination Criteria	1.75 V/cell	see note below	1.75 V/cell	1.75 V/cell
Recharge Energy, kWh	31.48	24.17	24.55	30.88
Coulombic Recharge, Ah	282.6	213.6	217.7	275.1
Recharge Time, h	14.0	12.6	12.7	13.8
Battery Temp. (Start of Discharge), °F	73.9	72.3	75.8	73.3
Battery Temp. (End of Discharge), °F	81.2	84.7	87.5	80.6
Battery Temp. (Start of Charge), °F	79.7	80.4	82.2	80.3
Battery Temp. (End of Charge), °F	94.2	92.3	93.0	94.2

<sup>a</sup>Operational problems with ETV-1-1 during this test, but test validity was not impaired.

<sup>b</sup>Invalid range test. Terminated at 84.86 V instead of 84.0 V.

DATA FROM TESTS OF THE GLOBE ISOA-2 BATTERY

Battery Cycle	65	66	67 <sup>a</sup>	68 <sup>b</sup>
Date (discharge)	3/29/82	3/30/82	4/1/82	4/7/82
Test Vehicle	ETV-1-1	ETV-1-1	ETV-1-1	--
Type of Discharge	D	D	45 mi/h	CC, 83 A
Distance Traveled, mi	48.30	58.36	12.65	--
Discharge Time, min	101.4	120.6	18.2	142.0
Discharge Energy from Battery, kWh	14.73	17.57	2.48	N.A.
Regen. Energy To Battery, kWh	1.63	1.93	0.05	--
Coulombic Battery Discharge, Ah	169.1	199.3	25.7	192.9
Coulombic Regen., Ah	15.48	18.35	0.44	--
Discharge Termination Criteria	1.3 V/cell	accel time	electrolyte levels	1.75 V/cell
Recharge Energy, kWh	22.52	24.68	N.A.	N.A.
Coulombic Recharge, Ah	205.0	223.0	N.A.	233.6
Recharge Time, h	12.2	12.8	N.A.	13.3
Battery Temp. (Start of Discharge), °F	69.8	85.4	71.7	70.8
Battery Temp. (End of Discharge), °F	90.7	105.7	74.1	78.0
Battery Temp. (Start of Charge), °F	84.8	92.0	N.A.	78.0
Battery Temp. (End of Charge), °F	90.3	92.2	N.A.	N.A.

<sup>a</sup>Test aborted because of low electrolyte level in some cells.

<sup>b</sup>Conditioning cycle. Adjusted gravities.

DATA FROM TESTS OF THE GLOBE ISOA-2 BATTERY

Battery Cycle	69 <sup>a</sup>	70	71 <sup>b</sup>	72 <sup>c</sup>
Date (discharge)	4/9/82	4/12/82	4/13/82	4/14/82
Test Vehicle	ETV-1-1	ETV-1-1	ETV-1-1	ETV-1-1
Type of Discharge	45 mi/h	FTP	FTP	FTP
Distance Traveled, mi	108.09	51.22	29.84	29.64
Discharge Time, min	146.7	218.1	126.5	122.9
Discharge Energy from Battery, kWh	18.55	16.37	9.60	9.48
Regen. Energy To Battery, kWh	0.03	1.93	1.17	1.20
Coulombic Battery Discharge, Ah	199.6	185.0	103.5	102.2
Coulombic Regen., Ah	0.33	18.28	11.00	11.24
Discharge Termination Criteria	1.75 V/cell	1.3 V/cell	30 mi	30 mi
Recharge Energy, kWh	27.28	23.10	14.56	14.14
Coulombic Recharge, Ah	257.1	203.9	125.1	122.0
Recharge Time, h	13.3	12.5	10.9	N.A.
Battery Temp. (Start of Discharge), °F	73.0	71.7	86.0	83.9
Battery Temp. (End of Discharge), °F	81.7	87.3	91.4	91.0
Battery Temp. (Start of Charge), °F	82.2	84.5	84.2	83.5
Battery Temp. (End of Charge), °F	92.6	91.3	89.5	87.8

<sup>a</sup>Invalid range test: operational problems with ETV-1-1.

<sup>b</sup>Partial discharge.

<sup>c</sup>Partial discharge.



DATA FROM TESTS OF THE GLOBE ISOA-2 BATTERY

Battery Cycle	73	74	75	76 <sup>a</sup>
Date (discharge)	4/15/82	4/16/82	4/19/82	5/3/82
Test Vehicle	ETV-1-1	ETV-1-1	ETV-1-1	--
Type of Discharge	FTP	45 mi/h	45 mi/h	CC, 83 A
Distance Traveled, mi	57.15	111.32	99.00	--
Discharge Time, min	251.1	149.7	134.6	N.A.
Discharge Energy from Battery, kWh	18.29	18.99	17.75	N.A.
Regen. Energy To Battery, kWh	2.21	0.05	0.05	--
Coulombic Battery Discharge, Ah	206.1	202.2	190.6	179.2
Coulombic Regen., Ah	20.89	0.51	0.49	--
Discharge Termination Criteria	1.3 V/cell	1.75 V/cell	1.75 V/cell	1.75 V/cell
Recharge Energy, kWh	24.54	26.87	26.44	N.A.
Coulombic Recharge, Ah	219.6	239.9	234.1	N.A.
Recharge Time, h	12.9	13.2	13.0	11.8
Battery Temp. (Start of Discharge), °F	82.2	83.7	72.8	74.0
Battery Temp. (End of Discharge), °F	96.9	89.5	81.7	83.0
Battery Temp. (Start of Charge), °F	92.3	89.7	80.0	81.4
Battery Temp. (End of Charge), °F	93.2	91.8	93.9	N.A.

<sup>a</sup>Conditioning cycle. Measured gassing rate during charge.



APPENDIX I

DATA FROM TESTS OF THE W-220-1 BATTERY



DATA FROM TESTS OF THE W-220-1 BATTERY

Battery Cycle	1 <sup>a</sup>	2	3	4 <sup>b</sup>
Date (discharge)	8/14/80	8/15/80	8/22/80	9/5/80
Test Vehicle	--	--	--	--
Type of Discharge	CC, 70 A	CC, 70 A	CC, 70 A	N.A.
Distance Traveled, mi	--	--	--	--
Discharge Time, min	N.A.	N.A.	N.A.	N.A.
Discharge Energy from Battery, kWh	N.A.	N.A.	N.A.	N.A.
Regen. Energy To Battery, kWh	--	--	--	--
Coulombic Battery Discharge, Ah	26	180	202	N.A.
Coulombic Regen., Ah	--	--	--	--
Discharge Termination Criteria	1.0 V/cell	KOH leak	1.0 V/cell	1.0 V/cell
Recharge Energy, kWh	N.A.	N.A.	N.A.	N.A.
Coulombic Recharge, Ah	70	273	348	35
Recharge Time, h	N.A.	N.A.	N.A.	N.A.
Battery Temp. (Start of Discharge), °F	N.A.	N.A.	N.A.	N.A.
Battery Temp. (End of Discharge), °F	N.A.	N.A.	N.A.	N.A.
Battery Temp. (Start of Charge), °F	N.A.	N.A.	N.A.	N.A.
Battery Temp. (End of Charge), °F	N.A.	N.A.	N.A.	N.A.

<sup>a</sup>Shakedown cycle.

<sup>b</sup>Partial charge prior to start of vehicle testing.

DATA FROM TESTS OF THE W-220-1 BATTERY

Battery Cycle	5 <sup>a</sup>	6 <sup>b</sup>	7 <sup>c</sup>	8
Date (discharge)	9/8/80	9/9/80	9/10/80	10/3/80
Test Vehicle	SCT-2	SCT-2	ETV-1-2	--
Type of Discharge	D	D	55 mi/h	CC, 112 A
Distance Traveled, mi	17.2	18.0	68.76	--
Discharge Time, min	36.1	37.2	76.8	N.A.
Discharge Energy from Battery, kWh	6.36	6.44	14.60	N.A.
Regen. Energy To Battery, kWh	0.14	0.16	0.07	--
Coulombic Battery Discharge, Ah	63.3	66.1	154.6	181.7
Coulombic Regen., Ah	1.1	1.3	0.58	--
Discharge Termination Criteria	vehicle failure	see note	1.0 V/cell	1.0 V/cell
Recharge Energy, kWh	N.A.	N.A.	N.A.	N.A.
Coulombic Recharge, Ah	364	100	103	348.3
Recharge Time, h	N.A.	N.A.	N.A.	N.A.
Battery Temp. (Start of Discharge), °F	91.6	84.4	84.2	N.A.
Battery Temp. (End of Discharge), °F	109.0	104.4	115.4	N.A.
Battery Temp. (Start of Charge), °F	N.A.	N.A.	N.A.	N.A.
Battery Temp. (End of Charge), °F	91.6	84.4	84.2	N.A.

<sup>a</sup>Invalid range test: terminated by vehicle failure.

<sup>b</sup>Invalid range test: terminated because battery terminals overheating.

<sup>c</sup>Battery was configured to 84 cells during this test.

DATA FROM TESTS OF THE W-220-1 BATTERY

Battery Cycle	9	10	11	12
Date (discharge)	10/6/80	10/7/80	10/8/80	10/10/80
Test Vehicle	SCT-2	SCT-2	ETV-1-2	--
Type of Discharge	CC, 112 A	CC, 112 A	CC, 112 A	CC, 112 A
Distance Traveled, mi	--	--	--	--
Discharge Time, min	N.A.	N.A.	N.A.	N.A.
Discharge Energy from Battery, kWh	N.A.	N.A.	N.A.	N.A.
Regen. Energy To Battery, kWh	--	--	--	--
Coulombic Battery Discharge, Ah	186.9	182.4	186.6	206.7
Coulombic Regen., Ah	--	--	--	--
Discharge Termination Criteria	80 V	80 V	80 V	80 V
Recharge Energy, kWh	N.A.	N.A.	N.A.	N.A.
Coulombic Recharge, Ah	297.6	278.8	280	348
Recharge Time, h	N.A.	N.A.	N.A.	N.A.
Battery Temp. (Start of Discharge), °F	N.A.	N.A.	N.A.	N.A.
Battery Temp. (End of Discharge), °F	N.A.	N.A.	N.A.	N.A.
Battery Temp. (Start of Charge), °F	N.A.	N.A.	N.A.	N.A.
Battery Temp. (End of Charge), °F	N.A.	N.A.	N.A.	N.A.

DATA FROM TESTS OF THE W-220-1 BATTERY

Battery Cycle	13	14	15	16
Date (discharge)	10/13/80	10/14/80	10/15/80	10/27/80
Test Vehicle	--	--	--	--
Type of Discharge	CC, 112 A	CC, 112 A	CC, 112 A	CC, 112 A
Distance Traveled, mi	--	--	--	--
Discharge Time, min	N.A.	N.A.	N.A.	N.A.
Discharge Energy from Battery, kWh	N.A.	N.A.	N.A.	N.A.
Regen. Energy To Battery, kWh	--	--	--	--
Coulombic Battery Discharge, Ah	212.4	199.9	188.8	200
Coulombic Regen., Ah	--	--	--	--
Discharge Termination Criteria	80 V	80 V	80 V	80 V
Recharge Energy, kWh	N.A.	N.A.	N.A.	N.A.
Coulombic Recharge, Ah	350	323	301.2	350.4
Recharge Time, h	N.A.	N.A.	N.A.	N.A.
Battery Temp. (Start of Discharge), °F	N.A.	N.A.	N.A.	129
Battery Temp. (End of Discharge), °F	N.A.	N.A.	N.A.	N.A.
Battery Temp. (Start of Charge), °F	N.A.	N.A.	N.A.	N.A.
Battery Temp. (End of Charge), °F	90	N.A.	N.A.	N.A.



# DATA FROM TESTS OF THE W-220-1 BATTERY

Battery Cycle	17	18	19	20
Date (discharge)	10/28/80	10/29/80	10/30/80	4/10/81
Test Vehicle	--	--	--	--
Type of Discharge	CC, 112 A	CC, 112 A	CC, 75 A	CC, 115 A
Distance Traveled, mi	--	--	--	--
Discharge Time, min	N.A.	N.A.	N.A.	N.A.
Discharge Energy from Battery, kWh	N.A.	N.A.	N.A.	N.A.
Regen. Energy To Battery, kWh	--	--	--	--
Coulombic Battery Discharge, Ah	212.8	206.8	211.7	123.9
Coulombic Regen., Ah	--	--	--	--
Discharge Termination Criteria	70 V	80 V	80 V	1.0 V/cell
Recharge Energy, kWh	N.A.	N.A.	N.A.	N.A.
Coulombic Recharge, Ah	354.3	353.5	354.3	420.1
Recharge Time, h	N.A.	N.A.	N.A.	N.A.
Battery Temp. (Start of Discharge), °F	88	88	N.A.	N.A.
Battery Temp. (End of Discharge), °F	130	130	125	N.A.
Battery Temp. (Start of Charge), °F	N.A.	N.A.	N.A.	N.A.
Battery Temp. (End of Charge), °F	89	88	85	N.A.

DATA FROM TESTS OF THE W-220-1 BATTERY

Battery Cycle	21	22	23 <sup>a</sup>	24 <sup>a</sup>
Date (discharge)	4/13/81	4/14/81	6/17/81	6/18/81
Test Vehicle	--	--	--	--
Type of Discharge	CC, 115 A	CC, 115 A	special	special
Distance Traveled, mi	--	--	--	--
Discharge Time, min	N.A.	N.A.	N.A.	N.A.
Discharge Energy from Battery, kWh	N.A.	16.85	N.A.	N.A.
Regen. Energy To Battery, kWh	--	--	--	--
Coulombic Battery Discharge, Ah	151.8	165.1	N.A.	N.A.
Coulombic Regen., Ah	--	--	--	--
Discharge Termination Criteria	90 V	90 V	N.A.	N.A.
Recharge Energy, kWh	N.A.	53.29	N.A.	N.A.
Coulombic Recharge, Ah	353.7	353.0	N.A.	N.A.
Recharge Time, h	N.A.	N.A.	N.A.	N.A.
Battery Temp. (Start of Discharge), °F	N.A.	N.A.	N.A.	N.A.
Battery Temp. (End of Discharge), °F	N.A.	N.A.	N.A.	N.A.
Battery Temp. (Start of Charge), °F	N.A.	N.A.	N.A.	N.A.
Battery Temp. (End of Charge), °F	N.A.	N.A.	N.A.	N.A.

<sup>a</sup>Tests conducted by Westinghouse personnel to select the best cells for use in the W-220-3 battery.

## APPENDIX J

### DATA FROM TESTS OF THE W-220-2 BATTERY



DATA FROM TESTS OF THE W-220-2 BATTERY

Battery Cycle	1	2	3	4
Date (Discharge)	2/3/81	2/4/81	2/5/81	2/12/81
Test Vehicle	--	--	--	--
Type of Discharge	CC, 115 A	CC, 115 A	CC, 115 A	CC, 115 A
Distance Traveled, mi	--	--	--	--
Discharge Time, min	N.A.	N.A.	N.A.	N.A.
Discharge Energy From Battery, kWh	N.A.	N.A.	N.A.	N.A.
Regen. Energy To Battery, kWh	--	--	--	--
Coulombic Battery Discharge, Ah	181.73	174	189	193.6
Coulombic Regen., Ah	--	--	--	--
Discharge Termination Criteria	1.0 V/cell	1.0 V/cell	1.0 V/cell	1.0 V/cell
Recharge Energy, kWh	N.A.	N.A.	N.A.	N.A.
Coulombic Recharge, Ah	350.0	350.7	350.0	352.0
Recharge Time, h	5.0	5.0	5.0	5.0
Battery Temp. (Start of Discharge), °F	N.A.	91.0	N.A.	N.A.
Battery Temp. (End of Discharge), °F	N.A.	100.0	N.A.	N.A.
Battery Temp. (Start of Charge), °F	N.A.	65.0	N.A.	N.A.
Battery Temp. (End of Charge), °F	N.A.	91.0	N.A.	120.0

DATA FROM TESTS OF THE W-220-2 BATTERY

Battery Cycle	5 <sup>a</sup>	6 <sup>b</sup>	7	8
Date (Discharge)	3/4/81	3/5/81	3/12/81	3/16/81
Test Vehicle	--	--	--	--
Type of Discharge	CC, 115 A	CC, 115 A	CC, 115 A	CC, 115 A
Distance Traveled, mi	--	--	--	--
Discharge Time, min	N.A.	N.A.	N.A.	N.A.
Discharge Energy From Battery, kWh	N.A.	N.A.	13.76	17.20
Regen. Energy To Battery, kWh	--	--	--	--
Coulombic Battery Discharge, Ah	186.8	149.0	133.7	167.1
Coulombic Regen., Ah	--	--	--	--
Discharge Termination Criteria	1.0 V/cell	Cell Failure	1.0 V/cell	1.0 V/cell
Recharge Energy, kWh	N.A.	N.A.	32.42	53.34
Coulombic Recharge, Ah	353.7	354.3	220.0	353.0
Recharge Time, h	N.A.	N.A.	N.A.	5.0
Battery Temp. (Start of Discharge), °F	89	94	91	88.2
Battery Temp. (End of Discharge), °F	105	N.A.	108	129.7
Battery Temp. (Start of Charge), °F	N.A.	80	77	80.2
Battery Temp. (End of Charge), °F	89	94	91	90.0

<sup>a</sup>Installed battery in SCT-2 before this test.

<sup>b</sup>Ruptured a cell during discharge. Battery removed from car. Ruptured cell and adjacent cell replaced.

DATA FROM TESTS OF THE W-220-2 BATTERY

Battery Cycle	9	10	11 <sup>a</sup>	12
Date (Discharge)	3/17/81	3/18/81	3/23/81	3/24/81
Test Vehicle	--	--	--	--
Type of Discharge	CC, 115 A	CC, 115 A	CC, 115 A	CC, 115 A
Distance Traveled, mi	--	--	--	--
Discharge Time, min	88.0	N.A.	N.A.	N.A.
Discharge Energy From Battery, kWh	17.55	18.13	17.77	17.97
Regen. Energy To Battery, kWh	--	--	--	--
Coulombic Battery Discharge, Ah	170.6	176.3	170.7	172.6
Coulombic Regen., Ah	--	--	--	--
Discharge Termination Criteria	1.0 V/cell	1.0 V/cell	1.0 V/cell	1.0 V/cell
Recharge Energy, kWh	52.40	52.96	53.63	53.56
Coulombic Recharge, Ah	352.4	353.2	354.4	351.4
Recharge Time, h	5.0	5.0	5.0	5.0
Battery Temp. (Start of Discharge), °F	90.8	92.8	83.8	85.5
Battery Temp. (End of Discharge), °F	131.8	125.8	122.8	127.5
Battery Temp. (Start of Charge), °F	104.2	N.A.	N.A.	72.8
Battery Temp. (End of Charge), °F	92.5	N.A.	N.A.	86.5

<sup>a</sup>Replaced two cells with low capacity before this cycle.

DATA FROM TESTS OF THE W-220-2 BATTERY

Battery Cycle	13 <sup>a</sup>	14	15	16
Date (Discharge)	3/25/81	3/27/81	3/30/81	3/31/81
Test Vehicle	--	--	--	--
Type of Discharge	CC, 115 A	CC, 115 A	CC, 115 A	CC, 115 A
Distance Traveled, mi	--	--	--	--
Discharge Time, min	N.A.	N.A.	N.A.	N.A.
Discharge Energy From Battery, kWh	18.39	18.68	19.07	19.19
Regen. Energy To Battery, kWh	--	--	--	--
Coulombic Battery Discharge, Ah	179.0	179.9	183.0	184.1
Coulombic Regen., Ah	--	--	--	--
Discharge Termination Criteria	1.0 V/cell	1.0 V/cell	1.0 V/cell	1.0 V/cell
Recharge Energy, kWh	60.75	53.86	54.16	53.19
Coulombic Recharge, Ah	400.0	353.9	353.8	350.4
Recharge Time, h	6.0	5.0	5.0	5.0
Battery Temp. (Start of Discharge), °F	86.5	85.0	88.8	89.2
Battery Temp. (End of Discharge), °F	119.8	132.8	125.2	133.8
Battery Temp. (Start of Charge), °F	N.A.	74.5	74.5	86.5
Battery Temp. (End of Charge), °F	N.A.	87.0	88.8	89.2

<sup>a</sup>Ruptured a cell during discharge. Replaced ruptured cell and adjacent cell. Replaced three cells having low capacity.



DATA FROM TESTS OF THE W-220-2 BATTERY

Battery Cycle	17	18	19 <sup>a</sup>	20 <sup>b</sup>
Date (Discharge)	4/1/81	4/2/81	4/3/81	4/24/81
Test Vehicle	--	--	--	--
Type of Discharge	CC, 115 A	CC, 115 A	--	CC, 75 A
Distance Traveled, mi	--	--	--	--
Discharge Time, min	N.A.	N.A.	--	N.A.
Discharge Energy From Battery, kWh	15.78	15.72	--	16.03
Regen. Energy To Battery, kWh	--	--	--	--
Coulombic Battery Discharge, Ah	151.3	149.5	--	162.5
Coulombic Regen., Ah	--	--	--	--
Discharge Termination Criteria	1.0 V/cell	1.0 V/cell	--	1.0 V/cell
Recharge Energy, kWh	32.60	32.69	N.A.	51.68
Coulombic Recharge, Ah	220.4	221.3	326.0	300.0
Recharge Time, h	N.A.	N.A.	N.A.	N.A.
Battery Temp. (Start of Discharge), °F	83.8	N.A.	--	79.8
Battery Temp. (End of Discharge), °F	116.8	N.A.	--	116.5
Battery Temp. (Start of Charge), °F	87.2	N.A.	74.5	80.0
Battery Temp. (End of Charge), °F	83.2	N.A.	88.8	81.8

<sup>a</sup>Two cells ruptured during charge. Replaced three damaged cells and five cells having low capacity.

<sup>b</sup>Measured voltage during charge at various currents.

DATA FROM TESTS OF THE W-220-2 BATTERY

Battery Cycle	21	22	23 <sup>a</sup>	24
Date (Discharge)	4/27/81	4/28/81	4/30/81	5/1/81
Test Vehicle	--	--	--	--
Type of Discharge	CC, 75 A	CC, 75 A	CC, 75 A	CC, 75 A
Distance Traveled, mi	--	--	--	--
Discharge Time, min	N.A.	N.A.	N.A.	N.A.
Discharge Energy From Battery, kWh	17.76	13.92	19.67	20.35
Regen. Energy To Battery, kWh	--	--	--	--
Coulombic Battery Discharge, Ah	165.38	165.5	185.3	194.3
Coulombic Regen., Ah	--	--	--	--
Discharge Termination Criteria	1.0 V/cell	1.0 V/cell	1.0 V/cell	80 V
Recharge Energy, kWh	43.98	45.50	N.A.	49.39
Coulombic Recharge, Ah	300.0	300.3	386.6	330.1
Recharge Time, h	N.A.	6.0	N.A.	6.0
Battery Temp. (Start of Discharge), °F	75.2	76.5	76.0	78.0
Battery Temp. (End of Discharge), °F	114.8	116.8	121.2	125.5
Battery Temp. (Start of Charge), °F	74.0	86.2	N.A.	N.A.
Battery Temp. (End of Charge), °F	76.2	76.0	N.A.	N.A.

<sup>a</sup>Charge was started on 4/29, finished on 4/30. Interrupted to repair leak in manifold.

DATA FROM TESTS OF THE W-220-2 BATTERY

Battery Cycle	25	26	27	28 <sup>a</sup>
Date (Discharge)	5/5/81	5/6/81	5/7/81	5/8/81
Test Vehicle	--	--	--	--
Type of Discharge	CC, 75 A	CC, 75 A	CC, 75 A	CC, 75 A
Distance Traveled, mi	--	--	--	--
Discharge Time, min	N.A.	N.A.	N.A.	N.A.
Discharge Energy From Battery, kWh	19.25	19.28	19.12	19.07
Regen. Energy To Battery, kWh	--	--	--	--
Coulombic Battery Discharge, Ah	181.9	182.7	182.4	182.6
Coulombic Regen., Ah	--	--	--	--
Discharge Termination Criteria	80 V	80 V	80 V	80 V
Recharge Energy, kWh	46.12	44.70	44.27	44.22
Coulombic Recharge, Ah	308.3	300.1	300.3	300.0
Recharge Time, h	N.A.	4.3	5.0	5.25
Battery Temp. (Start of Discharge), °F	91.0	91.8	88.2	88.8
Battery Temp. (End of Discharge), °F	125.2	125.0	122.5	122.8
Battery Temp. (Start of Charge), °F	75.8	83.2	N.A.	N.A.
Battery Temp. (End of Charge), °F	82.8	82.8	N.A.	N.A.

<sup>a</sup>Repaired leak in manifold prior to charge.

# DATA FROM TESTS OF THE W-220-2 BATTERY

Battery Cycle	29	30	31	32
Date (Discharge)	5/11/81	5/12/81	5/13/81	5/14/81
Test Vehicle	--	--	--	--
Type of Discharge	CC, 75 A	CC, 75 A	CC, 75 A	CC 75 A
Distance Traveled, mi	--	--	--	--
Discharge Time, min	N.A.	N.A.	N.A.	N.A.
Discharge Energy From Battery, kWh	19.05	19.03	18.78	18.95
Regen. Energy To Battery, kWh	--	--	--	--
Coulombic Battery Discharge, Ah	180.96	180.0	179.2	179.2
Coulombic Regen., Ah	--	--	--	--
Discharge Termination Criteria	80 V	80 V	80 V	80 V
Recharge Energy, kWh	44.33	44.15	44.10	44.18
Coulombic Recharge, Ah	300.2	300.7	300.0	300.1
Recharge Time, h	6.0	6.0	6.1	6.0
Battery Temp. (Start of Discharge), °F	88.8	91.8	89.2	90.8
Battery Temp. (End of Discharge), °F	122.5	125.0	121.0	122.0
Battery Temp. (Start of Charge), °F	76.2	96.5	87.8	87.8
Battery Temp. (End of Charge), °F	79.8	80.8	80.8	80.8

DATA FROM TESTS OF THE W-220-2 BATTERY

Battery Cycle	33	34 <sup>a</sup>	35	36
Date (Discharge)	5/15/81	5/18/81	6/1/81	6/2/81
Test Vehicle	--	--	SCT-2	SCT-2
Type of Discharge	CC, 75 A	CC, 75 A	45 mi/h	35 mi/h
Distance Traveled, mi	--	--	71.58	88.56
Discharge Time, min	N.A.	N.A.	96.7	159.2
Discharge Energy From Battery, kWh	18.56	18.77	15.16	16.22
Regen. Energy To Battery, kWh	--	--	0.018	0.01
Coulombic Battery Discharge, Ah	176.8	178.8	144.0	151.4
Coulombic Regen., Ah	--	--	0.13	0.05
Discharge Termination Criteria	80 V	0.89 V/cell	1.0 V/cell	1.0 V/cell
Recharge Energy, kWh	43.61	43.95	44.16	43.31
Coulombic Recharge, Ah	300.0	300.1	300.0	300.0
Recharge Time, h	7.5	N.A.	N.A.	N.A.
Battery Temp. (Start of Discharge), °F	85.2	N.A.	88.0	89.8
Battery Temp. (End of Discharge), °F	118.5	N.A.	120.8	120.0
Battery Temp. (Start of Charge), °F	97.5	N.A.	N.A.	N.A.
Battery Temp. (End of Charge), °F	77.0	N.A.	N.A.	N.A.

<sup>a</sup>Installed battery in SCT-2 after this cycle.

# DATA FROM TESTS OF THE W-220-2 BATTERY

Battery Cycle	37	38	39 <sup>a</sup>	40 <sup>a</sup>
Date (Discharge)	6/3/81	6/4/81	6/11/81	6/18/81
Test Vehicle	SCT-2	SCT-2	--	--
Type of Discharge	55 mi/h	45 mi/h	special	special
Distance Traveled, mi	49.98	73.35	--	--
Discharge Time, min	55.7	98.9	N.A.	N.A.
Discharge Energy From Battery, kWh	13.26	15.07	N.A.	N.A.
Regen. Energy To Battery, kWh	0.03	0.02	--	--
Coulombic Battery Discharge, Ah	129.8	142.1	N.A.	N.A.
Coulombic Regen., Ah	0.19	0.14	--	--
Discharge Termination Criteria	1.0 V/cell	1.0 V/cell	N.A.	N.A.
Recharge Energy, kWh	N.A.	N.A.	N.A.	N.A.
Coulombic Recharge, Ah	N.A.	N.A.	N.A.	N.A.
Recharge Time, h	N.A.	N.A.	N.A.	N.A.
Battery Temp. (Start of Discharge), °F	88.8	88.0	N.A.	N.A.
Battery Temp. (End of Discharge), °F	122.5	121.5	N.A.	N.A.
Battery Temp. (Start of Charge), °F	N.A.	N.A.	N.A.	N.A.
Battery Temp. (End of Charge), °F	N.A.	N.A.	N.A.	N.A.

<sup>a</sup>Tests conducted by Westinghouse personnel to select the best cells for use in the W-220-3 battery.

## APPENDIX K

### DATA FROM TESTS OF THE W-220-3 BATTERY





DATA FROM TESTS OF THE W-220-3 BATTERY

Battery Cycle	1 <sup>a</sup>	2 <sup>b</sup>	3	4
Date (discharge)	7/15/81	7/16/81	7/21/81	7/22/81
Test Vehicle	--	--	--	--
Type of Discharge	CC, 75 A	CC, 75 A	CC, 75 A	CC, 75 A
Distance Traveled, mi	--	--	--	--
Discharge Time, min	N.A.	N.A.	145.0	141.0
Discharge Energy from Battery, kWh	N.A.	19.2	18.86	18.72
Regen. Energy To Battery, kWh	--	--	--	--
Coulombic Battery Discharge, Ah	177.0	180.0	178.1	176.5
Coulombic Regen., Ah	--	--	--	--
Discharge Termination Criteria	1.0 V/cell	1.0 V/cell	1.0 V/cell	1.0 V/cell
Recharge Energy, kWh	N.A.	50.75	45.38	44.6
Coulombic Recharge, Ah	340.0	338.6	304.5	300.0
Recharge Time, h	8.0	8.0	4.9	5.2
Battery Temp. (Start of Discharge), °F	92.0	N.A.	87.0	86.5
Battery Temp. (End of Discharge), °F	138.0	N.A.	124.1	122.8
Battery Temp. (Start of Charge), °F	78.0	N.A.	75.0	75.0
Battery Temp. (End of Charge), °F	83.0	N.A.	87.0	86.5

<sup>a</sup>Conditioning/forming cycle.

<sup>b</sup>Conditioning/forming cycle.

DATA FROM TESTS OF THE W-220-3 BATTERY

Battery Cycle	5	6 <sup>a</sup>	7 <sup>b</sup>	8 <sup>c</sup>
Date (discharge)	7/23/81	7/24/81	8/11/81	8/12/81
Test Vehicle	--	--	SCT-2	SCT-2
Type of Discharge	CC, 75 A	CC, 75 A	45 mi/h	45 mi/h
Distance Traveled, mi	--	--	79.56	83.80
Discharge Time, min	N.A.	144.0	107.5	113.0
Discharge Energy from Battery, kWh	18.87	20.11	17.00	17.64
Regen. Energy To Battery, kWh	--	--	N.A.	0.02
Coulombic Battery Discharge, Ah	177.6	189.6	161.9	167.9
Coulombic Regen., Ah	--	--	N.A.	0.16
Discharge Termination Criteria	1.0 V/cell	1.0 V/cell	1.0 V/cell	1.0 V/cell
Recharge Energy, kWh	44.82	51.02	N.A.	45.17
Coulombic Recharge, Ah	300.0	340.3	300.0	300.0
Recharge Time, h	5.1	6.0	N.A.	N.A.
Battery Temp. (Start of Discharge), °F	88.0	87.5	87.0	85.2
Battery Temp. (End of Discharge), °F	123.0	127.2	124.8	126.2
Battery Temp. (Start of Charge), °F	75.0	73.0	N.A.	N.A.
Battery Temp. (End of Charge), °F	88.0	87.0	N.A.	N.A.

<sup>a</sup>Test to determine effect of extending taper charge an extra 40 Ah.

<sup>b</sup>Half-hour open-circuit stand between end of charge and start of discharge.

<sup>c</sup>Invalid range test: power interruption during charge resulted in a half-hour open-circuit stand part way through the charge.

DATA FROM TESTS OF THE W-220-3 BATTERY

Battery Cycle	9 <sup>a</sup>	10	11	12
Date (discharge)	8/13/81	8/14/81	8/18/81	8/19/81
Test Vehicle	SCT-2	SCT-2	SCT-2	SCT-2
Type of Discharge	D Cycle	45 mi/h	35 mi/h	45 mi/h
Distance Traveled, mi	45.02	86.51	100.40	83.93
Discharge Time, min	98.7	116.7	173.2	113.2
Discharge Energy from Battery, kWh	16.60	18.01	19.16	17.84
Regen. Energy To Battery, kWh	N.A.	0.02	0.01	0.02
Coulombic Battery Discharge, Ah	176.8	171.9	179.6	172.7
Coulombic Regen., Ah	2.84	0.15	0.06	0.20
Discharge Termination Criteria	accel time	1.0 V/cell	1.0 V/cell	1.0 V/cell
Recharge Energy, kWh	44.92	45.00	44.08	44.02
Coulombic Recharge, Ah	300.0	300.0	299.9	300.0
Recharge Time, h	N.A.	N.A.	N.A.	N.A.
Battery Temp. (Start of Discharge), °F	86.2	86.8	86.2	87.0
Battery Temp. (End of Discharge), °F	142.5	127.5	124.8	128.5
Battery Temp. (Start of Charge), °F	N.A.	N.A.	72.5	89.5
Battery Temp. (End of Charge), °F	N.A.	N.A.	85.3	85.3

<sup>a</sup>Invalid range test: motor overtemp resulted in current limiting after 32 cycles.

DATA FROM TESTS OF THE W-220-3 BATTERY

Battery Cycle	13	14	15	16 <sup>a</sup>
Date (discharge)	9/2/81	9/3/81	9/4/81	9/9/81
Test Vehicle	SCT-2	SCT-2	SCT-2	--
Type of Discharge	35 mi/h	C Cycle	55 mi/h	CC, 75 A
Distance Traveled, mi	95.85	47.75	57.35	--
Discharge Time, min	165.3	179.4	63.7	63.0
Discharge Energy from Battery, kWh	18.80	17.55	15.68	10.03
Regen. Energy To Battery, kWh	0.01	0.29	0.01	--
Coulombic Battery Discharge, Ah	174.6	175.0	155.3	90.2
Coulombic Regen., Ah	0.07	2.39	0.08	--
Discharge Termination Criteria	1.0 V/cell	accel time	1.0 V/cell	90 Ah
Recharge Energy, kWh	44.96	43.93	44.56	41.49
Coulombic Recharge, Ah	299.9	300.3	300.0	300.0
Recharge Time, h	N.A.	N.A.	N.A.	6.1
Battery Temp. (Start of Discharge), °F	89.5	89.0	89.0	88.0
Battery Temp. (End of Discharge), °F	128.5	136.5	132.0	105.0
Battery Temp. (Start of Charge), °F	74.8	100.5	104.0	75.0
Battery Temp. (End of Charge), °F	89.2	89.0	88.2	88.0

<sup>a</sup>Test to determine amount of overcharge required after a partial discharge.

DATA FROM TESTS OF THE W-220-3 BATTERY

Battery Cycle	17 <sup>a</sup>	18 <sup>a</sup>	19 <sup>b</sup>	20
Date (discharge)	9/10/81	9/11/81	9/16/81	9/17/81
Test Vehicle	--	--	SCT-2	SCT-2
Type of Discharge	CC, 75 A	CC, 75 A	55 mi/h	C
Distance Traveled, mi	--	--	54.68	45.89
Discharge Time, min	69.0	110.0	62.7	172.8
Discharge Energy from Battery, kWh	9.92	14.69	15.36	17.04
Regen. Energy To Battery, kWh	--	--	0.04	0.30
Coulombic Battery Discharge, Ah	90.7	138.2	152.4	171.2
Coulombic Regen., Ah	--	--	0.29	2.54
Discharge Termination Criteria	90 Ah	1.0 V/cell	1.0 V/cell	accel time
Recharge Energy, kWh	16.12	16.00	44.74	44.52
Coulombic Recharge, Ah	110.5	110.0	300.0	300.0
Recharge Time, h	1.7	1.8	N.A.	N.A.
Battery Temp. (Start of Discharge), °F	86.0	80.0	89.2	87.2
Battery Temp. (End of Discharge), °F	101.0	111.0	133.2	137.0
Battery Temp. (Start of Charge), °F	89.0	77.0	76.0	103.0
Battery Temp. (End of Charge), °F	86.0	80.0	88.0	86.2

<sup>a</sup>Test to determine amount of overcharge required after a partial discharge.

<sup>b</sup>No electrolyte circulation for first 27 min of discharge.

DATA FROM TESTS OF THE W-220-3 BATTERY

Battery Cycle	21	22	23	24
Date (discharge)	9/18/81	9/22/81	9/23/81	9/24/81
Test Vehicle	SCT-2	SCT-2	SCT-2	SCT-2
Type of Discharge	45 mi/h	55 mi/h	55 mi/h	35 mi/h
Distance Traveled, mi	82.21	58.16	56.52	98.77
Discharge Time, min	111.3	65.6	63.9	170.9
Discharge Energy from Battery, kWh	17.41	15.82	15.59	18.87
Regen. Energy To Battery, kWh	0.01	0.02	0.02	0.01
Coulombic Battery Discharge, Ah	165.8	156.5	154.9	175.2
Coulombic Regen., Ah	0.04	0.18	0.12	0.07
Discharge Termination Criteria	1.0 V/cell	1.0 V/cell	1.0 V/cell	1.0 V/cell
Recharge Energy, kWh	44.58	44.97	44.66	44.72
Coulombic Recharge, Ah	300.0	300.0	300.0	300.0
Recharge Time, h	N.A.	N.A.	N.A.	N.A.
Battery Temp. (Start of Discharge), °F	86.2	89.5	88.8	88.5
Battery Temp. (End of Discharge), °F	129.9	132.8	132.0	128.2
Battery Temp. (Start of Charge), °F	105.5	75.8	102.5	102.8
Battery Temp. (End of Charge), °F	86.0	89.0	88.2	88.2

DATA FROM TESTS OF THE W-220-3 BATTERY

Battery Cycle	25	26 <sup>a</sup>	27 <sup>b</sup>	28 <sup>c</sup>
Date (discharge)	9/25/81	9/28/81	10/5/81	10/13/81
Test Vehicle	SCT-2	SCT-2	SCT-2	SCT-2
Type of Discharge	35 mi/h	45 mi/h	45 mi/h	45 mi/h
Distance Traveled, mi	99.44	70.14	58.63	80.17
Discharge Time, min	171.8	95.0	79.7	107.9
Discharge Energy from Battery, kWh	19.05	15.26	12.87	16.92
Regen. Energy To Battery, kWh	0.01	0.01	0.01	0.02
Coulombic Battery Discharge, Ah	176.6	149.4	128.8	161.3
Coulombic Regen., Ah	0.05	0.09	0.12	0.15
Discharge Termination Criteria	1.0 V/cell	1.0 V/cell	1.0 V/cell	1.0 V/cell
Recharge Energy, kWh	44.60	44.99	44.92	45.36
Coulombic Recharge, Ah	300.0	300.0	300.0	300.0
Recharge Time, h	N.A.	N.A.	N.A.	N.A.
Battery Temp. (Start of Discharge), °F	89.5	85.0	78.2	82.2
Battery Temp. (End of Discharge), °F	129.2	122.0	114.0	122.2
Battery Temp. (Start of Charge), °F	103.2	78.2	77.5	75.5
Battery Temp. (End of Charge), °F	88.2	88.0	89.5	80.8

<sup>a</sup>Self-discharge test. 24-h open-circuit stand between end of charge and start of discharge.

<sup>b</sup>Self-discharge test. 72-h open-circuit stand between end of charge and start of discharge.

<sup>c</sup>Self-discharge test. 1-h open-circuit stand between end of charge and start of discharge.

DATA FROM TESTS OF THE W-220-3 BATTERY

Battery Cycle	29 <sup>a</sup>	30 <sup>b</sup>	31 <sup>b</sup>	32 <sup>b</sup>
Date (discharge)	10/21/81	10/30/81	11/2/81	11/3/81
Test Vehicle	SCT-2	--	--	--
Type of Discharge	45 mi/h	CC, 75 A	CC, 75 A	CC, 75 A
Distance Traveled, mi	79.61	--	--	--
Discharge Time, min	107.5	133.0	127.0	135.0
Discharge Energy from Battery, kWh	16.46	19.43	17.31	18.12
Regen. Energy To Battery, kWh	0.02	--	--	--
Coulombic Battery Discharge, Ah	157.2	178.2	162.0	169.5
Coulombic Regen., Ah	0.15	--	--	--
Discharge Termination Criteria	1.0 V/cell	1.0 V/cell	1.0 V/cell	1.0 V/cell
Recharge Energy, kWh	44.80	41.35	45.06	44.67
Coulombic Recharge, Ah	300.0	300.0	300.0	300.0
Recharge Time, h	N.A.	4.5	5.3	5.6
Battery Temp. (Start of Discharge), °F	87.3	117.0	85.0	83.0
Battery Temp. (End of Discharge), °F	125.5	142.0	112.2	123.0
Battery Temp. (Start of Charge), °F	78.8	N.A.	76.0	N.A.
Battery Temp. (End of Charge), °F	84.8	117.0	85.0	83.0

<sup>a</sup>Self-discharge test. 4-h open-circuit stand between end of charge and start of discharge.

<sup>b</sup>Conditioning cycle.



DATA FROM TESTS OF THE W-220-3 BATTERY

Battery Cycle	33	34 <sup>a</sup>	35 <sup>a</sup>	36 <sup>a</sup>
Date (discharge)	11/5/81	11/9/81	11/10/81	11/12/81
Test Vehicle	--	--	--	--
Type of Discharge	CC, 75 A	CC, 75 A	CC, 75 A	CC, 75 A
Distance Traveled, mi	--	--	--	--
Discharge Time, min	122.0	132.0	146.0	139.0
Discharge Energy from Battery, kWh	16.40	17.54	19.59	19.90
Regen. Energy To Battery, kWh	--	--	--	--
Coulombic Battery Discharge, Ah	153.2	166.4	183.2	185.3
Coulombic Regen., Ah	--	--	--	--
Discharge Termination Criteria	1.0 V/cell	1.0 V/cell	1.0 V/cell	1.0 V/cell
Recharge Energy, kWh	36.81	51.42	52.60	52.71
Coulombic Recharge, Ah	250.0	350.0	350.0	350.0
Recharge Time, h	5.5	N.A.	6.2	6.0
Battery Temp. (Start of Discharge), °F	79.5	84.5	92.5	89.8
Battery Temp. (End of Discharge), °F	117.8	116.8	129.0	130.2
Battery Temp. (Start of Charge), °F	78.8	77.2	88.2	87.2
Battery Temp. (End of Charge), °F	79.5	84.5	92.5	89.5

<sup>a</sup>Conditioning cycle.

DATA FROM TESTS OF THE W-220-3 BATTERY

Battery Cycle	37	38	39 <sup>a</sup>	40 <sup>b</sup>
Date (discharge)	11/13/81	11/16/81	11/17/81	12/3/81
Test Vehicle	--	--	--	--
Type of Discharge	CC, 75 A	CC, 75 A	CC, 75 A	CC, 75 A
Distance Traveled, mi	--	--	--	--
Discharge Time, min	139.0	139.0	135.0	130.0
Discharge Energy from Battery, kWh	18.64	18.82	18.36	17.26
Regen. Energy To Battery, kWh	--	--	--	--
Coulombic Battery Discharge, Ah	173.6	174.6	169.1	162.5
Coulombic Regen., Ah	--	--	--	--
Discharge Termination Criteria	1.0 V/cell	1.0 V/cell	1.0 V/cell	1.0 V/cell
Recharge Energy, kWh	44.86	45.15	44.11	46.65
Coulombic Recharge, Ah	300.0	300.2	300.0	340.1
Recharge Time, h	5.3	4.8	4.4	8.3
Battery Temp. (Start of Discharge), °F	88.8	91.5	106.8	84.6
Battery Temp. (End of Discharge), °F	128.0	130.0	137.8	117.0
Battery Temp. (Start of Charge), °F	82.5	81.2	101.5	80.2
Battery Temp. (End of Charge), °F	88.8	91.5	107.0	84.6

<sup>a</sup>No cooling water for first 210 Ah of charge.

<sup>b</sup>Conditioning cycle.

DATA FROM TESTS OF THE W-220-3 BATTERY

Battery Cycle	41 <sup>a</sup>	42	43 <sup>a</sup>	44 <sup>b</sup>
Date (discharge)	12/29/81	12/30/81	1/5/82	1/6/82
Test Vehicle	--	--	--	--
Type of Discharge	CC, 75 A	CC, 75 A	CC, 75 A	CC, 75 A
Distance Traveled, mi	--	--	--	--
Discharge Time, min	150.9	141.0	162.0	68.0
Discharge Energy from Battery, kWh	20.15	19.18	21.85	11.01
Regen. Energy To Battery, kWh	--	--	--	--
Coulombic Battery Discharge, Ah	189.9	176.7	204.6	90.0
Coulombic Regen., Ah	--	--	--	--
Discharge Termination Criteria	1.0 V/cell	1.0 V/cell	1.0 V/cell	90 Ah
Recharge Energy, kWh	64.82	45.23	71.67	44.41
Coulombic Recharge, Ah	430.0	300.0	475.0	300.0
Recharge Time, h	8.3	N.A.	8.5	4.6
Battery Temp. (Start of Discharge), °F	91.8	105.2	90.6	97.2
Battery Temp. (End of Discharge), °F	134.0	135.6	129.6	109.0
Battery Temp. (Start of Charge), °F	72.2	80.0	71.2	88.4
Battery Temp. (End of Charge), °F	91.6	105.2	90.6	97.2

<sup>a</sup>Conditioning cycle.

<sup>b</sup>Test to determine amount of overcharge required after a partial discharge.

DATA FROM TESTS OF THE W-220-3 BATTERY

Battery Cycle	45 <sup>a</sup>	46 <sup>a</sup>	47	48
Date (discharge)	1/7/82	1/8/82	1/11/82	1/12/82
Test Vehicle	--	--	--	--
Type of Discharge	CC, 75 A	CC, 75 A	CC, 75 A	CC, 75 A
Distance Traveled, mi	--	--	--	--
Discharge Time, min	71.0	N.A.	133.0	135.7
Discharge Energy from Battery, kWh	10.11	18.27	18.36	18.45
Regen. Energy To Battery, kWh	--	--	--	--
Coulombic Battery Discharge, Ah	90.3	146.5	169.8	170.5
Coulombic Regen., Ah	--	--	--	--
Discharge Termination Criteria	90 Ah	1.0 V/cell	1.0 V/cell	1.0 V/cell
Recharge Energy, kWh	18.27	18.34	44.94	44.56
Coulombic Recharge, Ah	126.0	126.0	300.0	300.0
Recharge Time, h	1.7	1.9	5.2	5.1
Battery Temp. (Start of Discharge), °F	95.8	98.0	89.2	91.2
Battery Temp. (End of Discharge), °F	N.A.	118.8	119.4	120.2
Battery Temp. (Start of Charge), °F	82.2	85.4	75.2	88.8
Battery Temp. (End of Charge), °F	96.4	95.8	89.2	91.2

<sup>a</sup>Test to determine amount of overcharge required after a partial discharge.

DATA FROM TESTS OF THE W-220-3 BATTERY

Battery Cycle	49 <sup>a</sup>	50 <sup>a</sup>	51 <sup>b</sup>	52
Date (discharge)	1/13/82	1/14/82	1/15/82	1/18/82
Test Vehicle	--	--	--	--
Type of Discharge	CC, 75 A	CC, 75 A	CC, 75 A	CC, 75 A
Distance Traveled, mi	--	--	--	--
Discharge Time, min	138.3	137.0	122.0	138.0
Discharge Energy from Battery, kWh	19.01	18.63	15.49	18.66
Regen. Energy To Battery, kWh	--	--	--	--
Coulombic Battery Discharge, Ah	176.0	169.5	140.7	173.8
Coulombic Regen., Ah	--	--	--	--
Discharge Termination Criteria	1.0 V/cell	1.0 V/cell	see note	1.0 V/cell
Recharge Energy, kWh	44.61	43.90	44.74	45.31
Coulombic Recharge, Ah	300.0	300.0	300.0	300.0
Recharge Time, h	5.1	5.0	5.3	5.7
Battery Temp. (Start of Discharge), °F	91.2	123.8	89.6	86.8
Battery Temp. (End of Discharge), °F	127.8	143.2	117.2	125.2
Battery Temp. (Start of Charge), °F	89.0	81.0	90.6	75.4
Battery Temp. (End of Charge), °F	91.2	91.0	89.4	86.8

<sup>a</sup>Conditioning cycle.

<sup>b</sup>Conditioning cycle. Discharge terminated when weakest group of five cells reached 1.0 V/cell.

DATA FROM TESTS OF THE W-220-3 BATTERY

Battery Cycle	53 <sup>a</sup>	54 <sup>a</sup>	55 <sup>a</sup>	56 <sup>b</sup>
Date (discharge)	2/12/82	2/16/82	2/17/82	2/19/82
Test Vehicle	--	--	--	--
Type of Discharge	CC, 75 A	CC, 75 A	CC, 75 A	CC, 75 A
Distance Traveled, mi	--	--	--	--
Discharge Time, min	82.0	110.0	110.8	128.0
Discharge Energy from Battery, kWh	11.04	15.30	14.67	17.62
Regen. Energy To Battery, kWh	--	--	--	--
Coulombic Battery Discharge, Ah	99.6	139.0	135.6	163.2
Coulombic Regen., Ah	--	--	--	--
Discharge Termination Criteria	1.0 V/cell	1.0 V/cell	1.0 V/cell	1.0 V/cell
Recharge Energy, kWh	30.44	44.70	52.29	44.44
Coulombic Recharge, Ah	200.6	300.0	350.1	300.0
Recharge Time, h	3.8	4.9	7.9	6.0
Battery Temp. (Start of Discharge), °F	75.2	86.4	77.4	77.4
Battery Temp. (End of Discharge), °F	92.0	105.4	110.0	113.8
Battery Temp. (Start of Charge), °F	68.4	74.0	87.4	87.8
Battery Temp. (End of Charge), °F	75.2	86.4	75.6	77.4

<sup>a</sup>Conditioning cycle.

<sup>b</sup>Measured gassing rate during charge.

DATA FROM TESTS OF THE W-220-3 BATTERY

Battery Cycle	57 <sup>a</sup>	58	59 <sup>b</sup>	60 <sup>c</sup>
Date (discharge)	2/22/82	2/26/82	3/2/82	3/3/82
Test Vehicle	--	--	--	--
Type of Discharge	CC, 75 A	CC, 75 A	CC, 75 A	CC, 75 A
Distance Traveled, mi	--	--	--	--
Discharge Time, min	126.0	117.2	126.0	122.8
Discharge Energy from Battery, kWh	17.26	16.79	17.30	N.A.
Regen. Energy To Battery, kWh	--	--	--	--
Coulombic Battery Discharge, Ah	159.1	153.7	157.5	153.0
Coulombic Regen., Ah	--	--	--	--
Discharge Termination Criteria	1.0 V/cell	1.0 V/cell	1.0 V/cell	1.0 V/cell
Recharge Energy, kWh	44.69	44.69	44.73	44.90
Coulombic Recharge, Ah	300.0	300.0	300.0	300.0
Recharge Time, h	5.8	5.2	5.3	5.8
Battery Temp. (Start of Discharge), °F	77.4	85.0	78.8	77.4
Battery Temp. (End of Discharge), °F	108.0	120.0	114.4	101.4
Battery Temp. (Start of Charge), °F	74.2	76.0	74.6	93.8
Battery Temp. (End of Charge), °F	78.0	85.0	78.8	77.4

<sup>a</sup>Conditioning cycle.

<sup>b</sup>Added 100 g LiOH before charge.

<sup>c</sup>Added 1 lb KOH before charge.

DATA FROM TESTS OF THE W-220-3 BATTERY

Battery Cycle	61 <sup>a</sup>	62 <sup>a</sup>	63 <sup>a</sup>	64 <sup>b</sup>
Date (discharge)	3/5/82	3/9/82	3/10/82	3/11/82
Test Vehicle	--	--	--	--
Type of Discharge	CC, 75 A	CC, 75 A	CC, 75 A	CC, 75 A
Distance Traveled, mi	--	--	--	--
Discharge Time, min	N.A.	117.8	121.0	N.A.
Discharge Energy from Battery, kWh	N.A.	N.A.	N.A.	N.A.
Regen. Energy To Battery, kWh	--	--	--	--
Coulombic Battery Discharge, Ah	140.2	147.2	154.6	106.5
Coulombic Regen., Ah	--	--	--	--
Discharge Termination Criteria	see note	see note	see note	cell failure
Recharge Energy, kWh	N.A.	N.A.	N.A.	N.A.
Coulombic Recharge, Ah	391.8	394.0	350.0	300.0
Recharge Time, h	N.A.	7.0	5.0	N.A.
Battery Temp. (Start of Discharge), °F	N.A.	82.2	83.4	90.0
Battery Temp. (End of Discharge), °F	103.0	107.2	117.2	N.A.
Battery Temp. (Start of Charge), °F	70.4	72.0	90.4	95.8
Battery Temp. (End of Charge), °F	82.6	82.2	83.4	90.0

<sup>a</sup>Conditioning cycle. Discharge terminated when weakest group of five cells reached 1.0 V/cell.

<sup>b</sup>Discharge terminated by cell failure after 106 Ah.



DATA FROM TESTS OF THE W-220-3 BATTERY

Battery Cycle	65 <sup>a</sup>	66 <sup>b</sup>	67	68 <sup>c</sup>
Date (discharge)	3/16/82	3/17/82	3/18/82	3/19/82
Test Vehicle	--	--	--	--
Type of Discharge	CC, 75 A	CC, 75 A	CC, 75 A	CC, 75 A
Distance Traveled, mi	--	--	--	--
Discharge Time, min	101.1	139.0	135.0	128.5
Discharge Energy from Battery, kWh	N.A.	N.A.	17.49	16.60
Regen. Energy To Battery, kWh	--	--	--	--
Coulombic Battery Discharge, Ah	126.4	167.3	169.4	160.6
Coulombic Regen., Ah	--	--	--	--
Discharge Termination Criteria	see note	1.0 V/cell	1.0 V/cell	1.0 V/cell
Recharge Energy, kWh	N.A.	N.A.	44.02	42.79
Coulombic Recharge, Ah	300.0	300.0	300.0	300.0
Recharge Time, h	6.5	5.0	5.8	11.5
Battery Temp. (Start of Discharge), °F	72.8	83.0	77.2	66.4
Battery Temp. (End of Discharge), °F	96.0	106.6	107.0	102.8
Battery Temp. (Start of Charge), °F	71.2	75.0	85.0	87.0
Battery Temp. (End of Charge), °F	78.6	N.A.	77.2	65.4

<sup>a</sup>Conditioning cycle. Replaced two cells before this cycle. Discharge terminated when weakest group of five cells reached 1.0 V/cell.

<sup>b</sup>Configured battery to 88 cells before this cycle.

<sup>c</sup>Experimental charge. Lowered voltage clamp so current would taper to 10 A by end of charge. Measured gassing rate during charge.

DATA FROM TESTS OF THE W-220-3 BATTERY

Battery Cycle	69	70 <sup>a</sup>
Date (discharge)	3/22/82	3/23/82
Test Vehicle	--	--
Type of Discharge	CC, 75 A	CC, 75 A
Distance Traveled, mi	--	--
Discharge Time, min	135.0	N.A.
Discharge Energy from Battery, kWh	17.84	15.82
Regen. Energy To Battery, kWh	--	--
Coulombic Battery Discharge, Ah	169.9	N.A.
Coulombic Regen., Ah	--	--
Discharge Termination Criteria	1.0 V/cell	1.0 V/cell
Recharge Energy, kWh	44.14	42.93
Coulombic Recharge, Ah	300.2	300.0
Recharge Time, h	N.A.	14.0
Battery Temp. (Start of Discharge), °F	88.4	66.8
Battery Temp. (End of Discharge), °F	111.8	N.A.
Battery Temp. (Start of Charge), °F	74.8	88.2
Battery Temp. (End of Charge), °F	88.4	66.8

<sup>a</sup>Experimental charge. Voltage clamp set so current tapered to 10 A by end of charge. Measured gassing rate during charge.

















